CARDIFF UNIVERSITY
PRIFYSGOL CAERDYDD

# ORCA – Online Research @ Cardiff

This is an Open Access document downloaded from ORCA, Cardiff University's institutional repository:https://orca.cardiff.ac.uk/id/eprint/101997/

This is the author's version of a work that was submitted to / accepted for publication.

Citation for final published version:

Lambert-Smith, James S. , Lawrence, David M., Müller, Wolfgang and Treloar, Peter J. 2016. Palaeotectonic setting of the south-eastern Kédougou-Kéniéba Inlier, West Africa: New insights from igneous trace element geochemistry and U-Pb zircon ages. Precambrian Research 274 , pp. 110-135. 10.1016/j.precamres.2015.10.013

Publishers page: http://dx.doi.org/10.1016/j.precamres.2015.10.013

Please note:
Changes made as a result of publishing processes such as copy-editing, formatting and page numbers may not be reflected in this version. For the definitive version of this publication, please refer to the published source. You are advised to consult the publisher's version if you wish to cite this paper.

This version is being made available in accordance with publisher policies. See http://orca.cf.ac.uk/policies.html for usage policies. Copyright and moral rights for publications made available in ORCA are retained by the copyright holders.

Accepted Manuscript

Title: Palaeotectonic setting of the south-eastern Kédougou-Kéniéba Inlier, West Africa: new insights from igneous trace element geochemistry and U-Pb zircon ages

Author: James S. Lambert-Smith David M. Lawrence Wolfgang Müller Peter J. Treloar

PII: S0301-9268(15)00348-4
DOI: http://dx.doi.org/doi:10.1016/j.precamres.2015.10.013
Reference: PRECAM 4384

To appear in: *Precambrian Research*

Received date: 14-1-2015
Revised date: 7-10-2015
Accepted date: 17-10-2015

Please cite this article as: Lambert-Smith, J.S., Lawrence, D.M., Müller, W., Treloar, P.J.,Palaeotectonic setting of the south-eastern Kédougou-Kéniéba Inlier, West Africa: new insights from igneous trace element geochemistry and U-Pb zircon ages, *Precambrian Research* (2015), http://dx.doi.org/10.1016/j.precamres.2015.10.013

This is a PDF file of an unedited manuscript that has been accepted for publication. As a service to our customers we are providing this early version of the manuscript. The manuscript will undergo copyediting, typesetting, and review of the resulting proof before it is published in its final form. Please note that during the production process errors may be discovered which could affect the content, and all legal disclaimers that apply to the journal pertain.

ACCEPTED MANUSCRIPT

# Palaeotectonic setting of the south-eastern Kédougou-Kéniéba Inlier, West Africa: new insights from igneous trace element geochemistry and U-Pb zircon ages

James S. Lambert-Smith[1*]; David M. Lawrence[2]; Wolfgang Müller[3]; Peter J. Treloar[1]

[1]School of Geography, Geology and the Environment, Kingston University London, Kingston upon Thames, Surrey, KT1 2EE, UK

[2]Randgold Resources Ltd, 3rd Floor, Unity Chambers, 28 Halkett Street, St Helier, Jersey, JE24W

[3]Department of Earth Sciences, Royal Holloway, University of London, Egham, Surrey, TW20 0EX

*Corresponding author (Telephone: +44 (0) 208417 9000 Ext. 62880; Email: J.S.Lambert-Smith@kingston.ac.uk)

## Abstract

New U-Pb zircon ages and geochemistry from the eastern Kédougou-Kéniéba Inlier are presented and integrated with published data to generate a revised tectonic framework for the westernmost Birimian terranes. The Falémé Volcanic Belt and Kofi Series are highly prospective, hosting several multi-million ounce gold deposits and a significant iron ore resource, but remain under-researched. It is therefore important to constrain the fundamental geological setting.

The igneous rocks of the eastern Kédougou-Kéniéba Inlier are dominantly of high-K calc-alkaline affinity, with fractionated REE patterns and negative Nb-Ta anomalies. The plutonic rocks in the Falémé Belt are dioritic to granodioritic in composition, with moderately fractionated REE patterns and metaluminous A/CNK signatures. Felsic, peraluminous granite stocks, dykes and plutons with fractionated REE patterns and negative Eu, Ti and P anomalies intruded both the Falémé Belt and Kofi Series. Albitisation masks the affinity

Accepted Manuscript

ACCEPTED MANUSCRIPT

of some units, although use of the Th-Co diagram shows that prior to albitisation, all igneous unitsbelonged to the high-K calc-alkaline series. New U-Pb age data for the Boboti and Balangouma plutons indicate crystallisation at 2088.5 ± 8.5 Ma and at 2112 ± 13 Ma, respectively. Inherited zircons in the Boboti pluton indicate magmatic activity in the Falémé Belt at 2218 ± 83 Ma coincided with the oldest dated units in the Mako Belt to the West.

Systematic changes in Dy/Yb, Sm/La, Nb/Zr, Rb concentration, Eu-anomaly and $\varepsilon Nd_t$ over ~200 Ma reveal that the tectonic setting in the KKI evolved from a volcanic island arc environment to an active continental margin. Crustal thickening, as a result of a shift to collisional tectonic setting, combined with magmatic differentiation, led to the generation of peraluminous, granitic melts with a significant crustal component. A small suite of more basic intrusive and extrusive rocks on the eastern margin of the Dialé-Daléma basin are highly metaluminous and display limited LILE enrichment, with normalised HREE values close to unity. The Daléma igneous rocks may have formed in an extensional back arc, related to the arc system.

## Key Words

Kédougou-Kéniéba Inlier; Birimian; geochemistry; U-Pb zircon ages; palaeotectonic setting

## 1 Introduction

The Birimian terranes of the West African Craton are considered to be an important record of crustal growth in the Palaeoproterozoic (Boher et al., 1992; Doumbia et al., 1998; Gasquet et al., 2003). The exact tectonic setting and geodynamic processes that gave rise to the Birimian terranes remain a subject of debate. In part this is because of the complex nature of the terranes, but also due to gaps in the geochemical and chronological datasets. The Kédougou-Kéniéba Inlier (KKI; Figure 1) represents the westernmost outcrop of the Birimian in the Leo-Man shield, and is separated from the majority of the Palaeoproterozoic terranes by the overlying Neoproterozoic sandstones of the Taoudeni Basin. The western part of the KKI is well studied, with most attention given to the Mako Volcanic Belt (MVB; Figure 1) in Eastern Senegal (e.g., Debat



Accepted Manuscript

ACCEPTED MANUSCRIPT

et al., 1984; Abouchami et al., 1990; Ledru et al., 1991; Dia, et al., 1997; Diallo, 2001; Gueye et al., 2008; Ngom et al., 2009; Treloar et al., 2014). By comparison, the eastern KKI (the Falémé Volcanic Belt and Kofi Series; Figure 1) is under-researched, despite hosting several world-class Au deposits, including the Loulo, Gounkoto, Sadiola and Tabakoto gold mines all of which are situated east of the Senegal-Mali Shear Zone (SMSZ; Bassot and Dommanget, 1986; Dommanget et al., 1993; Lawrence et al., 2013a and b). In addition to Au mineralisation, several magnetite-skarn deposits are hosted in the Falémé Volcanic Belt (FVB; Schwartz and Melcher, 2004). The KKI is clearly a highly prospective region in the Birimian; it is therefore important to constrain the fundamental geological setting.

The majority of geochemical studies in the KKI have focused on the tholeiitic lavas and belt-hosted granitoid plutons in the MVB (Debat et al., 1984; Abouchami et al., 1990; Boher et al., 1992; Diallo, 2001; Pawlig et al., 2006). Schwartz and Melcher (2004) published a geochemical study of the FVB, which concentrated on the genesis of the skarn-style iron ore deposits. However, niether the extensive Balangouma pluton in the north of the belt (Figure 2), or the numerous minor stocks and dykes throughout the FVB and Kofi Series have been studied geochemically. These lithologies are dominantly unaltered by hydrothermal processes, with well-preserved primary textures, despite greenschist facies metamorphism. However, some rocks in the area have been albitised due to hydrothermal fluid-rock interactions. This may hide the true tectonic and petrogenetic affinity of these lithologies, leading to incorrect conclusions as to their genesis.

Here we use new geochronological and geochemical datasets, combined with published data, to construct an improved geotectonic framework for the KKI, with an emphasis on the Falémé Volcanic Belt and Kofi Series. We aim to integrate trace element geochemistry with geochronology to show the secular evolution of Birimian magmas from primitive island arc granitoids to evolved syn-collisional granites. This reflects the shift from an ocean island arc setting to an accretionary regime with associated crustal thickening. In addition we aim to examine the key geochemical characteristics of altered igneous lithologies



Accepted Manuscript

ACCEPTED MANUSCRIPT

and show that Na-rich igneous rocks in the KKI are the product of albitisation of high-K calc-alkaline lithologies.

## 2 Geology of the Birimian of West Africa

The West African Craton (WAC) consists of Archaean and Palaeoproterozoic terranes; stable since ~2 Ga, they provide a valuable record of crustal growth processes and contain notable mineral wealth. The WAC is divided into three domains: 1) The Reguibat Rise in northern Africa; 2) The Leo-Man Rise in sub-Saharan West Africa and, 3) The Kayes and Kédougou-Kéniéba Inliers in the Sahel region, North West of the Leo-Man Rise. The Reguibat and Leo-Man rises both share contacts with Archaean continental nuclei and are collectively referred to as the Baoulé-Mossi Domain. The Birimian terranes consist of narrow, linear to arcuate, N to NNE trending volcanic belts, separated by broad sedimentary basins. The volcanic rocks are interpreted to be the base of the sequence, with coeval to slightly younger metasedimentary rocks (Béziat et al., 2000; Pouclet et al, 2006; Roddaz et al., 2007). The terranes were accreted and cratonised during a period of SE to NW directed crustal shortening, metamorphism and magmatic accretion from 2120 to 2080 Ma known as the Eburnean orogeny (Bonhomme, 1962; Oberthür et al., 1998; Feybesse et al., 2006). Peak metamorphic conditions were reached in the Ashanti belt of Ghana at ~2100 Ma based on U-Pb ages of metamorphic titanite (Oberthür et al., 1998). Peak metamorphic conditions are widely reported as amphibolite facies (500–600°C; 4–6 kbar; John et al., 1999; White et al., 2013), although greenschist facies assemblages are dominant across the region (Hirdes et al., 1996).

The volcanic belts consist of tholeiitic lavas and associated mafic intrusions interbedded with minor sequences of immature sedimentary, volcaniclastic and carbonate rocks. The sedimentary basins comprise isoclinally folded and deformed sequences of greywacke, argillite and arkose with calc-alkaline volcanic sequences. Extensive suites of plutonic rocks have intruded both units, and range in composition from tholeiitic gabbro to high-K calc-alkaline granite. The majority of plutonic rocks are grouped by their host

ACCEPTED MANUSCRIPT

terranes; i.e. 'belt-' and 'basin-type', and a post-Eburnean K-rich series (Leube et al., 1990; Hirdes et al., 1992).

The Birimian terranes formed over a period of ~180 Ma, between 2266 and 2088 Ma (Perrouty et al., 2012; White et al., 2014 and references therein; Parra-Avila et al., 2015). This period is divided into two phases, the age and terminology of each differs throughout the Birimian. In South western Ghana the Eburnean I (2266-2150 Ma) precedes the Eburnean II (2216-2088 Ma) (Allibone et al., 2002). In northern Ghana, the earlier event is referred to as the Eoeburnean (2195–2150 Ma) and the latter as the Eburnean (2148–2090 Ma) (de Kock et al., 2011). In Burkina Faso the Eburnean (2130 – 1980 Ma) is preceded by the Tangaean event (2170-2130 Ma) (Tshibubudze et al., 2009; Hein, 2010). Broadly speaking, the earlier event, in each case, consists of volcanism, granitoid emplacement and fold, thrust tectonics. This is followed by emplacement of younger granitoids, strike-slip deformation and mineralisation in the latter event. U-Pb zircon ages show that the Eburnean I encompasses early volcanism, between 2266 ± 2 and 2132 ± 3 Ma (Taylor et al., 1992; Loh et al., 1999), and early plutonism, from 2213 ± 3 to 2151 ± 7 Ma (Dia et al., 1997; Gueye et al., 2007; White et al., 2014 and references therein). Tshibubudze et al., (in press) suggest that the three early events are broadly the same tectonic event. U-Pb dating of detrital zircons shows that sedimentation was coeval with magmatism in the volcanic belts, from 2135 ± 5 Ma in Ghana (Oberthür et al., 1998; Davis et al., 1994) and from 2164.7 ± 0.9 Ma in the KKI (Hirdes and Davis et al., 2002). The Eburnean represents the final phase of magmatism in Ghana, where basin-type plutons were intruded between 2116 ± 2 and 2088 ± 1 Ma (U-Pb zircon) (Hirdes et al., 1992; Davis et al., 1994).

Though there are variations, models for crustal growth in the Birimian largely involve the development of juvenile volcanic arc magmas in an oceanic setting (Sylvester and Attoh, 1992; Dia et al., 1997; Pawlig et al., 2006; Soumaila et al., 2008; Baratoux et al., 2011). Recent P-T-t reconstructions in metasedimentary rocks record blueschist-facies metamorphic conditions diagnostic of subduction environments (Ganne et al., 2011).



Accepted Manuscript

ACCEPTED MANUSCRIPT

## 3 Lithostratigraphy of the KKI

The stratigraphy of the KKI from west to east consists of: 1) bimodal volcanics intruded by numerous plutonic complexes in the MVB; 2) detrital sedimentary rocks of the Dialé-Daléma basin, which are intruded by the Saraya batholith; 3) calc-alkaline volcaniclastic rocks of the FVB and; 4) siliciclastic sedimentary rocks of the Kofi Series, unconformably overlain by Neoproterozoic sedimentary rocks to the east (Figure 1). Age data for the KKI are summarised in Table 1.

### 3.1 The Mako Volcanic Belt

The MVB is a NNE trending ~20-40 km wide band of bimodal volcanic rocks which crop out in the west of the KKI. They are overlain to the west by the Pan-African Mauritanides belt. The Main Transcurrent Shear Zone (MTZ) marks the eastern edge of the MVB, with the Dialé-Daléma basin to the east (Figure 2). The lowermost units in the west consist of thick flows of massive and pillowed tholeiitic basalt. These are associated with dolerites and gabbros and intercalated with thin felsic tuffs, pyroclastites, rhyolites and minor clastic and carbonaceous sedimentary rocks (Dioh et al., 2006), which become more prominent to the east. The age of the Mako tholeiitic basalts is poorly constrained. Dia (1988) reported a whole-rock Pb-Pb age of 2195 ± 118 Ma. Given this large error, the upper age limit for the Sandikounda amphibolite-gneiss complex (SAG; Figure 1) is interpreted to be the younger age limit for their eruption as it intrudes the lava sequences. The volcanic sequence is capped by andesitic lava, tuff and pyroclastic rocks (Dia, et al., 1997; Ngom et al., 2009). An andesite flow in the east of the MVB yielded a Sm-Nd whole-rock age of 2160 ± 16 Ma (Boher et al., 1992).

The MVB is intruded by a plutonic complex known as the Kakadian batholith (Dia, 1985; Hirdes and Davis, 2002; Dioh et al., 2006; Gueye et al., 2007). The batholith is composed of three units in the north (Figure 1); 1) the Sandikounda amphibolite-gneiss complex (SAG); 2) the Sandikounda Layered Plutonic Complex (SLPC); and 3) the Laminia-Kaourou Plutonic Complex (LKPC). The south of the batholith is known as the Badon batholith. The SAG consists of tonalitic to dioritic gneiss containing amphibolite enclaves. This is the oldest unit in the north of the batholith. U-Pb data indicate crystallisation at 2205 ± 15 Ma (Gueye et al.,



Accepted Manuscript

ACCEPTED MANUSCRIPT

2007). The SLPC crystallised between 2171 ± 9 and 2158 ± 8 Ma (Pb-Pb and U-Pb zircon data; Dia et al., 1997; Goujou et al., 2010), and is composed of layered hornblende-gabbro, diorite, migmatite and hornblendite, with xenoliths of wherlite and pyroxenite. Elements of the SLPC intruded the SAG (Gueye et al., 2008). The LKPC consists of the Laminia and Kaourou plutons. Tonalite and granodiorite of the Laminia pluton were emplaced at 2138 ± 12 and 2105 ± 8 Ma (Pb-Pb zircon data; Dia et al., 1997; Gueye et al., 2008). The porphyritic monzogranite of the Kaourou pluton is younger at 2079 ± 6 Ma (Pb-Pb zircon data; Dia et al., 1997). Both plutons contain xenoliths of Mako volcanic rocks and the SLPC (Dia et al., 1997). The Badon batholith is composed of biotite-granodiorite; magmatic emplacement occurred at a similar time to the SAG at 2198 ± 2 Ma (Pb-Pb zircon data; Gueye et al., 2007). To the south east of the Badon batholith, the Mako belt was intruded by the Soukouta granite-granodiorite complex at 2142 ± 7 Ma (U-Pb zircon; Delor et al., 2010). Delor et al., (2010) and Goujou et al., (2010) dated (U-Pb zircon) a series of granitic plutons, which intruded the MVB between 2142 ±7 Ma and 2102 ±8 Ma. The minor Mamakono and Tinkoto plutons intruded the MVB at 2076 ± 3 Ma and 2074 ± 5 Ma, respectively (U-Pb and Pb-Pb zircon data; Hirdes and Davis, 2002; Gueye et al., 2007). Ar-Ar and K-Ar studies on hornblende by Gueye et al. (2007) showed that the SAG and Tinkoto plutons cooled to ~550 °C by 2112 ± 12 Ma and 2051 ± 16 Ma, respectively. The Badon batholith cooled to below ~300°C at 2098 ± 20 Ma (Ar-Ar and K-Ar in biotite; Gueye et al., 2007).

### 3.2 The Dialé-Daléma series

Cropping out to the east of the MVB, the Dialé-Daléma series consists of a thick sequence of isoclinally folded volcanoclastic, siliciclastic and minor carbonate rocks centrally intruded by the Saraya Batholith (Hirdes and Davis, 2002; Gueye et al., 2008; Figure 1). The dominant volcanoclastic component of the Dialé-Daléma sediments suggests that they represent a lateral facies equivalent of the MVB. Subordinate basalts are interbedded in the westernmost sequence (Diallo, 2001), where the youngest detrital zircons yield a maximum U-Pb age of 2165 ± 0.9 Ma (Hirdes and Davis, 2002). The Saraya batholith consists of several plutonic bodies, composed of biotite-muscovite-adamellite granite. These bodies were emplaced between

ACCEPTED MANUSCRIPT

2079 ± 2 Ma and 2061 ± 15 Ma (U-Pb zircon and monazite) and place a lower limit on sedimentation in the Dialé-Dalemé Basin (Hirdes and Davis, 2002; Delor et al., 2010).

### 3.3 The Falémé Volcanic Belt

The Falémé Volcanic Belt crops out to the east of the Daléma basin (Hirdes and Davis, 2002; Lawrence et al., 2103a). The FVB is a ~16 km wide NNE trending belt of volcanic and intrusive rocks. Outcrop is dominated by plutonic rocks, consisting of two plutonic complexes, each >100 $km^2$: 1) the Balangouma pluton in the north; and 2) the Boboti pluton in the centre and south of the belt. Several smaller plutons crop out in the southern and eastern regions of the FVB, including the South Falémé (Hirdes and Davis, 2002) and Garaboureya plutons (Figure 2). The volcanic sequences comprise pillowed andesite flows, subordinate rhyodacite lavas and pyroclastic rocks. These are interbedded with volcanoclastic rocks, wackes and carbonate rocks (Hirdes and Davis, 2002; Schwartz and Melcher, 2004). Magnetite skarn deposits are hosted in several of the smaller plutons and carbonate rocks (Schwartz and Melcher, 2004). Limited age data are available for the volcanic sequence in the FVB. U-Pb zircon ages date a several volcanic and sub-volcanic rhyolite units at 2099 ± 4 Ma, 2082 ± 8 Ma and 2064 ± 30 Ma, with inheritance at 2155 ± 34 Ma (Hirdes and Davis, 2002). Further U-Pb zircon geochronological data from the Boboti pluton and the South Falémé tonalite show ages of 2080.2 ± 0.9 Ma and 2081.5 ± 1.1 Ma, respectively (Hirdes and Davis, 2002).

### 3.4 The Kofi Series

The Senegal-Mali Shear Zone (SMSZ) is a sinistral brittle-ductile shear zone that forms a 1-10 km wide N-S trending corridor of varying deformation styles, and separates the Kofi Series from the FVB. Secondary and higher order splays off the SMSZ host the major Au deposits in the Kofi Series, including Gara, Yalea, Sadiola, Yatela and Gounkoto (Dommanget, et al., 1993; Lawrence et al., 2013a and b). The Kofi Basin is made up of detrital sedimentary and carbonate rocks and breccias intruded by minor mafic dykes and small intermediate to felsic stocks. The sedimentary rocks in the Kofi Series are dominantly wackes, with end member sandstone (rare) and argillite (common). Wackes and argillites are typically interbedded on a small scale (10s cm), although both rock types occur as thicker units (10s m), with gradational changes from quartz



Accepted Manuscript

ACCEPTED MANUSCRIPT

wacke through to argillite common. The siliciclastic component of wackes varies between quartz and feldspar rich, with clasts showing a large range in size (fine sand to pebbles) and shape (angular to well rounded). Certain packages of quartz wacke, particularly in the west of the series have been intensely tourmalinised (Lawrence et al., 2013a), while others have been albitised. The Kofi Series is carbonate-rich to the west, with proximity to the Falémé Volcanic Belt (Figure 1). These carbonate rocks are dominantly dolomitic marls. Silicic clasts are composed of fine grained and sub angular quartz and feldspar. All sedimentary lithologies in the Kofi Series show poly-phase deformation generated during the Eburnean orogeny (Dabo and Aïfa, 2010). The igneous rocks that intruded the Kofi Series include dolerite to monzodiorite dykes and small stocks of quartz feldspar porphyry. Two larger plutons of monzogranite composition also intruded the Kofi Series, namely the Gamaye and Yatea plutons.

The age of deposition in the Kofi Series is constrained by detrital zircons and intrusive plutonic rocks. Tourmalinized quartz wacke at the Gara deposit include a detrital zircon dated by Pb-Pb at 2093 ± 7 Ma (Boher et al., 1992). An older, deltaic deposit on the margin of the FVB yields a U-Pb detrital zircon age of 2125 ± 27 Ma (Boher et al., 1992), though it is unclear whether this belongs to the Kofi Series or the FVB. The Gamaye pluton has been dated at 2045 ± 27 Ma using the Rb-Sr whole-rock isochron method, providing a broad lower age limit for sedimentation (Bassot and Cean-Vachette, 1984).

## 4 Methods

### 4.1 Mineral chemistry and petrography

Major and trace-element mineral compositions were determined using an Oxford Instruments X-ACT Energy Dispersive System (EDS) detector mounted on a Zeiss EVO 50 Scanning Electron Microscope (SEM) at Kingston University London. EDS operation employed an accelerating voltage of 20 kV, a beam current of 1.5 na, and a detector process time of 4. Data collection and reduction was handled using the Oxford Instruments INCA analytical suite. The detection limit for all elements was approximately 0.20 wt %.



Accepted Manuscript

ACCEPTED MANUSCRIPT

### 4.2 Geochemistry

Geochemical sample preparation and analyses were conducted at Kingston University. Rock pulps were desiccated overnight at 60 °C, then tested for loss on ignition (LOI) at 900 °C. 0.25 g of each sample was mixed with 1.25 g of lithium metaborate ($LiBO_2$) flux and fused in graphite crucibles at 1050 °C. The melt was then dissolved in 150 ml of 0.5M nitric acid ($HNO_3$), filtered, and diluted to a concentration of 0.3M $HNO_3$.

Analysis of major elements was conducted using a JY Ultima 2C inductively coupled plasma atomic emission spectrometer (ICP-AES). Standard reference materials: GSJ JR2 (rhyolite), USGS BCR-2 (basalt), USGS AVG-2 (andesite) and USGS BHVO-2 (basalt), were prepared and run as unknowns to monitor accuracy and precision. Measured values were within 3 % of the recommended values and the precision was better than 3 % (1 SD). USGS W-2 (Centerville diabase) was analysed every five samples to monitor instrumental drift.

Analysis of trace and rare earth elements (REEs) employed an Agilent 7500c quadrupole inductively coupled plasma mass spectrometer (ICP-MS). Samples, standards and blanks were prepared as above, and then diluted x25 in 0.5 % HCl and 1 % $HNO_3$. Instrumental drift was monitored by regular analysis of a 10 ppb multi-element solution. Accuracy and precision were determined from analysis of the standard reference materials: USGS AGV-2, GSJ JR-2, USGS BHVO-2, USGS BCR-2, GSJ JP-1, GSJ JA-2, TDB, WMG-1, GH, BR, Bt-Mica-Fe and Phl-Mica-Mg. Total accuracy was <3 % and precision was <4% (1SD).

### 4.3 Geochronology

Laser ablation inductively coupled mass spectrometry (LA-ICP-MS) was conducted on magmatic zircons from four samples of the Falémé Volcanic Belt. Zircons were separated using conventional methods at Kingston University. Zircons were mounted in 25 mm epoxy resin blocks, polished, and examined under SEM-CL to identify internal zonation and mineral inclusions.

LA-ICP-MS analysis was conducted at the Department of Earth Sciences, Royal Holloway University of London using a 193 nm excimer laser-ablation system featuring a two-volume Laurin LA cell coupled to an



Accepted Manuscript

ACCEPTED MANUSCRIPT

Agilent 7500ce quadrupole ICP-MS (Müller et al., 2009) (Table 2). Using GeoStar software, ~150 spots analysis points of both unknowns (~100) and reference materials (standards; ~50) were selected, which comprise one 'run'. The primary standard GJ-1 (600.7 Ma, based on Jackson et al., 2004) was analysed every seventh analysis to monitor both downhole as well as long-term elemental fractionation. Acquisition time was 30 seconds per spot with 15 seconds background before and after, pulse rate was 5 Hz, spot size was 34 µm and laser fluence on target (energy density) was 3 J/cm$^2$. The standards Temora-2 (416.78 ± 0.33Ma; Black et al., 2004), 91500 (1065.4 ± 0.3 Ma; Wiedenbeck et al., 1995), Mud Tank (732 ± 5 Ma; Black and Gulson, 1978) and Plešovice (337.13 ± 0.37 Ma; Sláma et al., 2008) were analysed as unknowns in order to ensure accuracy and reproducibility. Reduction of raw analytical data was performed using the Iolite software package® (Paton et al., 2010) in Wavemetrics Igor Pro® by applying exponential downhole fractionation and long-term spline data derived from the primary standard to both unknowns and secondary standards; no common-Pb correction was required. Approximate U, Th, Pb concentrations and Th/U-ratios are based on using the generally fewer 91500 analyses as calibration standard. Isochron diagrams, concordia, discordia and weighted mean U-Pb and Pb-Pb ages were calculated using the Isoplot 4.15 Excel macro (Ludwig, 2003).

Analyses of four international zircon standards were conducted to assess the accuracy and precision of the instrument. Thirty seven analyses of Plešovice yielded a concordant age of 336.1 ± 1.4Ma (MSWD=0.73); this gives an error of 0.3 % and precisionof 0.8 % (2 SD). Twenty nine analyses of the 91500 standard yielded a concordant age of 1053.8 ± 8.7 Ma (MSWD=0.9); this gives an error of 1.1 % and precision of 1.7 % (2 SD). Seventeen analyses of Temora-2 yielded a weighted average age of 410.7 ± 2.6 Ma (MSWD=1.2), with error of 1.5 % and precision of 1.3 % (2 SD). Mud Tank yielded a concordant age of 715 ± 11 Ma (MSWD=0.74); with error of 2.3 % and precision of 3.1 % (2 SD). Low U concentration in Mud Tank may contribute to higher error and uncertainty. The unknowns contained significantly higher concentrations of U; therefore Mud Tank can be disregarded when calculating accuracy and precision. Long-term reproducibility of $^{238}U/^{206}Pb$ ages based on Plesovice and 91500 zircons is ± 1.5 % (2 RSD). Analytical data for zircon satndards is presented in Table 3.



Accepted Manuscript

ACCEPTED MANUSCRIPT

# 5 Petrographic data

## 5.1 The Falémé Volcanic Rocks

The earliest volcanism in the FVB is recorded by fine-grained porphyritic andesites that crop out in the Kabe West area, south of the Balangouma pluton. These plagioclase-amphibole porphyries contain abundant euhedral albite (15 %) and amphibole (15 %) phenocrysts (0.5-2 mm). The groundmass is made up of finer, bladed albite (60 %) with minor anhedral quartz (5 %). Albite is strongly sericitised (5 %) and amphibole is replaced by actinolite. Along the eastern margin of the Boboti pluton, porphyritic and equigranular andesite overlies albitised sub-volcanic diorite (Figure 3A). The andesites contain albite phenocrysts (10 %) and a groundmass of albite (65 %) and actinolite (25 %), with accessory rutile, ilmenite, apatite and zircon. The diorite is equigranular, medium to coarse-grained and richer in amphibole (35 %) and rutile than the andesite.

## 5.2 The Daléma Suite

This small suite of intrusive and extrusive rocks crop out over ~3 $km^2$ on the eastern margin of the Dialé-Daléma basin, west of the Balangouma pluton. In this location, a fine-grained porphyritic basaltic-andesite (Figure 3B) contains phenocrysts of plagioclase (10 %), olivine (10 %) and trace clinopyroxene. Plagioclase is dominant and occurs as 0.5 to 3 mm laths and rare coarse tabular crystals. Olivine is fine to medium grained and subhedral, with embayments and inclusions of the groundmass common. The groundmass (75 %) is very fine and contains a high proportion of magnetite (5 %), with plagioclase, olivine and accessory pyrite. To the north, a phaneritic gabbroic diorite (Figure 3C) contains phenocrysts of oligoclase (50 %) ($An_{23}$) (up to 7 mm), magnesio-hornblende and tschermakite (35 %) (Both ~1.5 cm). These are replaced by biotite (10 %) and minor chlorite with associated ilmenite and titanite. Minor quartz and K-feldspar (~5 %) occur in the groundmass, with allanite, chalcopyrite, apatite, pyrite, gypsum and zircon. In the same locality, a gabbroic diorite porphyry (Figure 3D) contains 1-6 mm, subhedral phenocrysts of oligoclase (10 %), biotite (5 %) and actinolite (5 %). The groundmass is composed of oligoclase (32 %) ($An_{22}$), biotite (5 %), amphibole (40 %) and quartz (2-3 %), with minor clinopyroxene, K-feldspar, zircon and apatite.



Accepted Manuscript

ACCEPTED MANUSCRIPT

## 5.3 The Balangouma Pluton

The Balangouma pluton occupies the majority (~200 $km^2$) of the northern FVB and is composed of intermediate to felsic lithologies. The northern lobe of the pluton crops out to the north west of the Gara mine has been sheared out along the SMSZ. The main unit varies slightly in composition between monzodiorite, monzonite, quartz monzonite and granodiorite, but the bulk of the pluton is a coarse-grained, mesocratic quartz monzodiorite (Figure 3E). This contains coarse (5-7 mm) K-feldspar (2 %) and ~1 mm oligoclase (5 %) ($An_{26}$) phenocrysts. These minerals are also present in the medium grained groundmass (13 % and 25 %, respectively) together with biotite (26 %), quartz (9 %), augite (5 %) ($Wo_{30}En_{40}Fs_{30}$) and hornblende (5 %). Pyroxenes and amphiboles are partially chloritised (10 %). Accessory phases include apatite, titanite, zircon and Cr-rich haematite. This unit is cross cut by 20-30 cm wide aplite dykes (Figure 3G) composed of medium grained intergrown plagioclase (10 %), K-feldspar (35 %) and quartz (50 %). Fine-grained (<100 μm) biotite (2 %) emphasises a weak shear fabric. Similar units crop out throughout the pluton as meter-scale stocks.

## 5.4 The Boboti Pluton

The Boboti pluton (~187 $km^2$) makes up the central intrusive complex of the FVB. Schwartz and Melcher, (2004) and Dioh et al., (2006) describe the Boboti pluton as a clinopyroxene-hornblende-bearing granodiorite. Field mapping and sampling from outcrop in the southern Boboti pluton has revealed it to be more complex and composed of a number of intermediate to felsic intrusive stocks. Lithologies range in composition from diorite to monzogranite.

The southern body of the pluton is a coarse porphyritic quartz monzodiorite with 7-8 mm phenocrysts of albite (5 %), and ~2 mm phenocrysts of biotite and pyroxene (1 %) (Figure 4A). The groundmass is composed of sericitized albite (35 %), K-feldspar (25 %), quartz (10 %), clino- and orthopyroxene (10 %), biotite (9 %) and actinolite (3 %). Pyroxenes have been largely replaced by titanite (1 %) and V-Cr-bearing magnetite (1 %). Accessory phases include apatite, ilmenite, chalcopyrite, monazite and zircon. Minor bodies of monzogranite (Figure 4B), ~1-2 $km^2$ in extent, intruded the centre of the southern Boboti pluton. These are



Accepted Manuscript

ACCEPTED MANUSCRIPT

equigranular (400 - 600 µm) with rare 2-3 mm plagioclase phenocrysts. Quartz (31 %), albite (32 %) and K-feldspar (29 %) make up the groundmass, with minor intergrown muscovite (1 %) and biotite (1 %). Unevenly distributed clusters of <100 µm euhedral tourmaline (1 %) grains are present throughout the rock. Accessory minerals include epidote, ilmenite, zircon, apatite and titanite. Extensive outcrops of porphyritic pyroxene-bearing quartz diorite (Figure 4C) occur to the west (Sample BOP4 in Figure 2). This is medium to coarse-grained with 4 mm albite phenocrysts (7 %), with finer biotite (1 %) and actinolite phenocrysts (<1 %). The groundmass is composed of albite (70 %), quartz (5 %), clino- and orthopyroxene (6 %), biotite (4 %), actinolite (2 %) and K-feldspar (1 %). Pyroxene grains contain abundant inclusions of titanite (2 %) and magnetite (1 %). Accessory phases include apatite, chalcopyrite, monazite and zircon.

### 5.5 Minor Falémé Intrusive rocks

To the south of the Balangouma pluton several small plutons crop out just north of the Kouroudiako magnetite skarn deposit in the Kabe West target area (Figures 2, 4D and 4E). These consist of medium to coarse-grained quartz diorite with minor carbonate-chlorite-epidote alteration and magnetite-pyrite mineralisation. Phenocrysts of plagioclase (1-6 mm) and actinolite (~1 mm) occur within a fine to medium grained groundmass of plagioclase, K-feldspar, quartz, biotite and minor orthopyroxene. To the west, several medium-grained dioritic plutons host a magnetite skarn deposit at Karakaene Ndi. These have a hiatal seriate texture, with medium to coarse-grained albite, biotite, actinolite and quartz in the groundmass. Biotite and actinolite replace primary hornblende. All the diorite plutons in this area have been albitised (feldspars have been altered to albite), with the characteristic assemblage of carbonate-chlorite-haematite in the groundmass.

The south Falémé pluton, south east of the Boboti pluton, is exposed along the Falémé River. It consists of albitised diorites, magmatic breccias, and a small suite of diorites. Fine-grained diorite porphyry contains phenocrysts of coarse euhedral albite (~1 cm) and medium-grained, subhedral actinolite. The groundmass comprises plagioclase and actinolite with accessory rutile.



Accepted Manuscript

ACCEPTED MANUSCRIPT

## 5.6 Igneous rocks of the Kofi Series

### *5.6.1 The Yatea granite and North Gara stock*

The Yatea granite, which crops out in the east of the Kofi Series, is of similar affinity to a small stock which crops out just north of the Gara mine. Both bodies are pink coloured, medium-grained (1-3 mm) monzogranite (Figure 4F). Orthoclase and microcline (45 %) are dominant over plagioclase (up to 25 %). The mafic assemblage is dominated by biotite (<10 %). Accessory phases include magnetite, monazite and titanite.

### *5.6.2 The Gamaye pluton*

The Gamaye pluton is the largest igneous body exposed in the Kofi Series (~138 $km^2$). It is composed of monzogranite (Figure 4G), which is porphyritic in the south and equigranular in the north. The pluton is cross-cut by tourmaline bearing pegmatite dykes. The northern part of the pluton is composed of phaneritic monzogranite. The mineralogy consists of medium grained (200 - 500 µm), subhedral albite (35 %), K-feldspar (30 %), quartz (27 %) and biotite (8 %). Accessory minerals include muscovite, allanite and apatite (200 - 400 µm), zircon, rutile and magnetite. Tourmaline is disseminated in 1-5 cm halos around pegmatite dykes. Feldspars are weakly sericitized. This unit becomes porphyritic ~15 km to the SE (MOU2; Figure 2). K-feldspar forms subhedral poikilitic phenocrysts (up to 7 mm), and contains inclusions of quartz, plagioclase and biotite. Sub-rounded, 1 to 15 cm mafic enclaves are present throughout the unit. A series of coarse-grained pegmatite dykes cross cut the pluton. These are 1-30 cm wide and composed of 10-15 mm albite, quartz and K-feldspar, and ~200 µm muscovite. Some dykes contain very coarse (up to 8 mm) tourmaline crystals. These are typically subhedral, with inclusions of quartz and apatite. Thin (1-2 mm) tourmaline veins cross cut the dykes.

### *5.6.3 Minor intrusive rocks in the Kofi Series*

The Kofi Series is intruded by numerous discordant dykes (typically <5 m) and small (sub-km scale) plutons. Some units are extremely fine-grained. These minor igneous units are typically intermediate, diorite



Accepted Manuscript

ACCEPTED MANUSCRIPT

361 to quartz monzodiorite in composition, though mafic dykes are also present. Many lithologies have been
362 albitised to variable degrees.

363 Small stocks of biotite-quartz-feldspar porphyry (QFP; Figure 4H) occur in the vicinity of the Gamaye
364 pluton. Quartz (16 %), plagioclase (16 %) and K-feldspar (2 %) phenocrysts are up to 8 mm, while biotite
365 phenocrysts (6 %) measure ~1 mm. The groundmass (~60 % of the rock) is composed of <20 µm mineral
366 phases (likely quartz, plagioclase, k-feldspar and biotite). Feldspars show weak to moderate sericite
367 alteration. Intensely albitised QFP stocks occur near the Baqata and Kolya target areas (Figure 2). These
368 contain coarse (up to 7 mm) relict phenocrysts of quartz and feldspar, the latter having been replaced by
369 glomeroblastic albite. The groundmass is composed of secondary <100 µm albite with interstitial ankerite
370 and very fine –grained haematite. Albite is weakly sericitized.

371 Medium to coarse grained quartz monzodiorite dykes have intruded the footwall of the Gounkoto
372 deposit. These contain phenocrysts of plagioclase (5 %) and amphibole (replaced by actinolite) in a
373 groundmass of plagioclase (60 %), k-feldspar (5 %), quartz (10 %), actinolite (10 %) and biotite (10 %).
374 Accessory phases include augite (primary), apatite, tourmaline, ilmenite, rutile, monazite and chromite. In
375 addition, dykes of medium grained diorite occur throughout the Kofi Series. The mineralogy consists of
376 plagioclase (75 %), biotite (20 %) and K-feldspar (5 %) with accessory rutile and pyrite. It is possible that
377 these were originally monzodiorite dykes which have undergone weak albitisation.

378 Mafic dykes 0.5 to 13 m wide have intruded the wall-rock at both the Gara and Yalea Au deposits. These
379 are discontinuous, deformed and metamorphosed, forming sharp contacts with the host sediments. The
380 intensity of alteration makes primary compositions difficult to identify.

381 *5.6.4 Hydrothermal albitite*

382 Albitite crops out primarily at two localities within the Kofi Series, one at Baqata on the Bambadji permit
383 and one 15 km to north, in the Falémé River, near Kolya. In outcrop the unit is massive and blocky, with no
384 definable sedimentary or igneous textures. The lithology is composed dominantly of equigranular albite (85-



Accepted Manuscript

ACCEPTED MANUSCRIPT

95 %) with accessory quartz, chlorite, apatite, rutile, allanite, zircon and biotite. Chlorite is associated with fractures cross cutting the groundmass. It is likely that this unit is the result of extreme alteration of an igneous protolith and therefore represents the most intense example of the sodic alteration seen in this region.

### *5.6.5 Post-Birimian dolerite dykes*

These dolerite dykes cross cut all lithologies in the KKI and show no clear evidence of deformation or hydrothermal alteration. These are more continuous than the Birimian dykes and vary in thickness from 2-200 m. Mineralogy consists of bytownite ($An_{71-79}$), clinopyroxene and rare orthopyroxene. Similar dykes elsewhere in the WAC belong to the 200 Ma Central Atlantic Magmatic Province (CAMP; Jessell et al., 2015) ± . Though some CAMP-aged dykes are no doubt present, the mafic dykes in the KKI are dominantly older. Mafic dyke swarms with ages of ~1350-1400 Ma are most abundant, but ages of ~900 Ma and 1150 Ma are also present (K-Ar whole-rock data; Delor et al., 2010).

## 6 Geochemistry

A total of 42 fresh (unaltered) and albitised whole-rock samples were analysed for major and trace element concentrations. Only samples with minimal weathered crust and hydrothermal alteration were selected for analysis, with the exception of 14 samples of albitised igneous rocks. These were included to investigate the geochemical characteristics of the regional sodic alteration. All trace element data has been normalized against Normal-Mid Ocean Ridge Basalt concentrations (N-MORB; data from Sun and McDonough, 1989). Whole rock geochemical data is summarised in tables 4, 5, 6 and 7.

The geochemical data from the FVB and Kofi Series show a suite of igneous rocks with high-K calc-alkaline affinities (Figure 5A and B) with compositions ranging from gabbroic through to granitic (Figure 6). The FVB is dominated by large plutons of intermediate composition, with metaluminous A/CNK values (mean = 0.8; Figure 7), relatively little REE fractionation (mean La/Lu = 22.3) and very minor Eu anomalies (Eu/Eu* = 0.9; Figure 8). The small suite of felsic stocks that intruded the Balangouma and Boboti plutons are



Accepted Manuscript

ACCEPTED MANUSCRIPT

409 more evolved ($SiO_2$ >73 %), with moderately fractionated REE patterns (mean La/Lu = 50), peraluminous
410 A/CNK values (mean =1.2) and more distinct negative Eu anomalies (mean Eu/Eu* = 0.6; Figure 8C). By
411 comparison to the FVB, the Kofi Series contains less exposure of igneous rock. These are dominantly highly
412 fractionated (mean La/Lu=113), peraluminous (mean A/CNK = 1.1) granites of similar affinity to the minor
413 felsic stocks of the FVB. Minor dykes and plutons of more intermediate compositions are largely albitised;
414 these exhibit metaluminous A/CNK values (mean of 0.99) and relatively little REE fractionation (La/Lu of
415 19.9). The rocks of the Daléma igneous suite form a separate group, consisting of unevolved gabbros and
416 dolerites with highly metaluminous A/NK and A/CNK values (Figure 7) and low La/Lu ratios (mean = 9.4).

417 All samples show enrichment in the light ion lithophile (LILE) elements, with granitic samples showing
418 considerably higher enrichment in both the Kofi Series and the FVB (Figure 8). All rocks from both terranes
419 show consistent negative Nb and Ta anomalies (Figure 8D to F). In addition, granitic rocks from the Falémé
420 Belt and Kofi Series show pronounced negative Ti and P anomalies (Figure 8F).

421 Albitised samples show consistently high $Na_2O$ concentrations (mean =7.8 wt. %), with correspondingly
422 low concentrations of most other major elements, most notably $K_2O$ (mean = 0.6 wt. %). As a result of this,
423 the albitised samples lie in the tholeiitic series of the $K_2O$ versus $SiO_2$ diagram (Figure 5A) and also
424 consistently plot above the alkaline-sub-alkaline divide on the TAS diagram (Figure 6); unaltered samples are
425 consistently of sub-alkali affinity. Use of the Th-Co diagram of Hastie et al. (2007) reveals that the albitised
426 samples should indeed belong to the calc-alkaline and high-K calc-alkaline series (Figure 5B), as do the
427 unaltered rocks of the eastern KKI. A/NK values in albitised rocks are significantly lower than in unaltered
428 rocks, yet A/CNK values are unperturbed (Figure 7). This reflects albitisation of both plagioclase (loss of $Ca^{2+}$)
429 and K-feldspar (loss of $K^+$), and likely replacement of other alkali-bearing mineral species (e.g. biotite).
430 Albitised rocks plot in the alkaline field of the TAS diagram as a direct result of Na metasomatism.

## 431 7 LA-ICP-MS U-Pb Zircon Geochronology



Accepted Manuscript

ACCEPTED MANUSCRIPT

## 7.1 Boboti Pluton

### *7.1.1 BOP1A*

Sample BOP1A was obtained from the Southern part of the Boboti pluton. This unit is a coarse quartz monzodiorite with albite, biotite and pyroxene phenocrysts (Figure 4A). A total of 71 zircon grains were analysed (84 spots in total). These were stubby, subhedral, fine-grained (<150 µm) and highly fractured. Growth zones revealed under SEM-CL are well developed in some grains and almost absent in others (Figure 9A, B, C and D). A systematic relationship between zonation, apparent age and the degree of discordance was not observed. Forty three analyses produced concordant ages within a 2σ error ellipse (Figure 10A); 19 of these were highly concordant (Figure 10B and C). The majority of the data (70 spots) formed a clear discordia trending toward the origin. This is interpreted to be caused by recent Pb-loss attributed to surface weathering. Analytical data for sample BOP1A is presented in Table 8.

A regression line fitted to the 70 concordant and discordant spots intersects the isochron at 2088.5 ± 8.5 Ma (MSWD=2.2), with a lower intercept around the origin (-5 Ma; Figure 10A). This corresponds well with a weighted average $^{206}Pb/^{238}U$ age from the 19 most concordant spots of 2093 ± 9.6 Ma (MSWD=1.6; Figure 10B) and a weighted average $^{207}Pb/^{206}Pb$ age of 2085 ± 11 Ma (MSWD=6.3; Figure 10C). In order to minimize the rejection of data points the upper discordia intercept of 2088.5 ± 8.5 Ma is interpreted to represent the age of magmatic emplacement.

In addition to the main population, 2 small grain populations show evidence for inheritance of older material at ~2200 Ma and 3000 Ma (Figure 11A and B). Two zircon grains 9 and 22 yield partially concordant (~99 %) $^{206}Pb/^{238}U$ ages at 2209 ± 34 Ma and 2215 ± 35 Ma respectively (Figure 9C and D). These yield a concordia age of 2226 ± 13 Ma (MSWD of 1.4; Figure 11A). CL imaging show bright cores with diffuse zonation surrounded by a dark 2-10 µm rim. Two grains (zircons 75 and 73; Figure 9E and F) yielded concordant $^{206}Pb/^{238}U$ ages at 3000 ± 120 and 3380 ± 160 Ma respectively (Figure 11B) and Pb-Pb ages of 2865 ± 84 Ma and 3152 ± 94 Ma. Both the Archaean aged grains are fractured and feature a luminescent,

ACCEPTED MANUSCRIPT

finely zoned core and with a dark rim (Figure 11B). These cores may be the inherited component, with the dark rim a later overgrowth related to magmatism at ~2 Ga.

These new data broadly agree with the published age of emplacement for the Boboti pluton at 2080.2 ± 0.9 Ma (Hirdes and Davies, 2002). However, our data show a more protracted period of emplacement with a more widely distributed age population and additional evidence of inheritance from early magmatism and possible Archaean material.

## 7.2 Balangouma Pluton

### *7.2.1 CLIB01*

Sample CLIB01 from the Balangouma pluton to the north west of the Loulo mine camp is a coarse grained, mesocratic quartz monzodiorite with coarse (5-7 mm) K-feldspar phenocrysts (Figure 3E). A total of 81 grains were analysed (94 spots in total). The majority of spots produced highly discordant ages. Grains were stubby, subhedral, fine-grained (<150 µm) and highly fractured (Figure 9G and H). As with sample BOP1A, growth zonation appears to bears no relationship to the age or concordance of the grains. Analyses of the cores and rims of zircons are also consistently within error of each other. Analytical data for sample CLIB01 is presented in Table 9.

A discordia line was fitted to a subset of 43 spots with an upper intercept of 2105.6 ± 9.8 Ma (MSWD=5.8) and a lower intercept at 28 ± 57 Ma (Figure 12A). The lower intercept near the origin implies that recent Pb-loss is responsible for the discordance. A weighted mean $^{207}Pb/^{206}Pb$ age of 2098 ± 6.3 Ma (MSWD=4.6; Figure 12B) corresponds well to the upper intercept age as does a weighted mean $^{206}Pb/^{238}U$ age calculated from the most concordant spots (n=7) of 2097 ± 25 Ma (MSWD=3.9; Figure 12C). The age of magmatic emplacement is best represented by the upper intercept of the discordia, with an age of 2105.6 ± 9.8 Ma. This sample showed no evidence of inheritance.

### *7.2.2 CLIB05*



Accepted Manuscript

ACCEPTED MANUSCRIPT

Sample CLIB05 was collected from the Balangouma pluton around 8.5 km south of CLIB01. This sample is a coarse grained quartz monzonite with K-feldspar phenocrysts (Figure 3F). A total of 69 zircon grains were analysed (81 spots in total). Grains were subhedral, fractured and fine grained (<150 μm). Examination under SEM-CL reveals fine concentric zonation in the majority of zircon grains (Figure 9I and J). Some grains show small, anhedral cores lacking zoning; spot analyses of these cores tend to yield discordant ages. Analytical data for sample CLIB05 is presented in Table 10.

A significant number of analysed spots produced highly discordant ages, generating a discordia with an upper intercept of 2118 ± 16 Ma (MSWD=2.3; n=43) and a lower intercept around 100 Ma (Figure 13A). A weighted average of the 13 most concordant $^{206}Pb/^{238}U$ ages yields a younger age of 2054 ± 24 Ma (MSWD=0.58; Figure 13B), however the weighted average for the equivalent $^{207}Pb/^{206}Pb$ ages gives an age of 2096.5 ± 9.3 Ma (MSWD=1.4; Figure 13C), which broadly agrees with the upper intercept of the discordia. This weighted average $^{207}Pb/^{206}Pb$ age remains relatively consistent even if a limited number of analyses are rejected, giving an average age of 2103 ± 20 Ma, though this does produce a very high MSWD of 26 (n=57; Figure 13D). On the basis of this broad agreement it seems likely that the upper discordia intercept age of 2118 ± 16 Ma represents the age of magmatic emplacement for this sample.

### *7.2.3 CLIB07*

Sample CLIB07 was collected from an outcrop approximately 1.2 km to the northwest of CLIB05 in the Balangouma pluton. The sample is a coarse porphyritic monzonite (Figure 3H). A total of 59 zircon grains were analysed (70 spots in total). Grains are euhedral, fine (<150 μm) and highly fractured with rare inclusions of apatite and quartz (Figure 9K and L). As with other samples, growth zonation shows no clear relationship to the age or concordance of spots. Where cores and rims have been analysed, $^{206}Pb/^{238}U$ ages are consistently within error of each other. Analytical data for sample CLIB07 is presented in Table 11.

The analyzed grains produced highly discordant ages for a large number of spots. A set of 56 spots form a discordia with an upper intercept at 2113 ± 15 Ma and a lower intercept at 76 Ma (MSWD=1.4; Figure 14A). This corresponds well to the weighted mean $^{207}Pb/^{206}Pb$ age for the same spots of 2102 ± 8.2 Ma

ACCEPTED MANUSCRIPT

(MSWD=7.3; Figure 14B). In addition the weighted mean of the $^{206}Pb/^{238}U$ ages of the 9 most concordant spots yields an age of 2086 ± 23 Ma (MSWD=0.27; Figure 14C). The upper discordia intercept is accepted as the most probable age for magmatic emplacement for this sample at 2113 ± 15 Ma. This is on the basis of the overlapping mean U-Pb and Pb-Pb ages and the minimal rejection of data points in order to construct a robust discordia. No evidence of inheritance was found in this sample.

Given that the overall reproducibility of our method is ±1.5 % (2 RSD), the three ages of emplacement for the Balangouma pluton are analytically indistinguishable. We therefore favour an unweighted mean age for each of these units (represented by CLIB01, 05 and 07) of 2112 ± 13 Ma.

# 8 Discussion

## 8.1 Tectonic setting of the KKI

The Falémé Volcanic Belt and the Kofi Series consist of high-K and uppermost calc-alkaline series volcanic and magmatic rocks with fractionated REE patterns, and immature, siliciclastic sedimentary rocks. This suggests an island arc or active continental margin setting, an interpretation further supported by persistent depletion in Nb-Ta relative to HFS elements (Figure 8). This phenomenon is attributed to magmas derived from partial melting of sub-arc mantle wedge. This is due to the insolubility of Nb and Ta in slab-derived aqueous fluids and strong partitioning into residual rutile (Brenan et al., 1994; Baier et al., 2008). Calc-alkaline volcanic and plutonic rocks in the MVB display similar LREE and LILE enrichment, and negative Nb anomalies (Boher et al., 1992; Dioh et al., 2006; Pawlig et al., 2006) suggesting a similar tectonic setting.

The least evolved rocks in the region belong to the Daléma Suite. The tectonic setting in which this unit formed is unclear; Nb-Ta depletion and high Th/La and positive Ce/Ce* inherited from subducted sediment (Plank, 2005; Hastie et al., 2013; Figure 15) all point to a volcanic arc environment. The Dy/Dy*-Dy/Yb diagram of Davidson et al. (2013; Figure16) is of use here as it can represent the shape of a REE pattern in a single point. This highlights the slight LREE-enriched MORB character in the Daléma samples. LILE



Accepted Manuscript

ACCEPTED MANUSCRIPT

527 enrichment and near-MORB HREE values (Figure 8) suggest a possible extensional (back-arc) setting. Back-
528 arc rocks commonly feature arc-like chemistries modified by an invading fertile mantle source below the
529 spreading centre (Taylor and Martinez, 2003).

530 The less evolved rocks, dominantly present in the FVB (typically silica oversaturated syeno-diorites),
531 show characteristics typical of volcanic arc granites (Figure 17). These include the predominance of
532 amphibole, biotite and pyroxene in ferromagnesian mineral assemblages, depleted medium to HREE (Figure
533 8; a function of amphibole fractionation) and metaluminous A/CNK (Figure 7; c.f. Pearce, 1996). Minor
534 negative P anomalies and enrichment in Zr and Hf compared to other HFS elements (Figure 8E), respectively
535 indicate minor apatite fractionation and zircon accumulation (Pearce et al., 1984). Th/La-Ce/Ce* ratios
536 (Hastie et al., 2013; Figure 16) indicate that the arc rocks in the eastern KKI contain a mix of slab derived
537 components. These are dominated by volcanic and continental detritus, with minor contribution from
538 hydrogenous Fe–Mn oxides linked to slow sedimentation rates.

539 The felsic rocks (granites *sensu stricto*) of the FVB and Kofi Series feature negative Eu, Ti and P
540 anomalies, not observed in the intermediate lithologies (Figure 8) and classify as syn-collision granites
541 (Figure 17). Negative Eu anomalism indicates that plagioclase fractionation took place under relatively
542 reduced conditions (increasing $Eu^{2+}/Eu^{3+}$) during magma evolution (Drake, 1975). Similarly, depletions in Ti
543 and P indicate fractionation of apatite and Ti oxides. The Dy/Dy*-Dy/Yb diagram (Figure 15) indicates that
544 felsic rock in the study area have incorporated significant amounts of sediment (Davidson et al., 2013).

545 Overall, the igneous rocks of the south-eastern KKI represent a volcanic arc, developed above a
546 subducting oceanic plate. This subsequently evolved into a collisional setting. The Dy/Dy*-Dy/Yb diagram
547 (Figure 15) adequately represents the evolution of the arc system, with the Daléma igneous rocks plotting in
548 the E-MORB field and the Balangouma pluton and some of the more intermediate intrusions in the Kofi
549 showing upper continental crust compositions. The bulk of the data sit along the trend of increasing
550 sediment incorporation, with the most felsic, peraluminous rocks showing the highest Dy/Yb values. The
551 Th/La-Ce/Ce* diagram (Figure 16) shows that the mantle wedge below the arc has a significant contribution



Accepted Manuscript

ACCEPTED MANUSCRIPT

552 of continental detritus and hydrogenous Fe–Mn oxides as well as minor volcanic detritus from the
553 downgoing slab.

554 The MVB differs significantly from the FVB, due to the presence of a lower sequence of tholeiitic igneous
555 rocks. It is generally agreed (Abouchami et al., 1990; Diallo, 2001), due to the presence of pillow lavas,
556 turbidite sequences, a lack of significantly older inherited material and consistently positive $\varepsilon_{Nd}t$ values (+4.9;
557 Ngom et al., 2009) that these tholeiites are juvenile. However, there is debate over specific tectonic setting
558 being attributed to either: 1) intra-plate oceanic plateau (Abouchami et al., 1990; Boher et al., 1992; Ngom
559 et al., 2009); or 2) an immature oceanic island arc (Sylvester and Attoh, 1992; Dia et al., 1997; Diallo, 2001;
560 Pawlig et al., 2006). Abouchami et al. (1990) and Boher et al. (1991) suggested an oceanic plateau setting
561 based on low Ti concentrations, LREE depletion and pronounced negative Ce anomalies, placing the MVB
562 tholeiites between MORB and island arc compositions. Sylvester and Attoh (1992) observed that the Mako
563 and other Birimian belts show petrogenetic similarities with modern island arcs. The granitic rocks (*sensu*
564 *lato*; >5 % quartz) in the MVB are characterised by persistent negative Nb-Ta anomalies and LILE enrichment
565 (Boher et al., 1992; Dioh et al., 2006; Pawlig et al., 2006). Dioh et al. (2006) reported that the majority of
566 calc-alkaline and high-K intrusive rocks in the MVB classify as volcanic arc granites. A small subset lies along
567 the divide between volcanic arc and syn-collisional granite, including granites (*sensu stricto*) from the
568 Kéniéba pluton. These share geochemical characteristics with syn-collisional granites in the FVB and Kofi
569 Series, including peraluminous A/CNK values (1.03-1.04), negative Eu anomalies (0.72-0.81) and high Dy/Yb
570 values (~3.2). These points suggest that, despite the absence of tholeiites in the FVB, plutonic rocks in the
571 western KKI developed in very similar tectonic settings to those in the east, evolving from juvenile volcanic
572 arc to a collisional setting.

573 ### 8.2 Geochronological framework for the Kédougou-Kéniéba Inlier

574 New U-Pb zircon age data presented here show that the Balangouma pluton crystallised at 2112 ± 13
575 Ma (Table 1; Figure 18). Additionally, evidence of inherited zircon cores from the ~2085 Ma Boboti pluton
576 (Hirdes and Davis, 2002 and this study), suggest an earlier phase of magmatism in the FVB at ca. 2226 ± 13



Accepted Manuscript

ACCEPTED MANUSCRIPT

577 Ma (Figure 18). This suggests the presence of underlying basement material which predates the SAG in the
578 Mako Belt at 2213 ± 3 Ma (Gueye et al., 2007).

579 In general, the intermediate to felsic rocks in the KKI are the younger units. They are also the most likely
580 to yield useable zircons for accurate and precise dating. The geochronological data presented here,
581 combined with existing data, allows the synthesis of a geochronological framework for the KKI. Much of the
582 available age data imply diachroneity, with the westernmost MVB containing the oldest units (the SAG and
583 Badon pluton; Figure 18); the FVB, sedimentary basins and silicic intrusive rocks are generally younger.
584 Inherited grains found in several units of the FVB indicate that volcanism may have occurred simultaneously
585 in both the Falémé and MVBs. The following sequence of events can be determined from the available data
586 (Figure 18):

587 1. The intrusion of the SAG and elements of the Badon pluton occurred between 2213 ± 3 Ma and 2194
588 ± 4 Ma (Dia et al., 1997; Gueye et al., 2007). The Mako tholeiitic lavas are assumed to be older.
589 However, it is possible that tholeiitic volcanism was cogenetic with emplacement of the SAG or
590 Badon pluton (Pawlig et al., 2006). Inherited zircon grains from the Boboti pluton imply
591 magmatism may have occurred at some time prior in the FVB at ~2226 Ma.

592 2. The SLPC intruded the Mako volcanics and the SAG between 2171 ± 9 Ma and 2158 ± 8 Ma (Dia et
593 al., 1997; Goujou et al., 2010) within the time frame for possible calc-alkaline magmatism in the
594 FVB at 2155 ± 34 Ma, based on inherited zircon grains from a rhyolite flow (Hirdes and Davis,
595 2002). Sedimentation began in the westernmost Dialé-Daléma basin at 2164.7 ± 0.9 Ma (Hirdes
596 and Davis, 2002), coinciding with andesitic volcanism at 2160 ± 16 Ma (Boher et al., 1992).

597 3. The southern portion of the MVB was intruded by the Soukouta granite at 2142 ± 7 Ma. The oldest
598 component of the LKPC was emplaced over 33 Ma, from 2138 ± 6 Ma to 2105 ± 8 Ma (Dia, 1988;
599 Dia et al., 1987). The latter stages of emplacement overlap with the main phase of magmatism in



Accepted Manuscript

ACCEPTED MANUSCRIPT

600 the FVB. The SAG cooled below 550 °C at 2112 ± 12 Ma (Gueye et al., 2007. Deltaic deposits
601 began to develop on the western margin of the Kofi basin at 2125 ± 27 Ma (Boher et al., 1992).

602 4. The Falémé plutonic rocks (including the Boboti, Balangouma and South Falémé plutons) were
603 emplaced into pre-existing volcanic and sedimentary units between 2112 ± 13 Ma and 2080 ±
604 0.9 Ma, coinciding with felsic volcanism at 2099 ± 4 Ma (Hirdes and Davis, 2002). During this
605 period (2103 to 2102 Ma), further granitic plutons intruded the northern MVB (Goujou et al.,
606 2010) and rhyodacite units erupt in the Dialé-Daléma Basin (2098 ± 13 Ma; Delor et al., 2010).
607 Sedimentation in the Kofi basin began at 2093 ± 7 Ma at the latest (Boher et al., 1992). A deltaic
608 deposit began developing at 2125 ± 27 Ma, as reported by (Boher et al., 1992); however it is
609 unclear if this deposit belongs to the Kofi Series or the Falémé Belt. In either case, it provides an
610 argument for syn-volcanic sedimentation.

611 5. The latter stages of magmatism in the FVB and MVB are broadly coincident. The youngest unit of the
612 LKPC (the Kaourou pluton) and the late calc-alkaline series plutons (Tinkoto and Mamakono) in
613 the MVB all crystallised between 2079 ± 6 Ma and 2074 ± 5 Ma (Dia et al., 1997; Hirdes and
614 Davis, 2002; Gueye et al., 2007). A period of felsic volcanism in the FVB between 2082 ± 8 Ma
615 and 2064 ± 30 Ma (Delor et al., 2010) coincided with calc-alkaline volcanism in the MVB at 2067
616 ± 12 Ma (Gueye et al., 2007) . The Tinkoto pluton cooled below 550 °C by 2051 ± 16 Ma (Gueye
617 et al., 2007). The Saraya batholith marks the youngest limit for the Dialé-Daléma basin at 2079 ±
618 2 Ma (Hirdes and Davis, 2002). Metamorphic monazites within the batholith formed at 2064 ± 4
619 Ma and the pluton is interpreted to have cooled below 350 °C by 2021 ± 11 Ma (Gueye et al.,
620 2007).

621 Sedimentation in the Kofi Series is considered to have ceased by 2045 ± 27 Ma; the best-known age of
622 crystallisation of the Gamaye pluton (Bassot and Cean-Vachette, 1984).The data summarised in Figure 18
623 suggest that the development of the volcano-sedimentary belts and sedimentary basins of the KKI occurred
624 broadly synchronously, with a suite of older units within the westernmost MVB likely representing the



Accepted Manuscript

ACCEPTED MANUSCRIPT

earliest development of upper crust in the region (Dia et al., 1997; Geuye et al., 2007). For the older units of the KKI, Gueye et al. (2007) reported prolonged cooling profiles; with K-Ar from amphibole and biotite apparently suggest that the plutons took ~80 Ma to cool from 900 to 550 °C and ~100 Ma to cool from 900 to 300 °C, respectively. Smaller, younger plutons such as the Tinkoto granodiorite yielded K-Ar in amphibole ages within error of the crystallisation age of 2079 ± 6 Ma. Assuming no disturbance of the K-Ar system, this suggests that the western KKI remained hot (~550°C) until ~2100 Ma. The early magmatism in the KKI (represented by the SAG, Badon granodiorite and SLPC) likely corresponds to the Eoeburnean/Eburnean I of Ghana (Allibone et al., 2002; de Kock et al., 2011) and the Tangaean of Burkina Faso (Tshibubudze et al., 2009; Hein, 2010). New inherited zircon data in the Boboti pluton, suggests that magmatism occurred at a similar time in the FVB (~2226 Ma).

Sedimentation coincides with the onset of calc-alkaline volcanism and magmatism in both volcanic belts, supporting derivation from erosion of the arcs (c.f. Roddaz et al., 2007). In general, the more evolved magmatic rocks (the Saraya batholith, Gamaye pluton and the minor felsic stocks in the FVB) post-date the intermediate lithologies, either absolutely (through dating) or based on field relationships. This reflects the temporal evolution of the magmatic systems in the KKI through the arc stage and into the Eburnean orogeny, when crustal thickening increased the amount of assimilation of crustal material during emplacement (Figure 15).

The Boboti pluton contained two zircon grains which were partially (~95 %) concordant at ~3.0 and 3.4 Ga respectively. Very little Archaean material has previously been reported in Birimian terranes. However, the Birimian is bounded by older Archaean domains, which may conceivably have been reworked during arc formation, basin opening and terrane accretion. The Leo-Man Rise, to the south of the KKI contains units between 3540 to 3050 Ma (Thiéblemont et al., 2004). Inherited material from the Boboti pluton fall within this age range. Begg et al., (2009) reported tomographic data which suggested the presence of reworked Archaean crust and subcontinental lithospheric mantle beneath large portions of the West Africa Craton. Such material may be reworked by melts generated in the lower crust or upper mantle. Alternatively, Lebrun



Accepted Manuscript

ACCEPTED MANUSCRIPT

et al. (2015) reported the presence of Archaean derived clasts of banded iron formation within the Birimian aged Kintinian conglomerates of the Siguiri Basin in Southern Mali. Similar detrital material could conceivably have been present in the country rocks in to which the Boboti pluton intruded. This material may then have been incorporated during emplacement. While two zircon grains cannot be considered statistically significant and contamination cannot be wholly ruled out, there may be scope for future investigation into possible crustal contamination from Archaean terranes.

### 8.3 Temporal constraints on tectonic setting

The igneous rocks of the KKI show some distinct variation in their trace, REE and major element chemistry, which cannot wholly be attributed to the affinity of their host terranes (i.e. belt versus basin-type plutons). As an example, the minor felsic stocks that intruded the Balangouma and Boboti plutons are distinctly more evolved than their hosts, with peraluminous A/CNK, fractionated REE patterns and distinct Eu anomalies. It is therefore necessary to examine these geochemical variations in a temporal rather than spatial context.

In Figure 19 several geochemical parameters have been plotted against absolute ages of plutons from across the KKI. The data show a distinct positive trend in Dy/Yb values with time indicating an increasing control on REE patterns by residual garnet in the magma source (Davidson et al., 2013). This indicates sufficient thickening of the lithosphere to allow garnet to become stable in the magma source region. The trend of decreasing Eu* with time reflects fractional crystallisation of Ca-plagioclase. Higher Nb/Zr and La/Sm reflect increasing HFSE and LREE enrichment, respectively. The positive trend in these two ratios represents increase in the concentration of incompatible elements as the magmas become more evolved and collision begins to take place (c.f. Draut and Clift, 2001). Rb content in magmas is increased by partial crustal melts, combined with further enhancement due to addition of a Rb-rich volatile component (Pearce et al., 1984; Pearce, 1996). Increase in the Rb content of igneous rocks in the KKI over time reflects the transition from volcanic arc to syn-collision magmatism (Figure 17A). The overall positive $\varepsilon_{Nd}$(2.1Ga) values may be explained by the juvenile nature of the newly formed Birimian crust (Abouchami et al., 1990; Boher



Accepted Manuscript

ACCEPTED MANUSCRIPT

et al., 1992; Pawlig et al., 2006; Ngom et al., 2009). However, $\varepsilon_{Nd}$(2.1Ga) data (from Boher et al., 1992; Pawlig et al., 2006) shows a general trend toward lower positive values, indicating a greater contribution of continental derived sediment with time (c.f. Draut and Clift, 2001). In addition, the time difference between Nd model ages (Boher et al., 1992; Pawlig et al., 2006) and absolute ages of crystallisation increases with time, suggesting that more evolved melts began to stall in the thickened crust (Brown and Rushmer, 2006).

While there are some anomalously evolved rocks present in the older Mako sequences, in general Figure 19 shows a trend with time towards more evolved magmas with a greater contribution of sediments. This represents thickening of the newly formed Birimian crust as the volcanic island arc became accreted and collisional magmatism set in.

### 8.4 Comparisons to other Birimian terranes

The majority of previous research has concluded that the growth of Birimian crust initially took place in an oceanic setting, with immature island arcs evolving to continental arcs through a process of subduction generated magmatism and terrane accretion (Sylvester and Attoh, 1992; Abouchami et al., 1990 and Boher et al., 1992; Salah et al., 1996; Dia et al., 1997; Pawlig et al., 2006; Baratoux et al., 2011; Tshibubudze et al., in press). Granitoid rocks in Cote D'Ivoire (Pouclet et al., 2006), Burkina Faso (Tapsoba et al., 2012), Niger (Salah et al., 1996) and Ghana (Sylvester and Attoh, 1992) all display geochemical characteristics consistent with those described in the KKI (REE fractionation and negative Nb-Ta, P, Ti and Eu anomalies). Many igneous units throughout the Birimian are described as tonalite–trondhjemite–granodiorite series (TTG; e.g. Soumaila et al., 2008; Vidal et al., 2009; de Kock et al., 2011; Baratoux et al., 2011; Tapsoba et al., 2012; Tshibubudze et al., in press). This is not the case for the plutonic rocks in the eastern KKI where tonalitic compositions result from widespread alkali metasomatism (Figure 5). As described in the MVB, the majority of Birimian volcanic belts feature a lower sequence of tholeiitic rocks (Abouchami et al., 1990; Sylvester and Attoh, 1992; Salah et al., 1996; Feybesse et al., 2006). These are entirely lacking in the FVB. The only truly mafic volcanic to sub-volcanic rocks observed in the south-eastern KKI are those of the Daléma suite. There is little to compare the Daléma igneous rocks to in the wider Craton, though Dampare (2008) reported a



Accepted Manuscript

ACCEPTED MANUSCRIPT

probable back-arc setting for tholeiitic basaltic andesite in the southern Ashanti Belt. Similarly, back-arc settings have been suggested for Birimian rocks in SW Niger (Soumaila et al., 2008) and in Cote Di'Ivoire (Vidal and Alric, 1994). This suggests that extensional arc settings are likely to have occurred elsewhere in the Baoulé-Mossi domain.

Though early volcanism in the KKI is not well constrained, inherited zircons in the MVB and FVB suggest that magmatism took place at ca. 2200 Ma related to coeval volcanism. This agrees with whole rock Sm-Nd ages of volcanic rocks in Ghana (2266 ± 2 to 2132 ± 3 Ma; Taylor et al., 1992; Davis et al., 1994; de Kock et al., 2011) as well as U-Pb zircon data from TTG suites in Burkina Faso (2203 ± 12 Ma and 2207 ± 38 Ma; Tshibubudze et al., in press) and in south western Niger (2174 ± 4 Ma; U-Pb zircon; Soumaila et al., 2008). Alternatively, these inherited zircons may represent basement material. Crystallisation ages of Pre-Birimian gneiss in the Oudalan-Gorouol belt in NE Burkina have been reported by Tshibubudze et al.,(2013) at 2253 ± 9 Ma to 2255 ± 26 Ma (U-Pb zircon). In addition, detrital zircons in micaschists from south western Niger indicate the presence of a calc-alkali protolith between 2273 and 2278 Ma (U-Pb ages; Soumaila et al., 2008).

In Ghana (Leube et al., 1990; Oberthür et al., 1998; Davis et al., 1994), Burkina Faso (Roddaz et al., 2007; Baratoux et al., 2011; Tshibubudze et al., in press) and the KKI (Hirdes and Davis, 2002), sedimentation and belt magmatism overlap , suggesting that the basins are lateral facies equivalents of the volcanic arcs. Crystallisation of the Badon batholith, SAG and SLPC occurred between 2200 and 2150 Ma, matching the age range of belt-type plutons in Ghana (White et al., 2014 and references therein) and Burkina Faso (Tshibubudze et al., in press). The two-phase Eburnean model applied elsewhere in the Birimian (Allibone et al., 2002; Tshibubudze et al., 2009; Hein, 2010; de Kock et al., 2011) is also applicable in the KKI. Two distinct peaks in magmatic zircon abundance occur at 2150 and 2075 Ma, the majority of age data for the KKI fall between these peaks and likely represent the main phase of Eburnean magmatism. An older peak around 2200 Ma may represent the pre-Eburnean event (Eoeburnean, Eburnean I, Tangaean) described in other Birimian terranes (Allibone et al., 2002; Tshibubudze et al., 2009; Hein, 2010; de Kock et al., 2011). With the

ACCEPTED MANUSCRIPT

724 exception of inherited zircons from the Boboti pluton, material of this age is entirely lacking in the area of
725 the south-eastern KKI studied. In

726 The general trend of increasingly felsic, peraluminous magmatism through time, as a result of crustal
727 thickening, seems common throughout the Birimian (e.g. Ama Salah et al., 1996; Perrouty et al., 2012;
728 Tapsoba et al., 2012).

729 ## 9 Conclusions

730 The igneous rocks that define the eastern KKI are dominantly of high-K calc-alkaline affinity. Though in
731 some units, this affinity is masked by albitisation. Nevertheless, use of the Th-Co diagram of Hastie et al.
732 (2007) shows that all igneous units, prior to albitisation, belonged to the high-K calc-alkaline series. Indeed,
733 the Falémé Volcanic Belt altogether lacks the tholeiitic igneous units common to other Birimian belts.

734 Fractionated REE patterns and ubiquitous negative Nb-Ta anomalies suggest a tectonic setting analogous
735 to modern volcanic arcs and active continental margins. Furthermore, changes in trace element ratios, Eu-
736 anomaly and $\varepsilon_{Nd}t$ over ~200 Ma (Figure 19) reveal the tectonic setting in the KKI to have evolved from a
737 volcanic arc environment to an active continental margin, with more peraluminous, granitic melts
738 developing as the crust thickened. The Daléma igneous rocks on the eastern margin of the Dialé-Daléma
739 basin are highly metaluminous and display limited LILE enrichment, with normalised HREE values close to
740 unity. These may have formed in an extensional back arc system.

741 New U-Pb zircon age data show that the Boboti and Balangouma plutons were emplaced at 2088.5 ± 8.5
742 Ma and 2112 ± 13 Ma, respectively. Zircons in the Boboti pluton showed evidence of inherited material from
743 2226 ± 13 Ma, ~3.0 and 3.4 Ga. The Palaeoproterozoic age coincides with the oldest dated units in the
744 Western Mako Belt, whereas the Archaean ages suggest the possible reworking of Archaean material either
745 within the detrital basins or at depth beneath the Birimian crust. The available data suggest that the south-
746 eastern KKI is one of the younger terranes in the wider Birimian, lacking any significant component (bar

ACCEPTED MANUSCRIPT

747 inherited material) that correlates to earlier Birimian events (>2150 Ma) either in the Mako Belt or in Ghana
748 and Burkina Faso.

749 ## Acknowledgements

750 The Authors wish to thank Randgold Resources for generously funding this research. Additional thanks
751 must go to technical staff at Kingston University and to Andrew Miles and Philip Bird who provided helpful
752 discussion while preparing the manuscript. Constructive reviews by L. Baratoux, K. Hein and the Editor J.
753 Miller are also gratefully acknowledged.

754 ## References

755 Abouchami, W., Boher, M., Michard, A. Albarede, F., 1990. A major 2.1 Ga event of mafic magmatism in
756 West Africa: an early stage of crustal accretion. Journal of Geophysical Research 95, 17605-17629.

757 Allibone, A., Teasdale, J., Cameron, G., Etheridge, M., Uttley, P., Soboh, A., Appiah-Kubi, J., Adanu, A.,
758 Arthur, R., Mamphey, J., Odoom, B., Zuta, J., Tsikata, A., Pataye, F. Famiyeh, S., 2002. Timing and structural
759 controls on gold mineralisation at the Bogoso gold mine, Ghana, West Africa. Economic Geology 97, 949-
760 969.

761 Baier, J., Audétat, A., Keppler, H., 2008. The origin of the negative niobium tantalum anomaly in
762 subduction zone magmas. Earth and Planetary Science Letters 267, 290-300.

763 Baratoux, L., Metelka, V., Naba, S., Jessell, M. W., Grégoire, M., Ganne, J., 2011. Juvenile

764 Paleoproterozoic crust evolution during the Eburnean orogeny (~ 2.2–2.0 Ga), western Burkina Faso.

765 Precambrian Research 191, 18-45.



Accepted Manuscript

ACCEPTED MANUSCRIPT

766 Bassot, J.P. and Caen-Vachette, M., 1984. Données géochronologiques et géochimiques nouvelles sur les
767 granitodes de l'Est du Sénégal: implications sur l'histoire geologique du Birrimien de cette région. In: Klerkx,
768 J. and Michot, J. (Eds.), African Geology. Tervuren, Belgium, pp. 196-209.

769 Bassot, J. P., Dommanget, A., 1986. Mise en évidence d'un accident majeur affectant le Protérozoïque
770 inférieur des confins Sénégalo-Maliens:new data on an important fault in lower Proterozoic on the borders
771 of Senegal and Mali, Comptes Rendus De l'Académie Des Sciences. Série 2, Mécanique, Physique, Chimie,
772 Sciences De l'Univers, Sciences De La Terre 302, 1101-1106.

773 Béziat, D., Bourges, F., Debat, P., Lompo, M., Martin, F. Tollon, F., 2000. A Palaeoproterozoic ultramafic-
774 mafic assemblage and associated volcanic rocks of the Boromo greenstone belt: fractionates originating
775 from island-arc volcanic in the West African Craton. Precambrian Research 101, 25-47.

776 Black, L. P., Gulson, B. L., 1978. The age of the mud tank carbonatite, strangways range, northern
777 territory. BMR Journal of Australian Geology and Geophysics 3, 227-232.

778 Black, L. P., Kamo, S. L., Allen, C. M., Davis, D. W., Aleinikoff, J. N., Valley, J. W., Mundil, R., Campbell, I.
779 H., Korsch, R. J., Williams, I. S. Foudoulis, C., 2004. Improved $^{206}Pb/^{238}U$ microprobe geochronology by the
780 monitoring of a trace-element-related matrix effect; SHRIMP, ID–TIMS, ELA–ICP–MS and oxygen isotope
781 documentation for a series of zircon standards. Chemical Geology 205, 115-140.

782 Boher, M., Abouchami, W., Michard, A., Albarede, F. Arndt, N.T., 1992. Crustal growth in West Africa at
783 2.1 Ga. Journal of Geophysical Research 97, 345-369.

784 Bonhomme, M., 1962. Contribution à l'ètude géochronologique de la plate-forme de l'Ouest africain.
785 Ph.D. Thesis, University of Clermont-Ferrand, France, 62 pp.

786 Brenan, J. M., Shaw, H. F., Phinney, D. L., Ryerson, F. J., 1994. Rutile-aqueous fluid partitioning of Nb, Ta,
787 Hf, Zr, U and Th: implications for high field strength element depletions in island-arc basalts. Earth and
788 Planetary Science Letters 128, 327-339.



Accepted Manuscript

ACCEPTED MANUSCRIPT

789 Brown, M., Rushmer, T., 2006. Evolution and differentiation of the continental crust. Cambridge
790 University Press, 564 p.

791 Dabo, M., Aïfa, T., 2010. Structural styles and tectonic evolution of the Kolia-Boboti sedimentary Basin,
792 Kédougou-Kéniéba inlier, eastern Senegal. Comptes Rendus Geoscience 342, 796-805.

793 Dampare, S. B., Shibata, T., Asiedu, D. K., Osae, S., Banoeng-Yakubo, B., 2008. Geochemistry of
794 Paleoproterozoic metavolcanic rocks from the southern Ashanti volcanic belt, Ghana: petrogenetic and
795 tectonic setting implications. Precambrian Research 162, 403-423.

796 Davidson, J., Turner, S., Plank, T., 2013. Dy/Dy*: variations arising from mantle sources and petrogenetic
797 processes. Journal of Petrology 54, 525-537.

798 Davis, D.W., Hirdes, W., Schaltegger, U. Nunoo, E.A., 1994. U-Pb age constraints on deposition and
799 provenance of Birimian and gold-bearing Tarkwaian sediments in Ghana, West Africa. Precambrian Research
800 67, 89-107.

801 De Kock, G. S., Armstrong, R. A., Siegfried, H. P., Thomas, E. 2011. Geochronology of the Birim
802 Supergroup of the West African craton in the Wa-Bolé region of west-central Ghana: Implications for the
803 stratigraphic framework. Journal of African Earth Sciences 59, 1-40.

804 Debat, P., Diallo, D. P., Ngom, P. M., Rollet, M., Seyler, M., 1984. La série de Mako dans ses parties
805 centrale et méridionale (Sénégal oriental, Afrique de l'Ouest). précisions sur l'évolution de la série
806 volcanosédimentaire et données géochimiques préliminaires sur les formations magmatiques post-
807 tectoniques', Journal of African Earth Sciences 2 , 71-79.

808 Delor, C., Couëffé, R., Goujou, J. C., Diallo, D. P., Théveniaut, H., Fullgraf, T., Ndiaye, P.M., Dioh, E., Blein
809 O., Barry, T.M.M., Le Métour, J., Martelet, G., Sergeev, S., Wemmer, K., 2010. Notice explicative de la carte
810 géologique à 1/200 000 du Sénégal, feuille Saraya-Kédougou Est. Ministère des Mines, de l'Industrie, de
811 l'Agro-Industrie et des PME, Direction des Mines et de la Géologie, Dakar.



Accepted Manuscript

ACCEPTED MANUSCRIPT

812 Dia, A., 1985. Le complexe plutonique de laminia: Un exemple d'associations acide - basique dans le
813 massif de granitoids de Kakadian (Sénégal est), 13th Colloquium of African Geology, Abstracts 13, 64.

814 Dia, A. 1988. Caractères et significations des complexes magmatiques et métamorphiques du secteur de
815 Sandikounda–Laminia (nord de la boutonnière de Kédougou, est Sénégal). un modèle géodynamique du
816 birimien de l'Afrique de l'Ouest, Unpublished PhD Thesis, University of Dakar, Sénégal, .

817 Dia, A., Van Schmus, W.R. Kröner, A., 1997. Isotopic constraints on the age and formation of a
818 Palaeoproterozoic volcanic arc complex in the Kédougou inlier, eastern Senegal, West Africa. Journal of
819 African Earth Sciences 24, 197-213.

820 Diallo, D.P., 2001. Le paléovolcanisme de la bordure occidentale de la boutonnierè de Kédougou,
821 Paléoprotérozoïque du Sénégal oriental: incidences géotectoniques. Journal of African Earth Sciences 32,
822 919-940.

823 Dioh, E., Béziat, D., Debat, P., Grégoire, M. Ngom, P.M., 2006. Diversity of the Palaeoproterozoic
824 granitoids of the Kédougou inlier (eastern Senegal): Petrographical and geochemical constraints. Journal of
825 African Earth Sciences 44, 351-371.

826 Dommanget, A., Milesi, J.P. Diallo, M., 1993. The Loulo gold and tourmaline-bearing deposit. Mineralium
827 Deposita 28, 253-263.

828 Drake, M. J., 1975. The oxidation state of europium as an indicator of oxygen fugacity. Geochimica et
829 Cosmochimica Acta 39, 55-64.

830 Draut, A. E., Clift, P. D. 2001. Geochemical evolution of arc magmatism during arc-continent collision,
831 South Mayo, Ireland. Geology 29, 543-546.

Accepted Manuscript

ACCEPTED MANUSCRIPT

Feybesse, J. Milési, J.P., 1994. The Archaean/Proterozoic contact zone in West Africa: a mountain belt of decollement thrusting and folding on a continental margin related to 2.1 Ga convergence of Archean cratons? Precambrian Research 69, 199-227.

Feybesse, J., Billa, M., Guerrot, C., Duguey, E., Lescuyer, J., Milési, J.P. Bouchot, V., 2006. The Palaeoproterozoic Ghanaian province: Geodynamic model and ore controls, including regional stress modelling. Precambrian Research 149, 149-196.

Ganne, J., De Andrade, V., Weinberg, R. F., Vidal, O., Dubacq, B., Kagambega, N., Naba, S., Baratoux, L., Jessell, M. Allibon, J., 2011. Modern-style plate subduction preserved in the Palaeoproterozoic West African craton. Nature geoscience 5, 60-65.

Goujou, J. C., Buscail, F., Théveniaut, H., Dioh, E., Delor, C., Blein, O., Diallo, D.P., Ndiaye, P.M., Le Métour, J., Fullgraf T., Caby, R., Couëffé, R., Martelet, G., Sergeev, S., Tegyey, M., Villeneuve, M., Wemmer, K., 2010. Notice explicative de la carte géologique à 1/200 000 du Sénégal, feuille Kossanto-Dalafi Est, 2010, Ministère des Mines, de l'Industrie, de l'Agro-Industrie et des PME. Direction des Mines et de la Géologie, Dakar.Gueye, M., Siegesmund, S., Wemmer, K., Pawlig, S., Drobe, M., Nolte, N. Layer, P., 2007. New evidence for an early Birimian evolution in the West African Craton: an example from the Kédougou-Kéniéba inlier, southeast Senegal. South African Journal of Geology 110, 511-534.

Gueye, M., Ngom, P.M., Diene, M., Thiam, Y., Siegesmund, S., Wemmer, K. Pawlig, S., 2008. Intrusive rocks and tectno-metamorphic evolution of the Mako Palaeoproterozoic belt (Eastern Senegal, West Africa). Journal of African Earth Sciences 50, 88-110.

Hastie, A. R., Kerr, A. C., Pearce, J. A., Mitchell, S. F., 2007. Classification of altered volcanic island arc rocks using immobile trace elements: development of the Th–Co discrimination diagram. Journal of Petrology 48, 2341-2357.

ACCEPTED MANUSCRIPT

854 Hastie, A. R., Mitchell, S. F., Treloar, P. J., Kerr, A. C., Neill, I., Barfod, D. N., 2013. Geochemical
855 components in a Cretaceous island arc: The Th/La–(Ce/Ce*)Nd diagram and implications for subduction
856 initiation in the inter-American region. Lithos 162, 57-69.

857 Hein, K. A., 2010. Succession of structural events in the Goren greenstone belt (Burkina Faso):
858 implications for West African tectonics. Journal of African Earth Sciences 56, 83-94.

859 Hirdes, W. Davis, D.W., 2002. U-Pb Geochronology of Palaeoproterozoic rocks in the southern part of the
860 Kédougou-Kéniéba inlier, Senegal, West Africa: evidence for diachronous accretionary development of the
861 Eburnean Province. Precambrian Research 118, 83-99.

862 Hirdes, W., Davis, D.W. Eisenlohr, B.N., 1992. Reassessment of Proterozoic granitoid ages in Ghana on
863 the basis of U/Pb zircon and monazite dating. Precambrian Research 56, 89-96.

864 Hirdes, W., Davis, D.W., Ludtke, G., Konan, G., 1996. Two generations of Birimian (Paleoproterozoic)
865 volcanic belts in northeastern Cote d'Ivoire (West Africa): consequences for the `Birimian controversy'.
866 Precambrian Research 80, 173-191.

867 Jackson, S.E., Pearson, N.J., Griffin, W.L., Belousova, E.A., 2004. The application of laser ablation-inductively
868 coupled plasma-mass spectrometry to in situ U-Pb zircon geochronology. Chemical Geology 211, 47-69.

869

870 John, T., Klemd, R., Hirdes, W. Loh, G., 1999. The metamorphic evolution of the Palaeoproterozoic
871 (Birimian) volcanic Ashanti belt (Ghana, West Africa). Precambrian Research 98, 11-30.

872 Junner, N.R., 1940. Geology of the Gold Coast and Western Togoland. Gold Coast Geological Survey
873 Bulletin 11, 1-40.

Accepted Manuscript

ACCEPTED MANUSCRIPT

874 Lawrence, D.M., Treloar P.J., Rankin, A.H., Harbidge, P., Holliday, J., 2013a The Geology and Mineralogy
875 of the Loulo Mining District, Mali, West Africa: Evidence for Two Distinct Styles of Orogenic Gold
876 Mineralization. Economic Geology 108, 199-227.

877 Lawrence, D.M., Treloar, P.J., Rankin, A.H., Boyce, A., Harbidge, P., 2013b, A fluid inclusion and stable
878 isotope study at the Loulo mining district, Mali, West Africa: Implications for multifluid sources in the
879 generation of orogenic gold deposits. Economic Geology 107, 229–257.

880 Le Maitre, R. W. 1989. A classification of igneous rocks and glossary of terms.Recommendations of the
881 International Union of Geological Sciences, Sub-commission on the Systematics of Igneous rocks: Oxford,
882 Blackwell.

883 Lebrun, E., Thébaud, N., Miller, J., Bourget, J., Ulrich, S., Terblanche, O., 2015. Geochronology and
884 lithostratigraphy of the Siguiri district: implications for gold mineralisation in the Siguiri Basin (Guinea, West
885 Africa). 13th SGA Biennial Meeting, Nacy, France, 1-4.Ledru, P., Pons, J., Milesi, J. P., Feybesse, J. L. Johan, V.,
886 1991. Transcurrent tectonics and polycyclic evolution in the lower Proterozoic of Senegal-Mali, Precambrian
887 Research 50, 337-354.

888 Leube, A., Hirdes, W., Mauer, R., Kesse, G.O. 1990. The early Proterozoic Birimian Supergroup of Ghana
889 and some aspects of its associated gold mineralisation. Precambrian Research 46, 139-165.

890 Loh, G., Hirdes, W., Anani, C., Davis, D.W., Vetter, U., 1999. Explanatory notes for the geological map of
891 Southwest Ghana 1: 100,000. Geologisches Jahrbuch B 93, 150.

892 Ludwig, K. R., 2003. User's manual for Isoplot 3.00: A geochronological toolkit for Microsoft Excel (No. 4).
893 Kenneth R. Ludwig, 76 .p

894 Maniar, P.D., Piccoli, P.M., 1989. Tectonic discrimination of granitoids. Geological Society of America
895 Bulletin 101, 635-643.



Accepted Manuscript

ACCEPTED MANUSCRIPT

Milési, J.P., Feybesse, J.L., Ledru, P., Dommanget, A., Ouedrago, M., Marcoux, E., Prost, A., Vinchon, C., Sylvain, J.P., Johan, V., Tegyey, M., Calvez, J.Y. Lagny, P., 1989. West African gold deposits in their Lower Proterozoic lithostructural setting. Chronique de la Recherche Miniere 497, 3-98.

Müller, W., Shelley, M., Miller, P., Broude, S., 2009. Initial performance metrics of a new custom-designed ArF excimer LA-ICPMS system coupled to a two-volume laser-ablation cell. Journal of Analytical Atomic Spectrometry 24, 209-214.

Ngom, P. M., Cordani, U. G., Teixeira, W. Janasi, V. A., 2009. Sr and nd isotopic geochemistry of the early ultramafic–mafic rocks of the Mako bimodal volcanic belt of the Kedougou-Kéniéba Inlier (Senegal). Arabian Journal of Geosciences 3 , 49-57.

Oberthür, T., Vetter, U., Davis, D.W. Amanor, J.A., 1998. Age constraints on gold mineralisation and Palaeoproterozoic crustal evolution in the Ashanti belt of southern Ghana. Precambrian Research 89, 129-143.

Parra-Avila, L. A., Belousova, E., Fiorentini, M. L., Baratoux, L., Davis, J., Miller, J., McCuaig, T. C., 2015. Crustal evolution of the Paleoproterozoic Birimian terranes of the Baoulé-Mossi domain, southern West African Craton: U–Pb and Hf-isotope studies of detrital zircons. Precambrian Research. doi:10.1016/j.precamres.2015.09.005.

Paton, C., Woodhead, J. D., Hellstrom, J. C., Hergt, J. M., Greig, A., Maas, R., 2010. Improved laser ablation U-Pb zircon geochronology through robust downhole fractionation correction. Geochemistry, Geophysics, Geosystems 11, Q0AA06, doi:10.1029/2009GC002618.

Pawlig, S., Gueye, M., Klisches, R., Schwarz, S., Wemmer, K. Siegesmund, S., 2006. Geochemical and Sr-Nd isotopic data on the Birimian of the Kédougou-Kéniéba Inlier (Eastern Senegal): Implications on the Palaeoproterozoic evolution of the West African Craton. South African Journal of Geology 109, 411-427.

Pearce, J. A., 1996. Sources and settings of granitic rocks. Episodes 19, 120-125.



Accepted Manuscript

ACCEPTED MANUSCRIPT

Pearce, J. A., 2008. Geochemical fingerprinting of oceanic basalts with applications to ophiolite classification and the search for Archean oceanic crust. Lithos 100, 14-48.

Pearce, J.A., Harris, N.B. Tindle, A.G., 1984. Trace element discrimination diagrams for the tectonic interpretation of granitic rocks. Journal of Petrology 25, 956-983.

Pearce, J. A., Peate, D. W., 1995. Tectonic implications of the composition of volcanic arc magmas. Annual Review of Earth and Planetary Sciences 23, 251-286.

Perrouty, S., Aillères, L., Jessell, M. W., Baratoux, L., Bourassa, Y., Crawford, B., 2012. Revised Eburnean geodynamic evolution of the gold-rich southern Ashanti Belt, Ghana, with new field and geophysical evidence of pre-Tarkwaian deformations. Precambrian Research 204, 12-39.

Plank, T., 2005. Constraints from thorium/lanthanum on sediment recycling at subduction zones and the evolution of the continents. Journal of Petrology 46, 921-944.

Pouclet, A., Doumbia, S. Vial, D.S., 2006. Geodynamic setting of the Birimian volcanism in central Ivory Coast (western Africa) and its place in the Palaeoproterozoic evolution of the Man Shield. Bulletin Societe Geologique de France 177, 105-121.

Rickwood, P.C.,1989. Boundary lines within petrologic diagrams which use oxides of major and minor elements. Lithos 22, 247-263.

Roddaz, M., Debat, P. Nikiéma, S., 2007. Geochemistry of Upper Birimian sediments (major and trace elements and Nd–Sr isotopes) and implications for weathering and tectonic setting of the Late Palaeoproterozoic crust. Precambrian Research 159, 197-211.

Salah, I. A., Liegeois, J. P., Pouclet, A., 1996. Evolution d'un arc insulaire océanique birimien précoce au Liptako nigérien (Sirba): géologie, géochronologie et géochimie. Journal of African Earth Sciences 22, 235-254.



Accepted Manuscript

ACCEPTED MANUSCRIPT

941 Schwartz, M.O. Melcher, F., 2004. The Falémé Iron District, Senegal. Economic Geology 99, 917-939.

942 Sláma, J., Košler, J., Condon, D. J., Crowley, J. L., Gerdes, A., Hanchar, J. M., Horstwood, M. S. A., Morris,
943 G. A., Nasdala, L., Norberg, N., Schaltegger, U., Schoene, B., Tubrett, M. N. Whitehouse, M. J., 2008.
944 Plešovice zircon—a new natural reference material for U–Pb and Hf isotopic microanalysis. Chemical
945 Geology 249, 1-35.

946 Soumaila, A., Henry, P., Garba, Z., Rossi, M., 2008. REE patterns, Nd-Sm and U-Pb ages of the
947 metamorphic rocks of the Diagorou-Darbani greenstone belt (Liptako, SW Niger): implication for Birimian
948 (Palaeoproterozoic) crustal genesis. Geological Society, London, Special Publications 297, 19-32.

949 Sun, S.S. Mcdonough,W. F., 1989. Chemical and isotope systematics of oceanic basalts: implications for
950 mantle composition and processes, in: SAUNDERS, A. D. and NORRY, M. J. (Eds.) Magmatism in the Ocean
951 Basins. Geological Society, London, Special Publications 42, 313-345.

952 Sylvester, P.J. Attoh, K., 1992. Lithostratigraphy and composition of 2.1 Ga greenstone belts of the West
953 African Craton and their bearing on crustal evolution and the Archean-Proterozoic boundary. Journal of
954 Geology 100, 377-393.

955 Tapsoba, B., Lo, C. H., Jahn, B. M., Chung, S. L., Wenmenga, U., Iizuka, Y., 2013. Chemical and Sr–Nd
956 isotopic compositions and zircon U–Pb ages of the Birimian granitoids from NE Burkina Faso, West African
957 Craton: Implications on the geodynamic setting and crustal evolution. Precambrian Research 224, 364-396.

958 Taylor, B., Martinez, F., 2003. Back-arc basin basalt systematics. Earth and Planetary Science Letters 210,
959 481-497.

960 Taylor, P.N., Moorbath, S., Leube, A. Hirdes, W., 1992. Early Proterozoic crustal evolution in the Birimian
961 of Ghana: constraints from geochronology and isotope geochemistry. Precambrian Research 56, 97-111.



Accepted Manuscript

ACCEPTED MANUSCRIPT

962 Thiéblemont, D., Goujou, J. C., Egal, E., Cocherie, A., Delor, C., Lafon, J. M., Fanning, C. M., 2004. Archean
963 evolution of the Leo Rise and its Eburnean reworking. Journal of African Earth Sciences 39, 97-104.

964 Treloar, P. J., Lawrence, D. M., Senghor, D., Boyce, A., Harbidge, P., 2014. The Massawa gold deposit,
965 Eastern Senegal, West Africa: an orogenic gold deposit sourced from magmatically derived fluids? Geological
966 Society, London, Special Publications 393, SP393-12.

967 Tshibubudze, A., Hein, K. A., Marquis, P., 2009. The Markoye Shear Zone in NE Burkina Faso. Journal of
968 African Earth Sciences 55, 245-256.Tshibubudze, A., Hein, K. A. A., Peters, L. F. H., Woolfe, A. J., McCuaig, T.
969 C., 2013. Oldest U-Pb crystallisation age for the West African craton from the Oudalan-Gorouol Belt of
970 Burkina Faso. South African Journal of Geology 116, 169-181.

971 Tshibubudze, A., Hein, K. A., McCuaig, T. C. (In Press). The relative and absolute chronology of strato-tectonic
972 events in the Gorom-Gorom granitoid terrane and Oudalan-Gorouol belt, northeast Burkina Faso. Journal
973 of African Earth Sciences.

974 Vidal, M. Alric, G., 1994. The Palaeoproterozoic (Birimian) of Haute-Comoé in the West African Craton,
975 Ivory Coast: a transtensional back-arc basin. Precambrian Research 65, 207-229.

976 Vidal, M., Gumiaux, C., Cagnard, F., Pouclet, A., Ouattara, G., Pichon, M., 2009. Evolution of a
977 Paleoproterozoic “weak type” orogeny in the West African Craton (Ivory Coast). Tectonophysics 477, 145-
978 159.

979 White, A., Burgess, R., Charnley, N., Selby, D., Whitehouse, M., Robb, L., Waters, D., 2014. Constraints on
980 the timing of late-Eburnean metamorphism, gold mineralisation and regional exhumation at Damang mine,
981 Ghana. Precambrian Research 243, 18-38.

982 Wiedenbeck, M., Hanchar, J. M., Peck, W. H., Sylvester, P., Valley, J., Whitehouse, M., Kronz, A.,
983 Morishita, Y., Nasdala, L., Fiebig, J., Franchi, I., Girard, J.-P., Greenwood, R.C., Hinton, R., Kita, N., Mason,
984 P.R.D., Norman, M., Ogasawara, M., Piccoli, P.M., Rhede, D., Satoh, H., Schulz-Dobrick, B., Skår, O., Spicuzza,



Accepted Manuscript

ACCEPTED MANUSCRIPT

985 Mj., Terada, K., Tindle, A., Togashi, S., Vennemann, T., Xie, Q. Zheng, Y.-F., 2004. Further Characterisation of
986 the 91500 Zircon Crystal. Geostandards and Geoanalytical Research 28, 9–39.

987 Figures

988 Figure 1. Geological map of the Kédougou-Kéniéba Inlier, including units of the Mako belt referred to in
989 the text (modified after Lawrence, 2010).

990 Figure 2. Detailed geology of the Falémé Volcanic Belt and Kofi Series, locations of whole-rock
991 geochemistry samples are indicated.

992 Figure 3. Hand specimen photographs of: A) medium grained diorite (BP31); B) porphyritic basaltic
993 andesite (CLIB08); C) phaneritic gabbroic diorite (CLIB09); D) coarse gabbroic diorite with biotite phenocrysts
994 (CLIB10); E) sheared quartz monzodiorite from near the sheared contact between the FVB and Kofi series
995 (CLIB01); F) a coarse grained quartz monzonite with K-feldspar phenocrysts (CLIB05); G) an aplite dyke
996 (CLIB06) that cross-cuts the Balangouma pluton; H) a coarse porphyritic monzonite (CLIB07).

997 Figure 4. Hand specimen photographs of: A) coarse porphyritic quartz monzodiorite (BOP1A); B)
998 porphyritic monzogranite (BOP2 and 3); C) porphyritic pyroxene-bearing quartz diorite (BOP4); D) hand
999 specimen of coarse grained quartz diorite (BO4); E) hand specimen of medium grained quartz diorite (BO5);
1000 F) pink, medium-grained monzogranite (PTG1); G) equigranular monzogranite (MAD01); H) biotite-quartz-
1001 feldspar porphyry (FDGI01).

1002 Figure 5. A) $K_2O$ versus Silica diagram (Rickwood, 1989) showing the plutonic and volcanic units of the
1003 eastern KKI, note the 'upper trend' represents unaltered samples of high-K calc-alkaline affinity and the
1004 'lower' calc-alkaline to tholeiitic trend represents albitised samples, see text for details; B) Th-Co
1005 discrimination diagram (Hastie et al., 2007) showing albitised and fresh samples plotting in the high-K and
1006 upper calc-alkaline series.



Accepted Manuscript

ACCEPTED MANUSCRIPT

Figure 6. Geochemical samples plotted on total alkali silica (TAS) classification diagram (after Le Maitre et al., 1989) showing lithology names for: A) intrusive-plutonic samples and B) extrusive (volcanic) from the FVB and Kofi Series.

Figure 7. A/NK versus A/CNK diagram (after Maniar and Piccoli, 1989) for igneous rocks from the eastern KKI. Albitised samples are highlighted in red, note that albitisation results in lower A/NK values due to increase in overall $N_2O$.

Figure 8. N-MORB normalised REE patterns for A) the Daléma Igneous rocks from the eastern margin of the Diale-Dalema Basin; B) the intermediate composition (diorite to granodiorite) igneous rocks of the FVB and Kofi Series (see key); C) the granitic rocks of the FVB and Kofi Series. N-MORB normalised trace element diagrams of for D) the Daléma Igneous rocks from the eastern margin of the Diale-Dalema Basin; E) the intermediate composition (diorite to granodiorite) igneous rocks of the FVB and Kofi Series (see key); F) the granitic rocks of the FVB and Kofi Series, note the consistent depletion of Nb-Ta compared to other HFSE. Albitised samples were excluded from multi-element plots (D, E and F) due to extreme perturbation of the trace element patterns.

Figure 9. Representative SEM-CL images of: A) and B) zircons from sample BOP1A of the Boboti Pluton; C) and D) zircons BOP1A-09 and BOP1A-22 from the Boboti pluton with U-Pb ages indicated inheritance at ~2200 Ma (BOP1A; ages given are from $^{206}Pb/^{238}U$); E) and F) zircons BOP1A-73 and BOP1A-75 with ablation spots marked; G) and H) zircons from sample CLIB01 of the Balangouma Pluton; I) and J) zircons from sample CLIB05 of the Balangouma Pluton K) and L) zircons from sample CLIB07 of the Balangouma Pluton

Figure 10. A) Concordia diagram showing discordia plotted from 70 concordant and discordant grains from sample BOP1A of the Boboti pluton, the discordia trends toward the origin and is likely a result of recent Pb-loss; B) Diagram of the weighted mean $^{206}Pb/^{238}U$ age of 19 concordant grains from BOP1A and; C) the weighted mean $^{207}Pb/^{206}Pb$ age of the same 19 grains from BOP1A.



Accepted Manuscript

ACCEPTED MANUSCRIPT

Figure 11. Evidence for inherited material in the Boboti pluton: A) two partially concordant grains at ~2230 Ma, corresponding to early volcanic activity in the Falémé Belt; B) two partially concordant Archaean U-Pb ages from zircons BOP1A-73 and BOP1A-75 in the Boboti pluton.

Figure 12. Diagrams of A) discordia plotted from 43 ablation spots in sample CLIB01 trending toward the origin indicating recent Pb-loss, age of intercept is indicated; B) weighted mean of $^{206}Pb/^{238}U$ ages from the 7 most concordant grains; C) weighted mean $^{207}Pb/^{206}Pb$ ages for 43 grains from CLIB01. Weighted mean ages and MSWD values are indicated.

Figure 13. Diagrams of A) discordia plot constructed from 43 concordant and discordant grains from sample CLIB05, upper intercept age is indicated; B) a weighted average of the 13 most concordant $^{206}Pb/^{238}U$ ages from CLIB05 yielding a younger age than the discordia intercept in A; C) a weighted average of the 13 equivalent $^{207}Pb/^{206}Pb$ ages; D) a weighted average of 57 $^{207}Pb/^{206}Pb$ ages with 9 outliers rejected.

Figure 14. Diagrams of A) discordia plotted from 56 discordant and concordant spots from CLIB07 with the upper intercept indicated; B) a weighted average $^{207}Pb/^{206}Pb$ age of the same 56 spots with 6 outliers rejected; C) a weighted average $^{206}Pb/^{238}U$ age calculated from the 9 most concordant spots from CLIB07.

Figure 15. Th/La–(Ce/Ce*)Nd diagram after Hastie et al. (2013) showing the affinity of slab derived components in the igneous rocks of the FVB and Kofi Series, albitised samples not plotted. Th/La values are generally inherited from subducting slab sediments, which typically have Th/La > island arc lavas and N-MORB. $(Ce/Ce^*)_{Nd} = Ce_{CN}/(La_{CN}^{2/3} \times Nd_{CN}^{1/3})$; this reflects enrichment of Ce relative to other REEs, which relates to different oxidation states in the marine environment. Subducting marine sediment end members: SSC-HD = slow sediment clay-hydrogenous and SSC-FH = slow sediment clay-fish debris/hydrothermal, as described in Hastie et al., (2013).

Figure 16. Dy/Dy* vs Dy/Yb diagram of Davidson et al. (2013), this diagram describes the slope (Dy/Yb) and curvature (Dy/Dy*) of REE patters as a single point for any given sample. MORB field includes N-MORB and E-MORB data from the East Pacific Rise. Decreasing Dy/Dy* values below the MORB array are largely



Accepted Manuscript

ACCEPTED MANUSCRIPT

controlled by fractionation of clinopyroxene and amphibole, whereas increasing Dy/Yb reflects increasing control of residual garnet on REE patterns. PM, primitive mantle; DM, depleted mantle; GLOSS, average global subducting sediment; see Davidson et al., (2013) for details. Note that data for the Dalema rocks falls within the field for LREE enriched MORB, whereas the majority of the plutonic rocks in the FVB and Kofi plot toward bulk crustal values or along a trend of increasing sediment contamination. The most felsic, peraluminous units display the highest Dy/Yb values.

Figure 17. The A) Rb versus (Y+Nb) and B) Ta versus Nb diagrams of Pearce et al. (1984) for discriminating the tectonic environment of granitic rocks. Albitised samples are highlighted in red.

Figure 18. Summary diagram of published age data for the KKI. Data source is indicated by the numbers below the Belt-Series labels (1) Bassot and Caen-Vachette (1984); (2) Dia (1988); (3) Milesi et al. (1989); (4) Calvez et al. (1990); (5) Boher et al. (1992); (6) Dia et al. (1997); (7) Hirdes and Davis (2002); (8) Gueye et al. (2007); (9) Goujou et al., (2010); (10) Delor et al., (2010).

Figure 19. Tectonic evolution of the KKI defined by the trace element chemistry and isotope geochemistry of plutonic rocks in the FVB, Mako Belt, Saraya Batholith and Kofi Series. $\varepsilon Nd_{(2.1Ga)}$ becomes less positive with time, indicating an increasing influence of continent derived material. Higher Nb/Zr and La/Sm reflect increasing HFSE and LREE enrichment, respectively. Decreasing Eu* reflects fractional crystallisation of Ca-rich plagioclase. Increasing Dy/Yb reflects greater control on REE pattern by residual garnet as a result of slab sediment melting. Error bars for the x-axis are 2σ. Trace element and geochronological data are form this study with the additional geochemical, isotopic and geochronological data compiled from Boher et al., (1992), Pawlig et al., (2006), Dioh et al., (2006) Bassot and Caen-Vachette (1984); Dia et al. (1997); Hirdes and Davis (2002); Gueye et al. (2007).

## Tables

Table 1 – A summary of published geochronological data from the Kédougou-Kéniéba Inlier. Published sources are referenced in the table.



Accepted Manuscript

ACCEPTED MANUSCRIPT

1078 Table 2 - LA-ICPMS instrumental parameters.

1079 Table 3 – LA-MC-ICP-MS data for analyses of standard zircon materials GJ-1, Temora-2, 91500, Mud Tank
1080 and Plešovice.

1081 Table 4 – A summary whole rock geochemical data collected from the South-eastern KKI as part of this
1082 study.

1083 Table 5 – A summary whole rock geochemical data collected from the South-eastern KKI as part of this
1084 study.

1085 Table 6 – A summary whole rock geochemical data collected from the South-eastern KKI as part of this
1086 study.

1087 Table 7 – A summary whole rock geochemical data collected from the South-eastern KKI as part of this
1088 study.

1089 Table 8 - LA-MC-ICP-MS data for analyses of sample BOP1A - Boboti pluton, quartz monzodiorite
1090 porphyry.

1091 Table 9 - LA-MC-ICP-MS data for analyses of sample CLIB01 - Balangouma pluton, quartz monzodiorite
1092 porphyry.

1093 Table 10 - LA-MC-ICP-MS data for analyses of sample CLIB05 – Balangouma pluton, quartz monzonite
1094 porphyry.

1095 Table 11 - LA-MC-ICP-MS data for analyses of sample CLIB07 - Balangouma pluton, monzonite porphyry.

1096

Accepted Manuscript

ACCEPTED MANUSCRIPT

1096 Table.1

| Terrane | Unit | Method | Date (Ma) | ± (Ma) | Event | Reference |
|---|---|---|---|---|---|---|
| Mako volcanic Belt | Badon granodiorite | Ar-Ar (biotite) | 2098 | 20 | Cooling below 300 °C | Gueye et al., (2007) |
| | | K-Ar (biotite | 2090 | 9 | Cooling below 300 °C | Gueye et al., (2007) |
| | | Pb-Pb (zircon) | 2213 | 3 | Inherited core | Gueye et al., (2007) |
| | | Pb-Pb (zircon) | 2198 | 2 | Magmatic emplacement (rim) | Gueye et al., (2007) |
| | SAG dioritic gneiss | Pb-Pb (zircon) | 2202 | 6 | Protolith crystallisation | Gueye et al., (2007) |
| | SAG tonalitic gneiss | Ar-Ar (horneblende) | 2112 | 12 | Cooling below 550 °C | Gueye et al., (2007) |
| | | K-Ar (hornblende) | 2118 | 31 | Cooling below 550 °C | Gueye et al., (2007) |
| | | Pb-Pb (zircon) | 2194 | 4 | Protolith crystallisation | Dia et al., (1997) |
| | | Pb-Pb (zircon) | 2194 | 4 | Protolith crystallisation | Gueye et al., (2007) |
| | | U-Pb (zircon) | 2205 | 15 | Protolith crystallisation | Gueye et al., (2007) |
| | SLP complex diorite | Pb-Pb (zircon) | 2158 | 8 | Magmatic emplacement | Dia et al., (1997) |
| | SLP complex migmatite | U-Pb (zircon) | 2171 | 9 | Migmatisation | Goujou et al., (2010) |
| | LKP granodiorite gneiss | Pb-Pb (zircon) | 2138 | 12 | Protolith crystallisation | Dia et al., (1997) |
| | LKP Kaourou Pluton | Pb-Pb (zircon) | 2079 | 6 | Magmatic emplacement | Dia et al., (1997) |
| | | Rb-Sr (WR) | 2189 | 23 | Possible inheritence | Dia et al., (1997) |
| | LKP Laminia Pluton | Pb-Pb (zircon) | 2105 | 8 | Magmatic emplacement | Dia (1988) |
| | | U-Pb (zircon) | 2127 | 6 | Magmatic emplacement | Dia et al., (1997) |
| | Mamakono rhyolite | Pb-Pb (zircon) | 2067 | 12 | Eruption | Gueye et al., (2007) |
| | Mamakono granodiorite | U-Pb (zircon) | 2076 | 3 | Magmatic emplacement | Hirdes and Davis (2002) |
| | Granite | U-Pb (zircon) | 2102 | 8 | Magmatic emplacement | Goujou et al., (2010) |
| | Granite | U-Pb (zircon) | 2103 | 11 | Magmatic emplacement | Goujou et al., (2010) |
| | Granite | U-Pb (zircon) | 2142 | 7 | Magmatic emplacement | Delor et al., (2010) |
| | Andesite lava | Sm-Nd (WR) | 2160 | 16 | Eruption | Boher et al., (1992) |
| | Tinkoto granodiorite | Ar-Ar (horneblende) | 2051 | 16 | Cooling below 550 °C | Gueye et al., (2007) |
| | | K-Ar (biotite | 2064 | 20 | Cooling below 300 °C | Gueye et al., (2007) |
| | | Pb-Pb (zircon) | 2074 | 5 | Magmatic emplacement | Gueye et al., (2007) |
| Dialé-Daléma Series | Metasedimentary rocks | U-Pb (zircon) | 2164.7 | 0.9 | Upper age of sedimentation | Hirdes and Davis (2002) |
| | Saraya Batholith | Ar-Ar (muscovite) | 2022 | 12 | Cooling below 350 °C | Gueye et al., (2007) |
| | | K-Ar (muscovite) | 2021 | 11 | Cooling below 350 °C | Gueye et al., (2007) |
| | | U-Pb (monazite) | 2079 | 2 | Magmatic emplacement | Hirdes and Davis (2002) |
| | | U-Pb (monazite) | 2064 | 4 | Metamorphic overprint | Hirdes and Davis (2002) |
| | | U-Pb (zircon) | 2072 | 10 | Magmatic emplacement | Delor et al., (2010) |
| | | U-Pb (zircon) | 2061 | 15 | Magmatic emplacement | Delor et al., (2010) |
| | | U-Pb (zircon) | 2075 | 10 | Magmatic emplacement | Goujou et al., (2010) |
| | Metasedimentary rocks | Pb-Pb (zircon) | 2096 | 8 | Upper age of sedimentation | Milesi et al., (1989) |
| | | Pb-Pb (zircon) | 2156 | 10 | Upper age of sedimentation | Milesi et al., (1989) |
| | Andesite dyke | Pb-Pb (zircon) | 2070 | 10 | Crystallisation | Milesi et al., (1989) |
| | | Pb-Pb (zircon) | 2072 | 9 | Crystallisation | Calvez et al., (1990) |
| | Rhyodacite | U-Pb (zircon) | 2098 | 13 | Eruption or crystallisation | Delor et al., (2010) |
| Faleme Volcanic Belt | Balangouma pluton | U-Pb (zircon) | 2118 | 16 | Magmatic emplacement | This study |

Accepted Manuscript

ACCEPTED MANUSCRIPT

| | | | | | | |
|---|---|---|---|---|---|---|
| | Boboti granodiorite | U-Pb (zircon) | 2105 | 9.8 | Magmatic emplacement | This study |
| | | U-Pb (zircon) | 2113 | 15 | Magmatic emplacement | This study |
| | | U-Pb (zircon) | 2080.2 | 0.9 | Magmatic emplacement | Hirdes and Davis (2002) |
| | | U-Pb (zircon) | 2088.5 | 8.5 | Magmatic emplacement | This study |
| | | U-Pb (zircon) | 3000 | 120 | Inherited core | This study |
| | | U-Pb (zircon) | 3380 | 160 | Inherited core | This study |
| | | U-Pb (zircon) | 2218 | 83 | Inherited core | This study |
| | South Falémé tonalite | U-Pb (zircon) | 2081.5 | 1.1 | Magmatic emplacement | Hirdes and Davis (2002) |
| | Rhyolite lava | U-Pb (zircon) | 2099 | 4 | Eruption | Hirdes and Davis (2002) |
| | Rhyolite lava | U-Pb (zircon) | 2155 | 34 | Inheritence | Hirdes and Davis (2002) |
| | Bofeto rhyolite | U-Pb (zircon) | 2082 | 8 | Eruption or crystallisation | Delor et al., (2010) |
| | Rhyolite lava | U-Pb (zircon) | 2064 | 30 | Eruption | Delor et al., (2010) |
| Kofi Series | Tourmalinised quartz wacke | Pb-Pb (zircon) | 2093 | 7 | Upper age of sedimentation | Boher et al., (1992) |
| | Deltaic deposits | U-Pb (zircon) | 2125 | 27 | Upper age of sedimentation | Boher et al., (1992) |
| | Gara Au deposit | U-Pb (mon-xen) | 2028 | 10 | Mineralisation | Vielriecher (2006) |
| | Gamaye pluton | Rb-Sr (WR) | 2045 | 27 | Magmatic emplacement | Bassot and Caen-Vachette (1984) |

1097

1098

Accepted Manuscript

ACCEPTED MANUSCRIPT

1098 Table. 2

| Laboratory & Sample Preparation | |
|---|---|
| Laboratory name | Dept. of Earth Science, Royal Holloway University of London (LA-ICPMS analyses) |
| Sample type/mineral | Igneous zircons |
| **Laser ablation system** | |
| Make, Model & type | Resonetics / ASI RESOlution M-50 with Compex 110 |
| Ablation cell & volume | Laurin two-volume cell (M-50), upper volume ~2 $cm^3$ |
| Laser wavelength (nm) | 193nm |
| Pulse width (ns) | 20 ns |
| Fluence ($J.cm^{-2}$) | 3 $J/cm^{-2}$ |
| Repetition rate (Hz) | 5Hz |
| Ablation duration (secs) | 30 s, 15 s background before and after |
| Signal smoothing | 'Squid' signal smoothing device included |
| Spot size (□m) | 34 □m |
| Sampling mode | Spot ablation |
| Carrier gas | He only through LA cell; $N_2$ & Ar carrier-gas combined before squid |
| Cell carrier gas flow (l/min) | 850 ml/min He |
| **ICPMS Instrument** | |
| Make, Model & type | Agilent 7500ce |
| Sample introduction | Laser ablation only |
| RF power (W) | 1200W |
| Carrier gas flow (l/min) | 450 ml/min Ar, 6 ml/min $N_2$ |
| Detection system | Dual-stage detector |
| Masses measured | m/z = 29, 31, 139, 140, 141, 172, 175, 177, 206, 207, 208, 232, 238 |
| Dwell time per peak (ms) | 5 – 60 ms |
| Total sweep time per reading (ms) | 202 ms |
| Th/ThO, $^{232}Th/^{238}U$ | <0.25%, >93 % |
| **Data Processing** | See text for details |

1099

1100

Accepted Manuscript

ACCEPTED MANUSCRIPT

For all tables: Alb = albitised lithologies; Unalt = unaltered lithologies

Table 4

| | Alb | Alb | Unalt | Unalt | Unalt | Unalt | Unalt | Unalt | Unalt | Unalt |
|---|---|---|---|---|---|---|---|---|---|---|
| Pluton/Area | | | | | Balangouma | | | | | |
| Sample | LR4 | WP174 | CLIB05 | CLIB06 | CLIB07 | LR5 | R35 | R36 | R37 | R41 |
| SiO2 | 64.5 | 75.7 | 64.3 | 73.3 | 62.3 | 63.7 | 64.0 | 55.7 | 58.6 | 62.3 |
| TiO2 | 0.5 | 0.1 | 0.7 | 0.1 | 0.7 | 0.8 | 0.4 | 0.6 | 0.8 | 0.7 |
| Al2O3 | 16.2 | 14.7 | 15.6 | 14.9 | 14.9 | 15.6 | 15.6 | 13.9 | 16.4 | 15.4 |
| Fe2O3T | 2.2 | 0.1 | 5.0 | 0.6 | 6.0 | 5.7 | 3.8 | 5.0 | 6.6 | 5.3 |
| MnO | 0.0 | 0.0 | 0.1 | 0.0 | 0.1 | 0.1 | 0.1 | 0.1 | 0.1 | 0.1 |
| MgO | 3.1 | 0.1 | 2.2 | 0.2 | 3.4 | 3.1 | 1.7 | 2.5 | 3.5 | 2.7 |
| CaO | 2.8 | 0.2 | 3.5 | 0.8 | 4.6 | 4.4 | 5.1 | 3.8 | 5.1 | 4.2 |
| Na2O | 8.5 | 8.2 | 4.4 | 4.4 | 3.8 | 4.1 | 4.1 | 3.5 | 4.5 | 4.1 |
| K2O | 0.3 | 0.2 | 3.7 | 4.6 | 3.2 | 2.4 | 2.6 | 2.7 | 2.2 | 3.0 |
| P2O5 | 0.2 | 0.1 | 0.2 | 0.0 | 0.2 | 0.2 | 0.2 | 0.2 | 0.2 | 0.2 |
| LOI | 0.8 | 0.3 | 0.6 | 0.5 | 0.6 | 0.9 | 1.3 | 11.0 | 1.0 | 0.8 |
| Total | 99.2 | 99.6 | 100.2 | 99.4 | 99.6 | 100.9 | 99.0 | 98.9 | 99.1 | 98.8 |
| | | | | | | | | | | |
| Sample | LR4 | WP174 | CLIB05 | CLIB06 | CLIB07 | LR5 | R35 | R36 | R37 | R41 |
| V | 67.2 | 3.7 | 67.8 | 5.9 | 103.0 | 87.6 | 55.3 | 88.5 | 124.4 | 78.0 |
| Cr | 88.9 | 32.8 | 79.2 | 16.2 | 146.2 | 92.3 | 42.9 | 79.4 | 101.1 | 78.2 |
| Co | 7.2 | 0.0 | 7.2 | 0.0 | 12.5 | 16.6 | 11.7 | 16.6 | 21.7 | 14.5 |
| Ni | 11.8 | 4.1 | 21.8 | 4.9 | 42.0 | 37.6 | 10.7 | 35.2 | 45.5 | 34.3 |
| Ga | 21.7 | 20.9 | 21.8 | 20.9 | 20.6 | 25.0 | 28.7 | 29.7 | 32.7 | 26.5 |
| Rb | 7.1 | 7.5 | 228.3 | 268.3 | 164.9 | 142.5 | 120.6 | 121.2 | 108.1 | 128.0 |
| Sr | 205.8 | 47.2 | 341.2 | 213.1 | 398.7 | 381.6 | 453.0 | 419.0 | 538.4 | 377.1 |
| Y | 14.0 | 2.7 | 17.8 | 6.6 | 21.4 | 11.2 | 9.6 | 16.2 | 16.4 | 16.5 |
| Zr | 149.2 | 73.0 | 268.8 | 79.9 | 201.5 | 195.8 | 131.5 | 252.9 | 212.2 | 190.4 |
| Nb | 7.6 | 7.6 | 12.5 | 7.8 | 10.1 | 12.1 | 6.6 | 12.2 | 10.6 | 13.0 |
| Ta | 0.9 | 1.6 | 0.6 | 1.9 | 1.5 | 1.2 | 0.9 | 1.1 | 1.0 | 1.1 |
| Mo | 1.0 | 0.0 | 0.2 | 1.3 | 0.3 | 3.2 | 2.4 | 2.1 | 1.6 | 5.3 |
| Cs | 0.1 | 0.2 | 16.9 | 9.1 | 9.2 | 6.8 | 1.9 | 5.0 | 7.9 | 4.8 |
| Ba | 183.2 | 36.1 | 534.8 | 543.1 | 663.8 | 359.8 | 490.7 | 668.1 | 590.8 | 588.8 |
| La | 29.3 | 2.8 | 32.0 | 19.7 | 35.3 | 24.9 | 24.7 | 35.5 | 35.0 | 32.2 |
| Ce | 52.1 | 9.0 | 72.5 | 39.6 | 74.9 | 51.4 | 47.9 | 69.0 | 64.9 | 62.1 |
| Pr | 6.4 | 1.2 | 7.8 | 4.7 | 8.7 | 5.8 | 5.3 | 7.7 | 7.3 | 6.9 |
| Nd | 22.3 | 5.0 | 26.1 | 15.4 | 29.9 | 21.8 | 20.9 | 28.8 | 29.3 | 25.9 |
| Sm | 4.1 | 1.2 | 4.9 | 3.1 | 5.8 | 3.2 | 3.3 | 5.0 | 5.6 | 4.7 |
| Eu | 1.1 | 0.2 | 1.1 | 0.7 | 1.3 | 1.1 | 1.0 | 1.3 | 1.5 | 1.2 |
| Gd | 3.5 | 1.0 | 4.0 | 2.3 | 4.8 | 3.4 | 3.1 | 4.8 | 5.2 | 4.2 |
| Tb | 0.5 | 0.1 | 0.5 | 0.3 | 0.6 | 0.5 | 0.4 | 0.6 | 0.6 | 0.6 |
| Dy | 2.8 | 0.5 | 2.9 | 1.2 | 3.6 | 2.2 | 1.8 | 3.4 | 3.4 | 2.8 |
| Ho | 0.5 | 0.0 | 0.6 | 0.2 | 0.7 | 0.5 | 0.4 | 0.6 | 0.6 | 0.5 |
| Er | 1.6 | 0.2 | 1.5 | 0.4 | 1.8 | 1.2 | 1.0 | 1.7 | 1.7 | 1.5 |
| Tm | 0.0 | 0.0 | 0.2 | 0.1 | 0.3 | 0.0 | 0.0 | 0.2 | 0.2 | 0.2 |
| Yb | 1.5 | 0.2 | 1.6 | 0.5 | 1.7 | 1.2 | 1.1 | 1.5 | 1.6 | 1.4 |
| Lu | 0.2 | 0.0 | 0.3 | 0.1 | 0.3 | 0.2 | 0.2 | 0.3 | 0.2 | 0.2 |
| Hf | 3.9 | 2.5 | 7.3 | 3.1 | 5.3 | 5.6 | 3.6 | 6.3 | 5.1 | 5.0 |
| Th | 10.4 | 9.4 | 18.1 | 9.5 | 13.2 | 9.4 | 2.9 | 11.3 | 7.7 | 13.7 |
| U | 5.1 | 2.3 | 5.8 | 8.5 | 3.2 | 5.1 | 1.4 | 3.3 | 2.3 | 2.6 |

*Table 5*

| | Alb | Alb | Unalt | Unalt | Unalt | Unalt | Unalt | Unalt | Unalt | Unalt |
|---|---|---|---|---|---|---|---|---|---|---|



Accepted Manuscript

ACCEPTED MANUSCRIPT

| Pluton/Area | Baqata | | Boboti | | | | | Daléma | | | |
|---|---|---|---|---|---|---|---|---|---|---|---|
| Sample | BAQ01 | BP08 | BOP1A | BOP1B | BOP2 | BOP3 | BOP4 | CLIB08 | CLIB09 | CLIB10 | |
| SiO2 | 72.4 | 65.0 | 60.9 | 61.7 | 74.0 | 74.8 | 60.0 | 51.8 | 49.9 | | 52.1 |
| TiO2 | 0.1 | 0.5 | 0.8 | 0.8 | 0.1 | 0.1 | 1.0 | 2.2 | 1.2 | | 1.1 |
| Al2O3 | 16.4 | 17.5 | 14.4 | 14.4 | 14.2 | 13.9 | 15.2 | 14.3 | 15.0 | | 14.8 |
| Fe2O3T | 0.3 | 0.9 | 6.2 | 6.2 | 0.8 | 0.6 | 8.4 | 14.6 | 12.0 | | 9.8 |
| MnO | 0.0 | 0.0 | 0.1 | 0.1 | 0.0 | 0.0 | 0.1 | 0.2 | 0.1 | | 0.1 |
| MgO | 0.3 | 1.5 | 3.7 | 3.7 | 0.2 | 0.1 | 3.7 | 4.1 | 6.9 | | 7.5 |
| CaO | 0.3 | 3.0 | 4.1 | 4.1 | 0.7 | 0.6 | 5.4 | 8.0 | 8.3 | | 7.9 |
| Na2O | 8.7 | 9.8 | 3.8 | 3.7 | 4.1 | 4.0 | 3.6 | 3.1 | 2.8 | | 3.4 |
| K2O | 0.5 | 0.5 | 3.8 | 3.9 | 4.8 | 5.1 | 2.9 | 1.6 | 1.6 | | 1.7 |
| P2O5 | 0.0 | 0.2 | 0.2 | 0.2 | 0.1 | 0.0 | 0.2 | 0.4 | 0.4 | | 0.3 |
| LOI | 0.5 | 0.8 | 0.6 | 0.5 | 0.4 | 0.4 | 0.3 | 0.0 | 1.0 | | 1.1 |
| Total | 99.4 | 99.7 | 98.5 | 99.4 | 99.4 | 99.5 | 100.8 | 100.3 | 99.3 | | 99.5 |
| | | | | | | | | | | | |
| Sample | BAQ01 | BP08 | BOP1A | BOP1B | BOP2 | BOP3 | BOP4 | CLIB08 | CLIB09 | CLIB10 | |
| V | 0.1 | 28.3 | 104.8 | 106.8 | 0.8 | 2.8 | 139.5 | 241.5 | 245.1 | | 224.0 |
| Cr | 10.1 | 39.1 | 206.6 | 206.2 | 20.2 | 11.7 | 120.9 | 37.1 | 224.2 | | 321.1 |
| Co | 0.0 | 0.0 | 15.6 | 15.4 | 0.0 | 0.0 | 20.7 | 37.4 | 27.9 | | 30.8 |
| Ni | 4.1 | 6.1 | 74.4 | 71.8 | 4.1 | 4.1 | 66.3 | 7.2 | 40.2 | | 93.1 |
| Ga | 13.3 | 18.5 | 21.5 | 21.2 | 23.8 | 21.0 | 20.5 | 22.1 | 23.0 | | 21.8 |
| Rb | 5.6 | 9.2 | 224.4 | 231.4 | 304.4 | 232.2 | 150.5 | 51.2 | 47.0 | | 61.1 |
| Sr | 137.3 | 114.5 | 317.8 | 320.2 | 95.9 | 107.2 | 339.9 | 440.4 | 495.5 | | 498.7 |
| Y | 3.2 | 16.5 | 20.2 | 20.3 | 5.3 | 9.5 | 19.9 | 33.1 | 33.8 | | 29.1 |
| Zr | 41.3 | 176.7 | 241.2 | 213.8 | 59.6 | 53.6 | 151.8 | 169.2 | 99.4 | | 153.0 |
| Nb | 0.3 | 7.5 | 13.4 | 13.2 | 5.6 | 3.9 | 9.4 | 14.9 | 6.4 | | 4.9 |
| Ta | 0.0 | 0.7 | 1.3 | 1.4 | 1.2 | 1.2 | 0.9 | 0.7 | 0.0 | | 0.2 |
| Mo | 0.0 | 0.7 | 3.4 | 3.7 | 1.2 | 0.0 | 2.3 | 0.7 | 0.0 | | 0.0 |
| Cs | 0.0 | 0.1 | 12.1 | 13.2 | 18.4 | 9.1 | 8.3 | 2.0 | 4.1 | | 32.3 |
| Ba | 128.9 | 258.2 | 696.8 | 727.4 | 301.8 | 426.0 | 527.5 | 636.6 | 462.6 | | 461.1 |
| La | 2.6 | 30.8 | 45.7 | 40.9 | 16.2 | 27.0 | 35.8 | 27.4 | 19.6 | | 18.1 |
| Ce | 3.3 | 68.9 | 103.1 | 94.1 | 35.9 | 54.7 | 74.9 | 65.7 | 53.6 | | 51.9 |
| Pr | 0.6 | 8.2 | 11.3 | 10.4 | 3.8 | 6.1 | 8.8 | 8.3 | 7.8 | | 7.5 |
| Nd | 1.9 | 28.7 | 38.8 | 35.9 | 12.3 | 18.7 | 31.1 | 32.8 | 34.0 | | 32.1 |
| Sm | 0.4 | 5.0 | 6.7 | 6.6 | 2.7 | 3.4 | 6.0 | 7.1 | 7.7 | | 7.6 |
| Eu | 0.1 | 1.3 | 1.4 | 1.5 | 0.4 | 0.6 | 1.5 | 2.3 | 2.0 | | 1.9 |
| Gd | 0.5 | 3.8 | 5.4 | 5.2 | 1.7 | 2.6 | 5.0 | 6.8 | 7.1 | | 6.3 |
| Tb | 0.0 | 0.5 | 0.7 | 0.7 | 0.2 | 0.3 | 0.7 | 1.0 | 1.0 | | 0.9 |
| Dy | 0.4 | 2.8 | 3.5 | 3.6 | 0.8 | 1.6 | 3.7 | 5.7 | 5.7 | | 5.0 |
| Ho | 0.0 | 0.5 | 0.7 | 0.7 | 0.1 | 0.2 | 0.7 | 1.2 | 1.2 | | 1.0 |
| Er | 0.2 | 1.4 | 1.7 | 1.8 | 0.4 | 0.7 | 1.8 | 2.9 | 3.1 | | 2.6 |
| Tm | 0.0 | 0.2 | 0.3 | 0.3 | 0.1 | 0.1 | 0.3 | 0.4 | 0.5 | | 0.4 |
| Yb | 0.1 | 1.4 | 1.5 | 1.6 | 0.3 | 0.7 | 1.6 | 2.7 | 2.9 | | 2.6 |
| Lu | 0.0 | 0.2 | 0.3 | 0.3 | 0.0 | 0.1 | 0.3 | 0.4 | 0.5 | | 0.4 |
| Hf | 1.4 | 4.8 | 6.7 | 5.9 | 2.7 | 1.9 | 4.7 | 4.8 | 3.2 | | 4.1 |
| Th | 0.4 | 5.6 | 15.7 | 15.0 | 8.2 | 12.7 | 14.2 | 3.7 | 1.4 | | 1.9 |
| U | 0.5 | 2.3 | 4.4 | 4.7 | 4.1 | 6.0 | 4.3 | 1.2 | 0.7 | | 0.7 |

1104

1105 *Table 6*

| | Unalt | Alb | Alb | Alb | Unalt | Unalt | Unalt | Unalt | Unalt | Alb |
|---|---|---|---|---|---|---|---|---|---|---|
| Pluton/Area | Fadougou | Falémé Volcanics | | | | Gamaye | | Gara | | Kolya |
| Sample | FDGI01 | BP31 | BP29 | BO8 | BP32 | MAD01 | MOU02 | LD23 | LD9 | BO1 |
| SiO2 | 71.2 | 59.8 | 57.4 | 63.5 | 54.8 | 72.1 | 70.9 | 53.1 | 48.0 | 74.9 |
| TiO2 | 0.2 | 0.7 | 0.7 | 0.5 | 0.8 | 0.3 | 0.0 | 0.8 | 0.5 | 0.1 |
| Al2O3 | 14.9 | 14.8 | 13.3 | 15.4 | 13.0 | 15.2 | 16.9 | 18.1 | 8.9 | 14.2 |
| Fe2O3T | 2.4 | 3.8 | 5.4 | 1.5 | 11.7 | 1.5 | 0.1 | 9.2 | 8.8 | 0.2 |
| MnO | 0.0 | 0.0 | 0.0 | 0.0 | 0.0 | 0.0 | 0.0 | 0.0 | 0.1 | 0.0 |

ACCEPTED MANUSCRIPT

| | | | | | | | | | | |
|---|---|---|---|---|---|---|---|---|---|---|
| MgO | 0.5 | 6.7 | 7.7 | 3.0 | 8.5 | 0.5 | 0.0 | 6.7 | 12.5 | 0.0 |
| CaO | 1.6 | 3.7 | 5.5 | 6.1 | 1.1 | 0.8 | 0.3 | 1.1 | 6.4 | 0.1 |
| Na2O | 4.0 | 7.4 | 6.2 | 8.9 | 3.2 | 4.7 | 4.6 | 3.8 | 0.1 | 8.0 |
| K2O | 4.4 | 0.3 | 1.2 | 0.1 | 4.4 | 4.2 | 4.3 | 2.1 | 1.4 | 0.1 |
| P2O5 | 0.0 | 0.3 | 0.3 | 0.1 | 0.3 | 0.3 | 1.2 | 0.3 | 0.2 | 0.0 |
| LOI | 0.5 | 1.3 | 1.1 | 0.7 | 1.6 | 0.4 | 0.9 | 4.5 | 12.6 | 0.5 |
| Total | 99.7 | 98.7 | 98.7 | 99.9 | 99.3 | 100.0 | 99.1 | 99.8 | 99.4 | 98.1 |

| Sample | FDGI01 | BP31 | BP29 | BO8 | BP32 | MAD01 | MOU02 | LD23 | LD9 | BO1 |
|---|---|---|---|---|---|---|---|---|---|---|
| V | 13.5 | 125.5 | 132.4 | 88.0 | 137.7 | 15.4 | 31.8 | 141.2 | 136.8 | 3.3 |
| Cr | 22.8 | 331.0 | 475.0 | 124.9 | 438.6 | 28.9 | 16.0 | 224.9 | 214.8 | 15.4 |
| Co | 0.0 | 3.5 | 23.0 | 0.0 | 16.7 | 0.0 | 214.6 | 17.6 | 16.8 | 0.0 |
| Ni | 5.7 | 119.7 | 213.3 | 35.2 | 328.9 | 4.1 | 110.2 | 14.6 | 10.3 | 4.1 |
| Ga | 20.8 | 19.4 | 19.7 | 20.1 | 23.2 | 26.3 | 25.4 | 28.2 | 28.0 | 20.4 |
| Rb | 188.2 | 0.9 | 42.4 | 0.0 | 264.8 | 641.1 | 269.2 | 54.3 | 55.4 | 0.0 |
| Sr | 222.7 | 155.6 | 216.1 | 162.8 | 103.4 | 232.1 | 236.3 | 451.8 | 455.1 | 26.6 |
| Y | 10.3 | 18.2 | 15.6 | 13.8 | 14.7 | 4.7 | 8.0 | 10.2 | 10.3 | 15.2 |
| Zr | 141.1 | 167.7 | 148.5 | 131.6 | 131.7 | 200.4 | 176.6 | 136.8 | 139.3 | 59.7 |
| Nb | 9.6 | 6.8 | 5.9 | 6.0 | 3.5 | 13.3 | 13.2 | 8.8 | 11.5 | 4.9 |
| Ta | 0.9 | 0.4 | 0.8 | 0.7 | 0.2 | 2.2 | 1.7 | 0.6 | 0.7 | 1.1 |
| Mo | 1.1 | 0.0 | 24.9 | 0.6 | 0.6 | 0.0 | 1.2 | 2.4 | 4.7 | 0.0 |
| Cs | 3.0 | 0.0 | 1.2 | 0.0 | 4.7 | 484.5 | 70.3 | 1.7 | 1.9 | 0.0 |
| Ba | 622.4 | 59.8 | 88.7 | 38.0 | 260.4 | 825.2 | 745.7 | 566.3 | 594.7 | 23.6 |
| La | 30.6 | 18.0 | 50.7 | 12.8 | 8.8 | 63.4 | 49.2 | 12.1 | 11.6 | 19.7 |
| Ce | 66.6 | 46.1 | 108.8 | 40.5 | 22.0 | 123.5 | 110.4 | 25.4 | 26.1 | 44.1 |
| Pr | 7.6 | 6.3 | 11.9 | 5.3 | 2.7 | 12.4 | 10.2 | 3.2 | 3.3 | 5.3 |
| Nd | 26.1 | 26.5 | 41.6 | 20.5 | 10.4 | 37.4 | 30.8 | 12.6 | 12.4 | 19.5 |
| Sm | 4.7 | 5.8 | 7.2 | 4.2 | 2.5 | 5.1 | 4.7 | 2.8 | 2.9 | 4.2 |
| Eu | 0.9 | 1.5 | 2.2 | 1.2 | 0.9 | 0.7 | 0.9 | 0.7 | 0.7 | 0.5 |
| Gd | 3.2 | 4.7 | 5.3 | 3.3 | 2.5 | 3.0 | 3.2 | 2.5 | 2.6 | 3.4 |
| Tb | 0.4 | 0.6 | 0.6 | 0.5 | 0.4 | 0.2 | 0.3 | 0.4 | 0.4 | 0.4 |
| Dy | 1.8 | 3.2 | 3.0 | 2.5 | 2.4 | 1.0 | 1.5 | 2.1 | 1.8 | 2.5 |
| Ho | 0.3 | 0.6 | 0.5 | 0.4 | 0.5 | 0.1 | 0.2 | 0.4 | 0.4 | 0.5 |
| Er | 0.8 | 1.6 | 1.3 | 1.2 | 1.3 | 0.3 | 0.6 | 1.2 | 1.2 | 1.3 |
| Tm | 0.1 | 0.2 | 0.2 | 0.2 | 0.2 | 0.0 | 0.1 | 0.0 | 0.0 | 0.2 |
| Yb | 0.8 | 1.5 | 1.2 | 1.2 | 1.3 | 0.3 | 0.6 | 1.4 | 1.5 | 1.3 |
| Lu | 0.1 | 0.2 | 0.2 | 0.2 | 0.2 | 0.0 | 0.1 | 0.2 | 0.2 | 0.2 |
| Hf | 4.5 | 4.6 | 4.1 | 3.6 | 3.9 | 5.5 | 5.1 | 3.7 | 3.9 | 2.3 |
| Th | 9.3 | 5.5 | 5.2 | 3.8 | 4.4 | 35.4 | 23.6 | 4.6 | 4.8 | 10.1 |
| U | 4.1 | 1.9 | 1.5 | 1.8 | 1.7 | 6.3 | 5.4 | 1.8 | 1.7 | 3.6 |

*Table 7*

| Pluton/Area | Alb | Alb Kabe West | Alb | Alb Karekeane | Alb | Unalt North Gara | Unalt | Unalt South Falémé | Alb Yalea | Unalt Yatea |
|---|---|---|---|---|---|---|---|---|---|---|
| Sample | BO4 | BO5 | BP21 | R21 | R25 | R42 | R43 | FDGI02 | UYP1 | PTG1 |
| SiO2 | 52.4 | 53.9 | 59.3 | 61.1 | 58.8 | 76.2 | 74.3 | 65.1 | 60.0 | 69.5 |
| TiO2 | 1.0 | 0.8 | 0.6 | 0.5 | 0.6 | 0.0 | 0.0 | 0.5 | 0.7 | 0.3 |
| Al2O3 | 15.4 | 16.4 | 15.5 | 15.5 | 16.2 | 13.7 | 13.8 | 14.7 | 14.6 | 15.4 |
| Fe2O3T | 5.4 | 8.8 | 2.9 | 3.0 | 3.4 | 0.4 | 0.5 | 4.2 | 4.6 | 1.9 |
| MnO | 0.0 | 0.0 | 0.0 | 0.0 | 0.0 | 0.0 | 0.0 | 0.0 | 0.0 | 0.0 |
| MgO | 4.1 | 4.6 | 2.8 | 2.6 | 3.2 | 0.1 | 0.1 | 3.5 | 3.1 | 0.8 |
| CaO | 5.7 | 4.6 | 5.9 | 5.3 | 6.2 | 0.3 | 0.4 | 2.7 | 2.7 | 1.5 |
| Na2O | 5.2 | 6.1 | 8.5 | 8.8 | 7.8 | 3.5 | 4.2 | 4.3 | 7.5 | 5.2 |
| K2O | 2.0 | 1.3 | 0.1 | 0.1 | 0.6 | 5.4 | 4.9 | 3.4 | 0.7 | 3.1 |
| P2O5 | 0.1 | 0.1 | 0.2 | 0.1 | 0.3 | 0.0 | 0.0 | 0.2 | 0.2 | 0.1 |
| LOI | 8.6 | 2.7 | 3.6 | 3.2 | 3.6 | 0.8 | 0.7 | 0.7 | 4.8 | 0.9 |
| Total | 100.0 | 99.4 | 99.5 | 100.3 | 100.7 | 100.3 | 98.9 | 99.3 | 99.0 | 98.7 |



Accepted Manuscript

ACCEPTED MANUSCRIPT

| Sample | BO4 | BO5 | BP21 | R21 | R25 | R42 | R43 | FDGI02 | UYP1 | PTG1 |
|---|---|---|---|---|---|---|---|---|---|---|
| V | 196.4 | 168.4 | 94.3 | 59.3 | 84.5 | 1.9 | 2.7 | 68.7 | 96.9 | 25.9 |
| Cr | 18.0 | 74.3 | 48.0 | 39.4 | 59.5 | 11.3 | 15.8 | 198.2 | 123.1 | 18.8 |
| Co | 0.0 | 18.8 | 36.7 | 11.7 | 11.9 | 1.8 | 2.0 | 9.1 | 14.3 | 4.2 |
| Ni | 25.7 | 44.5 | 38.1 | 16.7 | 33.1 | 5.4 | 3.7 | 75.3 | 54.3 | 8.0 |
| Ga | 18.1 | 20.3 | 19.8 | 16.6 | 15.9 | 21.6 | 23.7 | 20.5 | 18.4 | 34.4 |
| Rb | 38.1 | 30.0 | 4.7 | 2.0 | 26.3 | 265.8 | 270.8 | 133.4 | 10.1 | 79.1 |
| Sr | 105.8 | 151.7 | 140.0 | 93.4 | 234.0 | 53.4 | 74.6 | 496.9 | 104.0 | 691.5 |
| Y | 21.7 | 23.9 | 15.4 | 12.2 | 21.2 | 7.8 | 4.4 | 14.6 | 13.4 | 5.8 |
| Zr | 115.8 | 92.5 | 133.7 | 107.6 | 146.0 | 38.4 | 28.4 | 187.3 | 143.3 | 120.4 |
| Nb | 6.4 | 2.9 | 5.4 | 6.0 | 6.4 | 8.3 | 8.6 | 8.4 | 8.4 | 6.0 |
| Ta | 0.4 | 0.0 | 0.7 | 0.6 | 0.5 | 1.4 | 1.7 | 0.9 | 0.7 | 0.5 |
| Mo | 0.0 | 0.0 | 1.9 | 26.4 | 0.0 | 1.5 | 3.0 | 2.2 | 0.8 | 1.2 |
| Cs | 0.1 | 0.0 | 0.1 | 0.3 | 2.2 | 3.3 | 13.6 | 2.9 | 0.6 | 2.6 |
| Ba | 226.8 | 221.3 | 23.4 | 14.5 | 80.7 | 133.2 | 164.0 | 807.5 | 31.3 | 954.9 |
| La | 17.9 | 19.2 | 12.6 | 6.1 | 15.9 | 20.6 | 7.3 | 43.1 | 32.7 | 25.1 |
| Ce | 35.5 | 36.9 | 34.2 | 15.9 | 50.7 | 30.0 | 13.6 | 95.0 | 77.7 | 49.6 |
| Pr | 4.7 | 4.9 | 4.3 | 2.8 | 8.0 | 4.1 | 1.7 | 10.4 | 10.1 | 5.8 |
| Nd | 18.4 | 19.0 | 17.9 | 14.0 | 36.0 | 14.6 | 6.5 | 35.5 | 40.2 | 22.8 |
| Sm | 4.0 | 4.2 | 4.3 | 3.7 | 7.9 | 2.5 | 1.7 | 5.7 | 7.8 | 4.1 |
| Eu | 1.2 | 1.3 | 1.1 | 1.0 | 2.4 | 0.4 | 0.3 | 1.4 | 2.1 | 1.0 |
| Gd | 4.1 | 4.3 | 3.6 | 3.1 | 6.5 | 2.5 | 1.4 | 4.2 | 6.3 | 3.1 |
| Tb | 0.7 | 0.6 | 0.5 | 0.4 | 0.9 | 0.3 | 0.2 | 0.5 | 0.7 | 0.3 |
| Dy | 3.8 | 3.9 | 2.8 | 2.4 | 4.9 | 1.5 | 0.8 | 2.6 | 3.6 | 1.4 |
| Ho | 0.8 | 0.8 | 0.5 | 0.5 | 0.8 | 0.2 | 0.2 | 0.5 | 0.5 | 0.2 |
| Er | 2.0 | 2.1 | 1.3 | 1.3 | 2.2 | 0.6 | 0.4 | 1.2 | 1.2 | 0.6 |
| Tm | 0.3 | 0.3 | 0.2 | 0.2 | 0.3 | 0.0 | 0.0 | 0.2 | 0.0 | 0.0 |
| Yb | 2.0 | 1.9 | 1.2 | 1.2 | 1.9 | 0.5 | 0.4 | 1.3 | 1.0 | 0.5 |
| Lu | 0.3 | 0.3 | 0.2 | 0.2 | 0.2 | 0.1 | 0.1 | 0.2 | 0.2 | 0.1 |
| Hf | 3.5 | 2.4 | 3.8 | 3.2 | 3.6 | 1.8 | 1.8 | 5.3 | 3.6 | 3.1 |
| Th | 3.5 | 3.8 | 4.2 | 4.8 | 4.4 | 6.4 | 15.4 | 13.4 | 3.8 | 4.8 |
| U | 1.1 | 0.9 | 1.2 | 1.9 | 2.1 | 2.7 | 2.8 | 4.4 | 1.2 | 1.7 |

1108

1109

Accepted Manuscript

ACCEPTED MANUSCRIPT

| | Ratios | | | | | | | | | | Ages | | | | | | | | Concentrations (calculated from 91500) | | | | | | | |
|---|---|---|---|---|---|---|---|---|---|---|---|---|---|---|---|---|---|---|---|---|---|---|---|---|---|---|
| Standard - | 207Pb/235 | Propagatec | 206Pb/238 | Propagatec | Error Corre | 207Pb/206 | Propagatec | Error Corre | 208Pb/232 | Propagatec | 207Pb/235 | Propagatec | 206Pb/238 | Propagatec | 208Pb/232 | Propagatec | 207Pb/206 | Propagatec | U (ppm) | Internal 2 S | Th (ppm) | Internal 2 S | Pb (ppm) | Internal 2 S | U/Th | Internal 2 SE |
| GJ1 - 1 | 0.807 | 0.042 | 0.09713 | 0.0037 | 0.021621 | 0.0605 | 0.0014 | 0.33647 | 0.0303 | 0.0023 | 599 | 24 | 597.5 | 22 | 602 | 45 | 603 | 52 | 419.5 | 9.3 | 13.28 | 0.35 | 11.09 | 0.84 | 33.35 | 0.53 |
| GJ1 - 10 | 0.819 | 0.042 | 0.09816 | 0.0038 | 0.2019 | 0.0605 | 0.0013 | 0.2541 | 0.0308 | 0.0024 | 606 | 24 | 603.5 | 22 | 611 | 47 | 599 | 48 | 373.8 | 8.4 | 11.69 | 0.34 | 10.96 | 0.86 | 31.19 | 0.66 |
| GJ1 - 11 | 0.842 | 0.044 | 0.1003 | 0.0039 | 0.39482 | 0.0608 | 0.0013 | 0.067381 | 0.0299 | 0.0022 | 618.5 | 24 | 616.1 | 23 | 593 | 42 | 613 | 45 | 350.7 | 7.2 | 11.23 | 0.3 | 10.16 | 0.76 | 31 | 0.65 |
| GJ1 - 12 | 0.774 | 0.04 | 0.09479 | 0.0037 | 0.20309 | 0.0593 | 0.0014 | 0.24233 | 0.0308 | 0.0027 | 580.7 | 23 | 583.7 | 22 | 610 | 53 | 555 | 50 | 325.5 | 7.7 | 10.48 | 0.33 | 9.37 | 0.79 | 31.14 | 0.66 |
| GJ1 - 13 | 0.817 | 0.042 | 0.09895 | 0.0039 | 0.22596 | 0.06 | 0.0013 | 0.21116 | 0.0293 | 0.0023 | 606.2 | 24 | 608.1 | 23 | 583 | 44 | 587 | 48 | 304.7 | 6.5 | 10.03 | 0.29 | 8.51 | 0.61 | 30.81 | 0.74 |
| GJ1 - 14 | 0.788 | 0.042 | 0.09648 | 0.0038 | 0.35928 | 0.0594 | 0.0014 | 0.039334 | 0.029 | 0.0023 | 590 | 24 | 593.7 | 22 | 576 | 45 | 559 | 51 | 321.3 | 7.6 | 10.65 | 0.36 | 9.08 | 0.69 | 30.59 | 0.68 |
| GJ1 - 15 | 0.797 | 0.042 | 0.0951 | 0.0038 | 0.39748 | 0.0608 | 0.0013 | 0.12953 | 0.0307 | 0.0023 | 593 | 24 | 585.5 | 22 | 609 | 46 | 610 | 48 | 382.8 | 7.2 | 12.34 | 0.3 | 11.03 | 0.84 | 31.06 | 0.74 |
| GJ1 - 16 | 0.813 | 0.043 | 0.0977 | 0.0039 | 0.38528 | 0.06 | 0.0013 | 0.16734 | 0.0292 | 0.0026 | 602 | 24 | 601 | 23 | 580 | 51 | 593 | 48 | 385.9 | 9.4 | 12.37 | 0.39 | 10.38 | 0.88 | 31.43 | 0.82 |
| GJ1 - 17 | 0.812 | 0.042 | 0.0974 | 0.0039 | 0.3071 | 0.0602 | 0.0013 | 0.28943 | 0.0311 | 0.0024 | 602 | 24 | 599 | 23 | 618 | 47 | 595 | 49 | 315.9 | 6.9 | 10.6 | 0.33 | 9.49 | 0.67 | 31.52 | 0.89 |
| GJ1 - 18 | 0.823 | 0.044 | 0.0982 | 0.004 | 0.44961 | 0.0606 | 0.0014 | 0.053348 | 0.0299 | 0.0027 | 609 | 25 | 603.7 | 23 | 594 | 54 | 602 | 51 | 274.9 | 5.4 | 9.22 | 0.23 | 7.92 | 0.69 | 32.76 | 0.82 |
| GJ1 - 19 | 0.81 | 0.043 | 0.0971 | 0.0037 | 0.34257 | 0.0599 | 0.0014 | 0.16601 | 0.0301 | 0.0026 | 600 | 24 | 598.1 | 23 | 598 | 51 | 581 | 53 | 320.1 | 5 | 10.17 | 0.25 | 8.59 | 0.71 | 33.61 | 0.81 |
| GJ1 - 2 | 0.816 | 0.042 | 0.09852 | 0.0039 | 0.058626 | 0.0598 | 0.0014 | 0.27379 | 0.0296 | 0.0025 | 604.1 | 24 | 605.7 | 23 | 589 | 48 | 581 | 48 | 402.1 | 8.4 | 12.96 | 0.34 | 10.96 | 0.88 | 31.88 | 0.51 |
| GJ1 - 3 | 0.809 | 0.041 | 0.09768 | 0.0038 | 0.081061 | 0.0597 | 0.0012 | 0.25257 | 0.0315 | 0.0024 | 600.9 | 23 | 600.8 | 22 | 624 | 48 | 581 | 44 | 384.4 | 9.7 | 12.22 | 0.35 | 11.29 | 0.87 | 31.39 | 0.52 |
| GJ1 - 4 | 0.822 | 0.042 | 0.0978 | 0.0038 | 0.17192 | 0.0608 | 0.0012 | 0.23138 | 0.0289 | 0.0024 | 607.6 | 23 | 601.4 | 22 | 573 | 47 | 618 | 43 | 351.2 | 7.5 | 11.13 | 0.29 | 9.63 | 0.77 | 31.09 | 0.59 |
| GJ1 - 5 | 0.789 | 0.041 | 0.09663 | 0.0037 | 0.15777 | 0.0593 | 0.0013 | 0.22416 | 0.0298 | 0.0022 | 589.4 | 23 | 594.6 | 22 | 593 | 43 | 563 | 48 | 342.8 | 8.2 | 10.98 | 0.32 | 10.14 | 0.76 | 30.42 | 0.46 |
| GJ1 - 6 | 0.822 | 0.043 | 0.09778 | 0.0038 | 0.25927 | 0.061 | 0.0013 | 0.10714 | 0.0301 | 0.0024 | 607.9 | 24 | 601.3 | 22 | 598 | 47 | 632 | 44 | 342.5 | 7.7 | 11.01 | 0.29 | 10.19 | 0.83 | 30.65 | 0.5 |
| GJ1 - 7 | 0.812 | 0.042 | 0.09839 | 0.0038 | 0.098229 | 0.06 | 0.0013 | 0.31226 | 0.03 | 0.0024 | 601.9 | 24 | 604.9 | 22 | 596 | 47 | 582 | 49 | 343.5 | 6.3 | 11.24 | 0.3 | 10.11 | 0.78 | 30.78 | 0.62 |
| GJ1 - 8 | 0.813 | 0.043 | 0.09696 | 0.0037 | 0.15783 | 0.061 | 0.0014 | 0.21275 | 0.0313 | 0.0025 | 602.5 | 24 | 596.5 | 22 | 622 | 48 | 620 | 48 | 353.7 | 9.1 | 11.75 | 0.35 | 10.87 | 0.81 | 30.53 | 0.61 |
| GJ1 - 9 | 0.784 | 0.04 | 0.09634 | 0.0037 | 0.33215 | 0.0594 | 0.0012 | 0.17806 | 0.0296 | 0.0023 | 588.4 | 23 | 592.8 | 22 | 588 | 46 | 568 | 44 | 365.9 | 8.6 | 11.77 | 0.34 | 10.53 | 0.8 | 30.91 | 0.59 |
| Mudtank - | 0.9 | 0.13 | 0.1167 | 0.0062 | 0.10749 | 0.0569 | 0.0081 | 0.16927 | 0.0325 | 0.0046 | 582 | 81 | 710 | 35 | 639 | 90 | 230 | 250 | 9 | 0.19 | 3.41 | 0.11 | 3.04 | 0.43 | 2.815 | 0.091 |
| Mudtank - | 1.13 | 0.16 | 0.1158 | 0.007 | 0.072216 | 0.0721 | 0.0098 | 0.26493 | 0.0373 | 0.0059 | 676 | 83 | 703 | 40 | 730 | 110 | 550 | 270 | 8.01 | 0.2 | 2.96 | 0.11 | 3.19 | 0.49 | 2.73 | 0.11 |
| Mudtank - | 1.01 | 0.16 | 0.1164 | 0.0069 | 0.206 | 0.068 | 0.011 | 0.15434 | 0.035 | 0.0057 | 641 | 87 | 707 | 40 | 680 | 110 | 390 | 270 | 7.21 | 0.34 | 2.82 | 0.15 | 2.89 | 0.45 | 2.69 | 0.14 |
| Mudtank - | 1.12 | 0.17 | 0.1208 | 0.0073 | 0.30237 | 0.0671 | 0.0094 | 0.27275 | 0.0418 | 0.0067 | 659 | 90 | 732 | 42 | 810 | 130 | 450 | 270 | 7.75 | 0.3 | 2.83 | 0.13 | 3.2 | 0.49 | 2.86 | 0.17 |
| Mudtank - | 1.05 | 0.19 | 0.1265 | 0.0084 | 0.21129 | 0.061 | 0.011 | 0.1029 | 0.0458 | 0.009 | 614 | 97 | 770 | 49 | 880 | 170 | 250 | 300 | 6.32 | 0.26 | 2.54 | 0.11 | 3.02 | 0.49 | 2.84 | 0.18 |
| 91500 - 1 | 1.831 | 0.06 | 0.1762 | 0.0033 | 0.15467 | 0.0749 | 0.0022 | 0.19021 | 0.0535 | 0.0035 | 1050 | 22 | 1045.8 | 18 | 1053 | 67 | 1040 | 60 | 84.1 | 1.7 | 31.52 | 0.69 | 16 | 0.58 | 2.665 | 0.025 |
| 91500 - 1 | 1.86 | 0.049 | 0.1769 | 0.0029 | 0.11441 | 0.0766 | 0.0021 | 0.25292 | 0.0528 | 0.0023 | 1064 | 18 | 1049.6 | 16 | 1040 | 44 | 1075 | 57 | 80 | 1.5 | 29.99 | 0.61 | 15 | 0.52 | 2.666 | 0.024 |
| 91500 - 1 | 1.86 | 0.049 | 0.1769 | 0.0029 | 0.11441 | 0.0766 | 0.0021 | 0.25292 | 0.0528 | 0.0023 | 1064 | 18 | 1049.6 | 16 | 1040 | 44 | 1075 | 57 | 80 | 1.5 | 29.99 | 0.61 | 15 | 0.52 | 2.666 | 0.024 |
| 91500 - 1 | 1.814 | 0.095 | 0.1766 | 0.0083 | 0.24674 | 0.0757 | 0.002 | 0.16418 | 0.0542 | 0.0034 | 1048 | 33 | 1048 | 46 | 1067 | 65 | 1059 | 55 | 115 | 2.8 | 33.91 | 0.78 | 15.11 | 0.42 | 2.709 | 0.028 |
| 91500 - 10 | 1.835 | 0.1 | 0.1807 | 0.0086 | 0.30755 | 0.0736 | 0.0023 | 0.18936 | 0.0547 | 0.0038 | 1051 | 36 | 1070 | 47 | 1074 | 72 | 997 | 65 | 78.9 | 1.9 | 29.17 | 0.75 | 15.1 | 0.49 | 2.652 | 0.055 |
| 91500 - 11 | 1.871 | 0.1 | 0.1835 | 0.0088 | 0.29466 | 0.0742 | 0.0022 | 0.24041 | 0.0537 | 0.0038 | 1067 | 37 | 1085 | 48 | 1057 | 72 | 1014 | 64 | 80.4 | 2.1 | 30.12 | 0.78 | 14.99 | 0.57 | 2.662 | 0.056 |
| 91500 - 12 | 1.863 | 0.1 | 0.1785 | 0.0086 | 0.40286 | 0.0764 | 0.0024 | 0.12401 | 0.0546 | 0.0037 | 1066 | 37 | 1058 | 47 | 1074 | 70 | 1073 | 64 | 83.7 | 2.3 | 31.3 | 0.81 | 15.15 | 0.51 | 2.673 | 0.058 |
| 91500 - 13 | 1.824 | 0.1 | 0.1804 | 0.0088 | 0.40853 | 0.074 | 0.0023 | 0.14622 | 0.055 | 0.0038 | 1046 | 37 | 1068 | 48 | 1081 | 72 | 1008 | 67 | 79.6 | 2.1 | 29.84 | 0.85 | 14.85 | 0.55 | 2.67 | 0.058 |
| 91500 - 14 | 1.849 | 0.11 | 0.1799 | 0.0087 | 0.32559 | 0.0755 | 0.0027 | 0.17478 | 0.0539 | 0.0038 | 1060 | 38 | 1066 | 48 | 1061 | 72 | 1048 | 68 | 79.5 | 1.7 | 30.02 | 0.73 | 15.05 | 0.59 | 2.651 | 0.06 |
| 91500 - 15 | 1.787 | 0.099 | 0.1787 | 0.0087 | 0.42569 | 0.072 | 0.0021 | 0.15027 | 0.0546 | 0.004 | 1036 | 36 | 1061 | 49 | 1072 | 76 | 958 | 61 | 80.4 | 1.8 | 30.04 | 0.86 | 14.99 | 0.58 | 2.682 | 0.071 |
| 91500 - 2 | 1.891 | 0.058 | 0.1801 | 0.0034 | 0.044247 | 0.0764 | 0.0022 | 0.29991 | 0.0535 | 0.0035 | 1072 | 21 | 1067.3 | 18 | 1053 | 66 | 1066 | 58 | 80.4 | 1.8 | 30.37 | 0.72 | 15.63 | 0.54 | 2.646 | 0.025 |
| 91500 - 2 | 1.774 | 0.051 | 0.1769 | 0.0029 | 0.00405 | 0.0731 | 0.0022 | 0.33314 | 0.0544 | 0.0025 | 1032 | 19 | 1049.5 | 16 | 1070 | 48 | 970 | 65 | 80 | 1.8 | 30.05 | 0.7 | 15 | 0.56 | 2.665 | 0.026 |
| 91500 - 2 | 1.774 | 0.051 | 0.1769 | 0.0029 | 0.00405 | 0.0731 | 0.0022 | 0.33314 | 0.0544 | 0.0025 | 1032 | 19 | 1049.5 | 16 | 1070 | 48 | 970 | 65 | 80 | 1.8 | 30.05 | 0.7 | 15 | 0.56 | 2.665 | 0.026 |
| 91500 - 2 | 1.775 | 0.092 | 0.1743 | 0.0082 | 0.11613 | 0.0735 | 0.0021 | 0.32952 | 0.0517 | 0.0034 | 1036 | 34 | 1035 | 45 | 1018 | 66 | 1009 | 58 | 80.4 | 1.8 | 29.42 | 0.73 | 15.21 | 0.49 | 2.634 | 0.036 |
| 91500 - 3 | 1.856 | 0.058 | 0.1779 | 0.0035 | 0.18963 | 0.0754 | 0.0021 | 0.2349 | 0.0514 | 0.0033 | 1062 | 21 | 1055 | 19 | 1012 | 64 | 1056 | 59 | 81.2 | 1.8 | 30.39 | 0.65 | 15.41 | 0.54 | 2.683 | 0.027 |
| 91500 - 3 | 1.803 | 0.049 | 0.174 | 0.0028 | -0.11593 | 0.0755 | 0.0021 | 0.4418 | 0.0509 | 0.0025 | 1046 | 17 | 1034.1 | 15 | 1002 | 48 | 1053 | 59 | 80 | 1.7 | 29.95 | 0.65 | 15 | 0.62 | 2.671 | 0.026 |
| 91500 - 3 | 1.803 | 0.049 | 0.174 | 0.0028 | -0.11593 | 0.0755 | 0.0021 | 0.4418 | 0.0509 | 0.0025 | 1046 | 17 | 1034.1 | 15 | 1002 | 48 | 1053 | 59 | 80 | 1.7 | 29.95 | 0.65 | 15 | 0.62 | 2.671 | 0.026 |
| 91500 - 3 | 1.841 | 0.096 | 0.1733 | 0.008 | 0.27661 | 0.0765 | 0.002 | 0.12063 | 0.0487 | 0.0032 | 1055 | 34 | 1030 | 44 | 960 | 62 | 1087 | 52 | 80.5 | 2 | 29.45 | 0.68 | 14.6 | 0.47 | 2.658 | 0.033 |
| 91500 - 4 | 1.829 | 0.063 | 0.1797 | 0.0034 | 0.17195 | 0.0745 | 0.0023 | 0.12546 | 0.0526 | 0.0034 | 1051 | 22 | 1065.3 | 19 | 1035 | 65 | 1025 | 62 | 80.4 | 1.8 | 30.18 | 0.73 | 15.31 | 0.59 | 2.674 | 0.027 |
| 91500 - 4 | 1.848 | 0.054 | 0.1783 | 0.003 | 0.13286 | 0.0754 | 0.0022 | 0.25781 | 0.0556 | 0.0023 | 1056 | 19 | 1058 | 16 | 1093 | 44 | 1043 | 61 | 80 | 1.6 | 29.99 | 0.65 | 15 | 0.5 | 2.678 | 0.03 |
| 91500 - 4 | 1.848 | 0.054 | 0.1783 | 0.003 | 0.13286 | 0.0754 | 0.0022 | 0.25781 | 0.0556 | 0.0023 | 1056 | 19 | 1058 | 16 | 1093 | 44 | 1043 | 61 | 80 | 1.6 | 29.99 | 0.65 | 15 | 0.5 | 2.678 | 0.03 |
| 91500 - 4 | 1.807 | 0.096 | 0.1754 | 0.0082 | 0.0898 | 0.0744 | 0.0023 | 0.31033 | 0.05 | 0.0035 | 1042 | 35 | 1042 | 45 | 985 | 67 | 1013 | 63 | 76.9 | 1.9 | 29.05 | 0.73 | 14.81 | 0.58 | 2.613 | 0.035 |
| 91500 - 5 | 1.779 | 0.056 | 0.1807 | 0.0035 | 0.05125 | 0.0725 | 0.0021 | 0.31954 | 0.055 | 0.0035 | 1037 | 20 | 1071 | 19 | 1082 | 67 | 974 | 61 | 84.2 | 2 | 31.38 | 0.77 | 15.8 | 0.53 | 2.667 | 0.029 |
| 91500 - 5 | 1.913 | 0.051 | 0.1787 | 0.0029 | 0.23908 | 0.0773 | 0.0021 | 0.12412 | 0.052 | 0.0023 | 1080 | 18 | 1061.1 | 16 | 1023 | 44 | 1117 | 53 | 80.4 | 1.8 | 30.41 | 0.74 | 15.1 | 0.5 | 2.628 | 0.029 |
| 91500 - 5 | 1.913 | 0.051 | 0.1787 | 0.0029 | 0.23908 | 0.0773 | 0.0021 | 0.12412 | 0.052 | 0.0023 | 1080 | 18 | 1061.1 | 16 | 1023 | 44 | 1117 | 53 | 80.4 | 1.8 | 30.41 | 0.74 | 15.1 | 0.5 | 2.628 | 0.029 |
| 91500 - 5 | 1.702 | 0.091 | 0.1698 | 0.008 | 0.30333 | 0.0734 | 0.0022 | 0.15768 | 0.0522 | 0.0033 | 1004 | 34 | 1011 | 44 | 1027 | 64 | 990 | 60 | 77.2 | 1.6 | 29.67 | 0.62 | 15.19 | 0.47 | 2.714 | 0.039 |
| 91500 - 6 | 1.829 | 0.058 | 0.1778 | 0.0034 | 0.29015 | 0.0746 | 0.0022 | 0.1096 | 0.0558 | 0.0036 | 1053 | 20 | 1056 | 19 | 1100 | 69 | 1034 | 58 | 85.4 | 2.1 | 31.76 | 0.81 | 16.57 | 0.59 | 2.676 | 0.027 |
| 91500 - 6 | 1.876 | 0.054 | 0.1786 | 0.003 | 0.0236 | 0.0765 | 0.0023 | 0.33294 | 0.0518 | 0.0024 | 1069 | 19 | 1059 | 17 | 1020 | 45 | 1082 | 60 | 79.3 | 1.8 | 29.6 | 0.7 | 14.82 | 0.54 | 2.661 | 0.027 |
| 91500 - 6 | 1.876 | 0.054 | 0.1786 | 0.003 | 0.0236 | 0.0765 | 0.0023 | 0.33294 | 0.0518 | 0.0024 | 1069 | 19 | 1059 | 17 | 1020 | 45 | 1082 | 60 | 79.3 | 1.8 | 29.6 | 0.7 | 14.82 | 0.54 | 2.661 | 0.027 |
| 91500 - 6 | 1.796 | 0.096 | 0.1739 | 0.0083 | 0.28309 | 0.0741 | 0.0021 | 0.17231 | 0.0515 | 0.0034 | 1040 | 36 | 1033 | 45 | 1014 | 65 | 1022 | 62 | 76.3 | 1.4 | 29.83 | 0.6 | 15.05 | 0.42 | 2.664 | 0.041 |
| 91500 - 7 | 1.877 | 0.055 | 0.1778 | 0.0034 | 0.031307 | 0.0762 | 0.0019 | 0.26401 | 0.0536 | 0.0035 | 1068 | 20 | 1054.8 | 18 | 1054 | 68 | 1076 | 51 | 87.3 | 1.8 | 32.94 | 0.68 | 16.48 | 0.56 | 2.626 | 0.025 |
| 91500 - 7 | 1.846 | 0.056 | 0.1802 | 0.0029 | -0.02009 | 0.0746 | 0.0024 | 0.3389 | 0.0513 | 0.0023 | 1054 | 21 | 1068 | 16 | 1011 | 44 | 1004 | 72 | 80.2 | 1.6 | 30.05 | 0.64 | 15.07 | 0.53 | 2.696 | 0.028 |
| 91500 - 7 | 1.846 | 0.056 | 0.1802 | 0.0029 | -0.02009 | 0.0746 | 0.0024 | 0.3389 | 0.0513 | 0.0023 | 1054 | 21 | 1068 | 16 | 1011 | 44 | 1004 | 72 | 80.2 | 1.6 | 30.05 | 0.64 | 15.07 | 0.53 | 2.696 | 0.028 |
| 91500 - 7 | 1.849 | 0.099 | 0.1805 | 0.0086 | 0.43065 | 0.0748 | 0.0022 | 0.085427 | 0.0529 | 0.0035 | 1057 | 36 | 1069 | 47 | 1041 | 67 | 1031 | 58 | 77.4 | 2.1 | 29.86 | 0.8 | 14.89 | 0.5 | 2.675 | 0.045 |
| 91500 - 8 | 1.847 | 0.063 | 0.1799 | 0.0035 | 0.16401 | 0.0738 | 0.0022 | 0.20618 | 0.0546 | 0.0037 | 1055 | 22 | 1066 | 19 | 1073 | 71 | 996 | 65 | 74 | 1.6 | 27.27 | 0.64 | 14.07 | 0.57 | 2.7 | 0.032 |
| 91500 - 8 | 1.857 | 0.099 | 0.1746 | 0.0082 | 0.29002 | 0.0764 | 0.0022 | 0.18854 | 0.0506 | 0.0035 | 1060 | 36 | 1037 | 45 | 997 | 66 | 1076 | 61 | 81.4 | 1.9 | 31.1 | 0.74 | 15.28 | 0.52 | 2.644 | 0.045 |
| 91500 - 9 | 1.78 | 0.099 | 0.1689 | 0.0082 | 0.34652 | 0.0765 | 0.0025 | 0.22879 | 0.0542 | 0.0037 | 1031 | 36 | 1005 | 45 | 1066 | 70 | 1080 | 63 | 79.3 | 2.3 | 28.28 | 0.79 | 14.6 | 0.55 | 2.717 | 0.062 |
| GJ1 - 1 | 0.814 | 0.02 | 0.0976 | 0.0017 | 0.009488 | 0.0602 | 0.0012 | 0.35556 | 0.0293 | 0.003 | 604.3 | 11 | 600.3 | 10 | 582 | 58 | 591 | 43 | 318.9 | 7.5 | 9.9 | 0.26 | 2.71 | 0.22 | 32.2 | 0.48 |
| GJ1 - 1 | 0.814 | 0.014 | 0.09761 | 0.0014 | 0.14574 | 0.0606 | 0.0011 | 0.28686 | 0.0303 | 0.0026 | 603.8 | 8 | 600.3 | 8.3 | 602 | 51 | 608 | 39 | 321 | 6.1 | 9.9 | 0.23 | 2.81 | 0.22 | 32.59 | 0.54 |
| GJ1 - 1 | 0.807 | 0.04 | 0.09757 | 0.0043 | 0.03884 | 0.0617 | 0.0014 | 0.27618 | 0.0307 | 0.003 | 599.3 | 23 | 600.1 | 25 | 609 | 59 | 642 | 50 | 473.6 | 9.2 | 11.19 | 0.27 | 2.79 | 0.22 | 33.44 | 0.5 |
| GJ1 - 10 | 0.797 | 0.021 | 0.0975 | 0.0018 | 0.10902 | 0.0599 | 0.0013 | 0.23973 | 0.0304 | 0.0031 | 593.7 | 12 | 599.7 | 11 | 602 | 60 | 575 | 49 | 314 | 7.1 | 9.88 | 0.26 | 2.86 | 0.23 | 32.06 | 0.52 |
| GJ1 - 10 | 0.812 | 0.015 | 0.09811 | 0.0015 | 0.094649 | 0.06 | 0.0012 | 0.25911 | 0.0291 | 0.0027 | 603.3 | 8.8 | 603.3 | 8.6 | 578 | 53 | 596 | 44 | 341.2 | 7 | 11.03 | 0.27 | 3.02 | 0.27 | 31.14 | 0.47 |
| GJ1 - 10 | 0.796 | 0.04 | 0.09751 | 0.0045 | 0.30461 | 0.0593 | 0.0014 | 0.14787 | 0.0298 | 0.0029 | 592.8 | 22 | 599.7 | 26 | 591 | 56 | 555 | 50 | 311.4 | 7.6 | 9.93 | 0.31 | 2.81 | 0.22 | 32.1 | 0.69 |
| GJ1 - 11 | 0.804 | 0.022 | 0.09802 | 0.0018 | 0.16965 | 0.0598 | 0.0014 | 0.14968 | 0.0297 | 0.0029 | 599 | 12 | 602.7 | 11 | 590 | 56 | 567 | 51 | 312.7 | 7 | 9.95 | 0.28 | 2.83 | 0.23 | 31.57 | 0.47 |
| GJ1 - 11 | 0.809 | 0.016 | 0.09688 | 0.0014 | 0.10868 | 0.0606 | 0.0012 | 0.22765 | 0.0304 | 0.0031 | 601.7 | 9.3 | 596.1 | 8.2 | 602 | 60 | 616 | 45 | 353.1 | 7.1 | 11.26 | 0.28 | 3.25 | 0.3 | 31.49 | 0.45 |
| GJ1 - 11 | 0.82 | 0.043 | 0.0977 | 0.0046 | 0.31996 | 0.0602 | 0.0014 | 0.205 | 0.0308 | 0.0032 | 608 | 24 | 600.7 | 27 | 611 | 63 | 603 | 51 | 312.1 | 7.5 | 9.9 | 0.34 | 2.98 | 0.24 | 32.11 | 0.84 |
| GJ1 - 12 | 0.819 | 0.02 | 0.09778 | 0.0018 | 0.22393 | 0.0604 | 0.0012 | 0.17634 | 0.0298 | 0.0029 | 607.3 | 12 | 601.3 | 10 | 597 | 58 | 602 | 44 | 301.5 | 7 | 9.49 | 0.28 | 2.62 | 0.21 | 32.08 | 0.53 |
| GJ1 - 12 | 0.798 | 0.018 | 0.09654 | 0.0014 | 0.23079 | 0.06 | 0.0013 | 0.084028 | 0.0301 | 0.0026 | 594 | 10 | 594 | 8.5 | 596 | 52 | 584 | 46 | 351.6 | 8.5 | 11.44 | 0.32 | 3.29 | 0.26 | 30.91 | 0.49 |
| GJ1 - 12 | 0.814 | 0.041 | 0.098 | 0.0046 | 0.33922 | 0.0596 | 0.0015 | 0.14463 | 0.0299 | 0.0029 | 604 | 22 | 602.5 | 27 | 594 | 56 | 564 | 53 | 316.3 | 8.5 | 10.12 | 0.32 | 2.91 | 0.22 | 30.95 | 0.69 |

ACCEPTED MANUSCRIPT

| | | | | | | | | | | | | | | | | | | | | | | | | |
|---|---|---|---|---|---|---|---|---|---|---|---|---|---|---|---|---|---|---|---|---|---|---|---|---|
| GJ1 - 13 | 0.811 | 0.022 | 0.09687 | 0.0018 | 0.042152 | 0.06 | 0.0015 | 0.33675 | 0.0291 | 0.003 | 601 | 12 | 596 | 11 | 577 | 58 | 575 | 54 | 305.7 | 6 | 9.62 | 0.24 | 2.63 | 0.23 | 31.96 | 0.48 |
| GJ1 - 13 | 0.811 | 0.018 | 0.09775 | 0.0014 | 0.062712 | 0.0602 | 0.0013 | 0.27739 | 0.0301 | 0.0028 | 602 | 10 | 601.2 | 8.2 | 597 | 56 | 586 | 49 | 347.8 | 7.6 | 11.37 | 0.29 | 3.34 | 0.28 | 30.59 | 0.45 |
| GJ1 - 13 | 0.806 | 0.04 | 0.0971 | 0.0046 | 0.41503 | 0.0603 | 0.0013 | 0.15521 | 0.0303 | 0.0033 | 598.8 | 22 | 597.5 | 27 | 601 | 65 | 602 | 46 | 314.9 | 8.4 | 9.66 | 0.34 | 2.76 | 0.25 | 31.91 | 0.81 |
| GJ1 - 14 | 0.829 | 0.02 | 0.09859 | 0.0018 | 0.049349 | 0.0605 | 0.0013 | 0.29254 | 0.0316 | 0.0031 | 611.9 | 11 | 606.1 | 10 | 626 | 61 | 597 | 47 | 297.5 | 6.9 | 9.47 | 0.24 | 2.75 | 0.24 | 31.43 | 0.48 |
| GJ1 - 14 | 0.804 | 0.016 | 0.0976 | 0.0015 | 0.19107 | 0.0602 | 0.0012 | 0.21021 | 0.03 | 0.0024 | 599.8 | 9 | 600.3 | 8.9 | 596 | 48 | 591 | 43 | 348.9 | 7.3 | 11.5 | 0.3 | 3.43 | 0.25 | 30.48 | 0.45 |
| GJ1 - 14 | 0.806 | 0.041 | 0.0977 | 0.0046 | 0.36549 | 0.06 | 0.0015 | 0.083396 | 0.0294 | 0.0031 | 598 | 23 | 600.6 | 27 | 583 | 62 | 582 | 54 | 322.1 | 7.3 | 10.06 | 0.3 | 2.76 | 0.24 | 31.35 | 0.76 |
| GJ1 - 15 | 0.798 | 0.02 | 0.09712 | 0.0018 | 0.22069 | 0.0599 | 0.0012 | 0.16277 | 0.0303 | 0.0029 | 594.3 | 11 | 597.4 | 11 | 602 | 57 | 577 | 45 | 308.8 | 6.4 | 9.64 | 0.27 | 2.67 | 0.21 | 32.14 | 0.46 |
| GJ1 - 15 | 0.812 | 0.017 | 0.09701 | 0.0014 | 0.016686 | 0.0608 | 0.0013 | 0.32076 | 0.0311 | 0.0026 | 602.1 | 9.6 | 596.8 | 8.3 | 618 | 52 | 607 | 48 | 349.1 | 7.7 | 11.22 | 0.3 | 3.41 | 0.26 | 31.22 | 0.46 |
| GJ1 - 15 | 0.816 | 0.042 | 0.0977 | 0.0046 | 0.40421 | 0.0606 | 0.0016 | 0.078582 | 0.0306 | 0.0033 | 604 | 24 | 600.8 | 27 | 607 | 65 | 604 | 55 | 314.2 | 8.1 | 9.48 | 0.35 | 2.73 | 0.22 | 33.25 | 0.96 |
| GJ1 - 16 | 0.795 | 0.02 | 0.09748 | 0.0017 | 0.15657 | 0.0599 | 0.0012 | 0.22122 | 0.0331 | 0.0032 | 592.2 | 12 | 599.6 | 9.9 | 655 | 62 | 585 | 46 | 312.8 | 7.2 | 9.73 | 0.27 | 2.89 | 0.22 | 32.16 | 0.47 |
| GJ1 - 16 | 0.809 | 0.019 | 0.09728 | 0.0015 | 0.17176 | 0.0603 | 0.0014 | 0.13837 | 0.0291 | 0.0022 | 600 | 11 | 598.4 | 8.6 | 583 | 45 | 595 | 50 | 346.4 | 7.2 | 11.23 | 0.28 | 3.12 | 0.21 | 31.04 | 0.49 |
| GJ1 - 16 | 0.81 | 0.042 | 0.0977 | 0.0046 | 0.32548 | 0.0599 | 0.0015 | 0.14322 | 0.0306 | 0.0035 | 600 | 23 | 600.6 | 27 | 607 | 69 | 579 | 57 | 333.5 | 7.1 | 10.48 | 0.36 | 2.99 | 0.25 | 32.09 | 0.9 |
| GJ1 - 17 | 0.806 | 0.02 | 0.09759 | 0.0017 | 0.028225 | 0.0605 | 0.0013 | 0.32987 | 0.0269 | 0.0028 | 599.1 | 11 | 600.2 | 10 | 535 | 54 | 605 | 45 | 305 | 6.6 | 9.53 | 0.24 | 2.35 | 0.2 | 32.09 | 0.51 |
| GJ1 - 17 | 0.804 | 0.017 | 0.09868 | 0.0015 | 0.10991 | 0.0592 | 0.0013 | 0.25662 | 0.0307 | 0.0028 | 597.5 | 9.6 | 606.6 | 8.6 | 609 | 54 | 555 | 49 | 339.2 | 7.9 | 10.97 | 0.31 | 3.16 | 0.26 | 31.03 | 0.47 |
| GJ1 - 17 | 0.81 | 0.042 | 0.0975 | 0.0046 | 0.42166 | 0.0601 | 0.0014 | 0.11831 | 0.0293 | 0.0033 | 602 | 24 | 599.5 | 27 | 581 | 64 | 598 | 54 | 337.2 | 8.7 | 10.64 | 0.35 | 2.76 | 0.25 | 31.95 | 0.8 |
| GJ1 - 18 | 0.799 | 0.021 | 0.09761 | 0.0018 | 0.14883 | 0.0598 | 0.0013 | 0.20325 | 0.0303 | 0.003 | 594 | 12 | 600.3 | 11 | 601 | 59 | 569 | 50 | 310.5 | 6.7 | 9.78 | 0.23 | 2.72 | 0.22 | 31.67 | 0.49 |
| GJ1 - 18 | 0.801 | 0.018 | 0.097 | 0.0014 | 0.033422 | 0.0598 | 0.0014 | 0.24568 | 0.0308 | 0.0026 | 597 | 10 | 596.7 | 8.1 | 610 | 50 | 575 | 52 | 339.3 | 7.1 | 10.92 | 0.25 | 3.13 | 0.24 | 31.25 | 0.51 |
| GJ1 - 18 | 0.807 | 0.041 | 0.0977 | 0.0046 | 0.39819 | 0.0602 | 0.0014 | 0.067988 | 0.0305 | 0.003 | 599 | 23 | 600.7 | 27 | 606 | 58 | 586 | 53 | 336.2 | 8.6 | 10.52 | 0.35 | 2.84 | 0.23 | 32.53 | 0.97 |
| GJ1 - 19 | 0.816 | 0.021 | 0.09785 | 0.0018 | 0.062314 | 0.0604 | 0.0013 | 0.32402 | 0.0295 | 0.003 | 604.4 | 12 | 601.8 | 10 | 585 | 58 | 594 | 48 | 315.9 | 7 | 9.99 | 0.27 | 2.73 | 0.23 | 31.58 | 0.45 |
| GJ1 - 19 | 0.8 | 0.017 | 0.09726 | 0.0014 | 0.097823 | 0.0598 | 0.0014 | 0.35465 | 0.0301 | 0.0027 | 595.4 | 9.7 | 598.3 | 8.3 | 598 | 53 | 570 | 50 | 334.7 | 6.3 | 10.67 | 0.25 | 2.95 | 0.25 | 31.63 | 0.49 |
| GJ1 - 19 | 0.812 | 0.042 | 0.0979 | 0.0046 | 0.44836 | 0.0608 | 0.0015 | 0.12913 | 0.0299 | 0.0032 | 602 | 23 | 601.8 | 27 | 607 | 67 | 610 | 51 | 331.2 | 8.3 | 10.06 | 0.39 | 2.65 | 0.24 | 33.7 | 1.1 |
| GJ1 - 2 | 0.809 | 0.021 | 0.09756 | 0.0017 | 0.096566 | 0.0601 | 0.0013 | 0.23542 | 0.0294 | 0.0029 | 600.2 | 12 | 600.1 | 10 | 584 | 56 | 588 | 48 | 302.8 | 6.7 | 9.48 | 0.25 | 2.65 | 0.2 | 32.14 | 0.58 |
| GJ1 - 2 | 0.81 | 0.019 | 0.09829 | 0.0015 | 0.12019 | 0.0596 | 0.0014 | 0.17347 | 0.0293 | 0.0027 | 600 | 11 | 604.3 | 8.6 | 582 | 54 | 566 | 52 | 327.8 | 6.5 | 10.22 | 0.24 | 2.83 | 0.24 | 32.13 | 0.47 |
| GJ1 - 2 | 0.809 | 0.04 | 0.09762 | 0.0047 | 0.19934 | 0.0598 | 0.0014 | 0.14305 | 0.0291 | 0.0028 | 600.7 | 22 | 600.4 | 27 | 578 | 55 | 577 | 48 | 389.3 | 8.7 | 10.37 | 0.28 | 2.55 | 0.21 | 31.4 | 0.57 |
| GJ1 - 20 | 0.81 | 0.02 | 0.09739 | 0.0018 | 0.13462 | 0.0601 | 0.0012 | 0.24835 | 0.031 | 0.0031 | 601.2 | 11 | 599 | 11 | 614 | 61 | 592 | 45 | 315.3 | 7 | 10.07 | 0.29 | 2.88 | 0.24 | 31.22 | 0.49 |
| GJ1 - 20 | 0.819 | 0.017 | 0.09881 | 0.0015 | 0.010659 | 0.06 | 0.0012 | 0.34871 | 0.0294 | 0.0026 | 605.9 | 9.3 | 607.4 | 8.6 | 583 | 51 | 593 | 48 | 324.3 | 7.3 | 10.45 | 0.29 | 2.74 | 0.24 | 31.23 | 0.49 |
| GJ1 - 20 | 0.806 | 0.041 | 0.0968 | 0.0045 | 0.35369 | 0.0612 | 0.0015 | 0.16072 | 0.03 | 0.0031 | 598 | 23 | 595.6 | 27 | 595 | 61 | 622 | 54 | 335.8 | 8.7 | 10.31 | 0.37 | 2.79 | 0.25 | 32.94 | 0.82 |
| GJ1 - 21 | 0.817 | 0.02 | 0.09768 | 0.0017 | 0.01611 | 0.0601 | 0.0013 | 0.34732 | 0.0305 | 0.003 | 604.8 | 11 | 600.7 | 10 | 605 | 59 | 583 | 47 | 326.1 | 8 | 10.25 | 0.31 | 2.98 | 0.24 | 31.66 | 0.54 |
| GJ1 - 21 | 0.82 | 0.015 | 0.09793 | 0.0014 | 0.14025 | 0.061 | 0.0011 | 0.20445 | 0.0293 | 0.0028 | 607.9 | 8.2 | 602.2 | 8.1 | 582 | 56 | 621 | 40 | 329.7 | 6.8 | 10.39 | 0.26 | 2.76 | 0.26 | 32.03 | 0.56 |
| GJ1 - 21 | 0.809 | 0.042 | 0.0993 | 0.0047 | 0.55317 | 0.0595 | 0.0014 | 0.036829 | 0.0304 | 0.0032 | 600 | 24 | 610.1 | 28 | 602 | 63 | 561 | 52 | 312.2 | 8.5 | 9.91 | 0.33 | 2.78 | 0.24 | 31.55 | 0.95 |
| GJ1 - 22 | 0.805 | 0.018 | 0.09692 | 0.0014 | 0.082758 | 0.0604 | 0.0014 | 0.24201 | 0.0312 | 0.0027 | 599 | 9.9 | 596.3 | 8.2 | 619 | 54 | 599 | 49 | 323.6 | 6.3 | 10.1 | 0.26 | 2.96 | 0.24 | 32.17 | 0.55 |
| GJ1 - 22 | 0.793 | 0.043 | 0.096 | 0.0046 | 0.55307 | 0.0601 | 0.0016 | -0.09997 | 0.0298 | 0.0034 | 590 | 24 | 590.7 | 27 | 591 | 66 | 579 | 57 | 320.4 | 8.4 | 9.75 | 0.33 | 2.63 | 0.24 | 33 | 1.1 |
| GJ1 - 23 | 0.815 | 0.015 | 0.09895 | 0.0015 | 0.040211 | 0.0597 | 0.0012 | 0.33761 | 0.0299 | 0.0025 | 604 | 8.6 | 608.2 | 8.5 | 600 | 49 | 584 | 42 | 311.9 | 6.9 | 9.63 | 0.25 | 2.77 | 0.2 | 32.63 | 0.5 |
| GJ1 - 23 | 0.8 | 0.041 | 0.0972 | 0.0046 | 0.31888 | 0.0595 | 0.0015 | 0.20166 | 0.0306 | 0.0031 | 596 | 24 | 597.8 | 27 | 607 | 61 | 572 | 55 | 305.5 | 7.1 | 9.48 | 0.33 | 2.64 | 0.21 | 32.61 | 0.97 |
| GJ1 - 24 | 0.831 | 0.042 | 0.0992 | 0.0047 | 0.47511 | 0.0604 | 0.0014 | 0.22677 | 0.0298 | 0.003 | 612 | 23 | 609.2 | 28 | 592 | 60 | 596 | 50 | 300.9 | 8 | 9.39 | 0.32 | 2.57 | 0.21 | 32.02 | 0.98 |
| GJ1 - 3 | 0.808 | 0.021 | 0.09766 | 0.0018 | 0.071119 | 0.0602 | 0.0014 | 0.35388 | 0.0307 | 0.003 | 599.5 | 12 | 600.6 | 10 | 615 | 58 | 592 | 51 | 308.7 | 6.6 | 9.76 | 0.27 | 2.88 | 0.22 | 31.88 | 0.55 |
| GJ1 - 3 | 0.811 | 0.018 | 0.09743 | 0.0015 | 0.12504 | 0.0603 | 0.0013 | 0.23475 | 0.03 | 0.0027 | 601 | 10 | 599.3 | 8.8 | 596 | 52 | 599 | 47 | 317.8 | 6.3 | 9.88 | 0.24 | 2.88 | 0.22 | 32.2 | 0.45 |
| GJ1 - 3 | 0.813 | 0.04 | 0.09758 | 0.0046 | 0.22833 | 0.0599 | 0.0014 | 0.16763 | 0.0307 | 0.0029 | 603 | 23 | 600.2 | 27 | 609 | 58 | 583 | 50 | 336.1 | 7.3 | 9.92 | 0.29 | 2.91 | 0.23 | 31.18 | 0.59 |
| GJ1 - 4 | 0.802 | 0.02 | 0.0978 | 0.0018 | 0.12971 | 0.0598 | 0.0013 | 0.25143 | 0.0305 | 0.0029 | 596.2 | 12 | 601.5 | 10 | 606 | 57 | 570 | 48 | 300.6 | 6 | 9.51 | 0.25 | 2.81 | 0.21 | 31.92 | 0.49 |
| GJ1 - 4 | 0.802 | 0.017 | 0.09833 | 0.0015 | 0.013864 | 0.0592 | 0.0013 | 0.34459 | 0.031 | 0.0027 | 596.6 | 9.6 | 604.6 | 8.8 | 615 | 52 | 550 | 50 | 323.8 | 6.8 | 10.06 | 0.25 | 3.05 | 0.22 | 32.4 | 0.48 |
| GJ1 - 4 | 0.813 | 0.04 | 0.09763 | 0.0045 | -0.10892 | 0.0601 | 0.0013 | 0.45376 | 0.03 | 0.0029 | 602.9 | 22 | 600.5 | 27 | 596 | 57 | 592 | 50 | 290.2 | 6.2 | 9.18 | 0.25 | 2.83 | 0.21 | 32.14 | 0.63 |
| GJ1 - 5 | 0.813 | 0.022 | 0.09744 | 0.0018 | 0.032938 | 0.0607 | 0.0014 | 0.25036 | 0.0305 | 0.003 | 602 | 12 | 599.3 | 10 | 606 | 59 | 600 | 53 | 312.7 | 7 | 9.7 | 0.27 | 2.9 | 0.23 | 32.55 | 0.56 |
| GJ1 - 5 | 0.812 | 0.017 | 0.09803 | 0.0014 | 0.015862 | 0.06 | 0.0013 | 0.33293 | 0.0305 | 0.0027 | 601.7 | 9.5 | 602.8 | 8.4 | 606 | 53 | 580 | 48 | 332.8 | 6.3 | 10.53 | 0.27 | 3.09 | 0.24 | 31.87 | 0.57 |
| GJ1 - 5 | 0.802 | 0.041 | 0.09766 | 0.0045 | 0.27919 | 0.0594 | 0.0014 | 0.11176 | 0.0305 | 0.0029 | 596 | 23 | 600.6 | 26 | 606 | 58 | 559 | 52 | 291 | 6.5 | 9.34 | 0.24 | 2.88 | 0.22 | 32.56 | 0.59 |
| GJ1 - 6 | 0.807 | 0.022 | 0.09755 | 0.0018 | 0.27755 | 0.06 | 0.0013 | 0.056463 | 0.0309 | 0.0032 | 599 | 12 | 600 | 10 | 613 | 63 | 581 | 48 | 310.6 | 7 | 9.67 | 0.24 | 2.94 | 0.25 | 32.21 | 0.44 |
| GJ1 - 6 | 0.81 | 0.019 | 0.09708 | 0.0015 | 0.1191 | 0.0603 | 0.0014 | 0.20049 | 0.0296 | 0.0025 | 602 | 11 | 597.2 | 8.7 | 589 | 49 | 600 | 52 | 329.5 | 6.9 | 10.52 | 0.25 | 2.91 | 0.22 | 31.36 | 0.46 |
| GJ1 - 6 | 0.811 | 0.041 | 0.0974 | 0.0045 | 0.072265 | 0.0609 | 0.0015 | 0.38481 | 0.0294 | 0.003 | 601.6 | 23 | 599.1 | 26 | 583 | 59 | 610 | 52 | 282 | 5.3 | 9.15 | 0.26 | 2.51 | 0.22 | 32.5 | 0.66 |
| GJ1 - 7 | 0.81 | 0.02 | 0.09769 | 0.0017 | 0.029711 | 0.0599 | 0.0012 | 0.30324 | 0.0313 | 0.003 | 601.3 | 11 | 600.8 | 9.9 | 620 | 60 | 586 | 45 | 309.5 | 6.7 | 9.75 | 0.27 | 2.9 | 0.22 | 32.2 | 0.58 |
| GJ1 - 7 | 0.826 | 0.019 | 0.09793 | 0.0015 | 0.18154 | 0.0612 | 0.0013 | 0.15814 | 0.0296 | 0.003 | 610 | 10 | 602.2 | 8.5 | 587 | 59 | 624 | 47 | 329.1 | 8.1 | 10.55 | 0.31 | 2.77 | 0.26 | 31.44 | 0.49 |
| GJ1 - 7 | 0.81 | 0.039 | 0.09782 | 0.0045 | 0.25743 | 0.0594 | 0.0013 | 0.1978 | 0.0302 | 0.0031 | 601 | 22 | 601.6 | 26 | 600 | 61 | 573 | 48 | 283.1 | 5.8 | 9.4 | 0.27 | 2.73 | 0.23 | 31.72 | 0.67 |
| GJ1 - 8 | 0.819 | 0.02 | 0.09813 | 0.0018 | 0.16882 | 0.0602 | 0.0012 | 0.2075 | 0.0302 | 0.0029 | 605.8 | 11 | 603.4 | 11 | 600 | 57 | 591 | 43 | 312.6 | 7.1 | 9.96 | 0.27 | 2.96 | 0.24 | 31.71 | 0.48 |
| GJ1 - 8 | 0.796 | 0.018 | 0.09747 | 0.0014 | 0.13257 | 0.0592 | 0.0013 | 0.17403 | 0.0294 | 0.0025 | 592.8 | 9.9 | 599.5 | 8.4 | 583 | 50 | 550 | 48 | 339.7 | 7 | 10.87 | 0.29 | 2.93 | 0.24 | 31.49 | 0.45 |
| GJ1 - 8 | 0.808 | 0.041 | 0.09754 | 0.0045 | 0.31698 | 0.0599 | 0.0014 | 0.11964 | 0.0307 | 0.0031 | 599 | 23 | 599.9 | 27 | 608 | 61 | 583 | 52 | 291.6 | 6.1 | 9.16 | 0.26 | 2.8 | 0.22 | 33.32 | 0.78 |
| GJ1 - 9 | 0.807 | 0.021 | 0.09708 | 0.0018 | 0.064812 | 0.0606 | 0.0014 | 0.26057 | 0.0284 | 0.003 | 599 | 12 | 597.3 | 10 | 564 | 58 | 599 | 49 | 314.2 | 7.3 | 9.92 | 0.25 | 2.7 | 0.24 | 31.87 | 0.48 |
| GJ1 - 9 | 0.807 | 0.02 | 0.09685 | 0.0014 | 0.20869 | 0.0604 | 0.0014 | 0.094977 | 0.0322 | 0.0029 | 600 | 11 | 595.9 | 8.5 | 638 | 56 | 595 | 53 | 343.6 | 6.9 | 10.83 | 0.27 | 3.19 | 0.26 | 31.95 | 0.49 |
| GJ1 - 9 | 0.815 | 0.041 | 0.0976 | 0.0045 | 0.37826 | 0.0612 | 0.0014 | 0.11592 | 0.0298 | 0.003 | 605 | 22 | 600 | 27 | 592 | 59 | 624 | 50 | 301.1 | 6.9 | 9.59 | 0.26 | 2.67 | 0.21 | 32.41 | 0.67 |
| Mudtank - | 1.16 | 0.17 | 0.1161 | 0.0056 | 0.089146 | 0.077 | 0.012 | 0.28148 | 0.0409 | 0.0071 | 702 | 80 | 706 | 32 | 790 | 130 | 560 | 280 | 6.77 | 0.11 | 2.533 | 0.075 | 0.92 | 0.15 | 2.729 | 0.091 |
| Mudtank - | 1.06 | 0.15 | 0.118 | 0.0069 | 0.096207 | 0.064 | 0.0089 | 0.17972 | 0.0374 | 0.0064 | 642 | 86 | 717 | 40 | 730 | 120 | 420 | 260 | 7.76 | 0.17 | 2.531 | 0.081 | 0.81 | 0.13 | 2.72 | 0.098 |
| Mudtank - | 0.82 | 0.16 | 0.1154 | 0.0048 | -0.01478 | 0.054 | 0.011 | 0.25387 | 0.0312 | 0.0066 | 460 | 110 | 702 | 28 | 610 | 130 | 0 | 310 | 7.29 | 0.15 | 2.723 | 0.084 | 0.82 | 0.17 | 2.744 | 0.083 |
| Mudtank - | 1.02 | 0.16 | 0.1196 | 0.0074 | 0.055093 | 0.0605 | 0.0097 | -0.01961 | 0.0385 | 0.007 | 605 | 85 | 726 | 42 | 750 | 130 | 230 | 270 | 6.48 | 0.17 | 2.251 | 0.087 | 0.8 | 0.13 | 2.8 | 0.12 |
| Mudtank - | 1.01 | 0.18 | 0.1164 | 0.0053 | 0.088091 | 0.066 | 0.011 | 0.2643 | 0.0363 | 0.007 | 560 | 100 | 712 | 31 | 710 | 130 | 230 | 300 | 7.24 | 0.19 | 2.752 | 0.099 | 0.95 | 0.16 | 2.691 | 0.091 |
| Mudtank - | 0.99 | 0.14 | 0.1149 | 0.0069 | 0.10536 | 0.0641 | 0.0087 | 0.19838 | 0.0391 | 0.0059 | 624 | 76 | 699 | 40 | 770 | 110 | 360 | 240 | 6.48 | 0.15 | 2.417 | 0.084 | 0.95 | 0.13 | 2.78 | 0.11 |
| Mudtank - | 1.17 | 0.16 | 0.1181 | 0.007 | 0.12271 | 0.0718 | 0.0092 | 0.18105 | 0.0349 | 0.0063 | 712 | 82 | 718 | 40 | 680 | 120 | 600 | 250 | 6.9 | 0.33 | 2.66 | 0.14 | 0.86 | 0.14 | 2.81 | 0.15 |
| Plesovice - | 0.3939 | 0.0092 | 0.05335 | 0.00097 | 0.18855 | 0.05301 | 0.00098 | 0.2364 | 0.01771 | 0.0012 | 336.8 | 6.7 | 335 | 5.9 | 355 | 24 | 319 | 41 | 705 | 17 | 70.2 | 1.8 | 11.79 | 0.48 | 10.04 | 0.11 |
| Plesovice - | 0.3858 | 0.0093 | 0.05347 | 0.00079 | 0.11909 | 0.0521 | 0.0012 | 0.18782 | 0.01671 | 0.00085 | 330.5 | 6.9 | 335.8 | 4.9 | 335 | 17 | 282 | 52 | 579 | 11 | 53.04 | 0.98 | 8.38 | 0.36 | 10.891 | 0.091 |
| Plesovice - | 0.3889 | 0.02 | 0.05376 | 0.0026 | 0.11332 | 0.0525 | 0.0012 | 0.24071 | 0.01696 | 0.0011 | 333.7 | 14 | 337.6 | 16 | 340 | 22 | 297 | 51 | 904 | 22 | 73.9 | 2 | 10.42 | 0.42 | 9.974 | 0.087 |
| Plesovice - | 0.4042 | 0.021 | 0.05375 | 0.0021 | 0.19472 | 0.0545 | 0.0012 | 0.11618 | 0.01765 | 0.00069 | 344 | 15 | 337.5 | 13 | 353 | 14 | 371 | 50 | 755 | 12 | 78 | 1.2 | 39 | 1.6 | 10.008 | 0.086 |
| Plesovice - | 0.3909 | 0.02 | 0.05417 | 0.0025 | 0.43243 | 0.0525 | 0.0013 | 0.10223 | 0.01722 | 0.0013 | 334.3 | 15 | 340 | 16 | 345 | 25 | 289 | 52 | 642 | 13 | 61.1 | 1.2 | 9.46 | 0.43 | 10.51 | 0.15 |
| Plesovice - | 0.3991 | 0.02 | 0.0552 | 0.0026 | 0.32494 | 0.0532 | 0.0012 | 0.25567 | 0.01661 | 0.0012 | 340.3 | 15 | 346.3 | 16 | 333 | 24 | 321 | 51 | 703 | 15 | 70.3 | 1.6 | 10.48 | 0.47 | 9.96 | 0.16 |
| Plesovice - | 0.406 | 0.021 | 0.05577 | 0.0027 | 0.46502 | 0.0533 | 0.0014 | 0.11416 | 0.01628 | 0.0012 | 344.8 | 15 | 349.8 | 16 | 326 | 24 | 320 | 56 | 672 | 16 | 71 | 1.7 | 10.73 | 0.48 | 9.49 | 0.18 |
| Plesovice - | 0.4074 | 0.011 | 0.0535 | 0.00095 | 0.12576 | 0.0556 | 0.0012 | 0.21936 | 0.01637 | 0.0011 | 346.3 | 7.7 | 336 | 5.8 | 328 | 23 | 412 | 49 | 533.2 | 7.8 | 52.16 | 0.54 | 8.42 | 0.37 | 10.26 | 0.1 |
| Plesovice - | 0.4386 | 0.01 | 0.05384 | 0.00078 | -0.03978 | 0.0588 | 0.0013 | 0.35599 | 0.0227 | 0.0013 | 368.4 | 7 | 338.1 | 4.8 | 453 | 27 | 545 | 50 | 706 | 16 | 69.2 | 1.5 | 15.21 | 0.66 | 10.219 | 0.087 |
| Plesovice - | 0.4021 | 0.02 | 0.05425 | 0.0026 | 0.30911 | 0.053 | 0.0012 | 0.079703 | 0.01769 | 0.0012 | 342.6 | 15 | 340.5 | 16 | 354 | 24 | 317 | 49 | 763 | 19 | 70.6 | 2 | 11.21 | 0.45 | 9.55 | 0.11 |
| Plesovice - | 0.3859 | 0.02 | 0.05315 | 0.0021 | 0.18286 | 0.0526 | 0.0011 | 0.18773 | 0.01622 | 0.00056 | 330.8 | 15 | 333.8 | 13 | 325 | 11 | 306 | 47 | 755 | 21 | 78.1 | 2.2 | 39 | 1.5 | 9.374 | 0.095 |
| Plesovice - | 0.3895 | 0.0095 | 0.05377 | 0.00093 | 0.001402 | 0.0524 | 0.0011 | 0.32151 | 0.01631 | 0.0011 | 333.5 | 6.9 | 337.6 | 5.7 | 327 | 22 | 287 | 45 | 680 | 17 | 67.2 | 1.6 | 10.8 | 0.47 | 10.155 | 0.091 |
| Plesovice - | 0.3957 | 0.0085 | 0.054 | 0.00081 | -0.02999 | 0.0531 | 0.0012 | 0.37872 | 0.01664 | 0.00093 | 337.9 | 6.1 | 339 | 4.9 | 333 | 18 | 318 | 48 | 579.1 | 9.9 | 57.55 | 0.79 | 9.14 | 0.41 | 10.03 | 0.1 |

ACCEPTED MANUSCRIPT

| | | | | | | | | | | | | | | | | | | | | | | | | | | |
|---|---|---|---|---|---|---|---|---|---|---|---|---|---|---|---|---|---|---|---|---|---|---|---|---|---|---|
| Plesovice - | 0.3914 | 0.02 | 0.05334 | 0.0024 | 0.17504 | 0.0526 | 0.0012 | 0.16436 | 0.01573 | 0.0011 | 335.6 | 14 | 335 | 15 | 315 | 21 | 305 | 50 | 724 | 18 | 70.6 | 1.9 | 10.92 | 0.42 | 9.689 | 0.088 |
| Plesovice - | 0.3906 | 0.02 | 0.05343 | 0.0021 | 0.18433 | 0.053 | 0.0011 | 0.25569 | 0.01687 | 0.00064 | 334.3 | 15 | 335.5 | 13 | 338 | 13 | 322 | 46 | 757 | 23 | 77.9 | 2.9 | 39.1 | 1.9 | 9.82 | 0.12 |
| Plesovice - | 0.3866 | 0.011 | 0.0541 | 0.00097 | 0.22063 | 0.0521 | 0.0012 | 0.098467 | 0.01631 | 0.0012 | 331.1 | 7.7 | 339.6 | 5.9 | 327 | 24 | 276 | 49 | 636 | 15 | 60.8 | 1.5 | 9.57 | 0.5 | 10.478 | 0.082 |
| Plesovice - | 0.4005 | 0.0095 | 0.05354 | 0.0008 | 0.089796 | 0.0543 | 0.0013 | 0.25188 | 0.017 | 0.00089 | 341.2 | 6.8 | 336.2 | 4.9 | 341 | 18 | 367 | 52 | 644 | 17 | 65.2 | 1.8 | 10.9 | 0.47 | 9.869 | 0.079 |
| Plesovice - | 0.3876 | 0.019 | 0.05235 | 0.0024 | 0.10911 | 0.0533 | 0.0012 | 0.27444 | 0.01585 | 0.0011 | 332.1 | 14 | 328.9 | 15 | 318 | 21 | 326 | 51 | 672 | 18 | 68.5 | 2 | 11.35 | 0.44 | 9.971 | 0.093 |
| Plesovice - | 0.3977 | 0.021 | 0.0526 | 0.0021 | 0.30331 | 0.0548 | 0.0012 | 0.14264 | 0.01637 | 0.00065 | 339.4 | 15 | 330.5 | 13 | 328 | 13 | 386 | 47 | 752 | 19 | 78.1 | 2.2 | 38.9 | 1.8 | 9.33 | 0.1 |
| Plesovice - | 0.3913 | 0.011 | 0.05331 | 0.00094 | 0.1347 | 0.0523 | 0.0012 | 0.18907 | 0.01738 | 0.0012 | 334.6 | 7.8 | 334.8 | 5.8 | 348 | 24 | 288 | 50 | 635 | 15 | 60.8 | 1.4 | 9.85 | 0.44 | 10.423 | 0.082 |
| Plesovice - | 0.3928 | 0.0073 | 0.05311 | 0.00076 | -0.02977 | 0.0538 | 0.0011 | 0.3613 | 0.01601 | 0.00074 | 335.9 | 5.3 | 333.6 | 4.7 | 321 | 15 | 347 | 44 | 803 | 21 | 83.9 | 2.3 | 13.03 | 0.53 | 9.574 | 0.088 |
| Plesovice - | 0.3862 | 0.019 | 0.05241 | 0.0024 | 0.26645 | 0.0536 | 0.0013 | 0.11671 | 0.01706 | 0.0012 | 330.9 | 14 | 329.3 | 15 | 342 | 23 | 336 | 51 | 627 | 17 | 64.8 | 1.9 | 10.29 | 0.45 | 10.09 | 0.11 |
| Plesovice - | 0.3865 | 0.02 | 0.05211 | 0.0021 | 0.36639 | 0.0537 | 0.0012 | 0.088697 | 0.01677 | 0.00063 | 331.1 | 15 | 327.4 | 13 | 336 | 12 | 343 | 47 | 755 | 17 | 77.7 | 2.1 | 38.9 | 1.7 | 9.64 | 0.12 |
| Plesovice - | 0.3867 | 0.011 | 0.0533 | 0.00092 | 0.067492 | 0.0534 | 0.0013 | 0.3224 | 0.01581 | 0.0011 | 332 | 7.8 | 334.7 | 5.6 | 317 | 22 | 326 | 54 | 629 | 11 | 59.6 | 1 | 8.64 | 0.35 | 10.484 | 0.082 |
| Plesovice - | 0.394 | 0.0083 | 0.05378 | 0.00081 | 0.25592 | 0.0532 | 0.0011 | 0.095517 | 0.01615 | 0.00083 | 336.6 | 6.2 | 337.7 | 4.9 | 324 | 17 | 317 | 46 | 706 | 21 | 70.3 | 2.4 | 10.78 | 0.47 | 10.03 | 0.1 |
| Plesovice - | 0.3998 | 0.02 | 0.05341 | 0.0025 | 0.19658 | 0.0547 | 0.0013 | 0.26002 | 0.01552 | 0.0011 | 340.8 | 15 | 335.4 | 15 | 311 | 22 | 379 | 53 | 642 | 15 | 64.4 | 1.5 | 9.81 | 0.39 | 10.25 | 0.12 |
| Plesovice - | 0.3922 | 0.02 | 0.0527 | 0.0021 | 0.31995 | 0.0539 | 0.0011 | 0.10268 | 0.01676 | 0.00064 | 335.4 | 15 | 331 | 13 | 336 | 13 | 352 | 47 | 757 | 21 | 78.4 | 2.3 | 39.2 | 1.7 | 9.67 | 0.13 |
| Plesovice - | 0.3922 | 0.011 | 0.05408 | 0.00096 | 0.080774 | 0.0527 | 0.0012 | 0.24153 | 0.0174 | 0.0012 | 335.2 | 7.9 | 339.5 | 5.9 | 349 | 25 | 302 | 51 | 625.9 | 8.7 | 60.34 | 0.85 | 9.61 | 0.41 | 10.311 | 0.083 |
| Plesovice - | 0.4038 | 0.0092 | 0.05401 | 0.00081 | 0.24021 | 0.0542 | 0.0012 | 0.092503 | 0.01676 | 0.00097 | 343.6 | 6.7 | 339.1 | 4.9 | 336 | 19 | 358 | 50 | 544 | 15 | 54.4 | 2.1 | 8.76 | 0.48 | 10.28 | 0.13 |
| Plesovice - | 0.3843 | 0.019 | 0.05117 | 0.0024 | 0.2795 | 0.054 | 0.0013 | 0.15801 | 0.01643 | 0.0012 | 330.3 | 14 | 321.7 | 14 | 329 | 24 | 358 | 53 | 684 | 16 | 65.6 | 1.7 | 10.38 | 0.44 | 10.58 | 0.13 |
| Plesovice - | 0.3871 | 0.02 | 0.05248 | 0.002 | 0.25541 | 0.0535 | 0.0011 | 0.18269 | 0.01688 | 0.00062 | 331.8 | 15 | 329.7 | 12 | 338 | 12 | 334 | 45 | 758 | 21 | 78.2 | 2.3 | 39.2 | 1.7 | 9.77 | 0.11 |
| Plesovice - | 0.3991 | 0.011 | 0.05375 | 0.00094 | 0.053076 | 0.0537 | 0.0012 | 0.2531 | 0.01731 | 0.0012 | 340.3 | 7.7 | 337.5 | 5.8 | 347 | 24 | 335 | 50 | 629 | 15 | 58.7 | 1.4 | 9.52 | 0.43 | 10.663 | 0.091 |
| Plesovice - | 0.3877 | 0.02 | 0.05214 | 0.0024 | 0.35753 | 0.0539 | 0.0013 | 0.13344 | 0.01677 | 0.0012 | 332 | 14 | 327.6 | 15 | 336 | 23 | 350 | 52 | 690 | 15 | 65.8 | 1.5 | 10.53 | 0.45 | 10.11 | 0.14 |
| Plesovice - | 0.3862 | 0.02 | 0.05225 | 0.002 | 0.33507 | 0.0534 | 0.0012 | 0.12151 | 0.017 | 0.0007 | 330.9 | 15 | 328.3 | 12 | 341 | 14 | 331 | 48 | 752 | 18 | 77.7 | 1.7 | 38.6 | 1.6 | 9.56 | 0.11 |
| Plesovice - | 0.394 | 0.0099 | 0.05358 | 0.00094 | 0.17107 | 0.0531 | 0.0011 | 0.15029 | 0.01764 | 0.0013 | 337.4 | 7.4 | 336.5 | 5.7 | 353 | 26 | 317 | 45 | 671 | 22 | 63.2 | 2.2 | 10.64 | 0.58 | 10.569 | 0.091 |
| Plesovice - | 0.4005 | 0.02 | 0.0539 | 0.0025 | 0.25601 | 0.0537 | 0.0013 | 0.21714 | 0.01566 | 0.0011 | 342.1 | 14 | 338.4 | 15 | 314 | 22 | 346 | 54 | 732 | 16 | 73.2 | 1.8 | 11.01 | 0.44 | 9.84 | 0.14 |
| Plesovice - | 0.3932 | 0.021 | 0.05345 | 0.0021 | 0.49695 | 0.0531 | 0.0011 | -0.03749 | 0.01731 | 0.00072 | 336 | 15 | 335.7 | 13 | 347 | 14 | 319 | 47 | 757 | 18 | 78.2 | 2.1 | 39.2 | 1.8 | 10.07 | 0.14 |
| Temora - 1 | 0.488 | 0.024 | 0.06549 | 0.0014 | 0.11303 | 0.0539 | 0.0026 | 0.19008 | 0.01985 | 0.0014 | 400 | 16 | 408.8 | 8.6 | 397 | 27 | 317 | 95 | 93.6 | 2.4 | 47.5 | 1.2 | 8.98 | 0.4 | 1.964 | 0.018 |
| Temora - 1 | 0.516 | 0.032 | 0.0647 | 0.0014 | -0.05654 | 0.0579 | 0.0037 | 0.33478 | 0.0211 | 0.0015 | 414 | 21 | 403.9 | 8.3 | 422 | 31 | 430 | 130 | 65.1 | 1.1 | 24.21 | 0.49 | 4.78 | 0.32 | 2.682 | 0.03 |
| Temora - 1 | 0.531 | 0.031 | 0.0705 | 0.0015 | 0.010366 | 0.0546 | 0.0032 | 0.24567 | 0.0227 | 0.0018 | 425 | 21 | 439 | 9.3 | 453 | 36 | 310 | 110 | 84.2 | 2.5 | 28.53 | 0.97 | 6.16 | 0.39 | 2.943 | 0.038 |
| Temora - 2 | 0.525 | 0.023 | 0.06615 | 0.0013 | 0.025602 | 0.058 | 0.0024 | 0.23737 | 0.02053 | 0.0013 | 427 | 15 | 412.8 | 8.1 | 411 | 27 | 482 | 89 | 123.1 | 3.6 | 73.2 | 2.3 | 14.5 | 0.57 | 1.686 | 0.014 |
| Temora - 2 | 0.529 | 0.038 | 0.0668 | 0.0015 | 0.173 | 0.057 | 0.0039 | 0.059225 | 0.0183 | 0.0015 | 420 | 25 | 416.8 | 9.1 | 366 | 29 | 400 | 140 | 54.8 | 1.2 | 19.63 | 0.47 | 3.57 | 0.25 | 2.805 | 0.037 |
| Temora - 3 | 0.483 | 0.025 | 0.06699 | 0.0014 | 0.17967 | 0.0526 | 0.0026 | 0.081402 | 0.02064 | 0.0014 | 398 | 17 | 417.9 | 8.6 | 413 | 28 | 261 | 96 | 95.7 | 1.9 | 48.63 | 0.97 | 9.85 | 0.4 | 1.973 | 0.016 |
| Temora - 3 | 0.508 | 0.02 | 0.06579 | 0.0011 | 0.063224 | 0.0558 | 0.0021 | 0.2186 | 0.02029 | 0.0011 | 414 | 13 | 410.7 | 6.7 | 406 | 21 | 412 | 79 | 192.2 | 7.6 | 62.8 | 2.5 | 11.67 | 0.61 | 3.068 | 0.028 |
| Temora - 4 | 0.521 | 0.02 | 0.06586 | 0.0013 | 0.17114 | 0.0579 | 0.0021 | 0.10191 | 0.02041 | 0.0013 | 423 | 13 | 411.1 | 7.8 | 408 | 25 | 477 | 75 | 140.9 | 2.6 | 90.6 | 1.6 | 17.83 | 0.58 | 1.557 | 0.011 |
| Temora - 4 | 0.528 | 0.018 | 0.06939 | 0.0012 | 0.16532 | 0.0552 | 0.0018 | 0.15519 | 0.01986 | 0.00087 | 428 | 12 | 432.4 | 6.9 | 397 | 17 | 385 | 70 | 200.3 | 2.4 | 105 | 2.2 | 19.92 | 0.58 | 1.919 | 0.022 |
| Temora - 5 | 0.521 | 0.028 | 0.06565 | 0.0014 | 0.08197 | 0.0579 | 0.0031 | 0.34019 | 0.0207 | 0.0014 | 420 | 19 | 409.8 | 8.7 | 414 | 26 | 430 | 110 | 101.4 | 2.1 | 56.9 | 1.1 | 11.05 | 0.41 | 1.783 | 0.015 |
| Temora - 5 | 11.38 | 0.59 | 0.1629 | 0.0077 | 0.37924 | 0.513 | 0.026 | 0.51711 | 0.1088 | 0.0068 | 2520 | 49 | 968 | 43 | 2080 | 120 | 4228 | 86 | 4.9 | 0.23 | 12.02 | 0.7 | 12.1 | 0.55 | 0.443 | 0.018 |
| Temora - 6 | 0.491 | 0.029 | 0.0661 | 0.0015 | 0.036738 | 0.0531 | 0.0031 | 0.3068 | 0.0221 | 0.0017 | 399 | 20 | 412.4 | 8.8 | 441 | 33 | 280 | 110 | 80.3 | 1.6 | 29.72 | 0.68 | 6.06 | 0.32 | 2.705 | 0.028 |
| Temora - 6 | 0.492 | 0.029 | 0.0643 | 0.0013 | -0.0053 | 0.0558 | 0.0033 | 0.20239 | 0.0199 | 0.0012 | 399 | 20 | 401.6 | 8 | 397 | 23 | 370 | 120 | 92.1 | 2.5 | 35.65 | 0.92 | 6.85 | 0.37 | 2.577 | 0.028 |
| Temora - 7 | 0.522 | 0.029 | 0.0702 | 0.0016 | 0.065496 | 0.0549 | 0.0031 | 0.18761 | 0.0223 | 0.0018 | 420 | 19 | 436.9 | 9.7 | 446 | 35 | 350 | 110 | 77.4 | 2.6 | 24.91 | 0.95 | 5.04 | 0.29 | 3.116 | 0.04 |
| Temora - 7 | 0.5 | 0.02 | 0.06636 | 0.0012 | -0.05741 | 0.055 | 0.0023 | 0.34877 | 0.022 | 0.0012 | 410 | 14 | 414.1 | 7.1 | 439 | 24 | 372 | 89 | 128.3 | 2.7 | 41.62 | 0.98 | 8.46 | 0.42 | 3.092 | 0.03 |
| Temora - 8 | 0.565 | 0.036 | 0.0719 | 0.0018 | 0.22379 | 0.0569 | 0.0034 | 0.12033 | 0.0213 | 0.0022 | 452 | 24 | 447.2 | 11 | 426 | 44 | 410 | 120 | 55.8 | 1.9 | 15.99 | 0.55 | 3.15 | 0.27 | 3.46 | 0.052 |
| Temora - 8 | 0.515 | 0.021 | 0.06652 | 0.0011 | -0.00492 | 0.0565 | 0.0024 | 0.2727 | 0.02047 | 0.0011 | 418 | 14 | 415.1 | 6.8 | 409 | 21 | 415 | 88 | 151.4 | 2.8 | 55.67 | 0.96 | 11.05 | 0.45 | 2.71 | 0.025 |
| Temora - 9 | 0.526 | 0.027 | 0.0709 | 0.0016 | 0.080047 | 0.054 | 0.0028 | 0.34941 | 0.02202 | 0.0016 | 424 | 18 | 441.5 | 9.4 | 440 | 31 | 320 | 100 | 83 | 1.4 | 48.95 | 0.76 | 10.14 | 0.44 | 1.686 | 0.015 |
| Temora2 - | 0.496 | 0.031 | 0.06555 | 0.0032 | 0.15333 | 0.0543 | 0.0025 | 0.009433 | 0.02076 | 0.0013 | 405 | 21 | 409.2 | 19 | 415 | 27 | 342 | 96 | 129.9 | 2.8 | 59.6 | 1.8 | 10.61 | 0.44 | 1.864 | 0.025 |
| Temora2 - | no value | | no value | | NaN | no value | | NaN | no value | | no value | | no value | | no value | | no value | | 0.0036 | 0.0042 | 0.0049 | 0.0042 | 0.05 | 0.28 | no value | NAN |
| Temora2 - | 0.504 | 0.027 | 0.06522 | 0.0031 | 0.11145 | 0.0558 | 0.0018 | 0.263 | 0.01907 | 0.0012 | 412 | 19 | 407.3 | 19 | 381.7 | 24 | 409 | 69 | 185 | 5.5 | 124.2 | 4.3 | 24.77 | 0.94 | 1.53 | 0.015 |
| Temora2 - | 0.468 | 0.029 | 0.06061 | 0.0024 | 0.22871 | 0.0558 | 0.0022 | 0.10987 | 0.02031 | 0.00082 | 387 | 20 | 379.3 | 15 | 406 | 16 | 396 | 82 | 178.9 | 1.9 | 63.83 | 0.71 | 39.4 | 1.5 | 2.716 | 0.031 |
| Temora2 - | 0.496 | 0.029 | 0.06547 | 0.0026 | 0.27776 | 0.0549 | 0.0018 | 0.079771 | 0.02079 | 0.00057 | 408 | 20 | 408.7 | 16 | 416 | 11 | 379 | 71 | 227.9 | 2.9 | 141.4 | 1.5 | 87.3 | 2.3 | 1.594 | 0.017 |
| Temora2 - | 0.499 | 0.031 | 0.06411 | 0.0026 | 0.18527 | 0.0566 | 0.0023 | 0.16804 | 0.02017 | 0.00073 | 408 | 21 | 400.5 | 16 | 403 | 14 | 422 | 85 | 143.2 | 4.4 | 70.3 | 2.7 | 42.4 | 1.9 | 2.068 | 0.034 |
| Temora2 - | 0.469 | 0.031 | 0.0618 | 0.0026 | 0.14181 | 0.0554 | 0.0026 | 0.20139 | 0.02062 | 0.00078 | 386 | 22 | 386.2 | 16 | 412 | 15 | 369 | 97 | 148 | 3.4 | 76.8 | 2.1 | 47.1 | 2 | 1.923 | 0.026 |
| Temora2 - | 0.525 | 0.039 | 0.0695 | 0.0035 | 0.12973 | 0.055 | 0.0032 | 0.20942 | 0.0238 | 0.0022 | 421 | 26 | 432.6 | 21 | 474 | 43 | 350 | 120 | 76.1 | 2.2 | 21.64 | 0.73 | 4.68 | 0.31 | 3.506 | 0.082 |
| Temora2 - | no value | | no value | | NaN | no value | | NaN | no value | | no value | | no value | | no value | | no value | | 0.006 | 0.014 | 0.0036 | 0.007 | 0.39 | 0.35 | no value | NAN |
| Temora2 - | 0.51 | 0.032 | 0.0638 | 0.0027 | 0.4067 | 0.0576 | 0.0023 | 0.050255 | 0.02105 | 0.00083 | 417 | 22 | 398.7 | 16 | 421 | 16 | 464 | 82 | 191.3 | 2.7 | 77.6 | 1.5 | 46.1 | 1.7 | 2.674 | 0.052 |

Accepted Manuscript

ACCEPTED MANUSCRIPT

| Ratios | | | | | | | | | | | Ages | | | | | | | | Concentrations (calculated from 91500) | | | | | | | |
|---|---|---|---|---|---|---|---|---|---|---|---|---|---|---|---|---|---|---|---|---|---|---|---|---|---|---|
| Sample - ar | 207Pb/235 | Propagatec | 206Pb/238 | Propagatec | Error Corre | 207Pb/206 | Propagatec | Error Corre | 208Pb/232 | Propagatec | 207Pb/235 | Propagatec | 206Pb/238 | Propagatec | 208Pb/232 | Propagatec | 207Pb/206 | Propagatec | U (ppm) | Internal 2 S | Th (ppm) | Internal 2 S | Pb (ppm) | Internal 2 S | U/Th | Internal 2 SE |
| BOP1A - 1 | 6.965 | 0.13 | 0.3827 | 0.0068 | 0.27623 | 0.1318 | 0.0015 | 0.3076 | 0.1106 | 0.0064 | 2106 | 17 | 2089 | 31 | 2124 | 120 | 2117 | 21 | 131.3 | 2.6 | 78 | 1.5 | 82.4 | 1.5 | 1.679 | 0.015 |
| BOP1A - 2 | 6.95 | 0.15 | 0.3866 | 0.007 | 0.23096 | 0.1293 | 0.0023 | 0.29057 | 0.1086 | 0.0064 | 2103 | 19 | 2107 | 33 | 2083 | 120 | 2083 | 31 | 173.6 | 5.2 | 117 | 3.6 | 120.2 | 3.2 | 1.4812 | 0.0099 |
| BOP1A - 3 | 7.122 | 0.13 | 0.3939 | 0.0068 | 0.33797 | 0.131 | 0.0013 | 0.30045 | 0.1111 | 0.0064 | 2125.3 | 16 | 2140 | 32 | 2129 | 120 | 2108 | 18 | 199.4 | 4.8 | 113.8 | 2.7 | 121.4 | 2.4 | 1.749 | 0.012 |
| BOP1A - 4 | 7.043 | 0.14 | 0.3889 | 0.0068 | 0.27322 | 0.1316 | 0.0018 | 0.21181 | 0.1096 | 0.0063 | 2116 | 18 | 2117 | 31 | 2101 | 120 | 2112 | 24 | 114.7 | 3.7 | 64.5 | 2.2 | 67.4 | 2.1 | 1.782 | 0.014 |
| BOP1A - 5 | 7.274 | 0.14 | 0.3961 | 0.0069 | 0.29231 | 0.1333 | 0.0015 | 0.2765 | 0.1159 | 0.0066 | 2145 | 16 | 2151 | 32 | 2215 | 120 | 2136 | 20 | 146.7 | 4.2 | 109.5 | 3 | 121.7 | 2.7 | 1.337 | 0.01 |
| BOP1A - 6 | 5.55 | 0.13 | 0.3066 | 0.0073 | 0.93438 | 0.13152 | 0.0009 | 0.16882 | 0.1007 | 0.0063 | 1904 | 21 | 1722 | 36 | 1937 | 120 | 2117 | 12 | 553 | 22 | 284 | 11 | 266.7 | 4.7 | 1.952 | 0.011 |
| BOP1A - 7 | 7.063 | 0.13 | 0.3893 | 0.0067 | 0.27167 | 0.1319 | 0.0015 | 0.29472 | 0.1098 | 0.0064 | 2118 | 16 | 2119 | 31 | 2105 | 120 | 2122 | 20 | 163.3 | 4.5 | 88.3 | 2.6 | 93.1 | 2.2 | 1.853 | 0.014 |
| BOP1A - 8 | 6.91 | 0.12 | 0.3848 | 0.0066 | 0.23499 | 0.1308 | 0.0013 | 0.32826 | 0.1071 | 0.0061 | 2098.7 | 15 | 2098 | 31 | 2056 | 110 | 2107 | 18 | 207.5 | 9.5 | 141.8 | 7.4 | 146.5 | 7 | 1.485 | 0.017 |
| BOP1A - 9 | 7.95 | 0.18 | 0.4088 | 0.0075 | 0.66692 | 0.1418 | 0.0019 | -0.16324 | 0.1626 | 0.011 | 2221 | 21 | 2209 | 34 | 3040 | 200 | 2243 | 23 | 155.1 | 5.6 | 102.5 | 4.8 | 153.6 | 2.9 | 1.54 | 0.019 |
| BOP1A - 10 | 6.946 | 0.13 | 0.3854 | 0.0067 | 0.47879 | 0.1315 | 0.0013 | 0.17375 | 0.1106 | 0.0064 | 2103 | 16 | 2104 | 31 | 2120 | 120 | 2117 | 17 | 211 | 9.7 | 167.5 | 8 | 177.5 | 6.6 | 1.265 | 0.012 |
| BOP1A - 11 | 7.104 | 0.13 | 0.3916 | 0.0067 | 0.21887 | 0.1325 | 0.0014 | 0.36345 | 0.1136 | 0.0066 | 2125.6 | 16 | 2130 | 31 | 2175 | 120 | 2131 | 19 | 179.9 | 7.9 | 86.2 | 4 | 94.5 | 3.6 | 2.096 | 0.016 |
| BOP1A - 12 | 7.465 | 0.14 | 0.4075 | 0.0071 | 0.5236 | 0.1337 | 0.0014 | 0.10734 | 0.12 | 0.007 | 2167 | 17 | 2203 | 33 | 2289 | 130 | 2144 | 18 | 180.1 | 5.8 | 97.2 | 3 | 112.9 | 2.4 | 1.851 | 0.012 |
| BOP1A - 13 | 9.08 | 0.45 | 0.4177 | 0.0092 | 0.80389 | 0.1561 | 0.0054 | -0.60343 | 0.191 | 0.018 | 2316 | 42 | 2248 | 42 | 3490 | 300 | 2375 | 55 | 86 | 5.1 | 53.8 | 3.5 | 91.2 | 5 | 1.613 | 0.018 |
| BOP1A - 14 | 7.394 | 0.14 | 0.4037 | 0.0072 | 0.43723 | 0.1335 | 0.0014 | 0.29128 | 0.1205 | 0.0071 | 2158 | 17 | 2185 | 33 | 2299 | 130 | 2140 | 19 | 202 | 9.6 | 160.2 | 8.6 | 136.6 | 9.8 | 1.279 | 0.017 |
| BOP1A - 16 | 7.111 | 0.13 | 0.3939 | 0.0071 | 0.40345 | 0.1318 | 0.0014 | 0.30268 | 0.11 | 0.0063 | 2125 | 17 | 2140 | 33 | 2108 | 120 | 2120 | 19 | 138.6 | 4.4 | 99.9 | 3.5 | 107.2 | 3.4 | 1.398 | 0.014 |
| BOP1A - 17 | 7.13 | 0.16 | 0.3959 | 0.0072 | 0.29812 | 0.131 | 0.002 | 0.22402 | 0.1092 | 0.0065 | 2126 | 19 | 2150 | 33 | 2093 | 120 | 2106 | 28 | 90.4 | 2.6 | 47.8 | 1.3 | 53.4 | 1.3 | 1.891 | 0.017 |
| BOP1A - 19 | 5.093 | 0.098 | 0.2846 | 0.0054 | 0.80644 | 0.1301 | 0.001 | 0.12979 | 0.0877 | 0.0051 | 1833 | 17 | 1614 | 27 | 1699 | 94 | 2097 | 14 | 210 | 12 | 149.2 | 7.9 | 126.1 | 5.6 | 1.407 | 0.012 |
| BOP1A - 21 | 5.971 | 0.13 | 0.3298 | 0.0075 | 0.82157 | 0.1314 | 0.0012 | 0.12659 | 0.1053 | 0.006 | 1968 | 19 | 1836 | 36 | 2022 | 110 | 2116 | 16 | 311.1 | 4.8 | 171.4 | 3.8 | 177.5 | 3.7 | 1.831 | 0.018 |
| BOP1A - 22 | 8.04 | 0.19 | 0.4104 | 0.0077 | 0.78757 | 0.1425 | 0.0018 | -0.33434 | 0.145 | 0.0097 | 2231 | 20 | 2215 | 35 | 2731 | 170 | 2252 | 21 | 152 | 6.8 | 97.8 | 4.7 | 134.1 | 4 | 1.573 | 0.016 |
| BOP1A - 23 | 6.854 | 0.12 | 0.3842 | 0.0066 | 0.26622 | 0.1294 | 0.0013 | 0.31001 | 0.1084 | 0.0062 | 2091.4 | 15 | 2096 | 30 | 2079 | 110 | 2087 | 17 | 238 | 12 | 166.3 | 8.7 | 175.1 | 7.9 | 1.4441 | 0.0095 |
| BOP1A - 24 | 7.114 | 0.13 | 0.3865 | 0.0067 | 0.26175 | 0.1336 | 0.0016 | 0.33058 | 0.1138 | 0.0066 | 2124 | 17 | 2106 | 31 | 2177 | 120 | 2140 | 21 | 134.6 | 2.3 | 76.15 | 0.9 | 85.1 | 1.2 | 1.773 | 0.018 |
| BOP1A - 25 | 7.033 | 0.13 | 0.3917 | 0.0068 | 0.36904 | 0.1301 | 0.0013 | 0.30328 | 0.1115 | 0.0064 | 2114 | 16 | 2130 | 32 | 2135 | 120 | 2098 | 19 | 198.2 | 9.5 | 145.8 | 7.7 | 157.6 | 7.1 | 1.381 | 0.016 |
| BOP1A - 26 | 2.99 | 0.23 | 0.169 | 0.012 | 0.98314 | 0.1247 | 0.002 | -0.62953 | 0.0576 | 0.0047 | 1333 | 68 | 996 | 68 | 1128 | 90 | 2017 | 29 | 472 | 47 | 348 | 32 | 164.8 | 2.4 | 1.34 | 0.011 |
| BOP1A - 27 | 6.824 | 0.12 | 0.3804 | 0.0066 | 0.28122 | 0.1298 | 0.0014 | 0.27365 | 0.1051 | 0.006 | 2087.3 | 16 | 2078 | 31 | 2020 | 110 | 2091 | 19 | 273 | 37 | 80.1 | 2.8 | 120.1 | 6.5 | 3.24 | 0.29 |
| BOP1A - 29 | 6.747 | 0.13 | 0.3813 | 0.0068 | 0.36871 | 0.1281 | 0.0016 | 0.17894 | 0.104 | 0.0061 | 2076 | 17 | 2082 | 32 | 1999 | 110 | 2066 | 22 | 147.2 | 5.7 | 67.6 | 2.3 | 68.2 | 2.2 | 2.17 | 0.02 |
| BOP1A - 30 | 6.846 | 0.13 | 0.3875 | 0.0067 | 0.39073 | 0.1278 | 0.0014 | 0.23665 | 0.1078 | 0.0062 | 2091 | 17 | 2111 | 32 | 2068 | 110 | 2063 | 20 | 156.4 | 4.3 | 124 | 4 | 129.7 | 3.4 | 1.272 | 0.011 |
| BOP1A - 31 | 6.704 | 0.13 | 0.3799 | 0.0068 | 0.40688 | 0.1278 | 0.0015 | 0.26002 | 0.1057 | 0.0061 | 2073 | 17 | 2075 | 32 | 2031 | 110 | 2062 | 20 | 180.5 | 4.7 | 125.6 | 2.9 | 129.6 | 2.7 | 1.44 | 0.015 |
| BOP1A - 32 | 6.728 | 0.13 | 0.3835 | 0.0067 | 0.43676 | 0.127 | 0.0014 | 0.20627 | 0.1097 | 0.0063 | 2074 | 16 | 2092 | 31 | 2104 | 120 | 2055 | 19 | 156.7 | 4.4 | 111.1 | 3.6 | 118 | 3.3 | 1.42 | 0.011 |
| BOP1A - 33 | 6.846 | 0.13 | 0.387 | 0.0068 | 0.2491 | 0.128 | 0.0015 | 0.34127 | 0.1115 | 0.0064 | 2090 | 17 | 2109 | 32 | 2136 | 120 | 2066 | 21 | 164.3 | 5.6 | 107.2 | 3.7 | 116.1 | 3.6 | 1.538 | 0.01 |
| BOP1A - 34 | 6.898 | 0.13 | 0.391 | 0.0068 | 0.35283 | 0.1281 | 0.0015 | 0.23011 | 0.109 | 0.0063 | 2098 | 17 | 2127 | 32 | 2091 | 110 | 2066 | 21 | 157.6 | 4.8 | 117.3 | 4.5 | 123.3 | 3.9 | 1.361 | 0.014 |
| BOP1A - 35 | 6.909 | 0.13 | 0.3915 | 0.0068 | 0.32367 | 0.1282 | 0.0015 | 0.24829 | 0.1097 | 0.0064 | 2099 | 17 | 2129 | 32 | 2103 | 120 | 2069 | 21 | 159.3 | 3.7 | 95.9 | 2.8 | 101.6 | 2.3 | 1.674 | 0.016 |
| BOP1A - 36 | 7.056 | 0.13 | 0.4017 | 0.0071 | 0.29757 | 0.1278 | 0.0015 | 0.33037 | 0.1152 | 0.0068 | 2118 | 17 | 2176 | 32 | 2203 | 120 | 2062 | 21 | 131.9 | 4.5 | 75.5 | 3 | 83 | 2.7 | 1.768 | 0.018 |
| BOP1A - 37 | 9.29 | 0.22 | 0.4238 | 0.0082 | 0.68865 | 0.1599 | 0.0023 | -0.09408 | 0.2211 | 0.016 | 2362 | 21 | 2276 | 37 | 4020 | 250 | 2450 | 25 | 126 | 6.2 | 75.2 | 4.2 | 155.3 | 6.3 | 1.699 | 0.018 |
| BOP1A - 38 | 6.796 | 0.12 | 0.3891 | 0.0068 | 0.19544 | 0.1282 | 0.0014 | 0.43247 | 0.1085 | 0.0063 | 2083.6 | 16 | 2118 | 32 | 2081 | 110 | 2069 | 19 | 168.2 | 6.3 | 134 | 5.7 | 138.3 | 4.7 | 1.267 | 0.01 |
| BOP1A - 41 | 6.85 | 0.15 | 0.3889 | 0.0073 | 0.30959 | 0.1291 | 0.0021 | 0.26558 | 0.11 | 0.0063 | 2090 | 20 | 2117 | 34 | 2110 | 110 | 2081 | 29 | 257 | 11 | 128.2 | 6 | 142 | 4.8 | 2.36 | 0.22 |
| BOP1A - 42 | 6.841 | 0.12 | 0.391 | 0.0068 | 0.39009 | 0.1277 | 0.0013 | 0.28891 | 0.1109 | 0.0063 | 2089.6 | 16 | 2127 | 32 | 2126 | 120 | 2063 | 17 | 171.8 | 1.8 | 121.5 | 1 | 128.8 | 1.8 | 1.413 | 0.017 |
| BOP1A - 43 | 7.107 | 0.13 | 0.3974 | 0.0069 | 0.35649 | 0.1305 | 0.0015 | 0.30678 | 0.1158 | 0.0068 | 2123 | 16 | 2157 | 32 | 2215 | 120 | 2100 | 20 | 131.5 | 3.5 | 87.8 | 2.1 | 96.1 | 1.7 | 1.494 | 0.012 |
| BOP1A - 44 | 6.83 | 0.13 | 0.3876 | 0.0068 | 0.44605 | 0.1281 | 0.0015 | 0.17653 | 0.1107 | 0.0064 | 2088 | 17 | 2111 | 31 | 2122 | 120 | 2068 | 20 | 153.4 | 4.5 | 105.6 | 3.7 | 110 | 3.4 | 1.465 | 0.017 |
| BOP1A - 45 | 7.045 | 0.13 | 0.3971 | 0.007 | 0.35389 | 0.1287 | 0.0015 | 0.29839 | 0.1153 | 0.0067 | 2115 | 17 | 2155 | 32 | 2205 | 120 | 2076 | 21 | 158.7 | 2.3 | 117.5 | 1.7 | 127.9 | 2.2 | 1.354 | 0.019 |
| BOP1A - 46 | 6.931 | 0.12 | 0.3912 | 0.0067 | 0.39236 | 0.1284 | 0.0012 | 0.29186 | 0.1106 | 0.0064 | 2101.2 | 16 | 2128 | 31 | 2119 | 120 | 2073 | 16 | 174.8 | 6 | 108.9 | 3.8 | 112.7 | 3 | 1.607 | 0.011 |
| BOP1A - 47 | 6.802 | 0.14 | 0.3857 | 0.007 | 0.35362 | 0.1272 | 0.0018 | 0.38209 | 0.1084 | 0.0065 | 2085 | 18 | 2102 | 33 | 2079 | 120 | 2055 | 25 | 199.3 | 3.4 | 153.1 | 2.3 | 156.5 | 1.8 | 1.299 | 0.011 |
| BOP1A - 48 | 7.137 | 0.14 | 0.3872 | 0.0067 | 0.31084 | 0.1327 | 0.0016 | 0.27245 | 0.1222 | 0.0072 | 2127 | 17 | 2109 | 31 | 2329 | 130 | 2129 | 21 | 137.8 | 4.8 | 98.5 | 3.9 | 112 | 3.1 | 1.404 | 0.019 |
| BOP1A - 49 | 6.501 | 0.13 | 0.3649 | 0.0065 | 0.60294 | 0.1282 | 0.0013 | 0.10118 | 0.1068 | 0.0062 | 2044 | 17 | 2005 | 31 | 2051 | 110 | 2069 | 18 | 229.7 | 8.7 | 175.8 | 7 | 174.6 | 5.4 | 1.308 | 0.01 |
| BOP1A - 50 | 6.811 | 0.12 | 0.3854 | 0.0068 | 0.28753 | 0.1268 | 0.0014 | 0.28792 | 0.111 | 0.0064 | 2085.5 | 16 | 2101 | 32 | 2127 | 120 | 2052 | 19 | 182.1 | 5.8 | 98.9 | 3.2 | 102.5 | 3 | 1.84 | 0.013 |
| BOP1A - 51 | 6.97 | 0.14 | 0.3937 | 0.0079 | 0.82955 | 0.1266 | 0.0011 | 0.10892 | 0.116 | 0.0068 | 2105 | 18 | 2139 | 36 | 2217 | 120 | 2051 | 15 | 324 | 18 | 156.5 | 8.9 | 167 | 7.5 | 2.067 | 0.013 |
| BOP1A - 52 | 6.62 | 0.14 | 0.3743 | 0.0071 | 0.69157 | 0.1269 | 0.0014 | 0.089769 | 0.108 | 0.0063 | 2059 | 19 | 2049 | 34 | 2076 | 110 | 2052 | 19 | 171.8 | 7.8 | 104.3 | 2.8 | 106.2 | 2.7 | 1.64 | 0.033 |
| BOP1A - 53 | 8.889 | 0.16 | 0.4232 | 0.0075 | 0.2591 | 0.1506 | 0.0016 | 0.44706 | 0.474 | 0.028 | 2325.2 | 16 | 2274 | 34 | 7820 | 380 | 2351 | 18 | 132.7 | 4.8 | 71.6 | 1.6 | 324 | 12 | 1.818 | 0.027 |
| BOP1A - 54 | 6.884 | 0.13 | 0.386 | 0.0068 | 0.29622 | 0.1276 | 0.0014 | 0.38623 | 0.1118 | 0.0066 | 2095 | 16 | 2104 | 32 | 2140 | 120 | 2063 | 21 | 126.8 | 3.5 | 76.4 | 2.2 | 79.1 | 1.9 | 1.661 | 0.014 |
| BOP1A - 55 | 6.836 | 0.13 | 0.3826 | 0.0067 | 0.33042 | 0.1276 | 0.0013 | 0.28422 | 0.1111 | 0.0064 | 2089 | 16 | 2088 | 31 | 2129 | 120 | 2063 | 19 | 147 | 5.3 | 98 | 4.1 | 101.2 | 4.1 | 1.511 | 0.014 |
| BOP1A - 56 | 6.891 | 0.13 | 0.3856 | 0.0067 | 0.3469 | 0.1279 | 0.0014 | 0.22387 | 0.1141 | 0.0066 | 2097 | 17 | 2102 | 31 | 2183 | 120 | 2065 | 20 | 180.9 | 5.8 | 132.1 | 4.5 | 139.3 | 3.5 | 1.3699 | 0.0092 |
| BOP1A - 57 | 6.736 | 0.13 | 0.3821 | 0.0067 | 0.52998 | 0.1262 | 0.0013 | 0.006347 | 0.1071 | 0.0061 | 2076 | 17 | 2086 | 31 | 2055 | 110 | 2042 | 18 | 197.7 | 4.1 | 154.9 | 2.9 | 154 | 2.6 | 1.2722 | 0.0095 |
| BOP1A - 58 | 6.996 | 0.12 | 0.3934 | 0.0068 | 0.35294 | 0.1271 | 0.0011 | 0.30136 | 0.1148 | 0.0065 | 2109.8 | 15 | 2138 | 31 | 2196 | 120 | 2057 | 15 | 224.6 | 5.8 | 151.6 | 2.7 | 161.2 | 2.3 | 1.471 | 0.015 |
| BOP1A - 59 | 6.65 | 0.16 | 0.3661 | 0.008 | 0.69966 | 0.1301 | 0.0018 | 0.11454 | 0.1217 | 0.0082 | 2062 | 21 | 2010 | 38 | 2317 | 150 | 2093 | 24 | 144.2 | 7.8 | 98.4 | 7.6 | 114.2 | 5.6 | 1.558 | 0.038 |
| BOP1A - 60 | 6.761 | 0.13 | 0.3801 | 0.0067 | 0.12398 | 0.1279 | 0.0016 | 0.43392 | 0.1154 | 0.0069 | 2079 | 16 | 2077 | 31 | 2207 | 120 | 2063 | 23 | 147.2 | 5.5 | 95.6 | 4.4 | 100.8 | 3.8 | 1.557 | 0.018 |
| BOP1A - 61 | 6.64 | 0.14 | 0.3745 | 0.0078 | 0.80782 | 0.1275 | 0.0012 | 0.080639 | 0.1069 | 0.0062 | 2065 | 18 | 2049 | 37 | 2055 | 110 | 2063 | 16 | 255 | 16 | 193 | 11 | 186.5 | 8.3 | 1.307 | 0.011 |
| BOP1A - 62 | 6.965 | 0.12 | 0.3887 | 0.0067 | 0.56104 | 0.12902 | 0.00096 | 0.18214 | 0.1119 | 0.0064 | 2105.9 | 15 | 2117 | 31 | 2143 | 120 | 2084 | 13 | 321 | 14 | 168.8 | 6.4 | 172.9 | 5.1 | 1.88 | 0.016 |
| BOP1A - 63 | 7.104 | 0.14 | 0.4014 | 0.0071 | 0.40837 | 0.1281 | 0.0015 | 0.28693 | 0.1178 | 0.0069 | 2123 | 17 | 2175 | 33 | 2249 | 120 | 2069 | 21 | 159 | 7.8 | 109.5 | 6.8 | 116.1 | 5.8 | 1.486 | 0.021 |
| BOP1A - 64 | 6.679 | 0.13 | 0.3786 | 0.0067 | 0.31496 | 0.1279 | 0.0015 | 0.23453 | 0.1081 | 0.0062 | 2068 | 17 | 2069 | 31 | 2074 | 110 | 2067 | 21 | 153.2 | 2 | 95.8 | 1.4 | 95.3 | 1.6 | 1.595 | 0.013 |
| BOP1A - 65 | 6.69 | 0.12 | 0.3811 | 0.0066 | 0.22005 | 0.1282 | 0.0014 | 0.31274 | 0.1093 | 0.0063 | 2069.7 | 16 | 2081 | 31 | 2095 | 110 | 2073 | 19 | 190.7 | 4.1 | 123 | 2.4 | 123.3 | 2.2 | 1.543 | 0.01 |
| BOP1A - 66 | 6.948 | 0.12 | 0.3958 | 0.0069 | 0.42721 | 0.1285 | 0.0012 | 0.21671 | 0.1141 | 0.0065 | 2103.3 | 16 | 2149 | 32 | 2183 | 120 | 2074 | 17 | 210.5 | 3.6 | 124.3 | 1.5 | 130.2 | 1.7 | 1.68 | 0.014 |
| BOP1A - 67 | 6.691 | 0.12 | 0.3837 | 0.0067 | 0.10396 | 0.1278 | 0.0015 | 0.42869 | 0.1101 | 0.0063 | 2069.7 | 16 | 2093 | 31 | 2114 | 110 | 2063 | 21 | 173.1 | 8.2 | 113.7 | 6.8 | 113.9 | 6.2 | 1.554 | 0.021 |
| BOP1A - 68 | 6.681 | 0.12 | 0.3775 | 0.0066 | 0.2599 | 0.13 | 0.0015 | 0.3195 | 0.1086 | 0.0063 | 2068 | 16 | 2064 | 31 | 2083 | 110 | 2093 | 21 | 160.8 | 4.9 | 107.8 | 4.1 | 106.2 | 3.4 | 1.5 | 0.015 |
| BOP1A - 69 | 6.838 | 0.11 | 0.3896 | 0.0066 | 0.55688 | 0.12961 | 0.00078 | 0.26638 | 0.1137 | 0.0065 | 2089.9 | 14 | 2121 | 30 | 2176 | 120 | 2091 | 11 | 486 | 17 | 247.3 | 8.3 | 255.3 | 6.3 | 1.947 | 0.011 |
| BOP1A - 70 | 6.706 | 0.13 | 0.3849 | 0.0068 | 0.32808 | 0.1288 | 0.0016 | 0.28862 | 0.1138 | 0.0065 | 2074 | 17 | 2100 | 31 | 2177 | 120 | 2075 | 21 | 159.6 | 4.2 | 95.9 | 2.8 | 99.5 | 2.5 | 1.66 | 0.012 |
| BOP1A - 71 | 6.52 | 0.14 | 0.3696 | 0.0067 | 0.049876 | 0.1291 | 0.0021 | 0.39472 | 0.1038 | 0.0063 | 2047 | 19 | 2027 | 32 | 1995 | 120 | 2087 | 31 | 154.4 | 3.4 | 94.3 | 2.1 | 92 | 2.2 | 1.63 | 0.011 |
| BOP1A - 72 | 6.645 | 0.12 | 0.3769 | 0.0068 | 0.32299 | 0.1299 | 0.0015 | 0.31327 | 0.1132 | 0.0066 | 2064 | 16 | 2061 | 32 | 2168 | 120 | 2093 | 20 | 175.2 | 2.3 | 89 | 1.3 | 90.1 | 1.5 | 1.96 | 0.016 |
| BOP1A - 73 | 26.5 | 2.5 | 0.691 | 0.04 | 0.99717 | 0.26 | 0.013 | -0.98337 | 1.18 | 0.16 | 3210 | 110 | 3380 | 160 | 14600 | 1500 | 3152 | 94 | 135.6 | 3.7 | 85.2 | 2.3 | 884 | 93 | 1.582 | 0.012 |
| BOP1A - 74 | 6.856 | 0.13 | 0.3915 | 0.0069 | 0.41642 | 0.1287 | 0.0014 | 0.21752 | 0.1142 | 0.0067 | 2091 | 17 | 2129 | 32 | 2184 | 120 | 2076 | 19 | 152.5 | 5.5 | 84 | 3.6 | 86.9 | 2.9 | 1.811 | 0.02 |
| BOP1A - 75 | 19 | 1.5 | 0.601 | 0.028 | 0.99453 | 0.2154 | 0.0099 | -0.97852 | 1.28 | 0.17 | 2905 | 96 | 3000 | 120 | 14900 | 1700 | 2865 | 84 | 302 | 12 | 128.9 | 7.6 | 1190 | 110 | 2.428 | 0.049 |
| BOP1A - 77 | 6.93 | 0.12 | 0.39 | 0.0068 | 0.4051 | 0.1299 | 0.0013 | 0.22519 | 0.1134 | 0.0065 | 2101 | 16 | 2122 | 31 | 2171 | 120 | 2093 | 18 | 306.7 | 5.4 | 242.2 | 5.9 | 259.7 | 7.4 | 1.264 | 0.013 |
| BOP1A - 78 | 6.8 | 0.12 | 0.3877 | 0.0066 | 0.27152 | 0.128 | 0.0012 | 0.31914 | 0.1142 | 0.0065 | 2084.6 | 15 | 2111.9 | 31 | 2186 | 120 | 2067 | 17 | 212.2 | 4.8 | 129.3 | 3.5 | 135.3 | 3 | 1.638 | 0.013 |
| BOP1A - 79 | 7.112 | 0.13 | 0.4023 | 0.0071 | 0.53796 | 0.1286 | 0.0011 | 0.23805 | 0.1263 | 0.0072 | 2124 | 16 | 2179 | 33 | 2403 | 130 | 2077 | 16 | 285.8 | 3.1 | 184.3 | 4.5 | 215 | 5.5 | 1.565 | 0.032 |
| BOP1A - 80 | 6.96 | 0.14 | 0.3905 | 0.0071 | 0.35836 | 0.1299 | 0.0017 | 0.26383 | 0.1151 | 0.0067 | 2105 | 18 | 2125 | 33 | 2201 | 120 | 2093 | 23 | 167.4 | 4.3 | 108.7 | 1.8 | 116.1 | 1.8 | 1.53 | 0.02 |
| BOP1A - 81 | 6.837 | 0.13 | 0.391 | 0.0067 | 0.33938 | 0.127 | 0.0014 | 0.24156 | 0.1149 | 0.0067 | 2090 | 17 | 2127 | 31 | 2197 | 120 | 2051 | 20 | 185.5 | 5.9 | 128.1 | 4.1 | 135.4 | 3.5 | 1.441 | 0.011 |
| BOP1A - 82 | 6.996 | 0.13 | 0.3963 | 0.0069 | 0.35457 | 0.128 | 0.0014 | 0.31906 | 0.1179 | 0.0068 | 2109 | 16 | 2151 | 32 | 2252 | 120 | 2066 | 20 | 168.6 | 4.8 | 105.3 | 2.8 | 114.8 | 2.7 | 1.588 | 0.013 |
| BOP1A - 83 | 7.051 | 0.13 | 0.3968 | 0.007 | 0.55151 | 0.1286 | 0.0014 | 0.19046 | 0.1143 | 0.0067 | 2116 | 17 | 2154 | 32 | 2187 | 120 | 2075 | 19 | 146.2 | 5.4 | 82.7 | 3.4 | 86.7 | 2.8 | 1.772 | 0.015 |
| BOP1A - 84 | 7.007 | 0.13 | 0.3821 | 0.0066 | 0.30937 | 0.1327 | 0.0015 | 0.25147 | 0.1292 | 0.0076 | 2110.7 | 16 | 2086 | 31 | 2454 | 140 | 2130 | 19 | 208 | 5.5 | 121.7 | 3.4 | 145.7 | 2.4 | 1.7 | 0.011 |

% conc4

Accepted Manuscript

ACCEPTED MANUSCRIPT

| | Ratios | | | | | | | | | Ages | | | | | | | Concentrations (calculated from 91500) | | | | | | | | |
|---|---|---|---|---|---|---|---|---|---|---|---|---|---|---|---|---|---|---|---|---|---|---|---|---|---|
| Sample - ar | 207Pb/235 | Propagatec | 206Pb/238 | Propagatec | Error Corre | 207Pb/206 | Propagatec | Error Corre | 208Pb/232 | Propagatec | 207Pb/235 | Propagatec | 206Pb/238 | Propagatec | 208Pb/232 | Propagatec | 207Pb/206 | Propagatec | U (ppm) | Internal 2 S | Th (ppm) | Internal 2 S | Pb (ppm) | Internal 2 S | U/Th | Internal 2 SE |
| CLIB01 - 1 | 7.161 | 0.077 | 0.391 | 0.0056 | 0.27193 | 0.1328 | 0.0014 | 0.36332 | 0.1219 | 0.0042 | 2130.1 | 9.6 | 2127 | 26 | 2324 | 75 | 2132 | 19 | 180 | 4.2 | 63.6 | 1.6 | 74.1 | 2.2 | 2.832 | 0.024 |
| CLIB01 - 2 | 7.467 | 0.075 | 0.4027 | 0.0064 | 0.39087 | 0.1347 | 0.0014 | 0.49674 | 0.1363 | 0.0046 | 2167.7 | 9 | 2181 | 29 | 2582 | 81 | 2156 | 19 | 221.7 | 3.9 | 96.7 | 1.1 | 126.4 | 2.2 | 2.284 | 0.024 |
| CLIB01 - 3 | 6.81 | 0.1 | 0.3764 | 0.0063 | 0.55316 | 0.1308 | 0.0016 | 0.20052 | 0.1137 | 0.0042 | 2085 | 13 | 2059 | 30 | 2175 | 76 | 2106 | 22 | 145.6 | 7.5 | 63.6 | 3.6 | 67.3 | 2.8 | 2.308 | 0.023 |
| CLIB01 - 4 | 4.56 | 0.19 | 0.1804 | 0.0058 | 0.96019 | 0.1845 | 0.0035 | -0.74815 | 0.1553 | 0.0099 | 1742 | 39 | 1067 | 31 | 2900 | 170 | 2689 | 32 | 503 | 27 | 261 | 14 | 372 | 16 | 1.934 | 0.012 |
| CLIB01 - 5 | 3.32 | 0.14 | 0.1857 | 0.0087 | 0.95649 | 0.1301 | 0.0015 | 0.17863 | 0.0658 | 0.0029 | 1467 | 33 | 1093 | 46 | 1291 | 55 | 2094 | 21 | 367 | 26 | 194 | 12 | 116.2 | 3.8 | 1.852 | 0.02 |
| CLIB01 - 6 | 5.841 | 0.062 | 0.2639 | 0.0046 | 0.019479 | 0.1605 | 0.0025 | 0.74556 | 0.1502 | 0.0069 | 1951 | 9.1 | 1509 | 23 | 2822 | 120 | 2453 | 26 | 304.9 | 5.2 | 112.3 | 2.2 | 160 | 3.3 | 2.716 | 0.02 |
| CLIB01 - 7 | 6.19 | 0.18 | 0.2674 | 0.0092 | 0.8984 | 0.1704 | 0.0026 | 0.43427 | 0.1731 | 0.007 | 1996 | 25 | 1522 | 47 | 3223 | 120 | 2554 | 26 | 219.2 | 2.7 | 91.7 | 1.6 | 153.7 | 2.4 | 2.392 | 0.026 |
| CLIB01 - 8 | 7.138 | 0.099 | 0.3953 | 0.0067 | 0.60142 | 0.1305 | 0.0013 | 0.22647 | 0.1144 | 0.004 | 2126 | 12 | 2146 | 31 | 2187 | 71 | 2106 | 19 | 193.5 | 9.5 | 105.5 | 5 | 115 | 3.9 | 1.824 | 0.013 |
| CLIB01 - 9 | 6.861 | 0.071 | 0.3831 | 0.0054 | 0.40045 | 0.1295 | 0.0013 | 0.17934 | 0.1048 | 0.0036 | 2092.1 | 9.5 | 2090 | 25 | 2014 | 66 | 2087 | 18 | 183.3 | 6.5 | 77.4 | 3.1 | 78.6 | 2.8 | 2.379 | 0.019 |
| CLIB01 - 10 | 7.71 | 0.12 | 0.4145 | 0.0068 | 0.4385 | 0.1356 | 0.002 | 0.15172 | 0.1245 | 0.0048 | 2197 | 15 | 2234 | 31 | 2369 | 86 | 2163 | 26 | 70.2 | 2.2 | 37.8 | 1.3 | 45.6 | 1.2 | 1.863 | 0.023 |
| CLIB01 - 11 | 6.09 | 0.12 | 0.3303 | 0.0069 | 0.81672 | 0.1335 | 0.0016 | 0.001579 | 0.112 | 0.0042 | 1983 | 17 | 1838 | 33 | 2144 | 76 | 2140 | 21 | 194.6 | 3.5 | 67 | 1.3 | 74.3 | 2.1 | 2.915 | 0.032 |
| CLIB01 - 12 | 7.41 | 0.1 | 0.408 | 0.0061 | 0.17604 | 0.1318 | 0.0019 | 0.36529 | 0.1202 | 0.0049 | 2160 | 12 | 2205 | 28 | 2299 | 88 | 2114 | 25 | 108.3 | 3.8 | 47.7 | 1.7 | 55.5 | 1.2 | 2.271 | 0.021 |
| CLIB01 - 13 | 6.718 | 0.093 | 0.3717 | 0.0061 | 0.63678 | 0.1314 | 0.0013 | 0.1392 | 0.1017 | 0.0036 | 2076 | 12 | 2037 | 29 | 1956 | 66 | 2113 | 18 | 170.7 | 8 | 83.1 | 5.2 | 82.3 | 4.8 | 2.127 | 0.037 |
| CLIB01 - 14 | 7.43 | 0.11 | 0.4215 | 0.0071 | 0.22245 | 0.1277 | 0.0018 | 0.26358 | 0.1118 | 0.0044 | 2162 | 15 | 2267 | 32 | 2140 | 78 | 2058 | 23 | 67.2 | 2.2 | 26.4 | 1.6 | 29.5 | 2 | 2.611 | 0.079 |
| CLIB01 - 15 | 7.23 | 0.1 | 0.3969 | 0.0062 | 0.29931 | 0.1323 | 0.0019 | 0.33022 | 0.1103 | 0.004 | 2138 | 13 | 2154 | 28 | 2113 | 74 | 2120 | 25 | 117.9 | 5.5 | 77.4 | 3.9 | 82 | 3.3 | 1.541 | 0.019 |
| CLIB01 - 16 | 7.115 | 0.095 | 0.4034 | 0.0059 | 0.25693 | 0.1281 | 0.0016 | 0.26028 | 0.1069 | 0.0039 | 2124 | 12 | 2184 | 27 | 2051 | 71 | 2066 | 23 | 110.8 | 3.5 | 55.4 | 1.7 | 57.2 | 1.4 | 2.002 | 0.018 |
| CLIB01 - 17 | 6.37 | 0.13 | 0.3556 | 0.0081 | 0.90391 | 0.1296 | 0.0011 | 0.021057 | 0.103 | 0.004 | 2023 | 19 | 1959 | 39 | 1979 | 73 | 2092 | 14 | 296 | 16 | 128.3 | 7.4 | 123 | 4.3 | 2.327 | 0.019 |
| CLIB01 - 20 | 7.22 | 0.12 | 0.4061 | 0.0065 | 0.37762 | 0.1287 | 0.0018 | 0.24095 | 0.1128 | 0.0042 | 2136 | 14 | 2196 | 29 | 2159 | 76 | 2079 | 25 | 114.6 | 3.8 | 37.5 | 1.4 | 39.9 | 1.3 | 3.083 | 0.035 |
| CLIB01 - 22 | 4.15 | 0.13 | 0.0973 | 0.0021 | 0.81633 | 0.3077 | 0.0057 | -0.42426 | 0.1568 | 0.0067 | 1654 | 26 | 598.3 | 13 | 2937 | 120 | 3498 | 30 | 477 | 34 | 228 | 13 | 320.1 | 9.7 | 2.064 | 0.051 |
| CLIB01 - 24 | 7.2 | 0.11 | 0.4069 | 0.0069 | 0.57499 | 0.1286 | 0.0017 | 0.23461 | 0.1156 | 0.0043 | 2134 | 13 | 2200 | 32 | 2209 | 77 | 2073 | 23 | 120.9 | 5.3 | 56.3 | 2.6 | 59.3 | 2.1 | 2.157 | 0.018 |
| CLIB01 - 25 | 5.84 | 0.12 | 0.324 | 0.0073 | 0.86754 | 0.1304 | 0.0012 | 0.14801 | 0.0998 | 0.004 | 1948 | 18 | 1807 | 35 | 1920 | 74 | 2104 | 17 | 290 | 14 | 170.4 | 8.6 | 150.3 | 3.8 | 1.71 | 0.013 |
| CLIB01 - 26 | 6.84 | 0.12 | 0.3784 | 0.007 | 0.82933 | 0.131 | 0.0012 | 0.037313 | 0.1165 | 0.0042 | 2088 | 15 | 2067 | 33 | 2226 | 77 | 2109 | 16 | 234.1 | 9.3 | 107.3 | 4.2 | 112.8 | 2.8 | 2.183 | 0.014 |
| CLIB01 - 30 | 5.51 | 0.11 | 0.3027 | 0.0057 | 0.61965 | 0.132 | 0.002 | 0.15369 | 0.1017 | 0.0037 | 1897 | 16 | 1703 | 27 | 1956 | 67 | 2116 | 27 | 118.7 | 4.8 | 65.2 | 2.9 | 60.4 | 2.7 | 1.858 | 0.039 |
| CLIB01 - 31 | 5.81 | 0.19 | 0.3205 | 0.01 | 0.95078 | 0.1314 | 0.0012 | -0.06873 | 0.0977 | 0.0041 | 1935 | 28 | 1787 | 50 | 1881 | 75 | 2114 | 16 | 328 | 25 | 191 | 19 | 152.3 | 9.8 | 1.868 | 0.05 |
| CLIB01 - 32 | 4.931 | 0.087 | 0.2769 | 0.0057 | 0.8412 | 0.1291 | 0.0012 | 0.10854 | 0.0874 | 0.0028 | 1806 | 15 | 1574 | 29 | 1693 | 53 | 2082 | 17 | 333.6 | 6.6 | 162.5 | 4.2 | 129.1 | 3.4 | 2.068 | 0.019 |
| CLIB01 - 33 | 4.92 | 0.059 | 0.2589 | 0.0044 | 0.6243 | 0.1379 | 0.0013 | 0.3975 | 0.0802 | 0.0027 | 1804.1 | 9.7 | 1483 | 23 | 1559 | 50 | 2198 | 17 | 639 | 42 | 412 | 22 | 300 | 16 | 1.527 | 0.019 |
| CLIB01 - 34 | 6.895 | 0.081 | 0.3877 | 0.0055 | 0.49259 | 0.1287 | 0.0013 | 0.096526 | 0.1119 | 0.0037 | 2096 | 10 | 2112 | 25 | 2143 | 67 | 2079 | 17 | 211.2 | 4 | 122.4 | 3.6 | 124.4 | 3.1 | 1.751 | 0.025 |
| CLIB01 - 35 | 7.22 | 0.11 | 0.4036 | 0.0066 | 0.53409 | 0.1298 | 0.0017 | 0.18537 | 0.1167 | 0.0042 | 2136 | 14 | 2185 | 30 | 2230 | 78 | 2089 | 23 | 136.3 | 6 | 63.9 | 2.8 | 66.8 | 2.3 | 2.142 | 0.019 |
| CLIB01 - 36 | 3.278 | 0.048 | 0.1823 | 0.0029 | 0.59847 | 0.1303 | 0.0016 | 0.056694 | 0.0601 | 0.0021 | 1474 | 11 | 1079.4 | 16 | 1182 | 39 | 2099 | 21 | 422 | 18 | 290 | 13 | 159.7 | 7.5 | 1.4572 | 0.0094 |
| CLIB01 - 38 | 6.1 | 0.15 | 0.3144 | 0.0087 | 0.87915 | 0.1412 | 0.0016 | 0.46122 | 0.126 | 0.0051 | 1984 | 21 | 1758 | 43 | 2394 | 92 | 2238 | 20 | 264 | 19 | 114 | 12 | 121.3 | 7.9 | 2.504 | 0.059 |
| CLIB01 - 39 | 7.254 | 0.096 | 0.4059 | 0.0062 | 0.33251 | 0.1296 | 0.0017 | 0.31093 | 0.1156 | 0.0041 | 2142 | 12 | 2197 | 28 | 2209 | 75 | 2089 | 23 | 133.3 | 5.2 | 61.4 | 2.4 | 65.5 | 2.2 | 2.175 | 0.02 |
| CLIB01 - 41 | 7.201 | 0.073 | 0.4 | 0.0058 | 0.48579 | 0.1306 | 0.0012 | 0.30215 | 0.1194 | 0.004 | 2135.3 | 8.8 | 2168 | 27 | 2279 | 72 | 2104 | 16 | 240.7 | 8.6 | 117.9 | 3.9 | 130.8 | 3.5 | 2.037 | 0.015 |
| CLIB01 - 42 | 6.28 | 0.18 | 0.3449 | 0.0089 | 0.90937 | 0.1312 | 0.0016 | -0.33196 | 0.1103 | 0.0045 | 2004 | 25 | 1907 | 43 | 2113 | 82 | 2109 | 21 | 247 | 4.6 | 118 | 2.2 | 123 | 3.9 | 2.115 | 0.051 |
| CLIB01 - 43 | 8.31 | 0.11 | 0.4484 | 0.0073 | 0.70209 | 0.1342 | 0.0012 | 0.07475 | 0.1369 | 0.0047 | 2263 | 12 | 2387 | 32 | 2592 | 83 | 2153 | 16 | 262.6 | 2.7 | 118.1 | 1.8 | 152 | 3.7 | 2.24 | 0.027 |
| CLIB01 - 44 | 4.189 | 0.077 | 0.2099 | 0.0052 | 0.70202 | 0.1454 | 0.0022 | 0.48294 | 0.0779 | 0.0028 | 1668 | 15 | 1227 | 27 | 1516 | 52 | 2285 | 25 | 339 | 17 | 272 | 15 | 201 | 12 | 1.265 | 0.012 |
| CLIB01 - 45 | 7.21 | 0.13 | 0.405 | 0.0068 | 0.60906 | 0.1293 | 0.0018 | 0.022877 | 0.1162 | 0.0045 | 2133 | 16 | 2191 | 31 | 2219 | 83 | 2081 | 25 | 119.3 | 4.8 | 53.4 | 2.2 | 57.1 | 1.6 | 2.244 | 0.023 |
| CLIB01 - 46 | 20.3 | 2.2 | 0.686 | 0.047 | 0.98456 | 0.1973 | 0.0083 | -0.87395 | 0.81 | 0.12 | 2930 | 100 | 3290 | 170 | 10800 | 1200 | 2740 | 72 | 66.7 | 6.4 | 27.3 | 3.2 | 139 | 14 | 2.634 | 0.064 |
| CLIB01 - 47 | 7.12 | 0.1 | 0.3576 | 0.0075 | 0.6981 | 0.1447 | 0.0018 | 0.56796 | 0.1421 | 0.0049 | 2124 | 12 | 1968 | 36 | 2685 | 86 | 2282 | 22 | 206.2 | 3.2 | 127.4 | 2.1 | 172.3 | 2.4 | 1.619 | 0.017 |
| CLIB01 - 48 | 2.356 | 0.075 | 0.0811 | 0.0015 | 0.21127 | 0.2117 | 0.0076 | 0.53143 | 0.0727 | 0.0039 | 1221 | 22 | 502.7 | 8.9 | 1415 | 74 | 2874 | 61 | 369 | 35 | 240 | 23 | 183 | 23 | 1.537 | 0.014 |
| CLIB01 - 49 | 5.74 | 0.17 | 0.3165 | 0.0088 | 0.91356 | 0.1314 | 0.0014 | -0.10235 | 0.1119 | 0.0037 | 1926 | 24 | 1768 | 43 | 2144 | 67 | 2112 | 19 | 253 | 12 | 115.4 | 2.7 | 124.6 | 2.2 | 2.154 | 0.066 |
| CLIB01 - 50 | 6.628 | 0.081 | 0.3717 | 0.0053 | 0.23981 | 0.1293 | 0.0016 | 0.29178 | 0.1049 | 0.0035 | 2061 | 11 | 2037 | 25 | 2019 | 65 | 2083 | 22 | 178.9 | 4.4 | 89.3 | 2.3 | 90.4 | 2.2 | 2.005 | 0.015 |
| CLIB01 - 51 | 5.92 | 0.15 | 0.322 | 0.0088 | 0.88314 | 0.1336 | 0.0015 | 0.30223 | 0.1123 | 0.0044 | 1957 | 22 | 1796 | 44 | 2149 | 80 | 2142 | 20 | 212 | 16 | 101.4 | 8.7 | 102.8 | 5.9 | 2.155 | 0.029 |
| CLIB01 - 53 | 6.19 | 0.15 | 0.2917 | 0.0073 | 0.67203 | 0.1544 | 0.0028 | 0.29358 | 0.1712 | 0.0085 | 1996 | 21 | 1647 | 36 | 3180 | 150 | 2384 | 30 | 166.8 | 5.6 | 69.7 | 2.1 | 112.9 | 2.7 | 2.389 | 0.027 |
| CLIB01 - 54 | 6.624 | 0.076 | 0.3756 | 0.0053 | 0.37552 | 0.1277 | 0.0014 | 0.2522 | 0.1038 | 0.0034 | 2061 | 10 | 2055 | 25 | 1999 | 62 | 2062 | 20 | 174 | 2.3 | 113.2 | 1.6 | 115.6 | 1.8 | 1.5314 | 0.0097 |
| CLIB01 - 55 | 7.07 | 0.13 | 0.3942 | 0.0063 | 0.10311 | 0.1304 | 0.0025 | 0.4369 | 0.1155 | 0.0045 | 2117 | 15 | 2141 | 29 | 2207 | 83 | 2090 | 34 | 68.2 | 2 | 35.2 | 1.3 | 39.5 | 1.2 | 1.957 | 0.029 |
| CLIB01 - 56 | 3.421 | 0.091 | 0.0953 | 0.0047 | 0.9203 | 0.2703 | 0.006 | 0.80307 | 0.0995 | 0.0047 | 1509 | 21 | 585 | 28 | 1914 | 85 | 3292 | 36 | 686 | 11 | 464.3 | 7.7 | 457 | 12 | 1.485 | 0.027 |
| CLIB01 - 57 | 7.11 | 0.11 | 0.3915 | 0.007 | 0.66173 | 0.1317 | 0.0015 | 0.2287 | 0.1241 | 0.0045 | 2122 | 14 | 2128 | 32 | 2363 | 80 | 2116 | 20 | 172.8 | 6.9 | 87 | 3.1 | 105 | 2.3 | 1.973 | 0.019 |
| CLIB01 - 58 | 2.14 | 0.13 | 0.0953 | 0.0042 | 0.73028 | 0.1636 | 0.0055 | 0.13206 | 0.0583 | 0.0063 | 1139 | 37 | 585 | 25 | 1130 | 120 | 2450 | 61 | 618 | 18 | 359 | 34 | 176 | 12 | 2.23 | 0.18 |
| CLIB01 - 59 | 5.53 | 0.096 | 0.308 | 0.0056 | 0.78889 | 0.1301 | 0.0013 | -0.04157 | 0.0983 | 0.0039 | 1902 | 15 | 1730 | 28 | 1893 | 72 | 2095 | 18 | 312 | 16 | 137.4 | 6.7 | 129.1 | 3.7 | 2.262 | 0.017 |
| CLIB01 - 60 | 6.723 | 0.091 | 0.3683 | 0.0059 | 0.63021 | 0.1323 | 0.0013 | 0.15997 | 0.1133 | 0.0043 | 2073 | 12 | 2021 | 28 | 2166 | 78 | 2127 | 17 | 273.7 | 9.7 | 114.5 | 5.4 | 125 | 3.4 | 2.426 | 0.03 |
| CLIB01 - 61 | 6.865 | 0.093 | 0.3786 | 0.0054 | 0.55986 | 0.1318 | 0.0014 | -0.03889 | 0.112 | 0.0045 | 2092 | 12 | 2070 | 25 | 2151 | 83 | 2120 | 20 | 210.9 | 4.8 | 103 | 2 | 115 | 2.5 | 2.039 | 0.016 |
| CLIB01 - 62 | 7.59 | 0.11 | 0.4188 | 0.0065 | 0.48879 | 0.1315 | 0.0016 | 0.16334 | 0.1231 | 0.0046 | 2181 | 13 | 2254 | 29 | 2345 | 83 | 2112 | 22 | 138 | 2.5 | 57.2 | 1.1 | 69.6 | 1.2 | 2.412 | 0.023 |
| CLIB01 - 63 | 4.67 | 0.17 | 0.23 | 0.011 | 0.51406 | 0.1509 | 0.0045 | 0.44438 | 0.1103 | 0.0078 | 1748 | 29 | 1328 | 56 | 2100 | 140 | 2328 | 48 | 304 | 27 | 196 | 22 | 170 | 13 | 1.86 | 0.11 |
| CLIB01 - 64 | 10.91 | 0.93 | 0.351 | 0.018 | 0.93807 | 0.2269 | 0.0097 | -0.40077 | 0.476 | 0.052 | 2479 | 73 | 1932 | 85 | 7850 | 730 | 2967 | 72 | 346 | 25 | 102.7 | 3.3 | 505 | 51 | 3.23 | 0.13 |
| CLIB01 - 65 | 4.308 | 0.095 | 0.2179 | 0.0056 | 0.86617 | 0.1436 | 0.0016 | 0.38312 | 0.1049 | 0.0036 | 1689 | 18 | 1269 | 30 | 2016 | 65 | 2268 | 19 | 351 | 19 | 134.1 | 6.9 | 137.4 | 5.6 | 2.609 | 0.02 |
| CLIB01 - 66 | 7.71 | 0.15 | 0.3835 | 0.0056 | 0.41967 | 0.1457 | 0.0025 | -0.05236 | 0.1551 | 0.0083 | 2193 | 18 | 2092 | 26 | 2900 | 150 | 2285 | 31 | 157.1 | 3.9 | 78.8 | 2.1 | 116.9 | 3.2 | 1.994 | 0.017 |
| CLIB01 - 67 | 7.552 | 0.099 | 0.3937 | 0.006 | 0.42896 | 0.1391 | 0.0016 | 0.25267 | 0.1363 | 0.0051 | 2177 | 12 | 2139 | 27 | 2580 | 90 | 2214 | 20 | 125.1 | 4.5 | 57.8 | 2 | 76.7 | 1.9 | 2.157 | 0.021 |
| CLIB01 - 68 | 6.834 | 0.057 | 0.3831 | 0.0054 | 0.39092 | 0.1293 | 0.001 | 0.36045 | 0.1099 | 0.0036 | 2089.2 | 7.2 | 2091 | 25 | 2108 | 65 | 2085 | 14 | 295.9 | 8.6 | 131.2 | 3.6 | 141.6 | 3.3 | 2.247 | 0.014 |
| CLIB01 - 69 | 3.189 | 0.036 | 0.1439 | 0.0022 | 0.30031 | 0.1608 | 0.0019 | 0.36178 | 0.0897 | 0.0031 | 1453 | 8.7 | 866.7 | 12 | 1735 | 58 | 2459 | 20 | 586 | 26 | 260 | 12 | 230 | 12 | 2.259 | 0.019 |
| CLIB01 - 70 | 6.21 | 0.13 | 0.3498 | 0.008 | 0.91085 | 0.1287 | 0.0011 | 0.067516 | 0.0996 | 0.0038 | 2000 | 19 | 1931 | 38 | 1916 | 70 | 2077 | 15 | 286 | 17 | 145.8 | 8.6 | 135.5 | 5.3 | 1.97 | 0.016 |
| CLIB01 - 71 | 3.291 | 0.065 | 0.1927 | 0.0041 | 0.80658 | 0.1239 | 0.0013 | 0.11298 | 0.0644 | 0.0025 | 1475 | 15 | 1135 | 22 | 1260 | 47 | 2011 | 19 | 480 | 27 | 183 | 11 | 109.7 | 3.7 | 2.628 | 0.02 |
| CLIB01 - 72 | 6.9 | 0.1 | 0.3886 | 0.0057 | 0.32807 | 0.1287 | 0.0017 | 0.17624 | 0.1139 | 0.0039 | 2096 | 13 | 2116 | 26 | 2179 | 71 | 2074 | 24 | 126.1 | 4.6 | 58.3 | 2 | 64 | 1.8 | 2.156 | 0.023 |
| CLIB01 - 73 | 3.524 | 0.054 | 0.1798 | 0.0033 | 0.39874 | 0.1425 | 0.002 | 0.45867 | 0.0964 | 0.0033 | 1530 | 12 | 1066 | 18 | 1859 | 60 | 2250 | 26 | 253 | 14 | 117.7 | 4.8 | 108.4 | 4.2 | 2.115 | 0.035 |
| CLIB01 - 74 | 9.37 | 0.32 | 0.39 | 0.0066 | 0.74851 | 0.1732 | 0.0045 | -0.52654 | 0.326 | 0.023 | 2358 | 32 | 2122 | 31 | 5610 | 350 | 2564 | 45 | 137.3 | 5.8 | 53.6 | 2.7 | 151.9 | 7.3 | 2.599 | 0.033 |
| CLIB01 - 75 | 7.19 | 0.13 | 0.408 | 0.0065 | 0.26109 | 0.1278 | 0.0023 | 0.25181 | 0.1125 | 0.0039 | 2131 | 17 | 2207 | 29 | 2154 | 71 | 2054 | 33 | 62.4 | 1.8 | 48.2 | 1.5 | 51.6 | 1.5 | 1.298 | 0.014 |
| CLIB01 - 76 | 3.643 | 0.063 | 0.2041 | 0.0043 | 0.80135 | 0.1299 | 0.0014 | 0.25997 | 0.0704 | 0.0029 | 1557 | 14 | 1196 | 23 | 1373 | 55 | 2092 | 19 | 373 | 20 | 205 | 19 | 126.8 | 6.5 | 1.972 | 0.049 |
| CLIB01 - 77 | 1.281 | 0.03 | 0.04731 | 0.00086 | 0.2073 | 0.1966 | 0.0046 | 0.30053 | 0.03356 | 0.0013 | 834 | 13 | 298 | 5.3 | 667 | 27 | 2790 | 40 | 762 | 53 | 747 | 57 | 228 | 13 | 1.035 | 0.011 |
| CLIB01 - 78 | 5.738 | 0.097 | 0.3214 | 0.0056 | 0.57612 | 0.1295 | 0.0018 | 0.12278 | 0.1021 | 0.0038 | 1933 | 15 | 1796 | 27 | 1964 | 69 | 2084 | 25 | 168 | 6.3 | 70.2 | 2.4 | 67.5 | 2.1 | 2.387 | 0.025 |
| CLIB01 - 79 | 4.8 | 0.11 | 0.2491 | 0.0066 | 0.82031 | 0.1401 | 0.0019 | 0.32277 | 0.1041 | 0.0043 | 1778 | 19 | 1431 | 34 | 1999 | 78 | 2222 | 23 | 326 | 18 | 141.4 | 8.2 | 132.2 | 3.6 | 2.322 | 0.02 |
| CLIB01 - 80 | 2.778 | 0.089 | 0.1055 | 0.0044 | 0.87132 | 0.1938 | 0.0037 | 0.50776 | 0.0809 | 0.0046 | 1343 | 23 | 645 | 26 | 1568 | 85 | 2762 | 31 | 812 | 12 | 454 | 14 | 333 | 8.9 | 1.843 | 0.064 |
| CLIB01 - 81 | 6.157 | 0.079 | 0.3468 | 0.0059 | 0.67672 | 0.1291 | 0.0011 | 0.29608 | 0.107 | 0.0036 | 1996 | 11 | 1918 | 28 | 2054 | 66 | 2082 | 16 | 236 | 12 | 112.3 | 6.9 | 110.1 | 5 | 2.141 | 0.025 |
| CLIB01 - 82 | 4.258 | 0.059 | 0.2425 | 0.004 | 0.59504 | 0.1272 | 0.0014 | 0.22198 | 0.0703 | 0.0024 | 1683 | 11 | 1399 | 21 | 1376 | 45 | 2057 | 20 | 287 | 11 | 181.7 | 6.3 | 120 | 3.9 | 1.573 | 0.015 |
| CLIB01 - 83 | 6.09 | 0.078 | 0.2642 | 0.0055 | 0.58309 | 0.1677 | 0.0022 | 0.68215 | 0.1674 | 0.006 | 1987 | 11 | 1510 | 28 | 3124 | 100 | 2532 | 23 | 452 | 18 | 186.6 | 9.5 | 287 | 11 | 2.464 | 0.03 |
| CLIB01 - 84 | 7.09 | 0.097 | 0.3901 | 0.0066 | 0.60783 | 0.1319 | 0.0014 | 0.22789 | 0.1332 | 0.0046 | 2120 | 12 | 2122 | 30 | 2525 | 81 | 2119 | 19 | 212 | 14 | 81 | 5.5 | 98.1 | 5.4 | 2.647 | 0.029 |
| CLIB01 - 85 | 6.366 | 0.098 | 0.3465 | 0.006 | 0.46268 | 0.1337 | 0.0018 | 0.35627 | 0.1197 | 0.004 | 2026 | 13 | 1917 | 29 | 2285 | 72 | 2140 | 24 | 164.8 | 7.7 | 77.1 | 3.7 | 84.1 | 3.3 | 2.143 | 0.018 |
| CLIB01 - 86 | 5.36 | 0.22 | 0.1964 | 0.0041 | 0.77578 | 0.1961 | 0.0059 | -0.53491 | 0.1256 | 0.0075 | 1856 | 37 | 1155 | 22 | 2380 | 140 | 2758 | 54 | 395 | 17 | 249 | 11 | 265.9 | 8 | 1.585 | 0.011 |
| CLIB01 - 87 | 6.75 | 0.12 | 0.3808 | 0.0086 | 0.92656 | 0.1288 | 0.00087 | 0.19137 | 0.1107 | 0.0038 | 2075 | 16 | 2077 | 40 | 2121 | 70 | 2080 | 12 | 635 | 40 | 318 | 18 | 326 | 20 | 1.978 | 0.017 |
| CLIB01 - 88 | 7.083 | 0.082 | 0.395 | 0.0057 | 0.40005 | 0.1301 | 0.0013 | 0.25502 | 0.119 | 0.0038 | 2121 | 10 | 2146 | 26 | 2271 | 68 | 2097 | 19 | 204.1 | 6.8 | 97.2 | 3.1 | 104.9 | 3.1 | 2.102 | 0.015 |

ACCEPTED MANUSCRIPT

| | | | | | | | | | | | | | | | | | | | | | | | | | |
|---|---|---|---|---|---|---|---|---|---|---|---|---|---|---|---|---|---|---|---|---|---|---|---|---|---|
| CLIB01 - 89 | 5.48 | 0.14 | 0.2921 | 0.0085 | 0.83642 | 0.1363 | 0.002 | 0.25526 | 0.1105 | 0.004 | 1888 | 23 | 1648 | 42 | 2117 | 72 | 2175 | 27 | 149.3 | 6.2 | 77.2 | 3.1 | 76 | 2.5 | 1.939 | 0.037 |
| CLIB01 - 90 | 2.838 | 0.058 | 0.1514 | 0.0041 | 0.86624 | 0.1365 | 0.0016 | 0.57207 | 0.0732 | 0.0023 | 1362 | 16 | 908 | 23 | 1428 | 44 | 2178 | 21 | 470 | 32 | 185 | 11 | 121.8 | 7.6 | 2.518 | 0.025 |
| CLIB01 - 91 | 6.23 | 0.18 | 0.3241 | 0.0068 | 0.90309 | 0.1389 | 0.002 | -0.57257 | 0.1158 | 0.0066 | 2001 | 25 | 1808 | 33 | 2200 | 120 | 2206 | 25 | 317 | 12 | 184 | 7.5 | 177.9 | 3.7 | 1.736 | 0.014 |
| CLIB01 - 92 | 3.77 | 0.35 | 0.1247 | 0.0081 | 0.99516 | 0.2179 | 0.0056 | -0.85757 | 0.143 | 0.018 | 1556 | 60 | 753 | 44 | 2680 | 300 | 2950 | 39 | 832 | 44 | 377 | 22 | 508 | 87 | 2.231 | 0.022 |
| CLIB01 - 93 | 1.084 | 0.023 | 0.06523 | 0.0011 | 0.49365 | 0.1205 | 0.0022 | 0.059487 | 0.02916 | 0.0011 | 743 | 11 | 407.3 | 6.8 | 581 | 21 | 1951 | 33 | 554 | 36 | 408 | 26 | 106.9 | 7.1 | 1.3582 | 0.0093 |
| CLIB01 - 94 | 8.06 | 0.17 | 0.4276 | 0.0077 | 0.76996 | 0.1362 | 0.0019 | -0.12656 | 0.1551 | 0.0071 | 2232 | 18 | 2293 | 35 | 2910 | 120 | 2172 | 24 | 112.1 | 2.2 | 59.3 | 1.6 | 83.8 | 4 | 1.909 | 0.028 |
| CLIB01 - 96 | 4.94 | 0.15 | 0.236 | 0.012 | 0.88355 | 0.1575 | 0.0039 | 0.84761 | 0.1125 | 0.0042 | 1801 | 26 | 1358 | 60 | 2153 | 76 | 2408 | 42 | 258 | 35 | 129 | 17 | 127 | 16 | 1.961 | 0.025 |
| CLIB01 - 97 | 4.15 | 0.055 | 0.2316 | 0.0042 | 0.7372 | 0.1301 | 0.0012 | 0.26639 | 0.0806 | 0.0025 | 1662 | 11 | 1342 | 22 | 1566 | 46 | 2098 | 16 | 461 | 19 | 219.5 | 8.8 | 158.2 | 5.4 | 2.099 | 0.014 |
| CLIB01 - 98 | 9.5 | 0.15 | 0.4258 | 0.0071 | 0.72164 | 0.1614 | 0.0017 | -0.05288 | 0.2489 | 0.0098 | 2384 | 15 | 2286 | 32 | 4480 | 160 | 2469 | 18 | 203.1 | 9 | 84.9 | 3.8 | 191.6 | 9.6 | 2.395 | 0.017 |
| CLIB01 - 99 | 7.24 | 0.1 | 0.4075 | 0.0064 | 0.45324 | 0.1292 | 0.0017 | 0.23774 | 0.1191 | 0.004 | 2140 | 13 | 2202 | 29 | 2274 | 72 | 2080 | 24 | 106.5 | 3.3 | 46.7 | 1.5 | 50.4 | 1.4 | 2.285 | 0.021 |
| CLIB01 - 10 | 7.16 | 0.11 | 0.4013 | 0.0067 | 0.46324 | 0.1291 | 0.0019 | 0.27676 | 0.1217 | 0.0042 | 2128 | 14 | 2176 | 31 | 2326 | 76 | 2081 | 26 | 73.7 | 2.6 | 56 | 2.1 | 61.4 | 1.7 | 1.321 | 0.015 |
| CLIB01 - 10 | 4.26 | 0.14 | 0.1454 | 0.0052 | 0.89535 | 0.2137 | 0.0029 | 0.28923 | 0.2077 | 0.01 | 1673 | 28 | 873 | 29 | 3800 | 170 | 2930 | 22 | 304 | 26 | 106 | 10 | 179.2 | 8.9 | 2.942 | 0.036 |
| CLIB01 - 10 | 6.42 | 0.12 | 0.3586 | 0.007 | 0.68951 | 0.1297 | 0.0017 | 0.12268 | 0.1129 | 0.0044 | 2030 | 17 | 1974 | 33 | 2160 | 79 | 2089 | 24 | 117 | 5.8 | 43.5 | 2.2 | 44.1 | 1.5 | 2.694 | 0.03 |
| CLIB01 - 10 | 3.276 | 0.073 | 0.0917 | 0.0025 | 0.18455 | 0.2669 | 0.0091 | 0.74821 | 0.1082 | 0.0046 | 1473 | 17 | 565 | 15 | 2073 | 84 | 3250 | 55 | 877 | 34 | 525 | 21 | 511.3 | 9.2 | 1.668 | 0.014 |
| CLIB01 - 10 | 5.77 | 0.15 | 0.2842 | 0.0085 | 0.93156 | 0.1474 | 0.0014 | 0.18669 | 0.1057 | 0.0042 | 1939 | 22 | 1609 | 43 | 2029 | 77 | 2313 | 17 | 371 | 24 | 229 | 17 | 221 | 12 | 1.672 | 0.016 |
| CLIB01 - 10 | 6.761 | 0.067 | 0.3744 | 0.0056 | 0.39451 | 0.1309 | 0.0012 | 0.3773 | 0.1172 | 0.0041 | 2079.3 | 8.8 | 2050 | 26 | 2238 | 74 | 2107 | 16 | 250.5 | 5.4 | 98.6 | 2.7 | 108.7 | 1.9 | 2.543 | 0.026 |

Accepted Manuscript

ACCEPTED MANUSCRIPT

| | Ratios | | | | | | | | | Ages | | | | | | | | Concentrations (calculated from 91500) | | | | | | | | |
|---|---|---|---|---|---|---|---|---|---|---|---|---|---|---|---|---|---|---|---|---|---|---|---|---|---|---|
| Sample - ar | 207Pb/235 | Propagatec | 206Pb/238 | Propagatec | Error Corre | 207Pb/206 | Propagatec | Error Corre | 208Pb/232 | Propagatec | 207Pb/235 | Propagatec | 206Pb/238 | Propagatec | 208Pb/232 | Propagatec | 207Pb/206 | Propagatec | U (ppm) | Internal 2 S | Th (ppm) | Internal 2 S | Pb (ppm) | Internal 2 S | U/Th | Internal 2 SE |
| CLIB5_80 - | 2.82 | 0.19 | 0.0714 | 0.0042 | 0.97982 | 0.2847 | 0.0046 | -0.71018 | 0.1501 | 0.011 | 1346 | 49 | 444 | 25 | 2820 | 200 | 3385 | 25 | 1723 | 77 | 921 | 42 | 1280 | 46 | 1.865 | 0.03 |
| CLIB5_35 - | 2.223 | 0.17 | 0.0896 | 0.0055 | 0.73063 | 0.1772 | 0.0041 | -0.2371 | 0.0966 | 0.012 | 1185 | 46 | 553 | 32 | 1850 | 220 | 2613 | 37 | 622 | 42 | 260 | 12 | 275 | 28 | 2.255 | 0.08 |
| CLIB5_48 - | 2.104 | 0.11 | 0.1289 | 0.0065 | 0.83909 | 0.1193 | 0.0021 | -0.15397 | 0.0486 | 0.0036 | 1147 | 37 | 781 | 37 | 957 | 69 | 1943 | 31 | 630 | 28 | 228 | 10 | 104.7 | 4.7 | 2.693 | 0.035 |
| CLIB5_71 - | 2.929 | 0.16 | 0.1476 | 0.0079 | 0.87144 | 0.1465 | 0.0025 | 0.10138 | 0.0888 | 0.0057 | 1381 | 42 | 886 | 45 | 1724 | 110 | 2299 | 29 | 667 | 30 | 347 | 13 | 280 | 13 | 1.897 | 0.031 |
| CLIB5_51 - | 4.99 | 0.29 | 0.1502 | 0.0071 | 0.58252 | 0.2396 | 0.0078 | -0.20166 | 0.901 | 0.11 | 1800 | 52 | 902 | 40 | 12000 | 1300 | 3084 | 56 | 709 | 11 | 131 | 12 | 779 | 44 | 6.96 | 0.52 |
| CLIB5_56 - | 2.738 | 0.13 | 0.1513 | 0.0072 | 0.77691 | 0.131 | 0.002 | -0.05765 | 0.0731 | 0.0049 | 1337 | 37 | 909 | 41 | 1425 | 92 | 2111 | 28 | 471 | 25 | 165.8 | 9.3 | 109.4 | 3 | 2.836 | 0.039 |
| CLIB5_32 - | 2.637 | 0.13 | 0.1551 | 0.0071 | 0.70794 | 0.1219 | 0.0017 | 0.15724 | 0.05443 | 0.0032 | 1310.8 | 35 | 929.3 | 40 | 1071 | 62 | 1982 | 24 | 695 | 29 | 253 | 10 | 136.2 | 4.6 | 2.742 | 0.028 |
| CLIB5_30 - | 2.79 | 0.14 | 0.159 | 0.0078 | 0.88451 | 0.1271 | 0.0019 | -0.03804 | 0.0549 | 0.0032 | 1349 | 37 | 950 | 43 | 1080 | 62 | 2054 | 26 | 504 | 12 | 262.7 | 6.8 | 139.7 | 3.7 | 1.948 | 0.02 |
| CLIB5_60 - | 7.99 | 0.38 | 0.1615 | 0.0078 | 0.90874 | 0.3592 | 0.0044 | 0.27419 | 0.443 | 0.026 | 2226 | 44 | 965 | 43 | 7405 | 370 | 3745.1 | 18 | 865 | 37 | 390 | 15 | 1580 | 63 | 2.194 | 0.025 |
| CLIB5_3 - 1 | 3.204 | 0.16 | 0.169 | 0.0083 | 0.69945 | 0.1372 | 0.0023 | 0.62872 | 0.0867 | 0.0055 | 1456 | 37 | 1006 | 46 | 1679 | 100 | 2189 | 28 | 459 | 15 | 179.1 | 6 | 159.5 | 4.2 | 2.654 | 0.022 |
| CLIB5_41 - | 3.006 | 0.26 | 0.1742 | 0.014 | 0.7666 | 0.1254 | 0.0018 | 0.027024 | 0.062 | 0.005 | 1407 | 52 | 1035 | 73 | 1215 | 93 | 2030 | 25 | 362 | 11 | 164.6 | 5.7 | 99.4 | 3.1 | 2.125 | 0.039 |
| CLIB5_8 - 1 | 2.994 | 0.14 | 0.175 | 0.0081 | 0.86597 | 0.12513 | 0.0016 | 0.073651 | 0.0597 | 0.0034 | 1404 | 36 | 1039 | 45 | 1172 | 65 | 2029 | 23 | 736 | 35 | 319 | 14 | 179.1 | 6.1 | 2.389 | 0.02 |
| CLIB5_70 - | 3.161 | 0.17 | 0.1796 | 0.0093 | 0.89984 | 0.1295 | 0.002 | 0.16418 | 0.0766 | 0.0051 | 1441 | 39 | 1063 | 51 | 1490 | 95 | 2087 | 27 | 889 | 42 | 400 | 23 | 257.3 | 5.8 | 2.257 | 0.045 |
| CLIB5_49 - | 3.389 | 0.16 | 0.1912 | 0.0089 | 0.8921 | 0.1284 | 0.0019 | 0.10739 | 0.0564 | 0.0035 | 1500 | 37 | 1127 | 48 | 1108 | 67 | 2074 | 24 | 1089 | 44 | 1080 | 40 | 601 | 30 | 0.984 | 0.014 |
| CLIB5_82 - | 3.261 | 0.16 | 0.1912 | 0.0091 | 0.85068 | 0.1247 | 0.0018 | -0.08744 | 0.0686 | 0.0041 | 1468 | 39 | 1127 | 49 | 1340 | 77 | 2021 | 25 | 534 | 19 | 189.5 | 6.3 | 119.3 | 4.2 | 2.794 | 0.048 |
| CLIB5_11 - | 6.17 | 0.31 | 0.1933 | 0.0092 | 0.88758 | 0.2304 | 0.0033 | -0.29876 | 0.389 | 0.024 | 1994 | 44 | 1139 | 50 | 6610 | 350 | 3054 | 23 | 431 | 21 | 153.4 | 8 | 550 | 23 | 2.938 | 0.032 |
| CLIB5_59 - | 3.568 | 0.2 | 0.2035 | 0.012 | 0.69061 | 0.1269 | 0.003 | 0.23382 | 0.0633 | 0.0071 | 1540 | 53 | 1194 | 67 | 1241 | 130 | 2051 | 37 | 325.7 | 7 | 138.2 | 3.6 | 83.3 | 2 | 2.353 | 0.053 |
| CLIB5_61 - | 5.543 | 0.27 | 0.2136 | 0.011 | 0.67664 | 0.1882 | 0.0042 | 0.26157 | 0.2668 | 0.018 | 1905 | 46 | 1247 | 59 | 4776 | 290 | 2723 | 33 | 409.7 | 8.7 | 145.3 | 2.9 | 358.6 | 6.6 | 2.818 | 0.048 |
| CLIB5_75 - | 5 | 0.24 | 0.2293 | 0.012 | 0.59732 | 0.1596 | 0.0074 | 0.11 | 0.141 | 0.021 | 1815 | 45 | 1330 | 66 | 2660 | 270 | 2442 | 66 | 269 | 13 | 109.1 | 6.3 | 147.3 | 9.2 | 2.481 | 0.062 |
| CLIB5_68 - | 4.061 | 0.21 | 0.233 | 0.012 | 0.75039 | 0.1276 | 0.0016 | 0.19101 | 0.0854 | 0.0053 | 1645 | 47 | 1350 | 63 | 1657 | 99 | 2064 | 23 | 917 | 24 | 709 | 14 | 567 | 11 | 1.287 | 0.038 |
| CLIB5_50 - | 4.51 | 0.21 | 0.2533 | 0.012 | 0.81532 | 0.1292 | 0.0017 | 0.076472 | 0.0767 | 0.0049 | 1730 | 40 | 1455 | 61 | 1492 | 91 | 2085 | 23 | 558 | 25 | 337 | 16 | 245.1 | 9.1 | 1.642 | 0.022 |
| CLIB5_28 - | 5.026 | 0.25 | 0.2541 | 0.012 | 0.64162 | 0.1445 | 0.0027 | -0.10577 | 0.1506 | 0.011 | 1825 | 44 | 1459 | 62 | 2830 | 180 | 2281 | 33 | 372.8 | 8.8 | 123.1 | 4.1 | 178 | 12 | 3.118 | 0.062 |
| CLIB5_52 - | 4.675 | 0.22 | 0.2608 | 0.012 | 0.83726 | 0.1295 | 0.0017 | 0.073543 | 0.0892 | 0.0057 | 1760 | 40 | 1493 | 63 | 1726 | 110 | 2088 | 24 | 413 | 18 | 149.3 | 6.5 | 126.8 | 3.6 | 2.729 | 0.037 |
| CLIB5_25 - | 7.33 | 0.38 | 0.2711 | 0.013 | 0.40802 | 0.1978 | 0.0043 | 0.11597 | 0.787 | 0.057 | 2149 | 54 | 1546 | 67 | 11630 | 720 | 2799 | 38 | 494 | 18 | 90.2 | 2.7 | 670 | 42 | 5.571 | 0.087 |
| CLIB5_15 - | 4.92 | 0.23 | 0.2762 | 0.013 | 0.72245 | 0.1279 | 0.0018 | 0.010314 | 0.0823 | 0.005 | 1803 | 40 | 1572 | 64 | 1597 | 92 | 2068 | 25 | 362.8 | 8.1 | 132.7 | 2.6 | 108.4 | 1.9 | 2.83 | 0.028 |
| CLIB5_72 - | 5.289 | 0.25 | 0.2803 | 0.013 | 0.67788 | 0.1391 | 0.002 | 0.23121 | 0.1275 | 0.0076 | 1865 | 41 | 1592 | 66 | 2431 | 140 | 2212 | 24 | 401 | 18 | 176.5 | 8.5 | 201 | 9.2 | 2.279 | 0.031 |
| CLIB5_5 - 1 | 5.075 | 0.24 | 0.285 | 0.013 | 0.78548 | 0.1294 | 0.0018 | 0.11661 | 0.0935 | 0.0059 | 1829 | 40 | 1616 | 66 | 1805 | 110 | 2087 | 25 | 233 | 11 | 114.2 | 6.5 | 101.9 | 3.1 | 2.177 | 0.035 |
| CLIB5_40 - | 5.491 | 0.25 | 0.2961 | 0.014 | 0.65229 | 0.1348 | 0.0019 | 0.16986 | 0.1481 | 0.0089 | 1897 | 42 | 1672 | 68 | 2790 | 160 | 2157 | 25 | 283 | 9.1 | 77.6 | 2.3 | 111 | 3.4 | 3.511 | 0.066 |
| CLIB5_65 - | 7.99 | 0.44 | 0.308 | 0.014 | 0.024375 | 0.1878 | 0.0077 | 0.46427 | 0.349 | 0.025 | 2222 | 49 | 1730 | 72 | 6020 | 380 | 2716 | 57 | 415 | 10 | 135.2 | 7.8 | 436 | 41 | 3.2 | 0.11 |
| CLIB5_12 - | 6.088 | 0.29 | 0.3094 | 0.014 | 0.70005 | 0.142 | 0.0021 | 0.23562 | 0.1652 | 0.011 | 1986 | 42 | 1737 | 71 | 3080 | 190 | 2250 | 26 | 273 | 11 | 104.3 | 5 | 154.7 | 2.1 | 2.768 | 0.042 |
| CLIB5_76 - | 5.51 | 0.34 | 0.3141 | 0.019 | 0.79756 | 0.1281 | 0.0019 | -0.20908 | 0.0998 | 0.0067 | 1900 | 60 | 1760 | 95 | 1922 | 130 | 2068 | 25 | 235.5 | 4.7 | 114.7 | 4.6 | 110.1 | 5.5 | 2.073 | 0.096 |
| CLIB5_47 - | 6.04 | 0.28 | 0.3193 | 0.016 | 0.67898 | 0.1376 | 0.0031 | 0.27749 | 0.1728 | 0.016 | 1979 | 48 | 1785 | 81 | 3220 | 260 | 2193 | 36 | 242.8 | 6.8 | 65.2 | 2.2 | 102.2 | 3.4 | 3.64 | 0.1 |
| CLIB5_78 - | 5.68 | 0.27 | 0.3276 | 0.015 | 0.83454 | 0.1263 | 0.0017 | 0.049517 | 0.1034 | 0.006 | 1925 | 45 | 1825 | 76 | 1988 | 110 | 2044 | 23 | 282 | 14 | 94.5 | 4 | 93.1 | 3.9 | 2.965 | 0.065 |
| CLIB5_79 - | 6.11 | 0.3 | 0.3412 | 0.016 | 0.84146 | 0.1306 | 0.002 | -0.02635 | 0.1274 | 0.009 | 1988 | 43 | 1891 | 79 | 2420 | 160 | 2103 | 28 | 377 | 13 | 140.9 | 4.3 | 162.4 | 3.6 | 2.661 | 0.046 |
| CLIB5_44 - | 6.11 | 0.34 | 0.3428 | 0.019 | 0.84073 | 0.1296 | 0.002 | 0.055833 | 0.1059 | 0.0064 | 1988 | 64 | 1899 | 100 | 2033 | 120 | 2090 | 26 | 376 | 10 | 157.8 | 5.7 | 156.8 | 4.2 | 2.342 | 0.074 |
| CLIB5_53 - | 6.6 | 0.31 | 0.3499 | 0.016 | 0.67398 | 0.1361 | 0.002 | 0.24998 | 0.1528 | 0.0094 | 2059 | 43 | 1937 | 79 | 2871 | 160 | 2174 | 26 | 189.9 | 6.7 | 74.5 | 2.2 | 112.1 | 2.4 | 2.525 | 0.049 |
| CLIB5_14 - | 6.5 | 0.31 | 0.3519 | 0.016 | 0.49766 | 0.1332 | 0.0024 | 0.21615 | 0.1287 | 0.0081 | 2047 | 44 | 1943 | 78 | 2443 | 140 | 2136 | 31 | 83.8 | 2.1 | 28.83 | 0.65 | 35.35 | 0.85 | 3.025 | 0.049 |
| CLIB5_74 - | 6.37 | 0.31 | 0.3552 | 0.017 | 0.77153 | 0.1317 | 0.002 | 0.21448 | 0.1255 | 0.0075 | 2025 | 44 | 1958 | 84 | 2388 | 140 | 2116 | 27 | 220.5 | 5.4 | 100.6 | 2.8 | 116.8 | 3 | 2.21 | 0.063 |
| CLIB5_67 - | 6.76 | 0.33 | 0.3596 | 0.017 | 0.66392 | 0.1377 | 0.0022 | 0.20786 | 0.1524 | 0.01 | 2079 | 43 | 1979 | 80 | 2861 | 180 | 2194 | 29 | 254 | 14 | 86.7 | 2.1 | 115.8 | 2.8 | 2.87 | 0.12 |
| CLIB5_77 - | 6.53 | 0.32 | 0.3606 | 0.017 | 0.82873 | 0.1327 | 0.0019 | 0.085239 | 0.1437 | 0.0087 | 2047 | 43 | 1983 | 82 | 2713 | 150 | 2132 | 25 | 196.5 | 3.8 | 71.56 | 0.94 | 94.6 | 1.7 | 2.725 | 0.052 |
| CLIB5_21 - | 6.53 | 0.4 | 0.3647 | 0.022 | 0.7785 | 0.1308 | 0.0026 | -0.05379 | 0.106 | 0.0083 | 2047 | 82 | 2003 | 110 | 2036 | 160 | 2105 | 36 | 214.4 | 4.6 | 76.8 | 2.7 | 77.7 | 3.1 | 2.89 | 0.099 |
| CLIB5_31 - | 6.64 | 0.31 | 0.3684 | 0.017 | 0.75096 | 0.1296 | 0.0017 | 0.16262 | 0.1056 | 0.0063 | 2063 | 42 | 2021 | 82 | 2029 | 110 | 2090 | 23 | 307.2 | 9.1 | 134.9 | 4 | 138.9 | 3.2 | 2.301 | 0.025 |
| CLIB5_62 - | 6.76 | 0.37 | 0.369 | 0.021 | 0.791 | 0.1317 | 0.0024 | -0.15302 | 0.1228 | 0.0074 | 2076 | 59 | 2024 | 100 | 2341 | 130 | 2122 | 31 | 204.9 | 5 | 94.8 | 2.7 | 107.7 | 3.9 | 2.162 | 0.053 |
| CLIB5_46 - | 7.06 | 0.5 | 0.3719 | 0.019 | 0.67662 | 0.138 | 0.017 | 0.32907 | 0.1485 | 0.077 | 2117 | 52 | 2036 | 94 | 2810 | 970 | 2199 | 110 | 175 | 6.3 | 76.7 | 1.4 | 107.3 | 4.2 | 2.215 | 0.07 |
| CLIB5_73 - | 6.91 | 0.35 | 0.3723 | 0.018 | 0.56032 | 0.1362 | 0.0077 | 0.37613 | 0.1431 | 0.023 | 2097 | 45 | 2039 | 89 | 2700 | 370 | 2173 | 71 | 201.4 | 7.4 | 70.8 | 2.3 | 95.3 | 6.5 | 2.849 | 0.062 |
| CLIB5_6 - 1 | 6.586 | 0.31 | 0.3724 | 0.017 | 0.58824 | 0.1284 | 0.0017 | 0.2496 | 0.1054 | 0.0062 | 2055.9 | 41 | 2040 | 81 | 2025 | 110 | 2073 | 24 | 248.4 | 6.3 | 124.5 | 3.6 | 129.5 | 2.9 | 2.089 | 0.029 |
| CLIB5_20 - | 6.66 | 0.31 | 0.3732 | 0.02 | 0.71277 | 0.1301 | 0.0048 | 0.018705 | 0.1077 | 0.014 | 2065 | 47 | 2044 | 100 | 2065 | 230 | 2095 | 56 | 109.4 | 4.7 | 48 | 2.2 | 51.8 | 2.3 | 2.356 | 0.047 |
| CLIB5_4 - 1 | 6.707 | 0.32 | 0.374 | 0.017 | 0.59448 | 0.1296 | 0.0018 | 0.12177 | 0.1047 | 0.0063 | 2071 | 41 | 2048 | 81 | 2012 | 120 | 2089 | 25 | 136.5 | 7 | 67 | 5.1 | 70.1 | 4.2 | 2.214 | 0.046 |
| CLIB5_69 - | 6.61 | 0.31 | 0.3744 | 0.018 | 0.7691 | 0.1293 | 0.0018 | 0.24467 | 0.1149 | 0.0068 | 2059 | 42 | 2051 | 81 | 2197 | 120 | 2085 | 24 | 294 | 14 | 101.3 | 4.5 | 101.4 | 3.2 | 2.877 | 0.043 |
| CLIB5_54 - | 6.88 | 0.33 | 0.3754 | 0.018 | 0.71856 | 0.1322 | 0.0021 | 0.17672 | 0.131 | 0.0095 | 2092 | 43 | 2053 | 84 | 2485 | 160 | 2126 | 27 | 172.3 | 5.6 | 57.5 | 2.2 | 72.2 | 1.9 | 3.011 | 0.054 |
| CLIB5_1 - 1 | 6.775 | 0.32 | 0.3763 | 0.017 | 0.55245 | 0.1298 | 0.0018 | 0.16567 | 0.1062 | 0.0066 | 2081 | 42 | 2058 | 82 | 2039 | 120 | 2092 | 25 | 145.7 | 2.8 | 79 | 1.2 | 87.3 | 1.5 | 1.891 | 0.022 |
| CLIB5_9 - 1 | 6.764 | 0.32 | 0.3766 | 0.017 | 0.55521 | 0.1314 | 0.002 | 0.11712 | 0.1177 | 0.0067 | 2079 | 42 | 2060 | 82 | 2248 | 120 | 2113 | 26 | 165.6 | 5.9 | 112.6 | 3.2 | 124.2 | 2.3 | 1.522 | 0.017 |
| CLIB5_37 - | 6.89 | 0.35 | 0.3761 | 0.019 | 0.7266 | 0.1312 | 0.002 | 0.11709 | 0.1145 | 0.0068 | 2096 | 48 | 2060 | 91 | 2190 | 120 | 2109 | 27 | 170 | 10 | 95.8 | 5.3 | 108.3 | 5 | 1.739 | 0.031 |
| CLIB5_18 - | 6.78 | 0.32 | 0.3795 | 0.018 | 0.73977 | 0.1299 | 0.0018 | 0.026291 | 0.1076 | 0.0066 | 2080 | 43 | 2073 | 84 | 2064 | 120 | 2093 | 25 | 195.9 | 4.8 | 81.2 | 2.6 | 86.8 | 2.3 | 2.513 | 0.037 |
| CLIB5_23 - | 7 | 0.35 | 0.3959 | 0.019 | 0.91284 | 0.12943 | 0.0017 | -0.0969 | 0.1091 | 0.0068 | 2110 | 45 | 2148 | 87 | 2091 | 120 | 2088 | 22 | 323 | 11 | 163.6 | 5.5 | 170.1 | 6.4 | 2.023 | 0.034 |
| CLIB5_45 - | 7.24 | 0.4 | 0.4027 | 0.023 | 0.80965 | 0.1304 | 0.002 | 0.12473 | 0.1297 | 0.0076 | 2139 | 72 | 2180 | 120 | 2464 | 140 | 2100 | 26 | 373 | 19 | 150.8 | 8.5 | 182.9 | 8 | 2.402 | 0.061 |
| CLIB5_81 - | 9.88 | 0.52 | 0.4444 | 0.021 | 0.82565 | 0.1613 | 0.0031 | -0.34368 | 0.287 | 0.021 | 2413 | 51 | 2368 | 96 | 5070 | 330 | 2460 | 33 | 177.2 | 5 | 84.4 | 3.7 | 212.3 | 4.3 | 2.146 | 0.06 |

Accepted Manuscript

ACCEPTED MANUSCRIPT

| Ratios | | | | | | | | | | | Ages | | | | | | | | Concentrations (calculated from 91500) | | | | | | | |
|---|---|---|---|---|---|---|---|---|---|---|---|---|---|---|---|---|---|---|---|---|---|---|---|---|---|---|
| Sample - ar | 207Pb/235 | Propagatec | 206Pb/238 | Propagatec | Error Corre | 207Pb/206 | Propagatec | Error Corre | 208Pb/232 | Propagatec | 207Pb/235 | Propagatec | 206Pb/238 | Propagatec | 208Pb/232 | Propagatec | 207Pb/206 | Propagatec | U (ppm) | Internal 2 S | Th (ppm) | Internal 2 S | Pb (ppm) | Internal 2 S | U/Th | Internal 2 SE |
| CLIB7 - 1 | 5.86 | 0.29 | 0.3291 | 0.014 | 0.79388 | 0.1293 | 0.0017 | 0.017276 | 0.0976 | 0.0018 | 1952 | 48 | 1833 | 70 | 1882 | 32 | 2086 | 22 | 284.4 | 6.3 | 118.2 | 3.5 | 336 | 14 | 2.52 | 0.031 |
| CLIB7 - 2 | 5.965 | 0.37 | 0.3282 | 0.02 | 0.59279 | 0.1313 | 0.0021 | 0.1846 | 0.1019 | 0.0037 | 1969 | 80 | 1829 | 100 | 1960 | 68 | 2115 | 27 | 261.5 | 9.7 | 122.1 | 4.9 | 361 | 12 | 2.203 | 0.022 |
| CLIB7 - 3 | 6.194 | 0.3 | 0.3445 | 0.013 | 0.16488 | 0.13 | 0.0017 | 0.3767 | 0.1087 | 0.0017 | 2003.5 | 43 | 1908.2 | 64 | 2084 | 31 | 2094 | 23 | 290.7 | 6.3 | 131.6 | 2.6 | 406.4 | 5.6 | 2.265 | 0.022 |
| CLIB7 - 4 | 4.13 | 0.23 | 0.219 | 0.01 | 0.56152 | 0.1359 | 0.0017 | 0.18064 | 0.0821 | 0.0019 | 1659 | 43 | 1276 | 54 | 1594 | 36 | 2175 | 23 | 459 | 15 | 204 | 6.4 | 503 | 27 | 2.28 | 0.022 |
| CLIB7 - 5 | 6.872 | 0.33 | 0.3842 | 0.015 | 0.44984 | 0.129 | 0.0015 | 0.23145 | 0.1098 | 0.0015 | 2093.9 | 43 | 2095 | 68 | 2105 | 28 | 2083 | 19 | 274 | 10 | 128.3 | 4.5 | 405 | 11 | 2.158 | 0.017 |
| CLIB7 - 6 | 6.649 | 0.32 | 0.3665 | 0.014 | 0.29094 | 0.131 | 0.0017 | 0.30604 | 0.1165 | 0.0017 | 2064 | 43 | 2012 | 65 | 2226 | 30 | 2110 | 24 | 196.9 | 9.6 | 133.9 | 6.8 | 448 | 17 | 1.491 | 0.02 |
| CLIB7 - 7 | 6.801 | 0.33 | 0.3783 | 0.015 | 0.44261 | 0.1295 | 0.0014 | 0.14943 | 0.1094 | 0.0013 | 2084.7 | 44 | 2068 | 69 | 2098 | 24 | 2091 | 20 | 348.6 | 8.3 | 164.2 | 3.8 | 519.4 | 8.6 | 2.134 | 0.018 |
| CLIB7 - 10 | 4.15 | 0.2 | 0.212 | 0.0083 | 0.74257 | 0.14134 | 0.0013 | 0.26225 | 0.07647 | 0.00095 | 1663.6 | 41 | 1239.3 | 45 | 1489 | 18 | 2242.7 | 16 | 1380 | 82 | 1274 | 86 | 2870 | 170 | 1.086 | 0.011 |
| CLIB7 - 12 | 4.988 | 0.25 | 0.2748 | 0.011 | 0.79863 | 0.1312 | 0.0016 | 0.009777 | 0.0904 | 0.0018 | 1814 | 43 | 1564 | 55 | 1748 | 34 | 2111 | 21 | 321.5 | 8.9 | 159 | 3.9 | 428.2 | 7.9 | 1.992 | 0.036 |
| CLIB7 - 13 | 6.589 | 0.32 | 0.3688 | 0.014 | 0.35998 | 0.1297 | 0.0016 | 0.38179 | 0.1121 | 0.0017 | 2058 | 43 | 2024 | 68 | 2146 | 31 | 2090 | 21 | 228.3 | 8.7 | 128 | 7.2 | 421 | 18 | 1.786 | 0.039 |
| CLIB7 - 15 | 6.305 | 0.31 | 0.354 | 0.014 | 0.74864 | 0.1288 | 0.0015 | 0.095655 | 0.1042 | 0.002 | 2017 | 43 | 1953 | 66 | 2002 | 37 | 2081 | 20 | 317 | 14 | 205.4 | 9.8 | 634 | 20 | 1.506 | 0.014 |
| CLIB7 - 16 | 6.439 | 0.31 | 0.3583 | 0.014 | 0.17277 | 0.1302 | 0.0015 | 0.13234 | 0.1144 | 0.0018 | 2036.3 | 42 | 1974 | 65 | 2189 | 33 | 2098 | 20 | 241.4 | 6.2 | 112.5 | 3.3 | 392.4 | 7.8 | 2.09 | 0.018 |
| CLIB7 - 17 | 6.067 | 0.3 | 0.3414 | 0.014 | 0.61452 | 0.1289 | 0.0016 | 0.19483 | 0.1101 | 0.0015 | 1984 | 43 | 1893 | 65 | 2111 | 28 | 2079 | 22 | 262 | 6.6 | 132.1 | 4.9 | 442 | 15 | 1.948 | 0.029 |
| CLIB7 - 19 | 6.73 | 0.33 | 0.3794 | 0.015 | 0.37724 | 0.1287 | 0.0017 | 0.3005 | 0.1081 | 0.0015 | 2075 | 44 | 2073 | 68 | 2075 | 27 | 2078 | 23 | 168.2 | 3.5 | 89.2 | 1.7 | 296.7 | 4.8 | 1.826 | 0.015 |
| CLIB7 - 20 | 1.872 | 0.095 | 0.1182 | 0.0047 | 0.58773 | 0.115 | 0.0018 | 0.052832 | 0.04473 | 0.00074 | 1069 | 34 | 720.3 | 27 | 884 | 14 | 1873 | 29 | 494 | 21 | 194 | 8.3 | 267 | 10 | 2.472 | 0.019 |
| CLIB7 - 21 | 4.105 | 0.2 | 0.2325 | 0.009 | 0.70711 | 0.1285 | 0.0017 | -0.05196 | 0.0948 | 0.0035 | 1654 | 41 | 1347 | 47 | 1827 | 65 | 2073 | 23 | 360 | 14 | 112.1 | 4.1 | 317.3 | 5 | 3.116 | 0.029 |
| CLIB7 - 22 | 6.511 | 0.32 | 0.3654 | 0.014 | 0.54048 | 0.1299 | 0.0016 | 0.21625 | 0.1123 | 0.0018 | 2046 | 45 | 2007 | 69 | 2150 | 34 | 2094 | 22 | 229 | 4.5 | 129 | 2.7 | 438.8 | 8.9 | 1.73 | 0.027 |
| CLIB7 - 23 | 6.86 | 0.33 | 0.3869 | 0.015 | 0.578 | 0.1291 | 0.0016 | 0.15516 | 0.1172 | 0.0024 | 2093 | 44 | 2108 | 69 | 2238 | 44 | 2085 | 21 | 169.1 | 7.1 | 99.9 | 6 | 350 | 14 | 1.707 | 0.033 |
| CLIB7 - 24 | 3.863 | 0.2 | 0.2119 | 0.0087 | 0.89428 | 0.1324 | 0.0015 | -0.15087 | 0.096 | 0.0027 | 1602 | 41 | 1238 | 46 | 1852 | 50 | 2127 | 20 | 477 | 18 | 189.6 | 5.1 | 566 | 23 | 2.444 | 0.035 |
| CLIB7 - 25 | 6.972 | 0.34 | 0.3915 | 0.015 | 0.47127 | 0.1296 | 0.0015 | 0.24819 | 0.1083 | 0.0015 | 2106.5 | 43 | 2129 | 70 | 2081 | 28 | 2091 | 21 | 181.1 | 5.7 | 100.9 | 4.3 | 334 | 12 | 1.795 | 0.03 |
| CLIB7 - 26 | 2.46 | 0.12 | 0.1308 | 0.0055 | 0.60297 | 0.1381 | 0.0025 | 0.66815 | 0.0559 | 0.0015 | 1258 | 35 | 792 | 31 | 1099 | 28 | 2193 | 31 | 492 | 48 | 361 | 35 | 650 | 74 | 1.341 | 0.013 |
| CLIB7 - 27 | 6.065 | 0.29 | 0.3442 | 0.013 | 0.51099 | 0.1283 | 0.0015 | 0.23739 | 0.1072 | 0.0013 | 1984 | 43 | 1907 | 65 | 2059 | 25 | 2072 | 21 | 309.2 | 3.5 | 205.8 | 2.2 | 671 | 13 | 1.484 | 0.016 |
| CLIB7 - 28 | 7.154 | 0.35 | 0.3942 | 0.015 | 0.43229 | 0.132 | 0.0018 | 0.26634 | 0.1239 | 0.002 | 2129 | 44 | 2142 | 70 | 2361 | 36 | 2120 | 24 | 158.5 | 4.9 | 78.9 | 2.2 | 296.8 | 6.4 | 1.989 | 0.022 |
| CLIB7 - 29 | 6.728 | 0.33 | 0.3763 | 0.015 | 0.55353 | 0.1303 | 0.0016 | 0.23895 | 0.1169 | 0.0029 | 2076 | 44 | 2058 | 68 | 2232 | 52 | 2098 | 22 | 243 | 6.5 | 118.5 | 3.3 | 417.5 | 7.3 | 2.05 | 0.021 |
| CLIB7 - 30 | 7.67 | 0.41 | 0.3316 | 0.015 | 0.53784 | 0.1682 | 0.0033 | 0.43875 | 0.2967 | 0.015 | 2192 | 46 | 1845 | 70 | 5250 | 250 | 2537 | 37 | 233.8 | 4.1 | 82.7 | 1.5 | 764 | 14 | 2.83 | 0.048 |
| CLIB7 - 31 | 3.059 | 0.15 | 0.1743 | 0.0072 | 0.8361 | 0.1275 | 0.0014 | 0.17122 | 0.0503 | 0.0012 | 1422 | 38 | 1035 | 39 | 992 | 24 | 2062 | 19 | 822 | 50 | 600 | 46 | 945 | 83 | 1.429 | 0.037 |
| CLIB7 - 32 | 3.19 | 0.16 | 0.1776 | 0.0071 | 0.75559 | 0.1308 | 0.0016 | 0.1273 | 0.05334 | 0.00077 | 1452 | 39 | 1053 | 39 | 1050 | 15 | 2105 | 22 | 595 | 38 | 431 | 31 | 674 | 39 | 1.42 | 0.022 |
| CLIB7 - 33 | 5.971 | 0.3 | 0.3262 | 0.014 | 0.43586 | 0.1336 | 0.0016 | 0.29885 | 0.1176 | 0.0039 | 1970 | 52 | 1820 | 72 | 2246 | 71 | 2142 | 22 | 274 | 12 | 142 | 12 | 487 | 35 | 2.037 | 0.07 |
| CLIB7 - 34 | 4.93 | 0.26 | 0.2546 | 0.011 | 0.84515 | 0.1406 | 0.0019 | -0.32084 | 0.1155 | 0.0049 | 1799 | 46 | 1461 | 55 | 2201 | 89 | 2230 | 25 | 392 | 19 | 148 | 5.8 | 527 | 37 | 2.625 | 0.036 |
| CLIB7 - 35 | 4.815 | 0.24 | 0.2658 | 0.01 | 0.71708 | 0.1315 | 0.0015 | 0.21967 | 0.0914 | 0.0016 | 1787 | 40 | 1519 | 53 | 1767 | 29 | 2115 | 20 | 342 | 17 | 193 | 8.4 | 524 | 20 | 1.759 | 0.022 |
| CLIB7 - 36 | 6.578 | 0.32 | 0.3632 | 0.014 | 0.6364 | 0.132 | 0.0016 | 0.47399 | 0.1195 | 0.0016 | 2054.8 | 43 | 1996 | 67 | 2281 | 30 | 2124 | 21 | 243.7 | 6.2 | 126.8 | 2.1 | 461 | 11 | 1.896 | 0.025 |
| CLIB7 - 37 | 6.872 | 0.34 | 0.3846 | 0.015 | 0.61128 | 0.1296 | 0.0016 | 0.19045 | 0.1124 | 0.002 | 2094 | 43 | 2097 | 70 | 2151 | 37 | 2091 | 21 | 208.6 | 2.8 | 82.8 | 1 | 280.8 | 4.8 | 2.51 | 0.027 |
| CLIB7 - 38 | 5.616 | 0.27 | 0.3066 | 0.012 | 0.76023 | 0.133 | 0.0016 | 0.27454 | 0.1263 | 0.0035 | 1917 | 43 | 1723 | 60 | 2403 | 63 | 2136 | 21 | 501 | 13 | 127.6 | 3.6 | 485 | 10 | 3.863 | 0.069 |
| CLIB7 - 39 | 5.3 | 0.25 | 0.2943 | 0.012 | 0.33192 | 0.1309 | 0.0017 | 0.3283 | 0.1033 | 0.0022 | 1870 | 47 | 1663 | 63 | 1985 | 40 | 2112 | 22 | 225 | 7 | 99.1 | 3.6 | 322 | 14 | 2.214 | 0.038 |
| CLIB7 - 40 | 2.938 | 0.17 | 0.1668 | 0.009 | 0.93761 | 0.1274 | 0.0014 | -0.20622 | 0.04852 | 0.0015 | 1387 | 55 | 994 | 51 | 957 | 29 | 2060 | 20 | 1182 | 66 | 1041 | 61 | 1562 | 90 | 1.103 | 0.011 |
| CLIB7 - 42 | 6.665 | 0.33 | 0.376 | 0.015 | 0.49984 | 0.129 | 0.0017 | 0.36026 | 0.1081 | 0.0016 | 2066 | 44 | 2057 | 69 | 2075 | 29 | 2080 | 23 | 210.5 | 5.5 | 102.4 | 2.8 | 333.8 | 8.2 | 2 | 0.021 |
| CLIB7 - 43 | 6.91 | 0.35 | 0.3704 | 0.015 | 0.76714 | 0.1349 | 0.0017 | 0.054868 | 0.1351 | 0.0034 | 2097 | 45 | 2033 | 71 | 2558 | 61 | 2162 | 22 | 292 | 21 | 139 | 11 | 532 | 29 | 2.072 | 0.025 |
| CLIB7 - 44 | 6.722 | 0.33 | 0.3719 | 0.014 | 0.53847 | 0.1309 | 0.0015 | 0.18072 | 0.115 | 0.0014 | 2074 | 43 | 2038 | 67 | 2200 | 26 | 2107 | 20 | 284.7 | 6.6 | 140.5 | 2.7 | 483.4 | 8.5 | 1.973 | 0.021 |
| CLIB7 - 45 | 6.842 | 0.33 | 0.3833 | 0.015 | 0.52864 | 0.1292 | 0.0015 | 0.30324 | 0.1154 | 0.0017 | 2089.7 | 43 | 2091 | 69 | 2207 | 31 | 2086 | 21 | 254.2 | 7.2 | 121.5 | 3.3 | 415 | 8.1 | 2.06 | 0.023 |
| CLIB7 - 46 | 6.255 | 0.31 | 0.344 | 0.014 | 0.82655 | 0.1318 | 0.0015 | 0.14938 | 0.0746 | 0.0013 | 2009 | 43 | 1904 | 66 | 1454 | 25 | 2119 | 20 | 320 | 18 | 266 | 14 | 584 | 27 | 1.186 | 0.024 |
| CLIB7 - 48 | 6.531 | 0.32 | 0.3566 | 0.014 | 0.54732 | 0.1329 | 0.0017 | 0.26044 | 0.119 | 0.002 | 2048 | 48 | 1965 | 68 | 2272 | 37 | 2133 | 22 | 238 | 11 | 134.7 | 5.2 | 469 | 16 | 1.746 | 0.032 |
| CLIB7 - 49 | 3.553 | 0.17 | 0.2046 | 0.0081 | 0.74393 | 0.1259 | 0.0014 | 0.04249 | 0.0834 | 0.0021 | 1539 | 41 | 1200 | 44 | 1617 | 38 | 2038 | 21 | 402 | 22 | 170.5 | 9.8 | 416 | 16 | 2.367 | 0.028 |
| CLIB7 - 50 | 6.367 | 0.32 | 0.3531 | 0.014 | 0.59755 | 0.1308 | 0.0017 | 0.080057 | 0.1073 | 0.0016 | 2027 | 46 | 1949 | 69 | 2060 | 30 | 2107 | 22 | 180.3 | 4.5 | 107.3 | 2.7 | 338.7 | 7.1 | 1.686 | 0.021 |
| CLIB7 - 51 | 6.934 | 0.34 | 0.3917 | 0.015 | 0.59791 | 0.1283 | 0.0016 | 0.2789 | 0.112 | 0.0015 | 2101 | 44 | 2130 | 71 | 2146 | 28 | 2071 | 22 | 258.5 | 5.5 | 122 | 2.8 | 404.7 | 7.2 | 2.125 | 0.021 |
| CLIB7 - 52 | 4.607 | 0.24 | 0.2355 | 0.01 | 0.83738 | 0.1418 | 0.002 | 0.10392 | 0.1134 | 0.0036 | 1745 | 44 | 1362 | 53 | 2168 | 65 | 2244 | 24 | 414 | 18 | 182 | 11 | 577 | 32 | 2.374 | 0.057 |
| CLIB7 - 53 | 6.68 | 0.33 | 0.347 | 0.014 | 0.68237 | 0.1398 | 0.0017 | 0.02945 | 0.1672 | 0.004 | 2067 | 47 | 1920 | 68 | 3121 | 70 | 2221 | 21 | 214.9 | 7.1 | 90.4 | 3.4 | 450.5 | 8.2 | 2.404 | 0.037 |
| CLIB7 - 54 | 6.794 | 0.34 | 0.3835 | 0.015 | 0.66195 | 0.1285 | 0.0016 | 0.086907 | 0.1101 | 0.0019 | 2083 | 44 | 2092 | 70 | 2110 | 34 | 2074 | 22 | 169.4 | 4.2 | 90.2 | 2.3 | 295.1 | 6.4 | 1.888 | 0.023 |
| CLIB7 - 56 | 5.767 | 0.29 | 0.3192 | 0.013 | 0.67309 | 0.131 | 0.0017 | 0.16317 | 0.1108 | 0.0016 | 1939 | 43 | 1787 | 63 | 2123 | 29 | 2109 | 23 | 262.1 | 9.4 | 141.5 | 5.7 | 462 | 15 | 1.847 | 0.022 |
| CLIB7 - 57 | 2.103 | 0.11 | 0.0994 | 0.0046 | 0.86482 | 0.1541 | 0.0022 | 0.55856 | 0.1785 | 0.0051 | 1146 | 36 | 610 | 27 | 3314 | 87 | 2386 | 25 | 763 | 36 | 131.6 | 8.3 | 655 | 20 | 5.92 | 0.12 |
| CLIB7 - 59 | 6.714 | 0.33 | 0.3774 | 0.015 | 0.73944 | 0.1295 | 0.0014 | 0.065593 | 0.1099 | 0.0015 | 2075 | 46 | 2063 | 70 | 2107 | 27 | 2089 | 19 | 324.1 | 9.7 | 148.3 | 4.7 | 478 | 13 | 2.157 | 0.026 |
| CLIB7 - 60 | 4.807 | 0.26 | 0.2754 | 0.013 | 0.88131 | 0.1263 | 0.0013 | 0.077406 | 0.0872 | 0.0021 | 1783 | 54 | 1567 | 69 | 1689 | 40 | 2045 | 18 | 863 | 22 | 459 | 10 | 1195 | 29 | 1.862 | 0.026 |
| CLIB7 - 61 | 6.929 | 0.34 | 0.386 | 0.015 | 0.60192 | 0.13 | 0.0017 | 0.29225 | 0.1229 | 0.0025 | 2100 | 44 | 2103 | 71 | 2341 | 45 | 2094 | 24 | 164.8 | 5.8 | 75.2 | 2.8 | 265.9 | 6.9 | 2.207 | 0.031 |
| CLIB7 - 62 | 6.92 | 0.35 | 0.3769 | 0.015 | 0.74697 | 0.1329 | 0.0018 | 0.16292 | 0.1377 | 0.0025 | 2097 | 44 | 2060 | 71 | 2606 | 44 | 2132 | 24 | 175.8 | 7.7 | 66.5 | 2.2 | 265.7 | 8.3 | 2.648 | 0.048 |
| CLIB7 - 63 | 6.539 | 0.32 | 0.356 | 0.014 | 0.75725 | 0.1329 | 0.0015 | 0.16467 | 0.114 | 0.0025 | 2049 | 45 | 1962 | 69 | 2180 | 45 | 2134 | 19 | 308 | 11 | 123.7 | 2.6 | 418 | 12 | 2.505 | 0.051 |
| CLIB7 - 64 | 6.182 | 0.31 | 0.3381 | 0.013 | 0.66202 | 0.1321 | 0.0018 | 0.15689 | 0.1121 | 0.0018 | 1999 | 44 | 1876 | 64 | 2151 | 34 | 2124 | 23 | 200 | 4.2 | 112.3 | 1.9 | 366.8 | 6.1 | 1.883 | 0.028 |
| CLIB7 - 68 | 4.341 | 0.24 | 0.2268 | 0.011 | 0.82344 | 0.1379 | 0.0016 | 0.25784 | 0.0855 | 0.0014 | 1698 | 43 | 1317 | 58 | 1658 | 25 | 2197 | 21 | 369 | 23 | 195 | 11 | 494 | 29 | 2.056 | 0.033 |
| CLIB7 - 69 | 6.5 | 0.32 | 0.354 | 0.014 | 0.75781 | 0.1319 | 0.0016 | 0.21164 | 0.1105 | 0.0022 | 2043 | 45 | 1953 | 68 | 2117 | 40 | 2120 | 21 | 237.3 | 9 | 132.1 | 4.1 | 430 | 14 | 1.95 | 0.039 |
| CLIB7 - 70 | 5.481 | 0.27 | 0.3011 | 0.012 | 0.81966 | 0.1308 | 0.0015 | 0.073167 | 0.099 | 0.002 | 1894 | 43 | 1695 | 60 | 1906 | 36 | 2106 | 21 | 351 | 11 | 195.8 | 6.1 | 554.2 | 8.8 | 1.945 | 0.028 |

Accepted Manuscript

ACCEPTED MANUSCRIPT

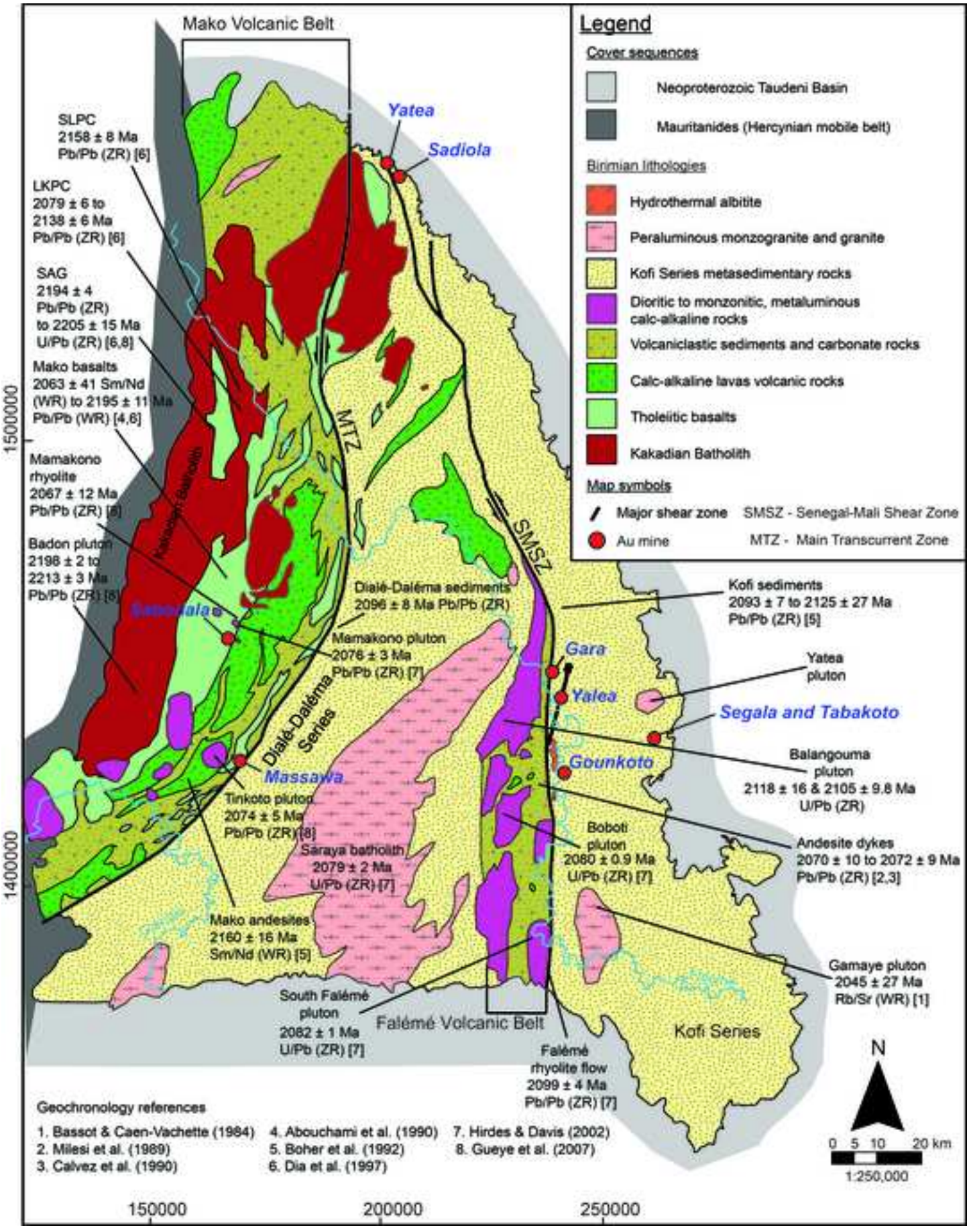

ACCEPTED MANUSCRIPT

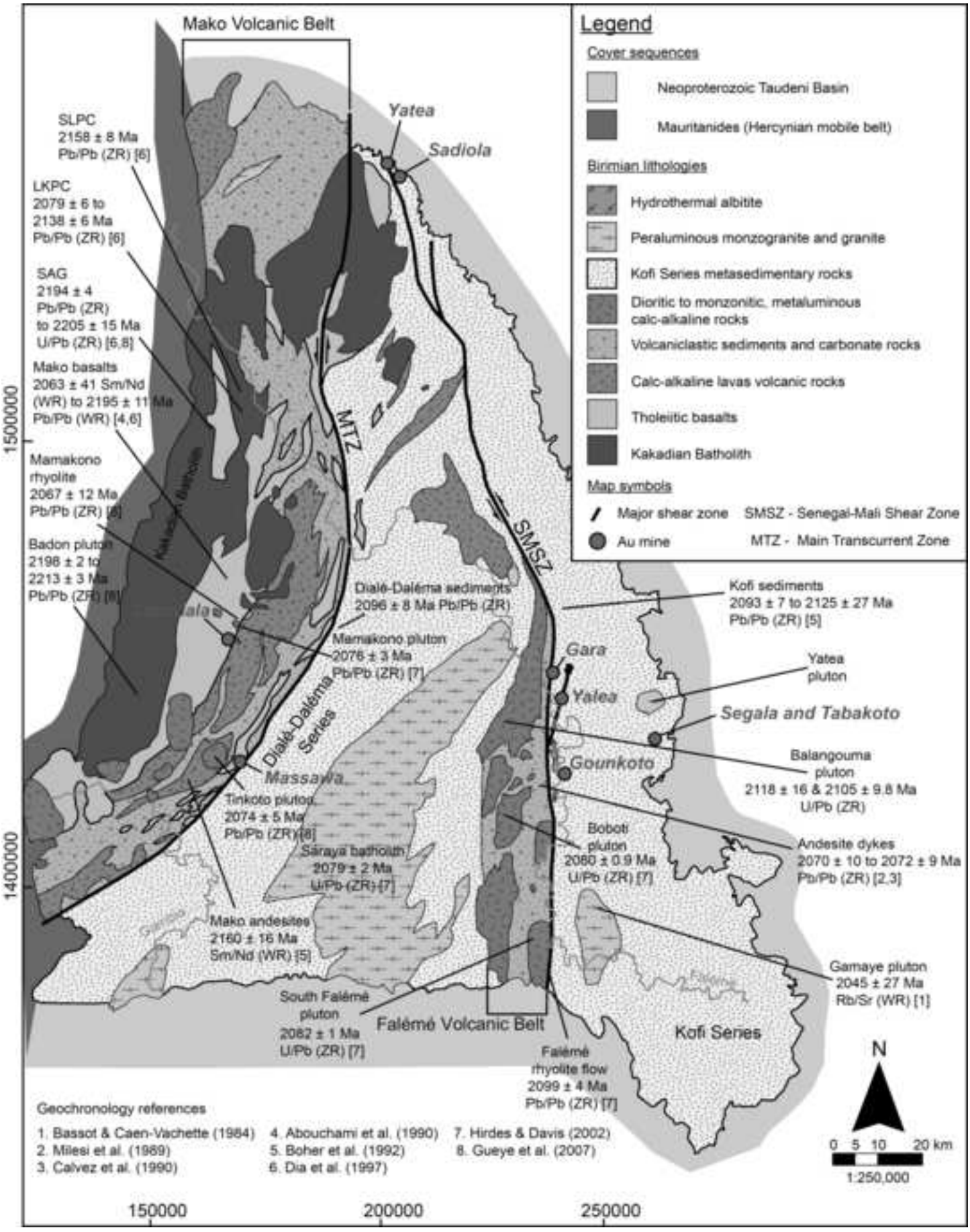

ACCEPTED MANUSCRIPT

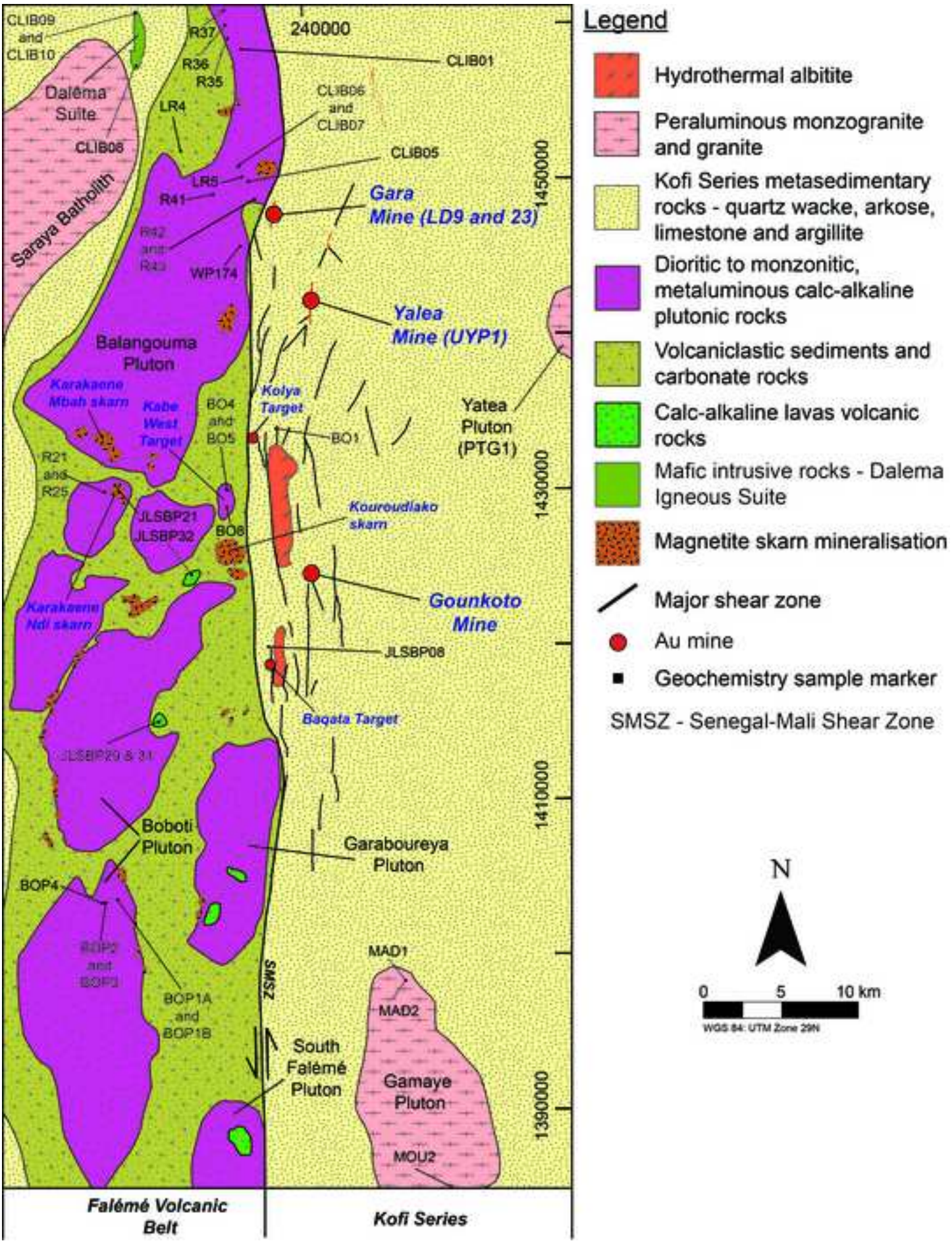

ACCEPTED MANUSCRIPT

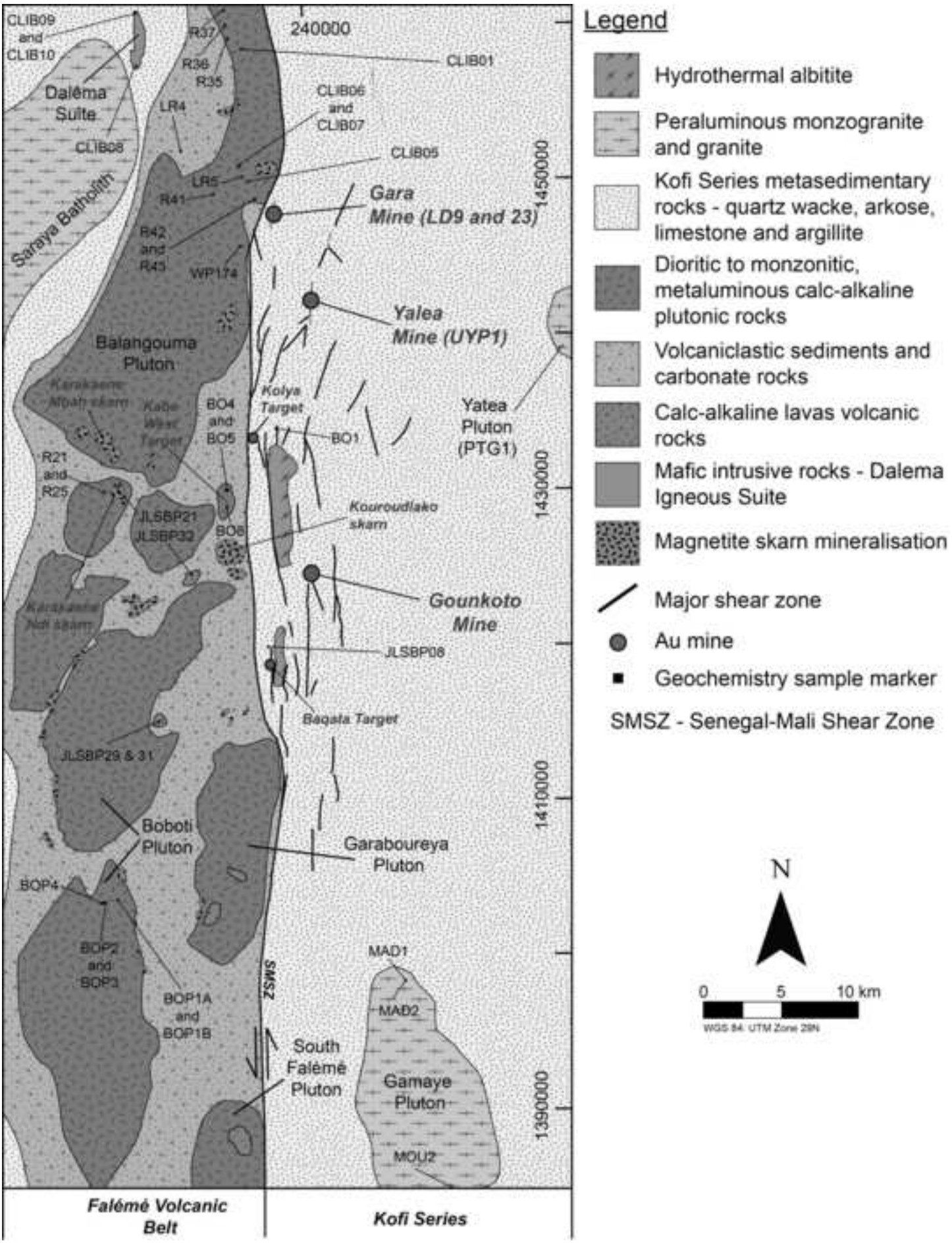

ACCEPTED MANUSCRIPT

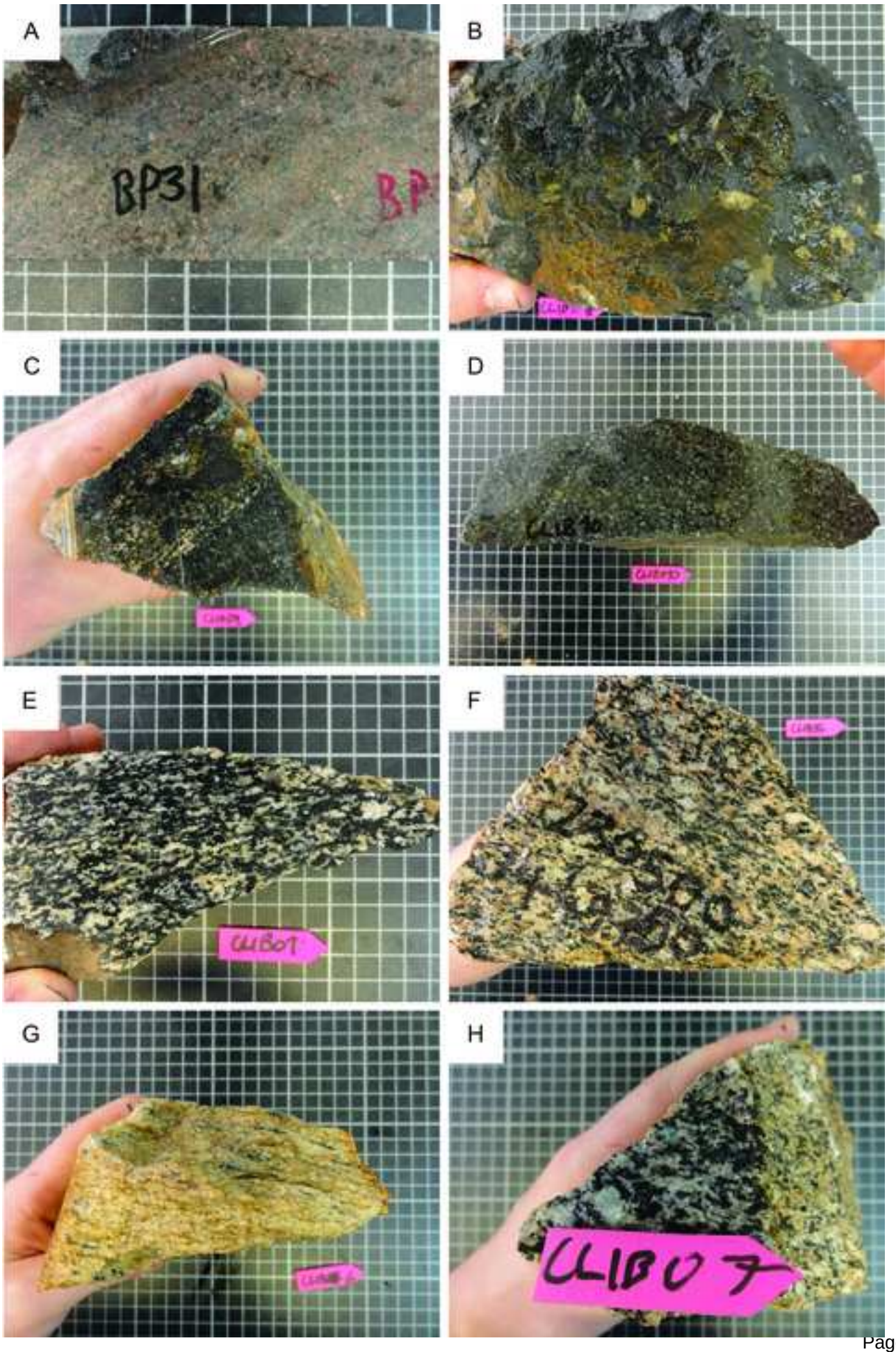

ACCEPTED MANUSCRIPT

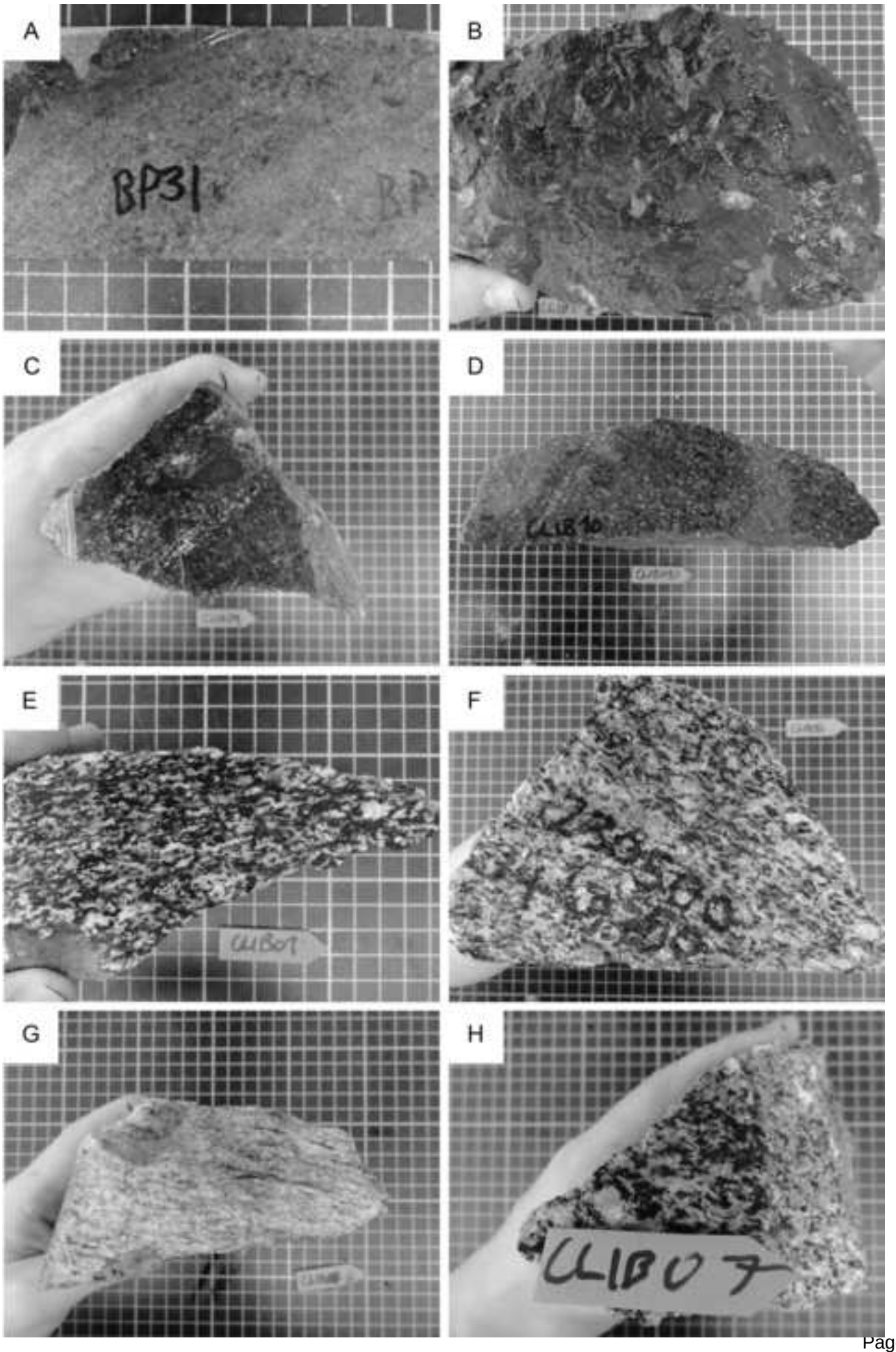

ACCEPTED MANUSCRIPT

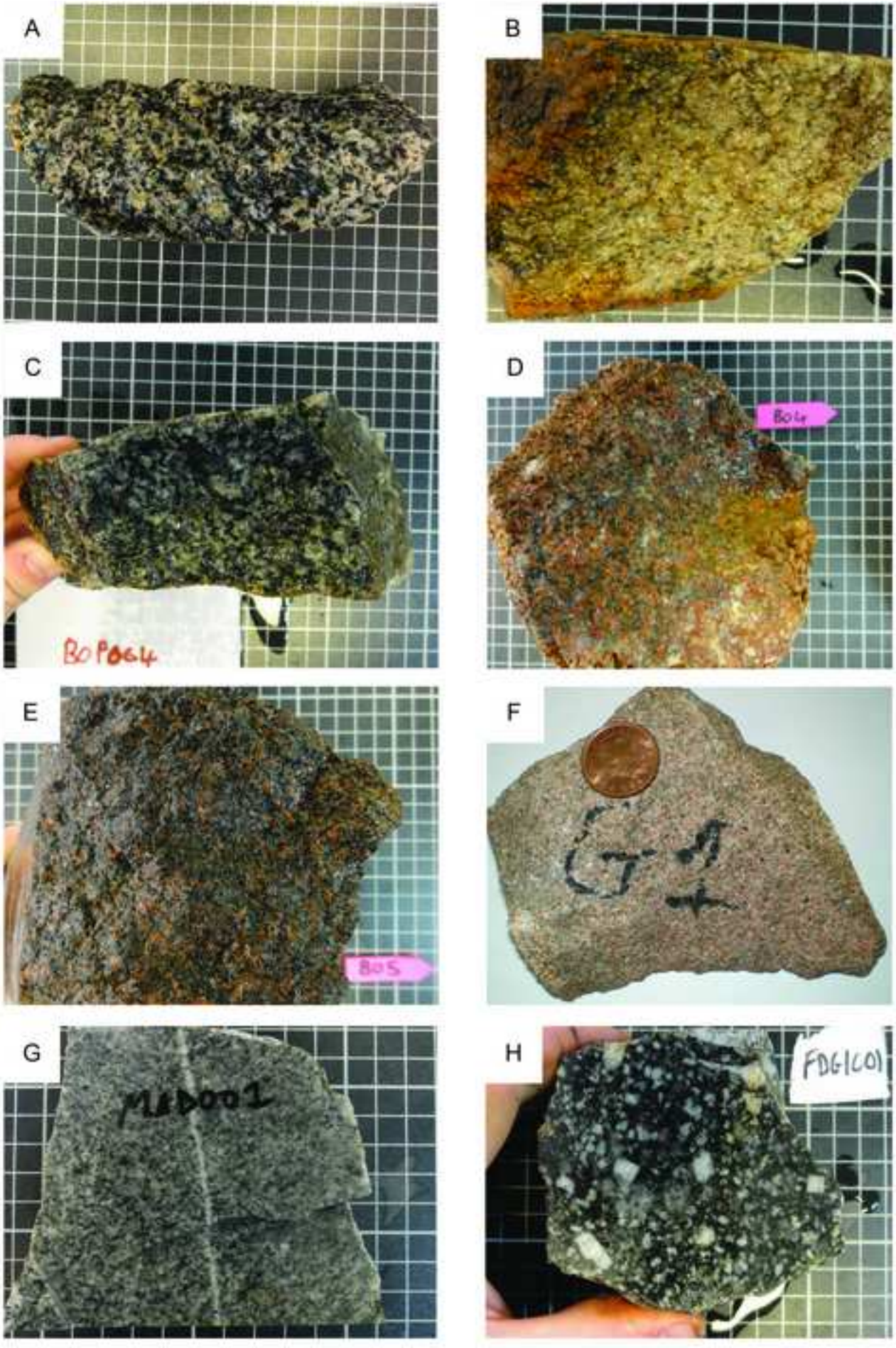

ACCEPTED MANUSCRIPT

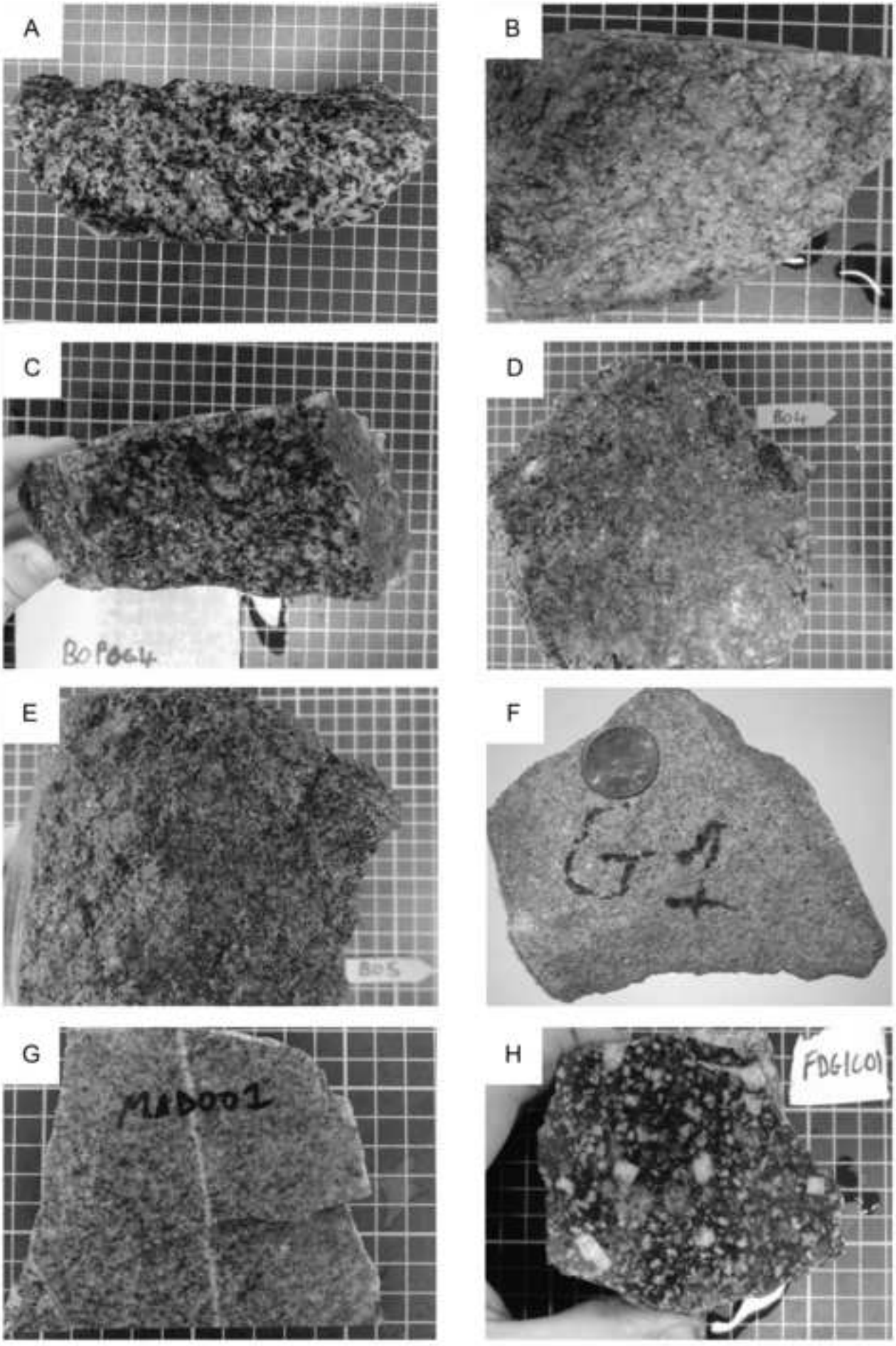

ACCEPTED MANUSCRIPT

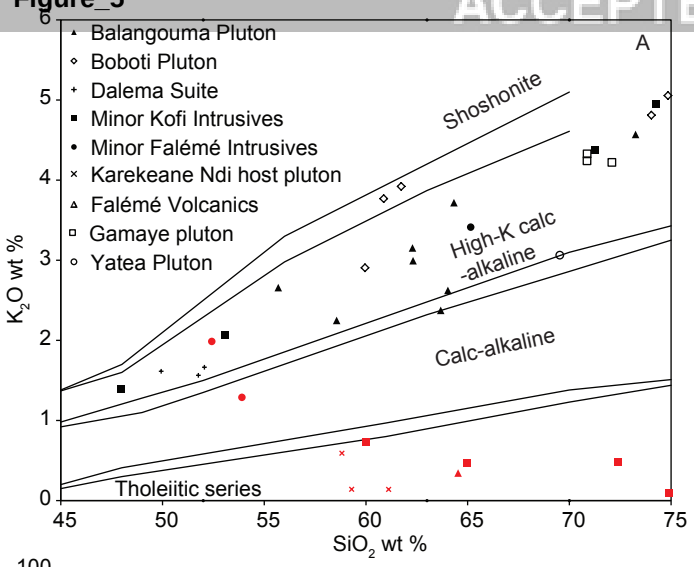


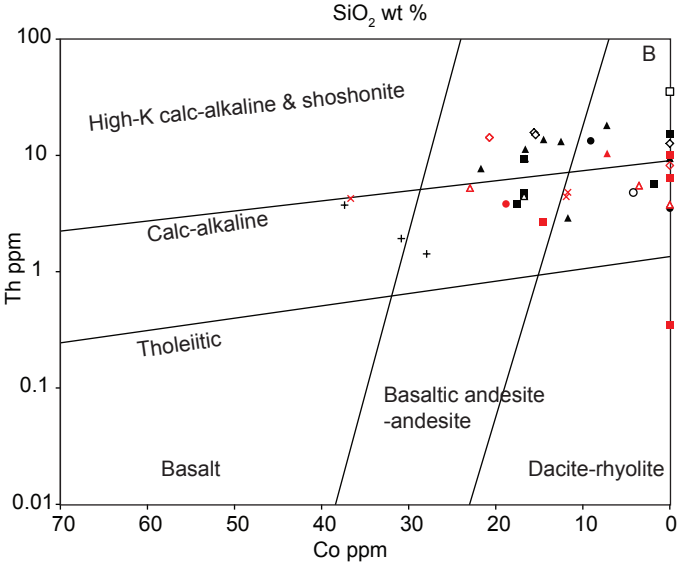


Accepted Manuscript

ACCEPTED MANUSCRIPT

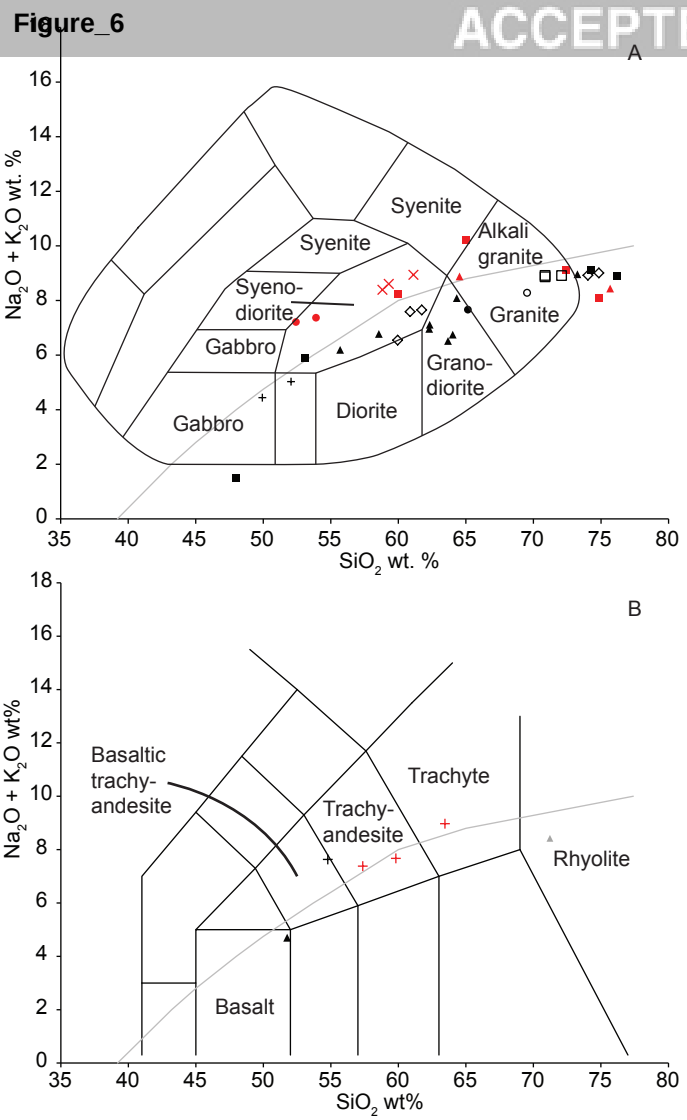





Legend

*Plutonic rocks*

- ▲ Balangouma
- ◇ Boboti
- \+ Dalema Suite
- ■ Minor Kofi Intrusives
- ● Minor Falémé Intrusives
- □ Gamaye pluton
- × Karekeane Ndi host pluton
- ○ Yatea

*Volcanic rocks*

- ▲ Dalema Suite
- ▲ Fadougou rhyolite
- \+ Falémé Volcanics

— Alkali-Sub-alkali division

Accepted Manuscript

ACCEPTED MANUSCRIPT

**Figure_7**

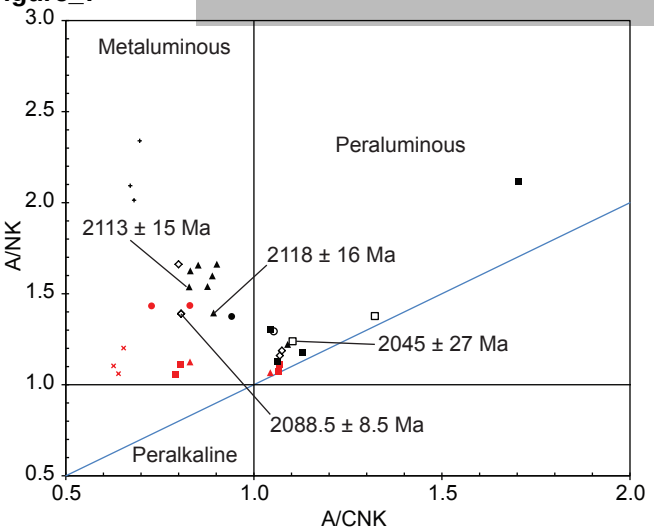


Legend

- ▲ Balangouma Pluton
- ◇ Boboti Pluton
- \+ Dalema Suite
- ■ Minor Kofi Intrusives
- ● Minor Falémé Intrusives
- □ Gamaye pluton
- × Karekeane Ndi host pluton
- ○ Yatea Pluton

Accepted Manuscript

ACCEPTED MANUSCRIPT

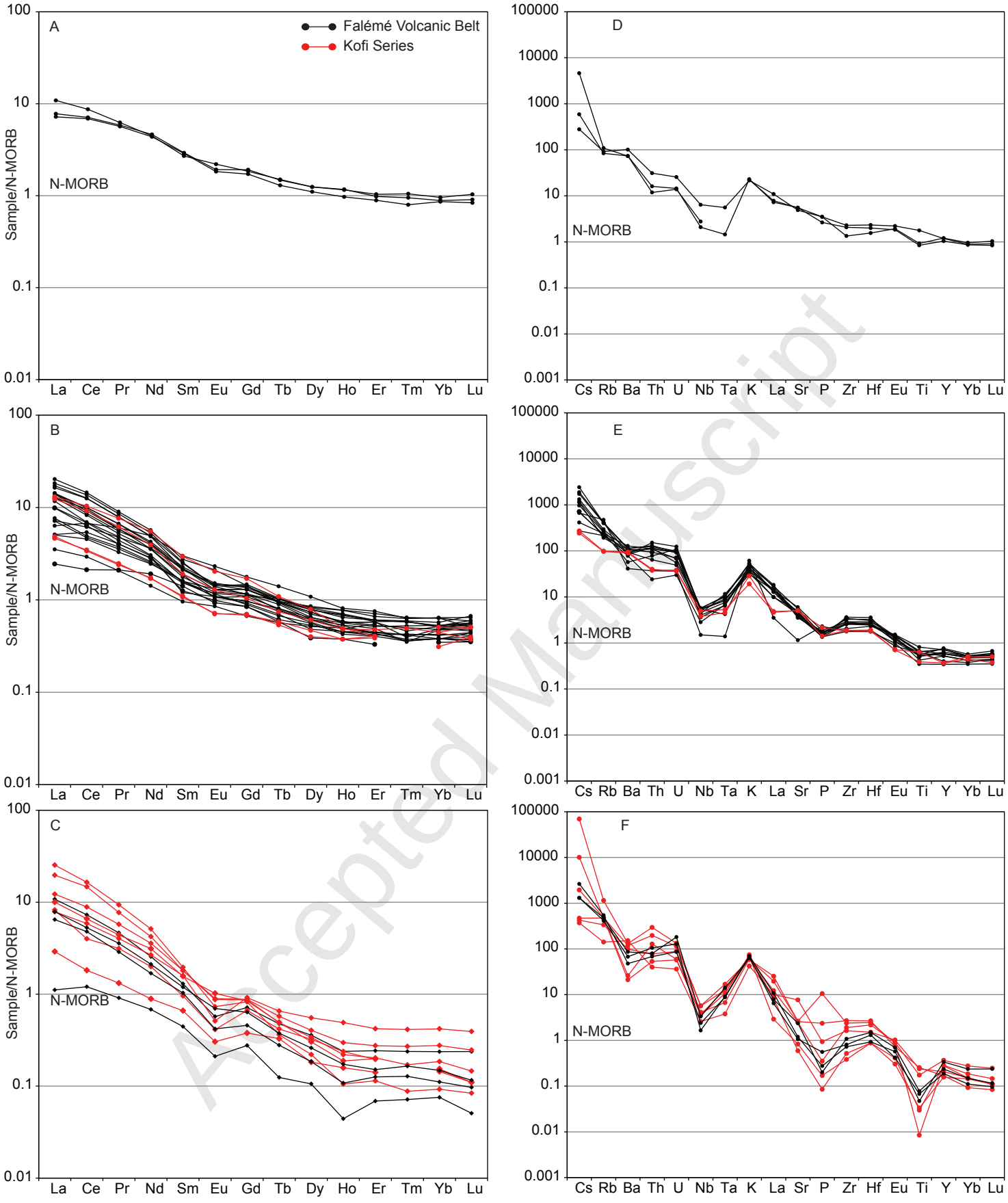


Accepted Manuscript

ACCEPTED MANUSCRIPT

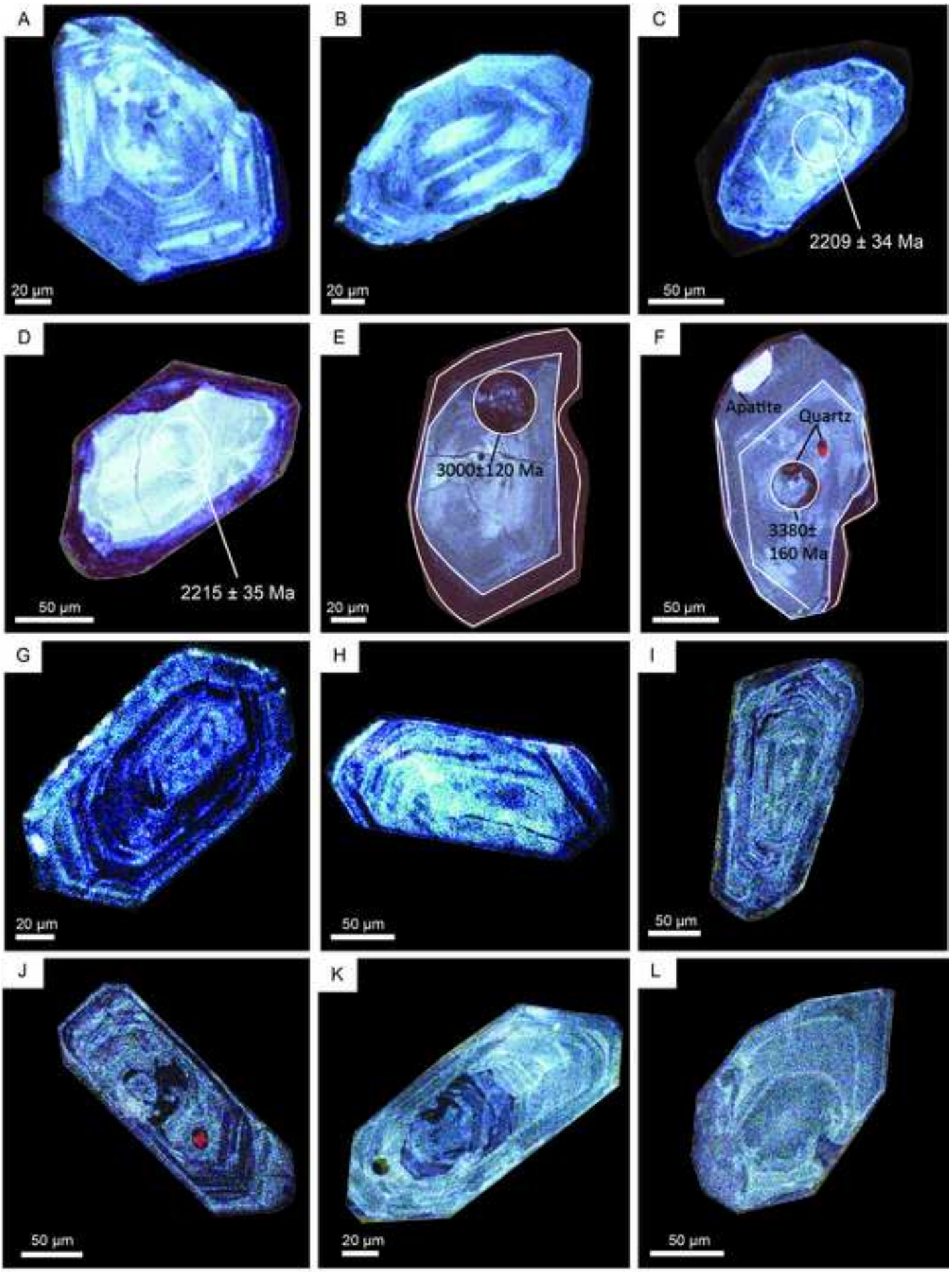

ACCEPTED MANUSCRIPT

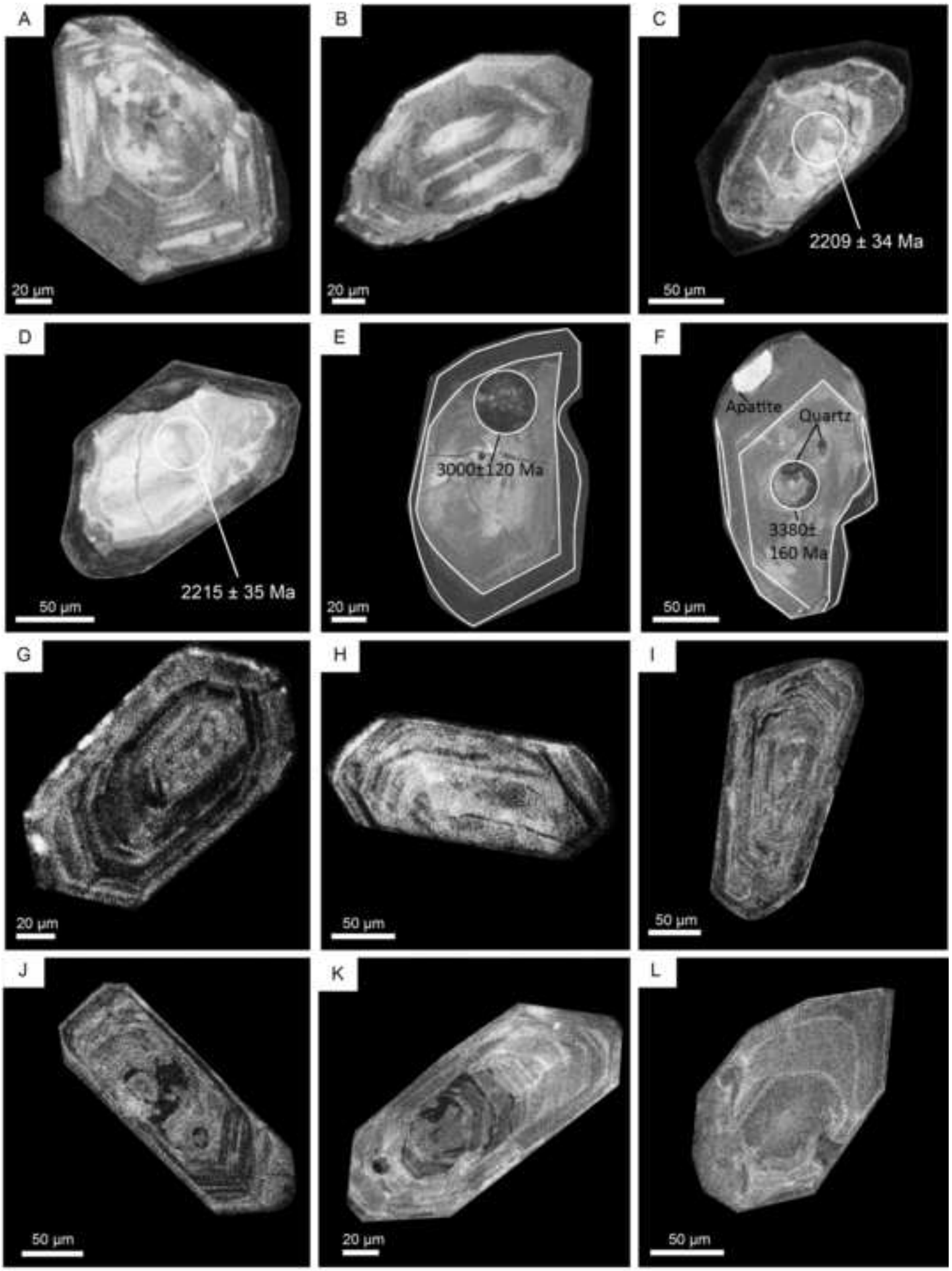

ACCEPTED MANUSCRIPT

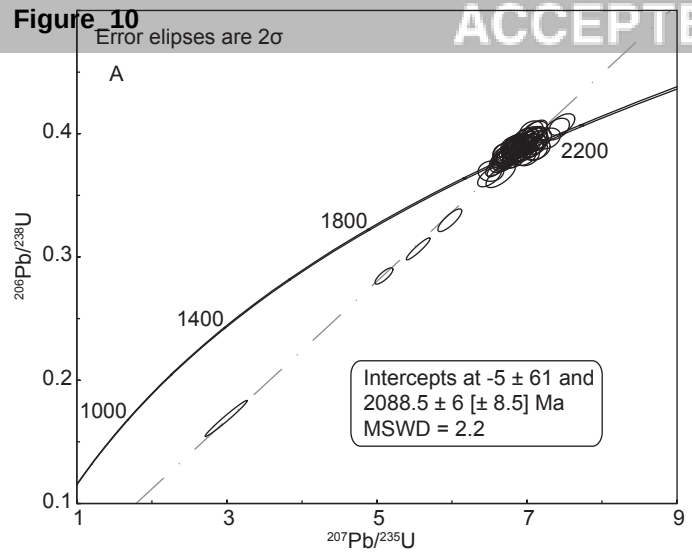


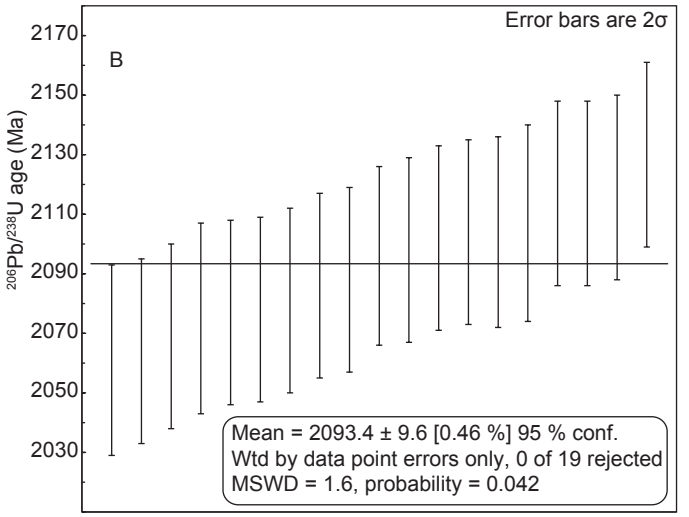


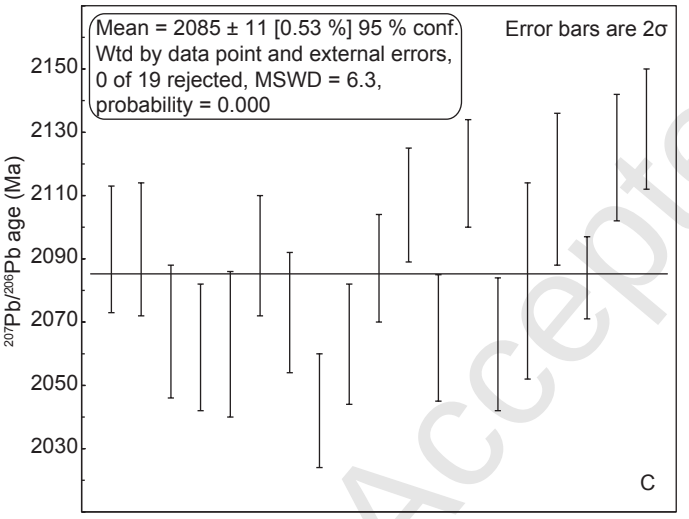


Accepted Manuscript

ACCEPTED MANUSCRIPT

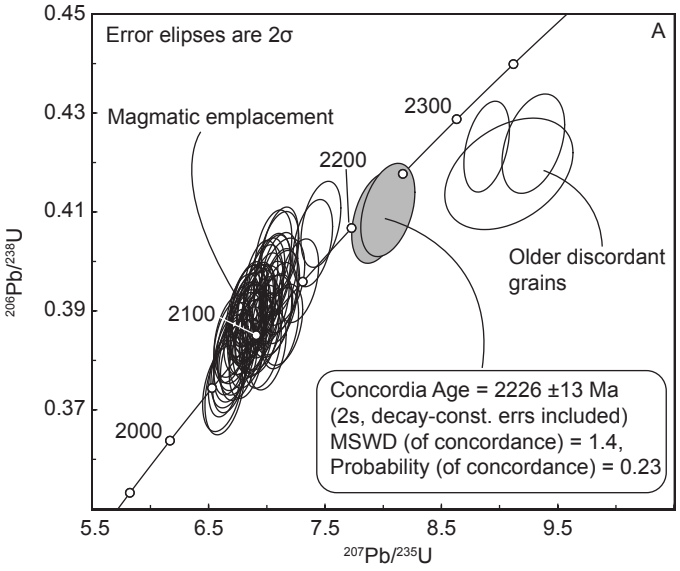


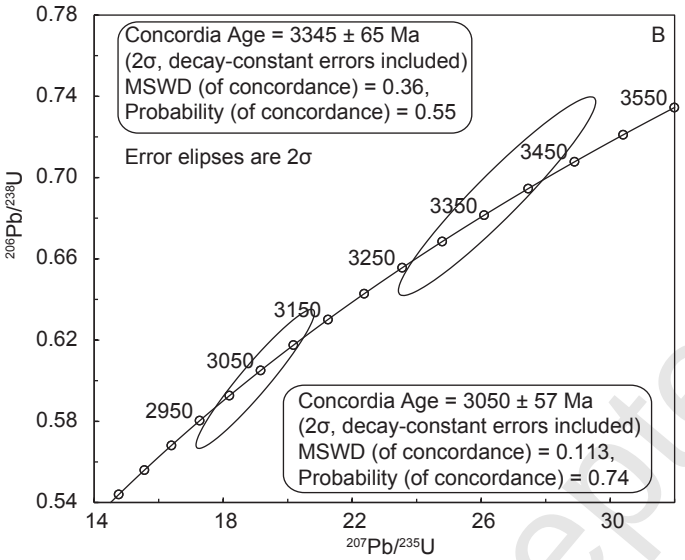


Accepted Manuscript

ACCEPTED MANUSCRIPT

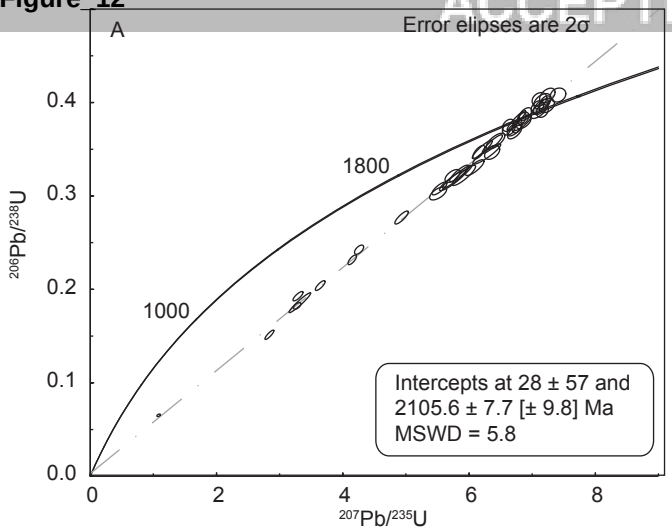


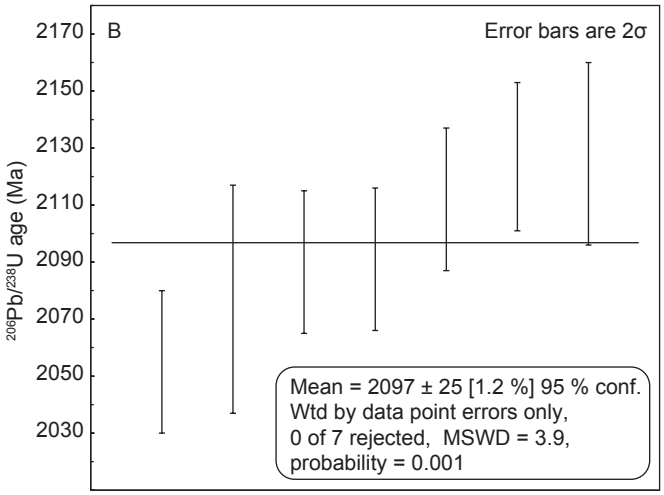


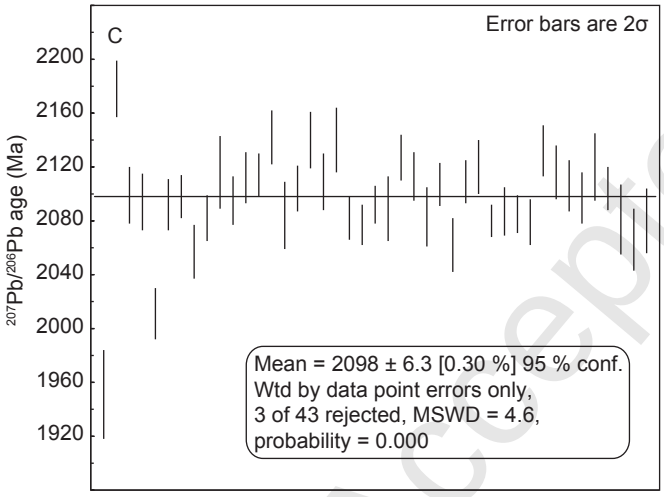


Accepted Manuscript

ACCEPTED MANUSCRIPT

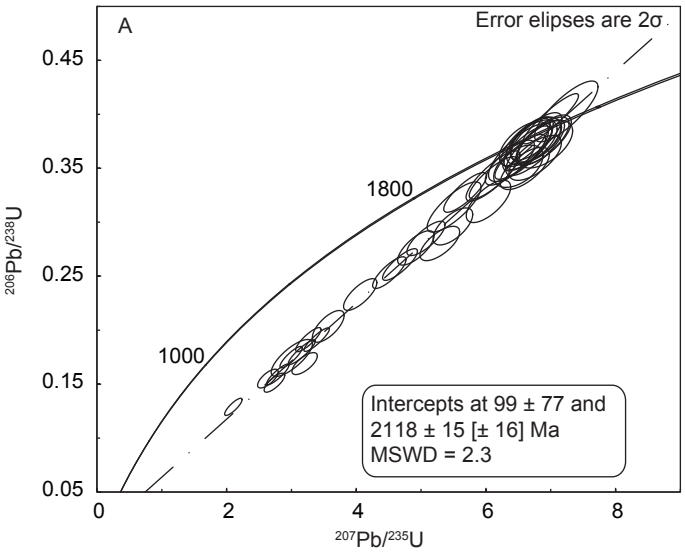


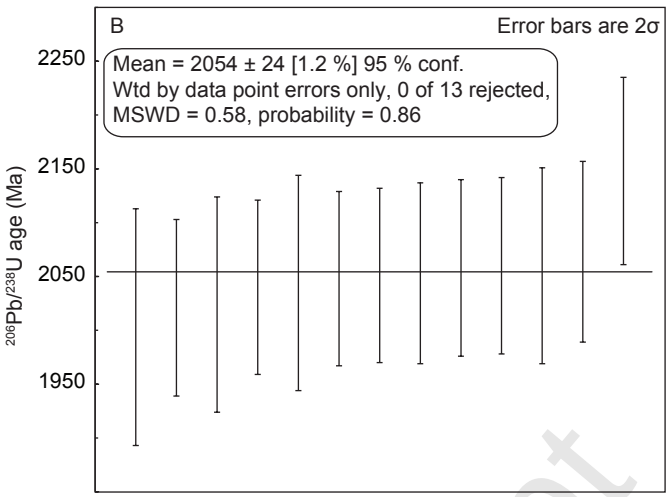


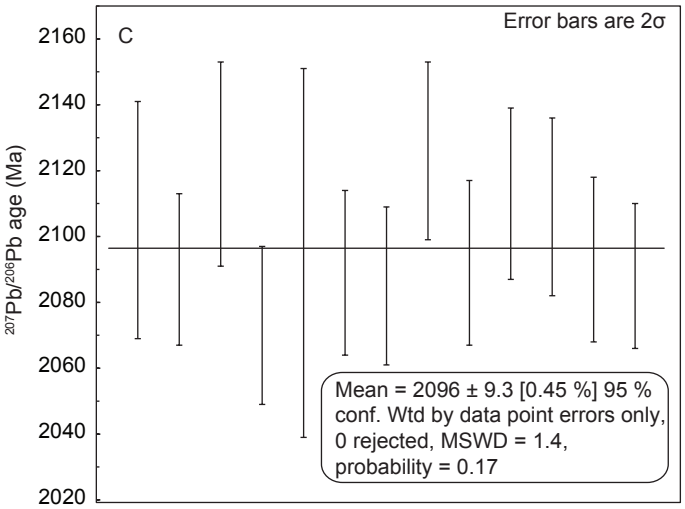


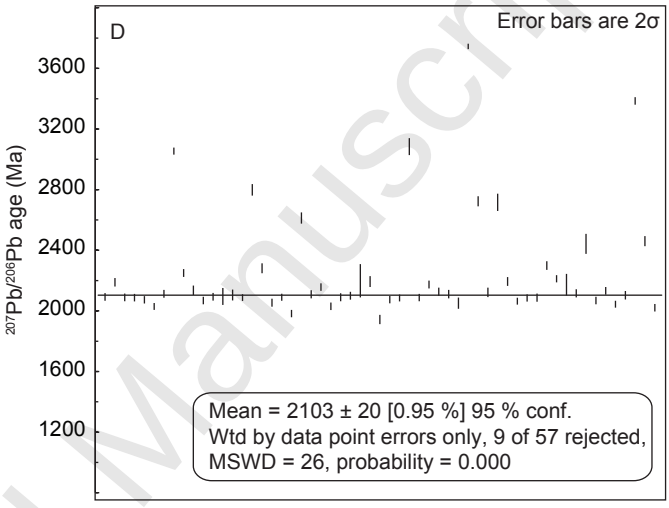


Accepted Manuscript

ACCEPTED MANUSCRIPT

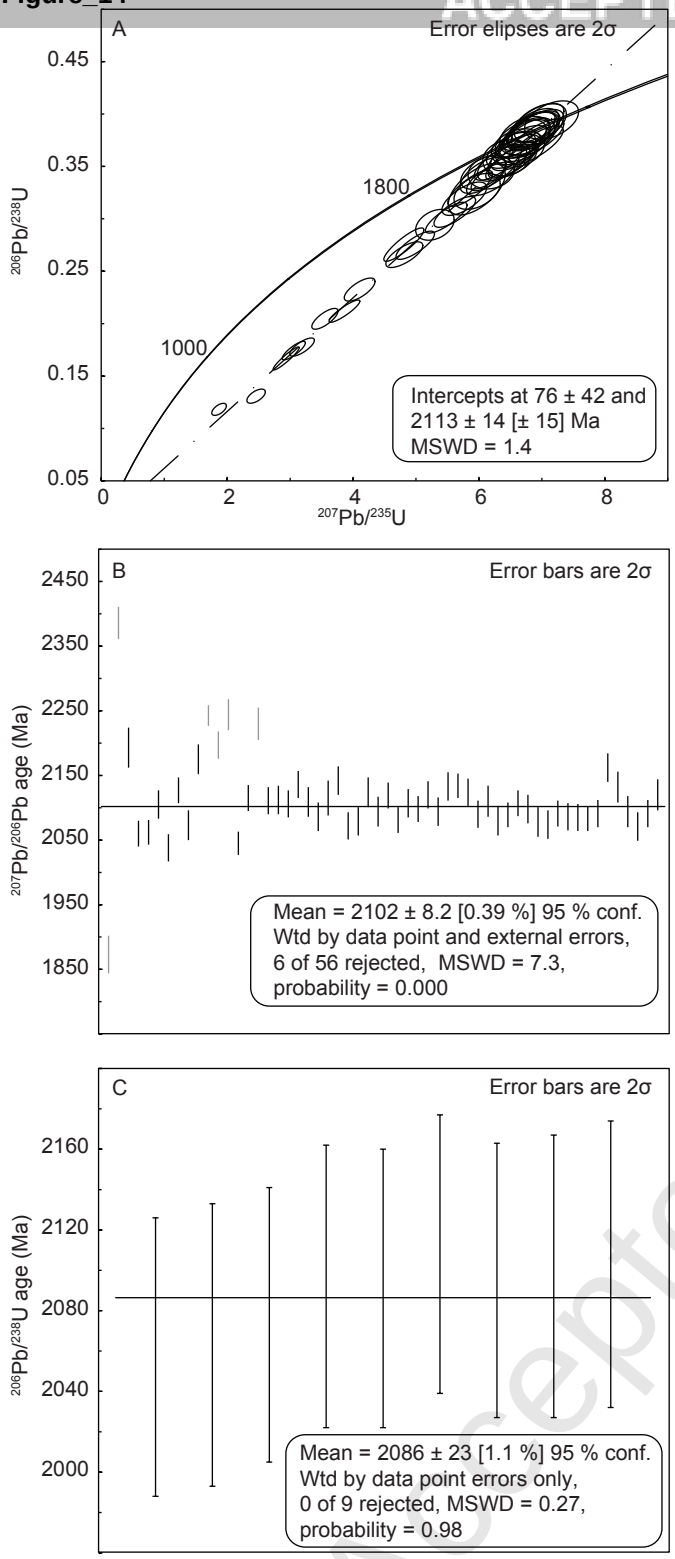


Accepted Manuscript

ACCEPTED MANUSCRIPT

**Figure_15**

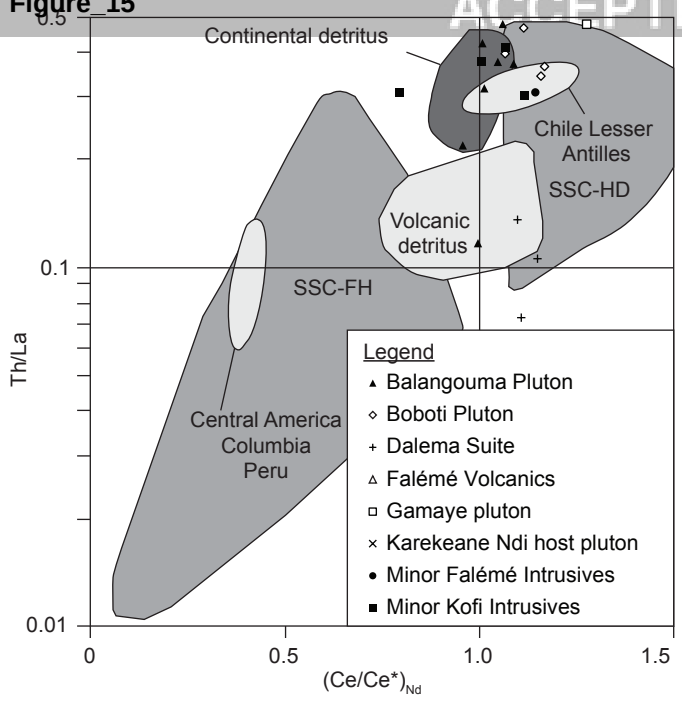


Accepted Manuscript

ACCEPTED MANUSCRIPT

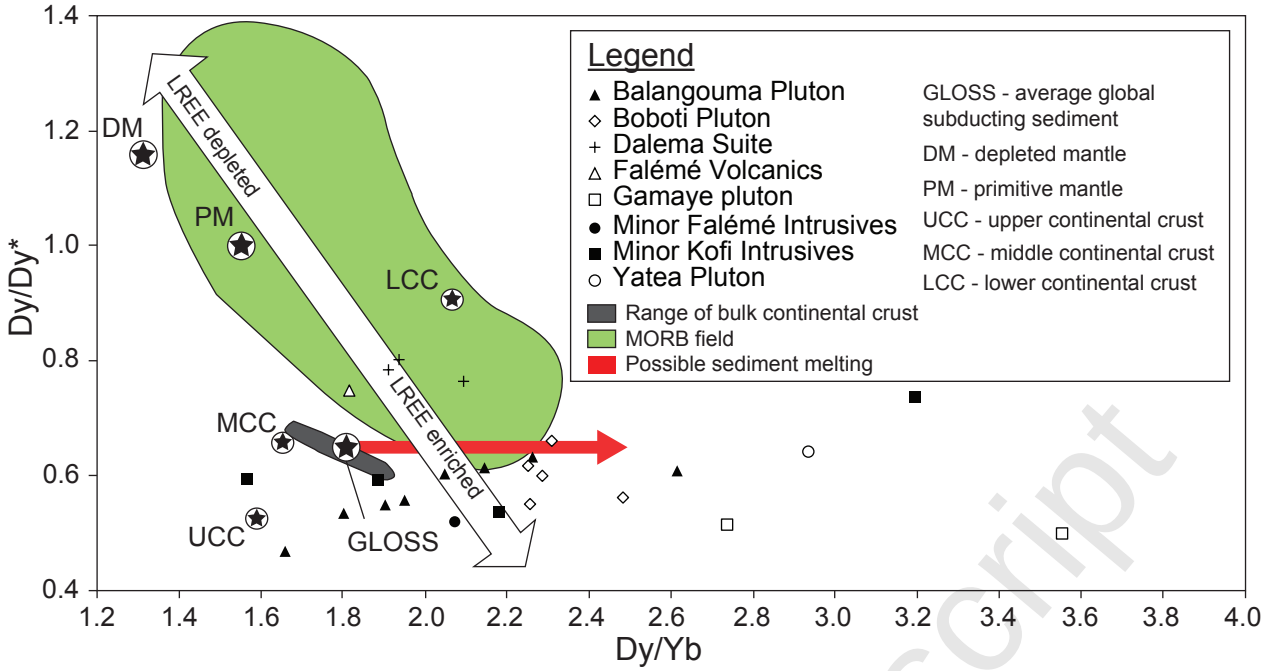


Accepted Manuscript

ACCEPTED MANUSCRIPT

Figure_17

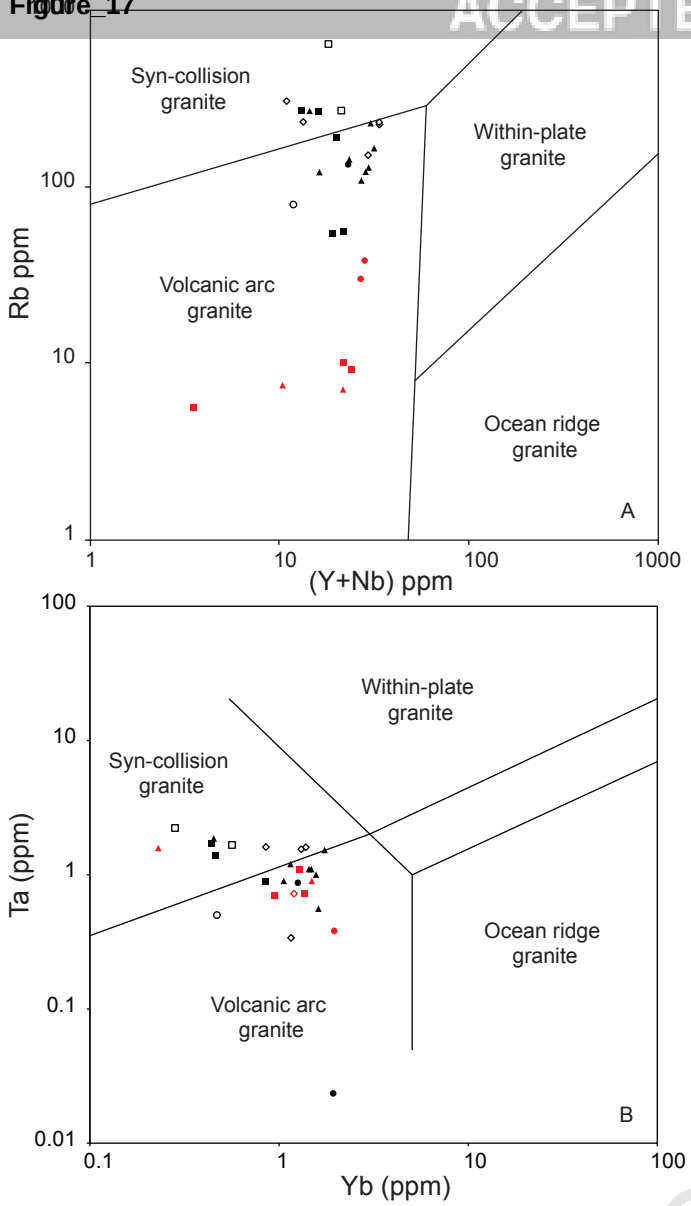





Legend

- ▲ Balangouma Pluton
- ◇ Boboti Pluton
- □ Gamaye pluton
- ● Minor Falémé Intrusives
- ■ Minor Kofi Intrusives
- ○ Yatea Pluton

Accepted Manuscript

ACCEPTED MANUSCRIPT

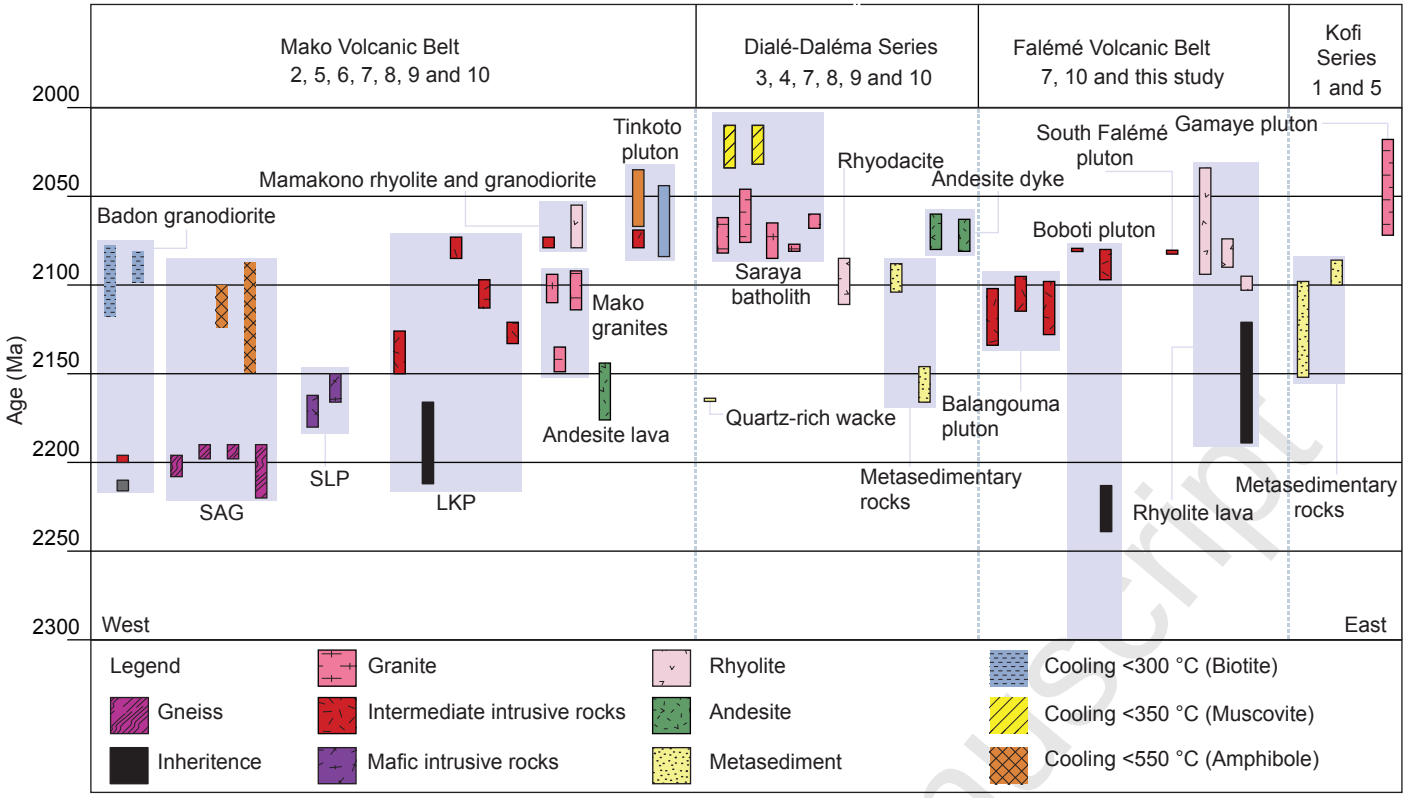


Accepted Manuscript

ACCEPTED MANUSCRIPT

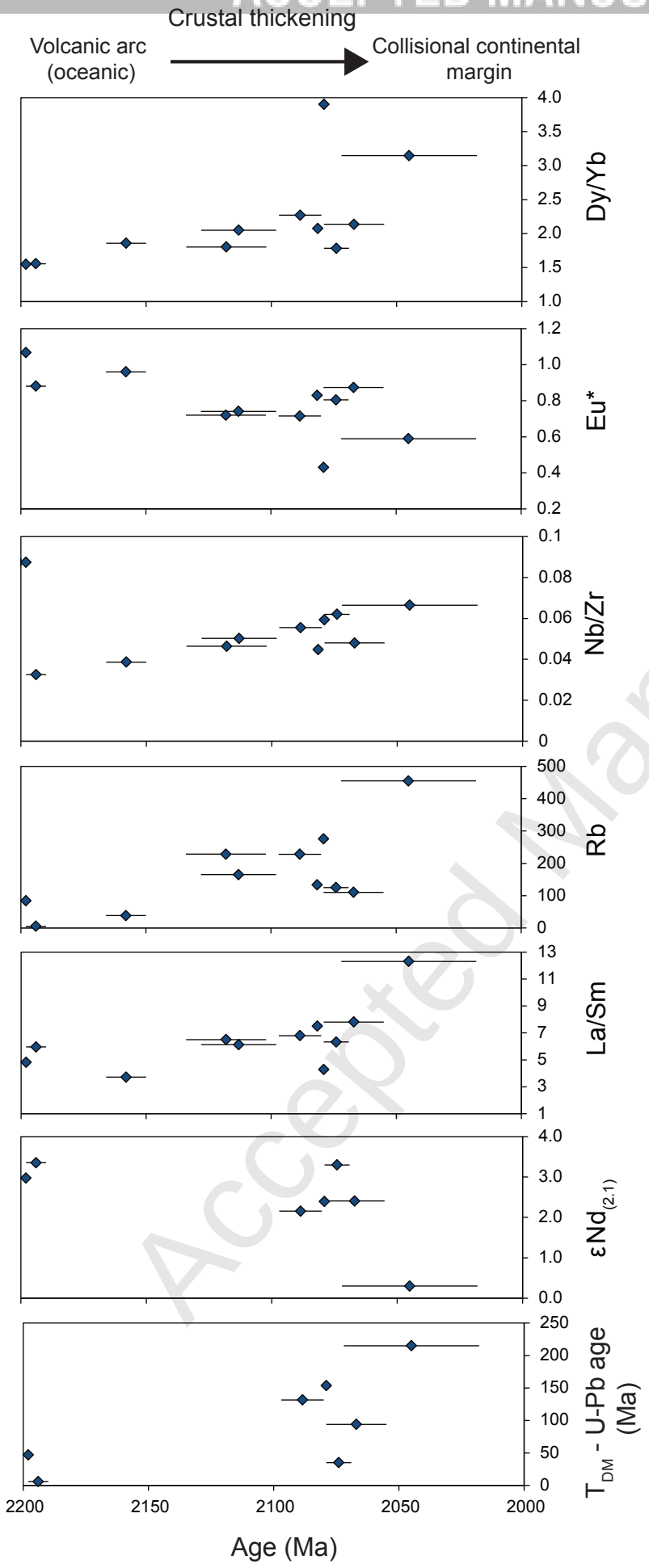


Accepted Manuscript

ACCEPTED MANUSCRIPT

- Highlights
- New U-Pb age data indicate the Balangouma pluton crystallised at 2112 ± 13 Ma.
- Inherited zircons indicate magmatic activity in the Falémé Belt at 2226 ± 13 Ma.
- The KKI evolved from a volcanic island arc environment to an active continental margin.
- Crustal thickening generated peraluminous, granitic melts with a crustal component.
- The Daléma igneous rocks may have formed in an extensional back arc setting.

Accepted Manuscript